

©2015 Yan Zhou

IMPROVING INTEGRATED SYSTEMS FOR ALGAL BIOFUELS AND WASTEWATER  
TREATMENT

BY

YAN ZHOU

DISSERTATION

Submitted in partial fulfillment of the requirements  
for the degree of Doctor of Philosophy in Agricultural and Biological Engineering  
in the Graduate College of the  
University of Illinois at Urbana-Champaign, 2015

Urbana, Illinois

Doctoral Committee:

Assistant Professor Lance C. Schideman, Chair  
Professor Yuanhui Zhang  
Associate Professor Tryg Lundquist  
Associate Professor Luis F. Rodriguez  
Assistant Professor Jeremy S. Guest

## ABSTRACT

The primary goal of this Ph.D. work is to promote synergistic integration of wastewater treatment and algal biofuel production. In particular, we proposed and then analyzed the impacts of a novel integrated system that treats wastewater and maximizes the beneficial reuse of wastewater nutrients and organics to produce bio-crude oil. Centered around this novel system, we investigated several important aspects that can improve performance of the integrated system and resolve several of the key limitations of current algal biofuel production schemes.

The novel system proposed in this study is referred to as “Environment-Enhancing Energy” (E<sup>2</sup>-Energy) because it can simultaneously improve conventional wastewater treatment by providing enhanced nutrient removal, while simultaneously producing a large amount of low-cost feedstock for biofuel production. The main components of the system are a mixed algal-bacterial cultivation process and a hydrothermal liquefaction (HTL) process with internal recycling of key resources between these processes. A series of algal cultivation and HTL experiments were conducted to confirm the feasibility of four key steps of the integrated system, which together facilitate *multi-cycle nutrient reuse* and *biomass amplification* to dramatically increase the biofuel potential of wastewater treatment systems. A mathematical model was developed using STELLA® to simulate the dynamic mass balances of E<sup>2</sup>-Energy operations that showed the potential to amplify biofuel production from wastewater by up to 10 times. Thus, the current amount of biosolids in manure, food processing wastes and municipal wastewater (153 million dry tons), could be amplified using E<sup>2</sup>-Energy to provide enough biofuel feedstocks to replace all U.S. petroleum imports (0.5 billion tons) using only wastewater inputs and CO<sub>2</sub>.

The mixed algal-bacterial cultivation process in the E<sup>2</sup>-Energy system was further investigated using a hybrid photobioreactor (PBR) that incorporated hollow-fiber membranes

and granular activated carbon (GAC). The PBR was used to monitor the long-term performance when treating a combination of municipal wastewater and post-HTL wastewater (PHWW), which is an important step in the E<sup>2</sup>-Energy system. During 800 days of operation covering a range of operating conditions (15-20 day SRT, 1% to 4% PHWW loading rate, with and without GAC), the PBR supported stable and efficient removal of organic carbon (79%-93% chemical oxygen demand, COD) and nitrogen (50%-99% NH<sub>4</sub><sup>+</sup>, and 27%-30% total nitrogen). Increasing PHWW loading rates generally reduced the removal of COD and NH<sub>4</sub><sup>+</sup>. Solids retention time (SRT) below 15 days lead to reactor failure without GAC present. The addition of GAC facilitated stable PBR performance with shorter SRTs and higher PHWW loading rates. GAC also improved COD removal from 70% to over 90%, improved NH<sub>4</sub><sup>+</sup> removal from 26% to 100%, and improved cytotoxicity removal of the combined wastewater from 40% to 60%.

The feasibility of treating PHWW via anaerobic digestion (AD) was also investigated, as a pretreatment step before the mixed algal cultivation. Successful AD occurred at concentrations of PHWW below 6.7%, producing a biogas yield of 0.5 ml/mg COD<sub>removed</sub>, with a methane content of ~70%, and organic removal efficiency of ~50%. Higher concentrations of PHWW (≥ 13.3%) had an inhibitory effect on the AD process, as indicated by delayed, slower, or no biogas production. Activated carbon effectively mitigated this inhibitory effect by enhancing biogas production and allowing digestion to proceed at PHWW concentrations up to 33.3%. Thus, AD is a feasible approach to remove and recover carbon from PHWW, which can improve the overall energy efficiency of E<sup>2</sup>-Energy system.

An algal-growth inhibition assay and response surface methodology were developed and used to study how HTL operating conditions affect the inhibition of algae by PHWW. The IC<sub>50</sub> values of 15 PHWW samples generated under various HTL operating conditions (260-300°C,

30-90min, 15-35% solids ratio) ranged from 0.34%-1.9%. As solids ratio increased from 15% to 25%, PHWW inhibition of algae increased significantly, and then decreased slightly as solids ratio increased from 25% to 35%. PHWW inhibition also generally increased as temperature and retention time increased. Gas chromatography-mass spectrometry (GC-MS) analysis revealed chemical compound differences between the most toxic and least toxic PHWW regarding the content of N, O heterocyclic compounds and straight chain oxygenates etc. COD,  $\text{NH}_4^+$ , and total nitrogen were all found to have moderate correlation with the PHWW inhibition. 280°C, 60min, and 15% solids ratio is recommended as HTL operating conditions that yields relatively high energy recovery (66.1%), and relatively low inhibition effect on algal growth ( $\text{IC}_{50}$  of 0.92%).

Finally, in order to provide useful insights about potential ways to improving photosynthetic efficiency in algal biofuel production systems, biochemical characteristics of a potentially advantageous “mutant” strain (IM) of *Chlamydomonas reinhardtii* were quantified and compared with its progenitor (KO), and to its wild-type (WT). IM grown under low light (10 and 20  $\mu\text{mol photons m}^{-2} \text{s}^{-1}$ ) had up to 27% higher dry weight than WT and KO cells. IM and KO cells, grown under 60  $\mu\text{mol photons m}^{-2} \text{s}^{-1}$ , also showed higher rates of net oxygen evolution and respiration than WT cells. The slow SM phase of chlorophyll a fluorescence transient was much reduced in IM cells, which is ascribed to a regulatory event called, “*state 2 to state 1 change*”. Additionally, when the IM strain is grown under low light, non-photochemical quenching of excited chlorophyll rose faster and recovered faster than in the other strains. Compared to WT cells, IM cells had more metabolites related to carbon metabolism and protection against oxidative stress. These results suggest that the IM strain has unique features that could improve algae productivity in optically dense cultures that are expected when integrating with wastewater treatment.

*To Father Maoqing Zhou and Mother Ningning Ren*

*For your love, support and understanding*

*and*

*To Husband Chao Mei and Daughter Xiaorui Mei*

*Who love me, and whom I dearly love.*

## ACKNOWLEDGEMENTS

First and foremost, I would like to express my deepest gratitude to my advisor, Professor Lance Schideman, for his guidance and support during the past six years. His wisdom, knowledge and commitment to the highest standards inspired and motivated me. I have benefited tremendously from working with and learning from him. I would like to thank him for his patience while training me to think as an engineer, and for encouraging me when I was facing difficulties. Also, I would like to thank the Schideman family for treating us to great food on Christmas Eve and countless other events, I really appreciate them.

Thanks to my committee members, Professor Yuanhui Zhang, who gave me a lot of constructive advice and helped throughout my Ph.D. research. I would like to thank my thesis committees: Professor Luis Rodrigues, Professor Tryg Lundquist, and Professor Jeremy Guest, for their encouragement, insightful comments, and support. Special thanks to Professor Govinjee, who guided me into the intricate details of the world of photosynthesis. I would like to thank him for walking me through my very earliest experiments with *Chlamydomonas* in Morrill Hall, and for continually teaching me how to think scientifically, and be a better person.

I thank my friends and colleagues in the Bioenvironmental Engineering group: Chih-ting Kuo, Peng Li, Ana Martin, Mengzi Wang, Wan-Ting Chen, Zhichao Wang, Guo Yu, Chao Gai, Peng Zhang, ZhongZhong Zhang, for the stimulating discussions, valuable support, and for all the fun we have had together.

Finally, I would like to thank my family, my parents and my husband Chao Mei, for always providing me support and love. It would not have been possible to write this doctoral thesis without the help and support from you.

## TABLE OF CONTENTS

<b>CHAPTER 1. INTRODUCTION .....</b>	<b>1</b>
1.1 Background .....	1
1.2 Research Objectives and Approaches .....	4
1.3 References .....	6
<b>CHAPTER 2. LITERATURE REVIEW .....</b>	<b>9</b>
2.1 Algae Based Wastewater Treatment Processes .....	9
2.2 Adsorbent Based Wastewater Treatment Processes .....	12
2.3 Characterization of Post-hydrothermal Liquefaction Wastewater .....	19
2.4 Effect of Operating Condition on Post-hydrothermal Liquefaction Wastewater .....	26
2.5 Light Utilization Efficiencies and Chlorophyll a Fluorescence .....	31
2.6 References .....	36
2.7 Figures and Tables .....	45
<b>CHAPTER 3. AN INNOVATIVE BIOENERGY PRODUCTION SYSTEM WHICH COMBINES ALGAL WASTEWATER TREATMENT AND HYDROTHERMAL LIQUEFACTION .....</b>	<b>50</b>
3.1 Introduction .....	50
3.2 Materials and Methods .....	52
3.3 Results and Discussion .....	63
3.4 Conclusions .....	79
3.5 References .....	79
3.6 Figures and Tables .....	85
<b>CHAPTER 4. ADSORBENT AMENDED HYBRID PHOTOBIOREACTOR FOR ENHANCED ALGAL WASTEWATER TREATMENT .....</b>	<b>97</b>
4.1 Introduction .....	97
4.2 Materials and Methods .....	99
4.3 Results and Discussion .....	103
4.4 Conclusions .....	122
4.5 References .....	122
4.6 Figures and Tables .....	126
<b>CHAPTER 5. ANAEROBIC TREATMENT OF AQUEOUS PRODUCT OF HYDROTHERMAL LIQUEFACTION TO INCREASE CARBON EFFICIENCY DURING BIOFUEL PRODUCTION .....</b>	<b>141</b>
5.1 Introduction .....	141
5.2 Material and Methods .....	143
5.3 Results and Discussion .....	144
5.4 Conclusions .....	153
5.5 References .....	153
5.6 Figures and Tables .....	157



**CHAPTER 6. EFFECT OF HTL OPERATING CONDITIONS AND WATER QUALITY ON THE INHIBITION CHARACTERISTICS OF POST HYDROTHERMAL LIQUEFACTION WASTEWATER..... 160**

6.1 Introduction ..... 160  
6.2 Materials and Methods ..... 163  
6.3 Results and Discussion ..... 168  
6.4 Conclusions ..... 178  
6.5 References ..... 179  
6.6 Figures and Tables..... 182

**CHAPTER 7. CHARACTERIZATION OF *CHLAMYDOMONAS REINHARDTII* MUTANT STRAINS WITH IMPROVED PHOTOSYNTHETIC EFFICIENCY UNDER LIGHT-LIMITED CONDITIONS ..... 191**

7.1. Introduction ..... 191  
7.2. Materials and Methods ..... 193  
7.3. Results ..... 198  
7.4. Discussion ..... 207  
7.5. Conclusions ..... 217  
7.6. References ..... 218  
7.7. Figures and Tables..... 227

# CHAPTER 1

## INTRODUCTION

### 1.1 Background

Current fossil fuel usage is widely recognized as unsustainable because of diminishing supplies and a significant contribution to greenhouse gas (GHG) emissions. Renewable, carbon-neutral fuels are necessary for environmental and economic sustainability, and biofuels from biomass are one of the most feasible alternatives to petroleum. Among biomass materials, algae are one of the most promising feedstocks for next generation biofuels because many algal species have higher biomass productivity than terrestrial crops, and algae can grow on marginal land and water bodies, which results in less competition with food production for arable land (U.S. DOE 2010). Algae also have an important environmental advantage because they can be grown in wastewater and improve water quality. In contrast, most biofuel paradigms increase the competition for fresh water resources (Sheehan et al. 1998).

Despite the apparent advantages of algal biofuels, significant economic, technical and environmental challenges remain to be solved for scaling-up of algal biofuel production. Most of the current algal biofuel technologies have focused on cultivating relatively pure, high-oil algal species and extracting the oil for conversion to biodiesel via transesterification. Maintaining a pure culture of high-oil algae is difficult, but attempts are made through species selection, genetic modification and/or strict control of cultivation conditions. However, high-oil algae tend to grow slower than most low-oil algal strains and bacteria (Mata et al. 2010; Rodolfi et al. 2009; Williams and Laurens 2010). Thus, the need for selective production of high-oil algae often leads to significant contamination problems (Sheehan et al. 1998).

Another key practical limitation for the algal biofuel industry is obtaining a net positive cost and energy balance for the extraction of biofuel from wet algal biomass (National Research Council 2012). Multiple recent life cycle analyses showed that drying algal biomass sufficiently for conventional oilseed extraction techniques consumes more than 90% of the energy content of the algal oils (Lardon et al. 2009; Xu 2011). Thus, future algal bio-energy schemes should avoid the need for dry algal biomass, and instead must be able to use wet biomass or algal species that excrete their oils from live cells.

Several reports have also raised concerns about the large amount of freshwater and fertilizer for large-scale algal biofuel production (U.S. DOE 2010; Clarens et al. 2010). It has been estimated that using algal feedstocks to meet the US Energy Independence and Security Act (EISA) federal mandates for producing one billion gallons of biomass-based diesel, would require 1,238 billion gallons/yr of fresh water (10% of US public water usage) and requires 564 million kg N (5% of US usage) (Yang et al. 2011). If purchased at current market prices, the water and nutrient inputs significantly raise the cost of algal biofuels. Lundquist et al. (2010) showed algal biofuels made with purchased inputs would exceed \$400/barrel, but integration with wastewater inputs and infrastructure could lower the net costs of algal biofuel production below \$30/barrel. Therefore, it is important to develop algal biofuel paradigms that are integrated with wastewater treatment.

Some important limitations with current algal wastewater treatment approaches include insufficient effluent water quality and low light utilization efficiencies. One challenge common to both conventional (bacteria based) wastewater treatment and novel algae based wastewater treatment is the need to improve effluent water quality in the face of mounting concerns about a variety of anthropogenic contaminants like residual pesticides from agriculture, pharmaceuticals

from household usage, and industrial chemicals from refineries, which are increasingly detected in various wastewater streams (Kolpin et al. 2002). These chemicals may exert deleterious impacts on human health and the natural environment if not treated properly and discharged into the environment (Petrovic et al. 2002). However, many of these chemicals are recalcitrant or slow-degrading compounds so that conventional biological treatment may not provide satisfactory removal. Therefore, some advanced wastewater treatment technologies are proposed to address these concerns and enhance treatment efficiency, such as using adsorbents (like activated carbon), or application of advanced oxidation process (like ozonation) to increase the biodegradability of the recalcitrant/slow degrading compounds.

Another important issue for the success of large-scale algal biomass production is maximizing their light utilization efficiency (Sheehan et al. 1998; Williams and Laurens 2010; Ogbonna and Tanaka 2000). Due to rapid light attenuation in dense algal cultures that absorb and scatter incoming light, significant spatial heterogeneity of light intensities occurs inside most photobioreactors. Cells at the surface can be damaged by excess light (through photoinhibition) (Adir et al. 2003) and lose absorbed radiant energy to heat dissipation. In contrast, cells located deeper in the culture may experience significant light limitations that would also decrease cell growth. For example, one previous study with dense cultures (1 g/L) found that 80-95% of the light path was severely light limited (Williams and Laurens 2010). Genetic and molecular studies have led to the development of strains that can tolerate high light and have better growth under high irradiance (Melis 2009; Polle et al. 2002; Polle et al. 2003; Beckmann et al. 2009; Kosourov et al. 2011; Perrine et al. 2012). On the other hand, developing algal strains that can make maximum use of low light conditions is also advantageous because there are likely to be significant areas of low irradiance in large-scale photobioreactor systems. Thus, algae with

improved light utilization efficiency and enhanced biomass production under low irradiance could thus be beneficial for improving overall algal production.

## **1.2 Research Objectives and Approaches**

The goal of this Ph.D. work is to promote synergistic integration of wastewater treatment and algal biofuel production, with each of the following chapters focusing on an innovative approach to resolve some of the key limitations and bottlenecks discussed above. Chapter 3 investigates a novel waste-to-energy system that integrates algal biomass production during wastewater treatment and hydrothermal liquefaction of that biomass into bio-crude oil. A key feature of this novel system is the concept of “multi-cycle nutrient reuse”, which is used to leverage the nutrients in wastewater for maximized bioenergy production. This system, which we refer to as, Environment-Enhancing Energy (E<sup>2</sup>-Energy), elegantly resolves several key bottlenecks for algal biofuels production including the contamination of target algal species, high energy demand for dewatering, and the high-cost inputs for nutrients and water. This chapter reported original experiments to provide a proof of concept for the key physicochemical and biological process steps of the E<sup>2</sup>-Energy process, and modeling to consider the net energy balance and overall mass balances in order to evaluate the national impact of this system. In this chapter, several critical issues for this novel system have also been identified, including effective treatment of post-hydrothermal liquefaction wastewater (PHWW) for environmental discharge and the inhibitory effects of PHWW on algal growth.

In Chapter 4, the mixed algal-bacterial cultivation process in the E<sup>2</sup>-Energy system was further investigated using a hybrid photobioreactor (PBR) that incorporated hollow-fiber membranes and granular activated carbon (GAC). The PBR was used to monitor the long-term performance when treating a combination of municipal wastewater and PHWW, which is an

important step in the E<sup>2</sup>-Energy system. The effect of using activated carbon to augment treatment performance and stability was also studied in this chapter. The adsorption process component, can improve effluent water quality by providing fast physicochemical capture of slowly-degrading/refractory and toxic compounds and the additional time needed for biological removal. In addition, adsorbents provide benefits such as buffering against shock loadings, toxic compounds, and fluctuations in biological performance due to temperature, pH, sunlight intensity, etc.

An alternative to directly treating PHWW is to add a pretreatment step before recycling it to an algal cultivation reactor. Chapter 5 studied the feasibility of using anaerobic digestion (AD) as a pretreatment of PHWW to reduce the organic content and recover additional energy content. This process provides potential detoxification before recycling PHWW into algal cultivation, which could amplify phototrophic biomass production and maximize the overall carbon capture and energy production of the E<sup>2</sup>-Energy system.

Chapter 6 investigated the inhibitory effect of PHWW on algal growth. An algal-growth inhibition assay and response surface methodology were used to study how HTL operating conditions affect the PHWW inhibition of algal growth, in order to provide guidance to produce PHWW suitable for algal cultivation. In addition, detailed chemical composition analysis, as well as analysis to elucidate the relationship between common water quality parameters and algal inhibition were conducted, which can help us to better understand the mechanism of PHWW inhibition and provide a rapid diagnosis about the inhibitory effects of PHWW.

Finally, Chapter 7 reported the biophysical and biochemical characterization of a spontaneous “mutant” strain of *Chlamydomonas reinhardtii*, which showed improved photosynthetic efficiency and up to 27% more biomass production under light-limited

conditions. *Chlamydomonas* has the flexibility to switch between photosynthesis and non-photosynthetic metabolism of carbon, which is an important feature for algae cultivations in wastewater. By elucidating the distinctive characteristics of the mutant in light utilization, we provide useful insights on potential ways to improve practical algal biofuel production systems. Ultimately, metabolic and genetic engineering could be used to transfer the desirable features of our *Chlamydomonas* mutant into other algae species to improve the efficiency of algal biofuel production systems (Dubini and Ghirardi 2014; Hong et al. 2014). The improved photosynthetic efficiency could also be used to enhance productivity of other algal biochemical manufacturing platforms (such as recombinant proteins, antioxidants, hormones) for industrial, nutritional and medical uses (Rasala and Mayfield 2014; Guarnieri and Pienkos 2014).

### 1.3 References

- Adir, N., H. Zer, S. Shochat and I. Ohad. 2003. Photoinhibition - a historical perspective. *Photosynthesis Research* 76(1-3): 343-370.
- Beckmann, J., F. Lehr, G. Finazzi, B. Hankamer, C. Posten and L. Wobbe. 2009. Improvement of light to biomass conversion by de-regulation of light-harvesting protein translation in *Chlamydomonas reinhardtii*. *Journal of Biotechnology* 142(1): 70-77.
- Clarens, A. F., E. P. Resurreccion, M. A. White and L. M. Colosi. 2010. Environmental Life Cycle Comparison of Algae to Other Bioenergy Feedstocks. *Environmental Science & Technology* 44(5): 1813-1819.
- Dubini, A. and M. L. Ghirardi. 2014. Engineering photosynthetic organisms for the production of biohydrogen. *Photosynthesis Research* 123(3): 241-253.
- Guarnieri, M. T. and P. T. Pienkos. 2014. Algal omics: unlocking bioproduct diversity in algae cell factories. *Photosynthesis Research* 123(3): 255-263.
- Hong, J. W., S. Jo and H. Yoon. 2014. Research and development for algae-based technologies in Korea: a review of algae biofuel production. *Photosynthesis Research* 123(3): 297-303.
- Kolpin, D. W., E. T. Furlong, M. T. Meyer, E. M. Thurman, S. D. Zaugg, L. B. Barber and H. T. Buxton. 2002. Pharmaceuticals, hormones, and other organic wastewater

- contaminants in US streams, 1999-2000: A national reconnaissance. *Environmental Science & Technology* 36(6): 1202-1211.
- Kosourov, S. N., M. L. Ghirardi and M. Seibert. 2011. A truncated antenna mutant of *Chlamydomonas reinhardtii* can produce more hydrogen than the parental strain. *International Journal of Hydrogen Energy* 36(3): 2044-2048.
- Lardon, L., A. Hélias, B. Sialve, J. P. Steyer and O. Bernard. 2009. Life-cycle assessment of biodiesel production from microalgae. *Environmental Science & Technology* 43(17): 6475-6481.
- Mata, T. M., A. A. Martins and N. S. Caetano. 2010. Microalgae for biodiesel production and other applications: a review. *Renewable & Sustainable Energy Reviews* 14(1): 217-232.
- Melis, A. 2009. Solar energy conversion efficiencies in photosynthesis: Minimizing the chlorophyll antennae to maximize efficiency. *Plant Science* 177(4): 272-280.
- National Research Council. 2012. Sustainable Development of Algal Biofuels. Washington, D.C.:The National Academic Press.
- Ogbonna, J. and H. Tanaka. 2000. Light requirement and photosynthetic cell cultivation - Development of processes for efficient light utilization in photobioreactors. *Journal of Applied Phycology* 12(3-5): 207-218.
- Perrine, Z., S. Negi and R. T. Sayre. 2012. Optimization of photosynthetic light energy utilization by microalgae. *Algal Research* 1(2): 134-142.
- Petrovic, M., M. Sole, M. J. L. de Alda and D. Barcelo. 2002. Endocrine disruptors in sewage treatment plants, receiving river waters, and sediments: Integration of chemical analysis and biological effects on feral carp. *Environmental Toxicology and Chemistry* 21(10): 2146-2156.
- Polle, J., S. Kanakagiri and A. Melis. 2003. tla1, a DNA insertional transformant of the green alga *Chlamydomonas reinhardtii* with a truncated light-harvesting chlorophyll antenna size. *Planta* 217(1): 49-59.
- Polle, J., S. Kanakagiri, E. Jin, T. Masuda and A. Melis. 2002. Truncated chlorophyll antenna size of the photosystems - a practical method to improve microalgal productivity and hydrogen production in mass culture. *International Journal of Hydrogen Energy* 27(11-12): 1257-1264.
- Rasala, B. A. and S. P. Mayfield. 2014. Photosynthetic biomanufacturing in green algae; production of recombinant proteins for industrial, nutritional, and medical uses. *Photosynthesis Research* 123(3):227-239.



- Rodolfi, L., G. C. Zittelli, N. Bassi, G. Padovani, N. Biondi, G. Bonini and M. R. Tredici. 2009. Microalgae for oil: strain selection, induction of lipid synthesis and outdoor mass cultivation in a low-cost photobioreactor. *Biotechnology and Bioengineering* 102(1): 100-112.
- Sheehan, J., T. Dunahay, J. Benemann and P. Roessler. 1998. *A Look Back at the U.S. Department of Energy's Aquatic Species Program: Biodiesel from Algae*. Golden: National Renewable Energy Laboratory
- U.S. DOE. 2010. National algal biofuels technology roadmap. U.S. Department of Energy, Office of Energy Efficiency and Renewable Energy, Biomass Program.
- Williams, P. J. L. B. and L. M. L. Laurens. 2010. Microalgae as biodiesel biomass feedstocks: Review analysis of the biochemistry, energetics economics. *Energy Environmental Science* 3(5): 554-590.
- Xu, L. 2011. Assessment of a dry and a wet route for the production of biofuels from microalgae: Energy balance analysis. *Bioresource Technology* 102(8): 5113-5122.
- Yang, J., M. Xue, X. Zhang, Q. Hu, M. Sommerfeld and Y. Chen. 2011. Life-cycle analysis on biodiesel production from microalgae: water footprint and nutrients balance. *Bioresource Technology* 102(1): 159-165.

## CHAPTER 2

### LITERATURE REVIEW

#### 2.1 Algae Based Wastewater Treatment Processes

##### 2.1.1 Nutrient removal by algae

Microalgae assimilate a significant amount of nutrients because they require high amounts of nitrogen and phosphorous for nucleic acids, phospholipids and proteins, which typically accounts for 45-60% of microalgae dry weight (Muñoz and Guieysse 2006). The nitrogen composition of algae ranges from 1% to 14% of algal dry weight and phosphorus ranges from 0.05% to 3.3% (Richmond 2004). Nutrient removal can also be further increased by NH<sub>3</sub> stripping or phosphorus precipitation due to an increase in pH associated with carbon dioxide fixation and removal during photosynthesis

Several algal species have been reported as useful for nutrient removal including *Botryococcus braunii*, *Chlamydomonas*, *Scenedesmus* and *Chlorella*. *Botryococcus braunii* has been cultivated successfully in secondary effluent in both batch and continuous experiments, with a removal efficiency of up to 99% for nitrate and 93% for phosphate (Sawayama et al. 1994; Sawayama et al. 1992). Tam and Wong (1996) reported removal of nitrogen by cultivating *Chlorella vulgaris* in wastewater, and found that the removal efficiency was inversely related to the initial nitrogen concentration: 100% nitrogen removal was achieved with initial nitrogen concentration lower than 20 mg/L, whereas 95% nitrogen removal was observed with 40-80 mg/L initial nitrogen concentration, and 50% removal with initial concentrations higher than 80 mg/L.

Mixed-cultures of algae can also achieve high efficiency in nutrient removal. For instance, the algae turf scrubber (ATS), has been reported to achieve 40-98% nitrogen removal

and 40-90% phosphorous removal in dairy and swine manure (Kebede-Westhead et al. 2003; Pizarro et al. 2006; Pizarro et al. 2002; Pizarro et al. 2002; Mulbry et al. 2008b; Mulbry et al. 2008a).

### **2.1.2 Organic removal by algae**

Microalgae have traditionally been used for N and P removal after most of the organics have been removed from wastewater by conventional secondary treatment such as activated sludge (Lavoie and Delanoue 1985; Martin et al. 1985). However, some recent studies have also reported that significant organic removal can be achieved by algae (Dilek et al. 1999; Hodaifa et al. 2008; Jail et al. 2010; Kamjunke et al. 2008).

Algae can take up organics like heterotrophic bacteria; however, the way they assimilate organics is more complicated. Algae can be classified as autotrophic algae, heterotrophic algae, mixotrophic algae, and photoheterotrophic algae (Neilson and Lewin 1974; Stewart 1974). Heterotrophy in algae implies the capacity for sustained growth and cell division in the dark, which appears to occur exclusively by aerobic dissimilation. They live just like heterotrophic bacteria-during respiration of substrate, oxygen is consumed and carbon dioxide is evolved. Except some colorless algae species, e.g., *Prototheca zopfii*, that are obligate heterotrophs, most heterotrophic algae can also grow photoheterotrophically. Mixotrophy occurs in a few algae that may have an impaired capacity to assimilate carbon dioxide in the light. Thus, mixotrophic algae require a supply of organic carbon even for growth in light. As a general rule, carbon dioxide is simultaneously assimilated in smaller amounts than that needed for phototrophic growth. Photoheterotrophy (photoassimilation) can be found in many algae. Many algae are unable to grow heterotrophically in the dark, but they are able to incorporate certain organic compounds into cellular material, including lipids, in the light. Many algae, such as *Chlamydomonas*, can

also assimilate exogenous acetate into lipids. Some algae are even able to incorporate long-chain fatty acids into lipids without their prior degradation (Neilson and Lewin 1974).

Although assimilation of organic substrates by algae are well established under certain laboratory conditions, algae generally have too low affinity for most of the substrates to compete effectively with other fast growing heterotrophic organisms such as heterotrophic bacteria (Neilson and Lewin 1974).

### **2.1.3 Algal-bacterial symbiosis**

The symbiotic relationship between algae and bacteria can support the aerobic degradation of various organic contaminants. Table 2-1 summarized the organic removal from literature. O<sub>2</sub> produced by algae can be used by heterotrophic bacteria for mineralizing organic pollutants, and the CO<sub>2</sub> released from bacterial respiration can be used by algae in photosynthesis, as shown in Figure 2-1. Mixed algal-bacterial wastewater treatment system is receiving increasing attention for two reasons. First, photosynthetic aeration can decrease the cost of mechanical aeration which accounts for more than 50% of the total energy consumption of typical aerobic wastewater treatments (Metcalf & Eddy et al. 2003). Second, algal biomass is promising as a potential biofuel feedstock (Rodolfi et al. 2009; Li et al. 2008; Chisti 2007; Gouveia and Oliveira 2009; Mata et al. 2010)

However, there are some challenges in combining algae and bacteria to treat wastewater, especially in keeping a balance between these two communities in order to achieve both decent organic and nutrient removal. First, algae are more sensitive to various organic pollutants and heavy metals (Muñoz and Guieysse 2006), which are common in various wastewater streams. Second, increased turbidity resulting from bacteria growth affects light delivery to algae. Furthermore, heterotrophic bacteria generally grow faster than heterotrophic algae (Kamjunke et

al. 2008) and can outcompete algae. Finally, algal uptake of pollutants and nutrients is generally more sensitive to changes in environmental conditions such as temperature and sunlight.

Therefore, the algal-bacterial combination for wastewater treatment must be carefully designed or controlled to provide a proper balance between them.

## **2.2 Adsorbent Based Wastewater Treatment Processes**

### **2.2.1 Adsorbent processes and models**

Adsorption processes use a solid adsorbent media for removing soluble substances from either liquid or gas. Any substance that is being removed from the liquid or gas phase is referred to as the adsorbate, and the adsorbent is the media onto which the adsorbate accumulates.

Adsorption occurs when the attractive forces at the adsorbent surface overcome the attractive forces of the liquid or gas originally containing the adsorbate (Metcalf & Eddy et al. 2003).

The equilibrium capacity of an adsorbent for a particular adsorbate is represented by adsorption isotherms, and the most common isotherm equations used to describe the experimental isotherm data were developed by Freundlich, Langmuir, and Brunauer, Emmet, and Teller (BET isotherm). Of the three, the Freundlich isotherm is used most commonly to describe the adsorption characteristics of the activated carbon used in water and wastewater treatment.

The empirically derived Freundlich isotherm is defined as follows:

$$q_e = K_f C_e^{1/n} \quad (2-1)$$

where  $q_e = \frac{x}{m}$  represents the mass of adsorbate ( $x$ ) per mass of adsorbent ( $m$ ) at equilibrium (mg/g),  $C_e$  represents the equilibrium liquid-phase concentration of the adsorbate (mg/L), and  $K_f$  and  $n$  are fitting parameters that depend on the adsorbent and adsorbate.  $K_f$  is an indicator of adsorption capacity, and when  $1/n$  values are similar, a higher  $K_f$  value indicates higher capacity.

1/n is a measure of intensity of adsorption, and higher 1/n values generally indicate that adsorption is more favorable. The Freundlich equation can be linearized using a log-log plot, and the temperature dependent constants  $K_f$  and 1/n can then be found by linear regression:  $\ln q_e = \ln K_f + \frac{1}{n} \ln C_e$ .

### **2.2.2 The application of activated carbon in wastewater treatment**

Activated carbon has a wide variety of applications for liquid phase treatment: food processing, preparation of alcoholic beverages, decolorization of oils and fats, product purification in sugar refining, purification of chemicals (acids, amines, glycerin, glycol, etc.), enzyme purification, decaffeination of coffee, gold recovery, refining of liquid fuels, and purification in the personal care, cosmetics, and pharmaceutical industries. Activated carbon is also the primary adsorbent used in adsorption processes in wastewater treatment applications.

There are two main size classifications of activated carbon: powdered activated carbon (PAC), which typically has a diameter of less than 0.074 mm (200 sieve) and can be added directly to the activated sludge process or other solids contacting processes. Granular activated carbon (GAC), which has a diameter greater than 0.1 mm (~140sieves), is generally used in filtration applications (Asano 2007). PAC has the advantage of faster adsorption rates, but has disadvantages associated with disposal because it is more difficult to separate from wastewater biosolids and sludges (Faust and Aly 1987).

Activated carbon has been used in both municipal wastewater treatment and industrial wastewater treatment. The primary purpose of using it for municipal wastewater treatment was to facilitate beneficial reuse of wastewater for industrial cooling water, irrigation of parks, etc. It has also been suggested for removing micropollutants in recent years, such as endocrine disruptor and pharmaceuticals, as more focus has been put on the potential hazards of these

micropollutants to the ecosystem and human health (Snyder et al. 2007; Servos et al. 2005). The main goal of using activated carbon in industrial wastewater treatment is to meet stringent regulations for discharge into receiving waters (Faust and Aly 1987).

There are a variety of locations within the conventional wastewater treatment scheme where activated carbon has been used. Activated carbon treatment can be placed after various physicochemical treatment steps such as coagulation/clarification, filtration, and dissolve air floatation, or it can be used as a tertiary or advanced treatment step subsequent to biological treatment for removal of refractory organics. Sometimes it has also been used prior to biological treatment to remove compounds that might be toxic to biological system. It can also be integrated directly into a biological treatment reactor, which can result in the removal or sequestering of refractory and inhibitory compounds (Metcalf & Eddy et al. 2003; Çe ğen and Aktas 2011).

#### *2.2.2.1 The removal of pollutants by physicochemical adsorption*

As a porous carbonaceous adsorbent, activated carbon can remove a broad variety of organic solutes as well as some inorganic solutes from wastewater by physicochemical adsorption. This pollutant removal mechanism has been used widely especially in removing dyes (Namasivayam and Kavitha 2002) and heavy metals (Amuda et al. 2007) from industrial wastewater, as well as removing refractory compounds and micropollutants as a tertiary/polishing treatment for municipal wastewater (Snyder et al. 2007). The adsorption process requires little or no energy inputs and generally requires only seconds or minutes of contact time with the water, which is significantly faster than the net rates of biological processes (Metcalf & Eddy et al. 2003). The group of organics that are generally amenable to adsorption onto activated carbon include pesticides, herbicides, aromatic solvents, polynuclear aromatics,

chlorinated aromatics, phenolic, chlorinated solvents, high-molecular-weight (HMW) aliphatic acids and aromatic acids, HMW amines, and aromatics amines, fuels, esters, ethers, alcohols, surfactants, and soluble organic dyes. Compounds having low molecular weight (LMW) and high polarity, such as LMW amines, nitrosamines, glycols, and certain ethers, are not amenable to adsorption (Çeçen and Aktas 2011).

The adsorption process takes place in four steps: 1) bulk solution transport, 2) film diffusion transport, 3) pore and surface transport, 4) adsorption (or sorption). The adsorption step involves the attachment of the material to be adsorbed to the adsorbent at an available adsorption site. Adsorption can occur on the outer surface of the adsorbent and in the macropores (>50 nm), mesopores (2-50 nm), micropores (micro-pore <2 nm). But the surface area of the macro and mesopores is small compared with the surface area of the micropores, and the amount of material adsorbed there is usually considered negligible. Many factors are known to have important influence on adsorption process including the material carbon is made of, carbon surface functionalities, pH value, oxygen availability, addition of electrolytes, etc.. Optimization of adsorption processes can generally enhance the removal of a specific compound (Bansal and Goyal 2010).

#### *2.2.2.2 The integration of activated carbon with biological treatment*

Adsorption and biological processes can take place in separate unit processes, or they can happen in the same reactor. The latter form of integration often offers synergy such that a higher degree removal is achieved than from adsorption or biodegradation alone, and it will be the focus of this literature review. For many pollutants that are considered slowly biodegradable or even nonbiodegradable, this integration may enhance the effectiveness of biological degradation. A



typical configuration of using activated carbon in wastewater treatment is shown as Figure 2-2 (using PAC as an example). There are mainly two forms, as described below.

- **The powdered activated carbon treatment (PACT) process**

PACT is a modified version of the conventional activated sludge process by the addition of PAC. It is an effective alternative for the removal of biodegradable and nonbiodegradable compounds, such as organic halogens (Orshansky and Narkis 1997; Bornhardt et al. 1997). PAC has also been integrated into membrane bioreactors (MBRs) as it can enhance contaminant removal and also prevent membrane biofouling (Munz et al. 2007). The PACT process is often employed in secondary treatment of high-strength industrial wastewaters and landfill leachates (Foo and Hameed 2009; Walker and Weatherley 1999; Pirbazari et al. 1996).

- **The biological activated carbon (BAC) process**

It is basically a GAC filtration bed where a large amount of aerobic biomass is accumulated or immobilized to exert the adsorption and biodegradable roles simultaneously. This results in a long operating time of the carbon before having to be regenerated and thus a low treatment cost (Xiaojian et al. 1991). BAC filtration is also used to some extent for the elimination of inorganics such as ammonia, perchlorate, and bromate (Walker and Weatherley 1999). Both the PACT and BAC system has also been adopted for anaerobic process (Park et al. 1999; Rajeshwari et al. 2000; Bertin et al. 2004).

The integration of activated carbon process enhances the degradation of slow-degrading compounds. Upon adsorption onto activated carbon, the retention time of an organic substance in a biological system is considerably increased. For example, in the PACT process, dissolved organics adsorbed on activated carbon are retained in the system for about 10-50 days, while in conventional biological systems they will be kept for a period equal to the hydraulic retention

time (HRT), typically 6-36 hour. The retention of organics may even be longer in a BAC reactors since the GAC is kept for a very long period of time in the reactor. The long retention of the pollutants on carbon surface enables the acclimating of attached and suspended microorganisms to these organics, eventually leading to their efficient biodegradation (Çeçen and Aktas 2011; Xiaojian et al. 1991)

The integration of activated carbon and biological system can also enhance the degradation of inhibitory and toxic compounds. Some organic and inorganic compounds may exert inhibitory or toxic effects on biological processes. This situation is usually encountered during industrial wastewater treatment, such as leachate treatment, or in public owned treatment works receiving a significant input of these wastewaters. Many of the inhibitory or toxic organic pollutants are amenable to adsorption onto activated carbon. Their adsorption from bulk water onto activated carbon lead to the protection of biomass, which is retained in the biological reactor in suspended or attached form. Moreover, microbial processes can take place on the surface of activated carbon that convert a specific toxic organic pollutant into an innocuous one. For example, phenol and phenolic compounds are well known for their inhibitory effect on biological processes. Lee et al. reported that the addition of PAC enabled the biodegradation of phenol, *p*-methylphenol, *p*-ethylphenol and *p*-isopropylphenol (Lee and Lim 2005). Another study reported that the addition of PAC to activated sludge enabled continuous operation with inlet concentrations of phenol up to 1000 mg/L (Sundstrom et al. 1979). In anaerobic digestion of coal gasification wastewater, which contains various inhibitory and toxic compounds (such as aromatic compounds and nitrogen containing compounds, including pyridine, methyl-, dimethyl-, and ethyl-substituted pyridines), it was reported that the presence of GAC served to

sequester the inhibitory and non-biodegradable components in the wastewater and permit the breakdown of degradable compounds during anaerobic digestion (Suidan et al. 1983).

Bioregeneration happens when simultaneous adsorption and biodegradation of compounds occurred (de Sa 1992). In this case, the activated carbon serves as a buffer, where the initial adsorption process helps to decrease the pollutants concentration in a shocking load or the level of any toxic compound, and thereby enhances microbial growth and survival. As the remaining aqueous phase compounds are degraded, adsorbed compounds slowly desorb and are re-released into the aqueous phase. Microbes then have an opportunity to degrade the released compounds without experience the inhibitory effects. Bioregeneration of activated carbon has been reported and discussed many several previous studies including anaerobic digestion of coal gasification wastewater and the aerobic biodegradation of phenolic compounds (Lee and Lim 2005) and aromatic compounds (De Jonge et al. 1996; Vinitnantharat et al. 2001), micropollutants (Speitel Jr and DiGiano 1987). Bioregeneration is a very valuable process since it can decrease the need to periodically replace or thermally regenerate the activated carbon. This process is dependent on many factors including biodegradability, absorbability, and desorbability of the adsorbed compounds, as well as the characteristics of activated carbon, and process configurations (Aktaş and Çeçen, 2007).

In summary, adsorbents can provide fast physicochemical capture of slowly-degrading and toxic compounds to accommodate the time needed for biological removal. Adsorbents can improve effluent quality by maintaining consistently lower effluent concentrations of organics, and then slowly release the organics as they are taken up by the microbes. Therefore, the adsorption process is much less sensitive to upset and natural variations in operating conditions, and can temporarily store organic substrates while microbes are adapting to changed conditions.

Adsorbents provide benefits such as buffering against shock loadings, toxic compounds, and fluctuations in biological performance due to temperature, pH, sunlight intensity, etc. This will improve reactor stability and effluent water quality, which is obviously important for wastewater applications.

## **2.3 Characterization of Post-hydrothermal Liquefaction Wastewater**

Biomass liquefaction technology, especially using algae as feedstock has had a relatively short development life. Since the oil product is in general the central interest as a liquid fuel alternative, there are few studies that emphasize on the aqueous phase product. Much of the information about the aqueous phase product, which is actually the most abundant product of HTL, has been only presented as a side issue in most articles and studies. It is not until recent couple of years, several research group started to investigate the properties of the aqueous product, as well as the way of utilizing it and recovering resources from it.

### **2.3.1 General wastewater quality of PHWW**

#### *2.3.1.1 pH and appearance*

PHWW is a high strength wastewater with high organic and nutrient content, as well as various minerals. Table 2-2 summarizes the general water quality parameters of PHWW from algae conversion. Generally, the PHWW had a basic pH around 7.2-9.3 (Jena et al. 2011b; Biller et al. 2012; Zhou et al. 2013). The slight alkalinity in PHWW might be related to high amount of ammonia. Yu et al. reported more acidic pH value (5-6) of PHWW when the reaction temperature was less than 200 °C, although as temperature further increased the pH kept increasing and stabilized at around 8 when the reaction temperature was beyond 260°C. Jena et al. (2011b) also reported that the pH of PHWW increased from 7.2 to 8.5 as reaction temperature

increased from 200°C to 380°C. The relatively low pH at lower operating temperature indicates that at lower temperature large amount of acid is produced; as temperature increases, they were composed/consumed, or more alkaline products are produced, like ammonia. The appearance of PHWW depends on the HTL conditions. For example, Jean et al. (2011a) reported that the PHWW obtained at 200°C and higher temperature were light brown in color, while the PHWW obtained at 200°C and 250°C were dark in color, viscous and having an acute odor.

#### *2.3.1.2 Organic content*

PHWW contains high organic content, indicated by either chemical oxygen demand (COD) or total organic carbon (TOC), as shown in Table 2-2. The COD was found to be in the range of 50-190 g/L, at different operating conditions, which is very high compared to typical wastewaters, even high-strength industrial wastewaters. For example, landfill leachate is well known to be difficult to treat and it normally has a COD of 5-70g/L (Renou et al. 2008). The high values of COD in PHWW suggest the presence of a higher amount of organics that could pose problems for safe discharge. From the perspective of utilizing PHWW as growth medium for algae, high organics levels could potentially be beneficial if the microalgae are capable of using these organics for mixotrophic or heterotrophic growth. However, ideally it would be more beneficial if more organics are directly converted into bio-crude oil from the perspective of carbon and energy efficiency during HTL process for biofuel production.

#### *2.3.1.3 Nutrient content*

High amounts of nitrogen were also found in various PHWW samples. As shown in Table 2-2, the total nitrogen content in PHWW was found to have a wide range, between 3.5-30 g/L. Nitrogen in PHWW is from the thermal decomposition of proteins which are important constituents of algal biomass. Therefore the total nitrogen (TN) content in PHWW is largely

dependent upon the biochemical content of the microalgae. For example, Biller et al. (2012) reported that among the PHWW produced from four different algal biomass under same HTL condition, *Scenedesmus* and *Chlorogloeopsis* had the lowest amounts of TN in PHWW due to the low nitrogen content in the algae, while *Spirulina* on the other hand had the highest value of TN in PHWW corresponding to its high protein and nitrogen content in the feedstock. Ammonia nitrogen was found to be a big portion of TN in PHWW, as high as almost 80% (Jena et al. 2011a). Ammonia was the product of protein break down and remained in the dissolved form in the PHWW. Phosphorus was also in general detected in PHWW, ranging from around 300-1600 mg/L total phosphorous (TP). Elemental analysis of PHWW indicated that O is the dominant element present (~80%) with H, C and N consisting of the balance (Jena et al. 2011b).

#### 2.3.1.4 Micronutrients

Besides C, N, P, H and O as discussed above, there are also a variety minerals in PHWW that originate from biomass feedstocks, including algae. Du et al. (2012) found K, Mg, Mn, Fe, Na, B, Ni and Cr in PHWW from converting *Nannochloropsis oculata*. Jena et al. (2011a) reported the existence of K, Cl, Fl, Al, B, Ca, Cd, Cr, Cu, Fe, Mg, Mn, Mo, Na, Pb, S, Si, Zn in PHWW, and also found that these minerals were present in significant quantities when compared to the standard growth culture medium such as BG11, modified Allen's medium, Bolds' Basal medium, etc.

#### 2.3.2 Organic composition of PHWW

Various organic compounds have been detected in PHWW, including sugars, alcohols, dianhydromannitol, 1-(2-furanyl)-ethanone (acetylfuran), isosorbide, indole, 3-amino-phenol and 2-cyclopenten-1-one, carboxylic acids, alcohols, ketones, various cyclic hydrocarbons, and many nitrogen-containing compounds (such as amides, azines, and pyrroles) (Elliot 1993; Appleford

2005). This literature review focuses on three important major groups of organic compounds: organic acid, cyclic hydrocarbons and nitrogenous organic compounds.

### 2.3.2.1 Organic acid

Organic acids were products of breakdown of larger molecules at elevated temperature, such as protein and carbohydrate. Various organic acids have been detected in PHWW, including formic acid, acetic acid, propionic acid, butyric acid, isobutyric acid, valeric acid, hexanoic acid, palmitic acid, succinic acid, glutaric acid, adipic acid, methylsuccinic acid etc (Elliot 1993).

These organic acids sometimes can be one of the biggest components in PHWW with very high concentrations, depending on HTL operating conditions. Tommaso et al. (2014) found that the short chain organic acid (C<sub>2</sub>-C<sub>4</sub>) was between 25-35% of the total detected compounds (according to relative peak area by gas chromatography-mass spectrometry (GC-MS) analysis) in PHWW, and long chain organic acid was between 3%-5%, when processing mixed algal biomass under 300°C and with retention time longer than 30 min. Jena et al. found that the formates concentration could be as high as 8110 mg/L, and acetates to be 3662 mg/L in PHWW when processing *Spirulina*.

These acids in PHWW are potentially advantageous for algal cultivation since many dissolved carboxylic acids, such as acetic, citric, fumaric, glycolic, lactic, malic, pyruvic, and succinic can support heterotrophic algal growth (Perez-Garcia et al. 2011). Many algae species that have been successfully cultivated in PHWW are known to be able to utilize various acids, including *Chlorella* spp. (such as *Chlorella vulgaris*), *Scenedesmus obliquus*, and *Chlamydomonas reinhardtii*. Among all the acids, acetic acid has been repeatedly reported in various studies of PHWW (Biller et al. 2012; Jena et al. 2011a; Ross et al. 2010; Tommaso et al. 2014). It is of particular interest since it is one of the most common carbon sources for many

microbial species. Biller et al. (2012) reported the existence of acetate (1290-7131 mg/L) in PHWW when converting four different algal biomass. Jena et al. (2011a) found the highest acetate concentration to be 3662 mg/L when processing *Spirulina* at 380°C. Just as a comparison, Tris–acetate–phosphate (TAP) medium, a widely used medium for mixotrophic algal cultivation contains 17.4 mM acetate, which is about 1027 mg/L acetate. Therefore, the acetate in PHWW could potentially be a very good source for algae cultivation.

#### 2.3.2.2 *Cyclic hydrocarbons*

Large amount of aromatic compounds and heterocycles are found in PHWW, including phenol, furfural, 1,2-dihydroxybenzene, methoxypheonol, phenolic aldehyde, 1,4-benzenediol (Elliot 1993; Appleford 2005). Phenol is one of the most reported compound. The presence of phenols in PHWW can be attributed to the depolymerization and repolymerization reactions forming a series of hydrocarbon compounds during the liquefaction process. Its concentration has been reported to be between 50-200 ppm depending on the HTL operating conditions (Biller et al. 2012; Jena et al. 2011a). Phenols and phenolic compounds are toxic compounds and have been shown to have inhibitory effects on algal growth (Lu et al. 2008; Agrawal and Gupta 2009; Tišler and Zagorc-Končan 1997).

#### 2.3.2.3 *Nitrogenous organic compounds*

Nitrogen organic compounds is another major component in PHWW. Many have been detected including pyrrole, pyrrole derivatives, indole, 3-ammino-phonol, amides, azines, pyridine, ethyl-substituted pyridines, quinolone (Elliot 1993; Anastasakis and Ross 2011). Tommaso et al. (2014) found the nitrogen heterocycles to be between 21-55% of the total detected compounds in PHWW (according to relative peak area by GC-MS analysis) when processing mixed algal biomass. Pham et al. (2013) identified the existence of 9 nitrogen



heterocycles in PHWW from *Spirulina* including 3-dimethylamino-phenol, 2,2,6,6-tetramethyl-4-piperidone, 2,6-dimethyl-3-pyridinol, 2-picoline, pyridine, 1-methyl-2-pyrrolidinone,  $\sigma$ -valerolactam, 2-pyrrolidinone,  $\epsilon$ -caprolactam, and found their concentrations to be between 0.052-139 mg/L. The formation of these compounds was likely related to cross-reactions of proteins with carbohydrates (Torri et al. 2012). In general, the higher the protein content, the higher amount the phenols and nitrogen heterocycles present in oil.

### **2.3.3 Regulatory considerations**

Because of the high concentrations of organic and nutrients in PHWW, direct discharge to surface waters is not possible, and treatment is needed to comply with the requirements of EPA effluent guidelines. Effluent guidelines are national standards for wastewater discharges to surface waters or to publicly owned treatment works (POTW, sometimes also called municipal wastewater treatment plants). EPA issues effluent guidelines for categories of existing sources and new sources under Title III of the Clean Water Act. The standards are technology-based, meaning they are based on the typical performance of specific treatment technologies rather than being based on risk or impacts to receiving waters. Although no official regulatory classification has yet been made, PHWW is likely to be categorized as petroleum refining point source category, integrated subcategory, and as a new source. There are two choices for treatment in this category: pretreatment for the discharge to POTWs, or treatment for direct discharge into surface waters. The treatment standards of these two options are summarized in Table 2-3 (U.S. EPA 2012). For the pretreatment option, there are significantly fewer requirements which includes oil, grease and ammonia nitrogen content. However, none of previously reported PHWW water quality data would meet the ammonia standard ( $\leq 1100$  mg/L as N). Thus, pretreatment would be required to reduce ammonia.

For discharge of PHWW directly to a surface water, the regulatory standards includes requirements for biological oxygen demand (BOD), COD, phenolic compounds, pH, and other parameters shown in Table 2-3. Except for pH, none of the requirements for water quality are met in PHWW. Therefore, treatment is necessary before any kind of discharge of PHWW. However, we note that it is generally challenging to effectively treat this kind of high strength wastewater with complicated compositions including some potentially toxic compounds. Thus, a fairly complex treatment scheme is usually needed (Metcalf & Eddy et al. 2003).

#### **2.3.4 Algal cultivation in PHWW**

Recently, a few studies have investigated utilizing PHWW as an organic and nutrient source to cultivate algae/algal-bacterial biomass, for bioenergy production. Results showed that PHWW could be used successfully for algal cultivation, however, significant dilution is needed (Biller et al. 2012; Jena et al. 2011a; Du et al. 2012; Minowa and Sawayama 1999). Both Biller et al. and Jena et al. reported that algae grew slower and reached a lower final concentration on the diluted process water than on standard medium, probably due to high concentration of inhibitors, including fatty acids, phenols and other toxic compounds produced in HTL (Biller et al. 2012; Jena et al. 2011a). Du et al, on the other hand, reported much higher growth of *Chlorella vulgaris* in diluted PHWW (Du et al. 2012). They postulated that under relatively low processing temperature (200 °C) used, polysaccharides and proteins were mainly hydrolyzed to monosugars and amino acids, which are in general less toxic than products obtained under higher reaction temperature, and can be readily used by algae as adequate carbon and nitrogen nutrients. During algal cultivation, both organic and nutrients level were reported to decrease. For example, up to 60% COD, TN, and 95% TP was reported to be removed during the cultivation of chlorella in PHWW (Du et al. 2012).

## **2.4 Effect of Operating Condition on Post-hydrothermal Liquefaction Wastewater**

HTL is a chemical process used to convert wet biomass (algae, wood, manure) into crude-like oil. Hot compressed subcritical water has some characteristics very different from water at standard conditions: a lower permittivity causes a rise in solubility of hydrophobic organic compounds; the hydrogen bonds are fewer and weaker; and the ionic product of water is two orders of magnitude higher ( $10^{-12}$  compared to  $10^{-14}$  at 25°C), promoting a high availability of  $H^+$  and  $OH^-$  for acid- and base-catalyzed reactions such as hydrolysis. These properties change at supercritical conditions, where radical reactions dominate, enhancing gasification reactions (Toor et al. 2011; López Barreiro et al. 2013).

The mechanism of HTL has not yet been clearly elucidated. The influence of various factors, like temperature, catalyst, retention time, feedstock composition, remain unclear. It is generally stated in the literature that in hot compressed liquid water, close to the critical point (374 °C and 22.1 MPa), competition between two reactions takes place: hydrolysis and repolymerization. The first one has more importance at the early stages of the process, when the microalgae are decomposed and depolymerized to small compounds. These compounds may be highly reactive, thus polymerizing and forming biocrude oil, gas and solid compounds. When increasing the reaction time or the temperature, repolymerization, condensation and decomposition of the components from the different phases may occur (Toor et al. 2011; Akhtar and Amin 2011; Zhang 2010).

### **2.4.1 Effect of reaction temperature**

Reaction temperature has been reported as an important factor influencing various HTL products. Yu et al. (2011) reported that the appearance of raw oil products had substantial changes with temperature, which can reflect the underlying reactions at different temperatures

and also help to predict the appearance of the PHWW, which was not reported in the study. It was reported that under relatively low temperatures, the oil formation did not occur, algae biomass remained as green algal cakes. This indicates that the associated PHWW generated at this condition probably only contained products from hydrolysis of algal biomass, and not too many oil components. As temperature increased, carbonization started to happen, converting algae into a black solid or asphalt like product. At this point, we would expect that the soluble portion of the asphalt like products would exist in PHWW, as well as other complex organics like those associated with petrochemicals, especially high molecular weight compounds. As temperature continued to increase beyond a certain level, self-separating oil started to form, and as a result the PHWW was expected to contain more oil like components. In another study, it was also reported that the appearance of PHWW was directly associated with temperature: the PHWW obtained at conversion temperature of 300 °C and higher were light brown in color, whereas the PHWW obtained at 200 °C and 250 °C were dark in color, viscous and had an acute odor (Jena et al. 2011b).

The pH of PHWW was also affected by reaction temperature. Yu et al. (2011) reported that when converting *Chlorella*, the pH of PHWW first decreased when the reaction temperature increased from 100 °C to 180 °C, and then started to increase with reaction temperature. This trend indicates that some acids and free hydrogen ions were produced first in the HTL process and then decomposed. They further explained the acid formation to be the result from amino acids or other short carbon chain organic acids from protein breakdown under relatively low temperatures. These organic acids could be further broken down to produce carbon monoxide and hydrogen ions, therefore enabling other recombination reactions as the temperature

continued to increase. Jena et al. (2011) also observed that PHWW pH changed from neutral (7.2) to slight alkaline (9.4) as temperature increased from 200 °C to 350 °C.

The organic and nutrient content in PHWW comes from the hydrolysis of proteins and hydrocarbons in the algal biomass. Up to 40% of carbon and up to 80% of nutrients in the original materials have been reported to be converted into water soluble matters (Tommaso et al. 2014; Yu et al. 2011). The organic and nutrient content of PHWW is significantly affected by reaction temperature (T), although different studies reported divergent trends. Both Jena et al. (2011) and Valdez et al. (2012) reported that organic content in PHWW decreased with increasing temperature, suggesting further conversion of water soluble compounds into highly volatile constituents and gaseous production. This was also supported by the observation that as temperature (or retention time) increased, the inorganic carbon portion of total carbon kept increasing and reached a maximum at the most severe conditions (Valdez et al. 2012). Other studies have reported different trends. For example, Yu et al. (2011) reported that as temperature increased from 100 °C to 320 °C, the carbon content in PHWW initially increased and then decreased slightly when the temperature was beyond 260 °C. Another study reported the opposite trend, finding that as temperature increased from 260 °C to 320 °C, the organic content of PHWW first decreased and then increased (Tommaso et al. 2014).

Nitrogen content was also reported to be affected by temperature in different ways. Yu et al. (2011) reported that as temperature (or retention time) increased, nitrogen recovery in PHWW kept increasing and stabilized at 70% after 240 °C. Tommaso et al. (2014) and Jena et al. (2011) both reported the opposite observation: the nitrogen content kept decreasing as temperature increased. Some other studies reported that there was no obvious influence of temperature on the nitrogen content in PHWW. For example, one study reported that about two-thirds of the initial

nitrogen in the feedstock was immediately distributed into the aqueous phase even at the mildest liquefaction temperature and any further increase in temperature beyond that did not affect the nitrogen content in PHWW significantly (López Barreiro et al. 2013). Ideally, all of the nitrogen would be distributed to the aqueous phase so that it could possibly be recovered and re-used for algae cultivation. Also, if all of the nitrogen were distributed to the aqueous phase, then there would be none in the biocrude oil, which would also be a desirable outcome.

#### **2.4.2 Effect of retention time**

The effect of retention time (RT) is closely linked to the temperature, many studies reported similar effect of retention time as temperature. Yu et al. (2010) reported that both carbon recovery and nitrogen recovery in aqueous product increased with the retention time (similar with the effect of temperature). Opposite from Yu's study, both Jena et al. (2010) and Valdez et al. (2012) reported that as retention time increased, the organic content in aqueous product decreased (the effect of temperature also showed similar effect in these two studies). They explained it as a result of conversion of soluble products into highly volatile, lighter compounds and gas products. Tommaso et al. (2014) reported that the COD decreased first and then increased as retention time (or reaction temperature) increased. Some studies also reported that the retention time did not show a big influence on the PHWW water quality. For example, Gai et al. (2014) found that while solid ratio and temperature had obvious effect on the water quality parameters of PHWW, the effect of retention time was not obvious. Tommaso et al. (2012) reported there was no obvious change in ammonia nitrogen, total nitrogen content in PHWW as retention time increased.

One study reported the change of individual compound/group of compounds as the retention time increased when processing mixed algal biomass (Tommaso et al. 2014). Organic

acids increased with reaction time first, and then decreased when the reaction lasted for 1.5 h. In contrast, cyclic amines and amides, which may be degraded from proteins, appeared at the very beginning of the HTL reaction and greatly decreased when the reaction lasted for more than 0.5 h. These results indicated that the decomposition of proteins was more complete when reaction time lasted for more than 0.5 h. When reaction time increased from 1 h to 1.5 h, fatty acid derivatives increased, indicating that fatty acids were synthesized.

### **2.4.3 Effect of solids ratio**

Experiments with microalgae solid ratio in the range of 4-50% have been studied. In general, the higher solids ratio it is, the more substance available for reaction, and the more end product there is. The substance in PHWW comes from two sources: the biomass that dissolved into aqueous phase, reacted, and remained; and the part comes from getting contact with oil phase. Both of these two components increase as the solid ratio increases. Gai et al. (2014b) reported that both the organic and nitrogen content in PHWW, as well as the weight of biocrude product increased as the solid ratio of feedstock increased from 15% to 35%. Another study reported that increasing the solid ratio in the feed from 10% to 20% led to an increase of more than 20% in the biocrude oil yield (Jena et al. 2011b).

Some studies showed that at relatively high solid ratio, the reaction/conversion is less efficient although the end product quantity may increase as the solid ratio increases. One study reported that as solid ratio increased from 7.5% to 17.5%, the biocrude oil yield continuously decreased, although the weight of the oil product kept increasing (Zou et al. 2010). Gai et al. (2014b) reported that organic content in PHWW increased dramatically as solid ratio increased from 15% to 25%, and had very slight increase from 25% to 35%. Both of these studies indicate that at higher solid ratio, less increase of absolute quantity of material ended up in oil or aqueous

product. It was postulated that at high solid ratio, the interactions among molecules of biomass and those of water is less influential, which can suppress the dissolution of the biomass components, resulting in lower oil yield as well as lower amount of end product in aqueous phase. The solubility of various end product may also influence the end product quantity in PHWW; many compounds might have already reached or have been very close to the maximum solubility in aqueous phase at a certain solid ratio, and further increase in solid ratio would not significantly increase the soluble content in PHWW.

## **2.5 Light Utilization Efficiencies and Chlorophyll a Fluorescence**

### **2.5.1 Photosynthesis process**

The energy in sunlight is introduced into the biosphere by a process known as photosynthesis, which occurs in plants, algae, and photosynthetic bacteria. The reaction inputs of photosynthesis are carbon dioxide (CO<sub>2</sub>), water (H<sub>2</sub>O), minerals and light, and the output are, directly or indirectly, carbohydrates, lipids and proteins. The process can be simplified as  $6\text{CO}_2 + 6\text{H}_2\text{O} + \text{Light} = (\text{CH}_2\text{O})_6 + 6\text{O}_2$  (Hall and Rao 1999). Living creatures, including humans, consume the products of photosynthesis to derive energy from them by “respiration”, where organic compounds are oxidized back to carbon dioxide and water. All the fuel we are using now to make our world work, coal, natural gas, and petroleum, are the photosynthetic product of the past where the sun’s energy has been stored. Photosynthesis therefore serves as a vital link between the light energy of the sun and all living creatures. Photosynthesis is driven primarily by visible light (wavelengths from 400 to 700 nm) that is absorbed by pigment molecules (mainly chlorophyll a and b and carotenoids). This spectral range of solar radiation that photosynthetic organisms are able to use in the process of photosynthesis is called photosynthetically active radiation (PAR).



The process of photosynthesis is arbitrarily divided into two major phases: a light-dependent phase (the “Light Reactions”) and a light-independent phase (the “Dark Reactions”). In the light reactions, two things happen: First, the electrons are transferred from water to NADP+ (nicotinamide adenine nucleotide phosphate, the oxidized form) by a scheme that is called the "Z Scheme", as shown in Figure 2-3 (Govindjee and Veit 2010). The products of this process are oxygen and NADPH (the reduced form of NADP). Second, the ADP (adenosine diphosphate) is converted to energy rich compound ATP (adenosine tri phosphate). In the dark reactions, these two compounds (NADPH and ATP) are used to convert CO<sub>2</sub> to sugars, and the ADP and NADP are made available to carry on the process. In the light induced reaction, when one molecule of chlorophyll absorbs one photon, an electron of chlorophyll transferred to a higher energy level (excited state). This energy-rich but unstable electron is then transferred to a neighboring electron acceptor with a strong electronegative redox potential. The transfer of the electron from the activated chlorophyll to the first acceptor is the first photochemical phase of photosynthesis. Right after a strongly electronegative substance has been produced, the electron flow precedes with electron acceptors of less negative redox potentials.

In order to better understand some of the measurements presented in later chapters, we provide a brief background on the photosynthesis in the chloroplasts of *Chlamydomonas* cells (including electron transfer pathways and carbon assimilation), as shown in Figure 2-4, which is adapted from Alric (2010). When a chloroplast is illuminated, the antenna of both photosystems, PSI and PSII, absorb light energy that is transferred rapidly to their reaction centers, P680 (PSII) and P700 (PSI), where primary charge separation (photochemistry) is initiated, followed by a chain of redox reactions. PSII ultimately oxidizes water and reduces electron carriers in the cytochrome (Cyt) b6/f, whereas PSI oxidizes Cyt b6/f, and reduces nicotinamide adenine

dinucleotide phosphate (NADP<sup>+</sup>) to NADPH. In addition to the linear electron flow, ferredoxin-mediated cyclic electron flow also occurs around PSI. Further, a proton motive force, *pmf* (i.e., a pH gradient,  $\Delta\text{pH}$ , plus a membrane potential,  $\Delta\psi$ ) is built across the thylakoid membrane during photosynthetic electron transfer, which is then used for ATP synthesis. The resulting NADPH and ATP are used in the Calvin–Benson cycle for CO<sub>2</sub> fixation that leads to the formation of sugars and starch. In mitochondria, acetate (both from the growth medium and that formed from glycolysis) is assimilated via acetyl-CoA into the Krebs (tricarboxylic acid) cycle. Extra NADPH and ATP can also be produced through starch breakdown in the chloroplast stroma; in addition, ATP may be produced through glycolysis in the cytosol (Hoefnagel et al. 1998). Moreover, when respiration is inhibited, malate can accumulate in the mitochondrion, and be transferred to the chloroplast by a reversible malate/oxaloacetate shuttle, which generates extra NADPH. The excess reducing power can be transferred to the plastoquinone (PQ) pool via a monomeric type-II NADH (Mus et al. 2005), and dissipated through the activity of plastid terminal oxidase (PTOX).

In summary, cooperation of two light reactions and two pigment systems leads to the production of reducing power (in the form of NADPH) and ATP, which are both subsequently used in the carbon-fixation pathway leading to the formation of carbohydrates. In Figure 2-4, we also show that there is an interaction between chloroplasts and mitochondria, where acetate from the culture medium for growing *Chlamydomonas* may fit into the highlighted metabolic pathways.

## 2.5.2 Chlorophyll a fluorescence

### 2.5.2.1 *Chlorophyll a fluorescence and fluorescence transient*

When Chlorophyll (Chl) absorbs light it is excited from the ground state to its singlet excited state,  $^1\text{Chl}^*$ . Excited Chl has several ways to relax back to the ground state. It can decay by emitting light, seen as fluorescence. Its excitation can also be used to fuel photosynthetic reactions, which is referred to as photochemical quenching (qP) of Chlorophyll (Chl) a fluorescence. Or it can de-excite by dissipating heat, which is referred to as non-photochemical quenching (NPQ). Both of the latter two pathways reduce the amount of fluorescence. The three processes, fluorescence, qP and NPQ occur in competition, such that any increase in the efficiency of one will result in a decrease in the yield of the other two. Therefore, information about the changes in the efficiency of photochemistry and heat dissipation can be obtained by measuring the yield of chlorophyll fluorescence. Although the total amount of chlorophyll fluorescence is very small (only 1 or 2% of total light absorbed) (Maxwell and Johnson 2000), measurement is quite easy. The spectrum of fluorescence is different to that of absorbed light, with the peak of fluorescence emission being of longer wavelength. Last,  $^1\text{Chl}^*$  can, by intersystem crossing, produce  $^3\text{Chl}^*$ , which in turn is able to produce  $^1\text{O}_2^*$ , a very reactive oxygen species (Muller et al. 2001).

When transferring photosynthetic material from the dark into the light, the intensity of the chlorophyll fluorescence shows characteristic changes. These changes were found by Kautsky and Hirsch in 1931 and have been termed fluorescence transients, or Kautsky effect (Govindjee 1995). When the light is switched on, the fluorescence intensity increases with a time constant in the microsecond or millisecond range. After a few seconds the intensity falls again and finally reaches a steady-state level. The initial rise of the fluorescence intensity is attributed to the

progressive saturation of the reaction centers in the photosynthesis pathway. Therefore the quenching of the fluorescence by the photosynthesis decreases with the time of illumination, with a corresponding increase of the fluorescence intensity. The quenching by the photosynthesis pathway is called “photochemical quenching” (Maxwell and Johnson 2000). The slow decrease of the fluorescence intensity at later times is termed “non-photochemical quenching”. Non-photochemical quenching is most likely due to a protection mechanism the plant has to avoid photodamage. The process that leads to non-photochemical quenching is often referred to as “photoinhibition”. Photoinhibition is a series of reactions that inhibit different activities of PSII (Adir et al. 2003), which may result in irreversible damage and to the extent of total inhibition, both of which would compound losses in productivity (Prince and Kheshgi 2005). In a typical plant, changes in these two processes will be complete within about 15-20 min and an approximate steady-state is attained, although the time taken to reach this state can vary significantly between plant species.

#### 2.5.2.2 *Non-photochemical quenching*

The non-photochemical quenching (NPQ) of the excited state of Chl *a* is a process that down-regulates excitation pressure in the photosynthetic apparatus by increasing de-excitation, as heat, of the singlet excited state of Chl *a* (Demmig-Adams et al. 2006; Demmig-Adams et al. 2014 (in press)), in parallel with a decrease in Chl *a* fluorescence yield.

Several types of NPQ have been identified (Muller et al. 2001), each one characterized by a particular kinetic behavior: pH-dependent (qE) (Nilkens et al. 2010; Jahns and Holzwarth 2012; Ruban et al. 2012), state change-dependent (qT) (Minagawa 2011), and photoinhibition-dependent (qI) (Tyystjärvi 2013). Although we note that qT in most plants is not a true NPQ process because it does not involve changes in the rate constants of the de-excitation processes of singlet excited

Chl *a*, but rather only changes in the antenna size of the two photosystems (Minagawa 2011; Papageorgiou and Govindjee 2011). However, in *Chlamydomonas*, during state 1 to state 2 transition, part of mobile phosphorylated LHCII trimers were shown to form arrays in the membrane, in which non photochemical quenching (of qE type) takes place (Iwai et al. 2010; Papageorgiou and Govindjee 2014 (in press)), as mentioned above.

The qE quenching is the most rapid component of NPQ and is triggered by a pH gradient ( $\Delta$  pH) that builds-up across the thylakoid membrane (see Figure 2-4). Therefore, qE is affected by all processes that influence  $\Delta$  pH, including ATP synthase activity, the linear and PSI-dependent cyclic electron transport flow, and ATP and NADPH consumption by the Calvin–Benson cycle (see Figure 2-4). However, in contrast to higher plants, qE in *Chlamydomonas* is not dependent on the presence of PsbS (Bonente et al. 2008), but on other proteins, such as Light-Harvesting Complex Stress-Related proteins (e.g., LhcSR1 and LhcSR3), which can sense pH changes and, unlike PsbS, can also bind pigments (Chl *a* and *b*, violaxanthin, zeaxanthin, and lutein) (Bonente et al. 2011; Tokutsu and Minagawa 2013; Peers et al. 2009).

## 2.6 References

- Abeliovich, A. and D. Weisman. 1978. Role of heterotrophic nutrition in growth of alga *Scenedesmus-Obliquus* in high-rate oxidation ponds. *Applied and Environmental Microbiology* 35(1): 32-37.
- Adir, N., H. Zer, S. Shochat and I. Ohad. 2003. Photoinhibition - a historical perspective. *Photosynthesis Research* 76(1-3): 343-370.
- Agrawal, S. and S. Gupta. 2009. Survival and Reproduction of Some Blue-Green and Green Algae As Affected by Sewage Water, Fertilizer Factory Effluent, Brassica Oil, Phenol, Toluene and Benzene. *Folia Microbiologica* 54(1): 67-73.
- Akhtar, J. and N. A. S. Amin. 2011. A review on process conditions for optimum bio-oil yield in hydrothermal liquefaction of biomass. *Renewable and Sustainable Energy Reviews* 15(3): 1615-1624.

- Alric, J. 2010. Cyclic electron flow around photosystem I in unicellular green algae. *Photosynthesis Research* 106(1-2): 47-56.
- Amuda, O., A. Giwa and I. Bello. 2007. Removal of heavy metal from industrial wastewater using modified activated coconut shell carbon. *Biochemical Engineering Journal* 36(2): 174-181.
- Anastasakis, K. and A. B. Ross. 2011. Hydrothermal liquefaction of the brown macro-alga *Laminaria Saccharina*: Effect of reaction conditions on product distribution and composition. *Bioresource Technology* 102(7): 4876-4883.
- Appleford, J. M. 2005. Analyses of the products from the continuous hydrothermal conversion process to produce oil from swine manure. PhD Dissertation. Champaign, IL: University of Illinois at Urbana-Champaign.
- Asano, T. 2007. *Water Reuse: Issues, Technologies, and Applications*. New York: McGraw-Hill.
- Bansal, R. C. and M. Goyal. 2010. *Activated Carbon Adsorption*. Boca Raton, FL: CRC press.
- Bertin, L., S. Berselli, F. Fava, M. Petrangeli-Papini and L. Marchetti. 2004. Anaerobic digestion of olive mill wastewaters in biofilm reactors packed with granular activated carbon and “Manville” silica beads. *Water Research* 38(14–15): 3167-3178.
- Biller, P., A. B. Ross, S. C. Skill, A. Lea-Langton, B. Balasundaram, C. Hall, R. Riley and C. A. Llewellyn. 2012. Nutrient recycling of aqueous phase for microalgae cultivation from the hydrothermal liquefaction process. *Algal Research* 1(1): 70-76.
- Bonente, G., M. Ballottari, T. B. Truong, T. Morosinotto, T. K. Ahn, G. R. Fleming, K. K. Niyogi and R. Bassi. 2011. Analysis of LhcSR3, a protein essential for feedback de-excitation in the green alga *Chlamydomonas reinhardtii*. *PLoS Biology* 9(1): e1000577.
- Bonente, G., F. Passarini, S. Cazzaniga, C. Mancone, M. C. Buia, M. Tripodi, R. Bassi and S. Caffarri. 2008. The Occurrence of the psbS Gene Product in *Chlamydomonas reinhardtii* and in Other Photosynthetic Organisms and Its Correlation with Energy Quenching. *Photochemistry and Photobiology* 84(6): 1359-1370.
- Bornhardt, C., J. Drewes and M. Jekel. 1997. Removal of organic halogens (AOX) from municipal wastewater by powdered activated carbon (PAC)/activated sludge (AS) treatment. *Water Science and Technology* 35(10): 147-153.
- Çeçen, F. and Ö. Aktas. 2011. *Activated Carbon for Water and Wastewater Treatment: Integration of Adsorption and Biological Treatment*. Hoboken, NJ: John Wiley & Sons.
- Chisti, Y. 2007. Biodiesel from microalgae. *Biotechnology Advances* 25(3): 294-306.
- De Jonge, R. J., A. M. Breure and J. G. Van Andel. 1996. Bioregeneration of powdered activated carbon (PAC) loaded with aromatic compound. *Water Research* 30(4): 875-882.

- de Sa, C. 1992. Bioregeneration of granular-activated carbon. *Water Science and Technology* 4, 26 (9-11): 2293-2295.
- Demmig-Adams, B., G. Garab, W. Adams III and Govindjee. 2014. *Non-Photochemical Quenching and Energy Dissipation In Plants, Algae and Cyanobacteria*. Dordrecht: Springer.
- Demmig-Adams, B., W. Adams III and A. K. Mattoo. 2006. *Photoprotection, Photoinhibition, Gene Regulation, and Environment*. Dordrecht: Springer.
- Dilek, F. B., H. M. Taplamacioglu and E. Tarlan. 1999. Colour and AOX removal from pulping effluents by algae. *Applied Microbiology and Biotechnology* 52(4): 585-591.
- Du, Z., B. Hu, A. Shi, A. Ma, X. Cheng, Y. Chen, P. Liu, Y. Lin and X. R. Roger. 2012. Cultivation of a microalga *Chlorella vulgaris* using recycled aqueous phase nutrients from hydrothermal carbonization process. *Bioresource Technology* 126: 354-357.
- Elliot, D. C. 1993. Evaluation of wastewater treatment requirements for thermochemical biomass liquefaction. In *Advances in Thermochemical Biomass Conversion*, 1299-1313. Netherlands: Springer.
- Faust, S. D. and O. M. Aly. 1987. *Adsorption Processes for Water Treatment*. Dordrecht: Springer.
- Foo, K. and B. Hameed. 2009. An overview of landfill leachate treatment via activated carbon adsorption process. *Journal of Hazardous Materials* 171(1): 54-60.
- Gai, C., Y. Zhang, W. Chen, Y. Zhou, L. Schideman, P. Zhang, G. Tommaso, C. Kuo and Y. Dong. 2015. Characterization of aqueous phase from the hydrothermal liquefaction of *Chlorella Pyrenoidosa*. *Bioresource Technologies* 184: 328-335
- Gouveia, L. and A. C. Oliveira. 2009. Microalgae as a raw material for biofuels production. *Journal of Industrial Microbiology and Biotechnology* 36(2): 269-274.
- Govindjee. 1995. Sixty-three years since Kautsky: Chlorophyll a fluorescence. *Australian Journal of Plant Physiology* 22(2): 131-160.
- Govindjee and W. Veit. 2010. Personal communication about Z-scheme of electron transport in photosynthesis.
- Hall, D. O. and K. K. Rao. 1999. *Photosynthesis*. 6th ed. Cambridge ; New York: Cambridge University Press.
- Hodaifa, G., M. E. Martinez and S. Sanchez. 2008. Use of industrial wastewater from olive-oil extraction for biomass production of *Scenedesmus obliquus*. *Bioresource Technology* 99(5): 1111-1117.

- Hoefnagel, M. H., O. K. Atkin and J. T. Wiskich. 1998. Interdependence between chloroplasts and mitochondria in the light and the dark. *Biochimica et Biophysica Acta (BBA)-Bioenergetics* 1366(3): 235-255.
- Iwai, M., M. Yokono, N. Inada and J. Minagawa. 2010. Live-cell imaging of photosystem II antenna dissociation during state transitions. *Proceedings of the National Academy of Sciences of the United States of America* 107(5): 2337-2342.
- Jahns, P. and A. R. Holzwarth. 2012. The role of the xanthophyll cycle and of lutein in photoprotection of photosystem II. *Biochimica et Biophysica Acta (BBA)-Bioenergetics* 1817(1): 182-193.
- Jail, A., F. Boukhoubza, A. Nejmeddine, S. Sayadi and L. Hassani. 2010. Co-treatment of olive-mill and urban wastewaters by experimental stabilization ponds. *Journal of Hazardous Materials* 176(1-3): 893-900.
- Jena, U., N. Vaidyanathan, S. Chinnasamy and K. C. Das. 2011a. Evaluation of microalgae cultivation using recovered aqueous co-product from thermochemical liquefaction of algal biomass. *Bioresource Technology* 102(3): 3380-3387.
- Jena, U., K. C. Das and J. R. Kastner. 2011b. Effect of operating conditions of thermochemical liquefaction on biocrude production from *Spirulina platensis*. *Bioresource Technology* 102(10): 6221-6229.
- Kamjunke, N., B. Köhler, N. Wannicke and J. Tittel. 2008. Algae as Competitors for Glucose with Heterotrophic Bacteria. *Journal of Phycology* 44(3): 616-623.
- Kebede-Westhead, E., C. Pizarro, W. W. Mulbry and A. C. Wilkie. 2003. Production and nutrient removal by periphyton grown under different loading rates of anaerobically digested flushed dairy manure. *Journal of Phycology* 39(6): 1275-1282.
- Lavoie, A. and J. Delanoue. 1985. Hyperconcentrated cultures of *Scenedesmus-Obliquus* - a new approach for waste-water biological tertiary-treatment. *Water Research* 19(11): 1437-1442.
- Lee, K. M. and P. E. Lim. 2005. Bioregeneration of powdered activated carbon in the treatment of alkyl-substituted phenolic compounds in simultaneous adsorption and biodegradation processes. *Chemosphere* 58(4): 407-416.
- Li, Q., W. Du and D. Liu. 2008. 3 Perspectives of microbial oils for biodiesel production. *Applied Microbiology and Biotechnology* 80(5): 749-756.
- López Barreiro, D., W. Prins, F. Ronsse and W. Brilman. 2013. Hydrothermal liquefaction (HTL) of microalgae for biofuel production: state of the art review and future prospects. *Biomass and Bioenergy* 53: 113-127.



- Lu, G., C. Wang and X. Guo. 2008. Prediction of toxicity of phenols and anilines to algae by quantitative structure-activity relationship. *Biomedical and Environmental Sciences* 21(3): 193-196.
- Martin, C., J. Delanoue and G. Picard. 1985. Intensive cultivation of fresh-water microalgae on aerated pig manure. *Biomass* 7(4): 245-259.
- Mata, T. M., A. A. Martins and N. S. Caetano. 2010. Microalgae for biodiesel production and other applications: A review. *Renewable & Sustainable Energy Reviews* 14(1): 217-232.
- Maxwell, K. and G. Johnson. 2000. Chlorophyll fluorescence - a practical guide. *Journal of Experimental Botany* 51(345): 659-668.
- Metcalf & Eddy, G. Tchobanoglous, F. L. Burton and H. D. Stensel. 2003. *Wastewater Engineering: Treatment and Reuse*. 4th ed. Boston: McGraw-Hill.
- Minagawa, J. 2011. State transitions—The molecular remodeling of photosynthetic supercomplexes that controls energy flow in the chloroplast. *Biochimica et Biophysica Acta (BBA)-Bioenergetics* 1807(8): 897-905.
- Minowa, T. and S. Sawayama. 1999. A novel microalgal system for energy production with nitrogen cycling. *Fuel* 78(10): 1213-1215.
- Mulbry, W., S. Kondrad and J. Buyer. 2008a. Treatment of dairy and swine manure effluents using freshwater algae: fatty acid content and composition of algal biomass at different manure loading rates. *Journal of Applied Phycology* 20(6): 1079-1085.
- Mulbry, W., S. Kondrad, C. Pizarro and E. Kebede-Westhead. 2008b. Treatment of dairy manure effluent using freshwater algae: Algal productivity and recovery of manure nutrients using pilot-scale algal turf scrubbers. *Bioresource Technology* 99(17): 8137-8142.
- Muller, P., X. Li and K. Niyogi. 2001. Non-photochemical quenching. A response to excess light energy. *Plant Physiology* 125(4): 1558-1566.
- Muñoz, R., M. Jacinto, B. Guieysse and B. Mattiasson. 2005. Combined carbon and nitrogen removal from acetonitrile using algal-bacterial bioreactors. *Applied Microbiology & Biotechnology* 67(5): 699-707.
- Munoz, R., C. Rolvering, B. Guieysse and B. Mattiasson. 2005. Aerobic phenanthrene biodegradation in a two-phase partitioning bioreactor. *Water Science and Technology* 52(8): 265-271.
- Muñoz, R. and B. Guieysse. 2006. Algal-bacterial processes for the treatment of hazardous contaminants: A review. *Water Research* 40(15): 2799-2815.
- Munz, G., R. Gori, G. Mori and C. Lubello. 2007. Powdered activated carbon and membrane bioreactors (MBRPAC) for tannery wastewater treatment: long term effect on biological and filtration process performances. *Desalination* 207(1): 349-360.

- Mus, F., L. Cournac, V. Cardellini, A. Caruana and G. Peltier. 2005. Inhibitor studies on non-photochemical plastoquinone reduction and H<sub>2</sub> photoproduction in *Chlamydomonas reinhardtii*. *Biochimica et Biophysica Acta (BBA)-Bioenergetics* 1708(3): 322-332.
- Namasivayam, C. and D. Kavitha. 2002. Removal of Congo Red from water by adsorption onto activated carbon prepared from coir pith, an agricultural solid waste. *Dyes and Pigments* 54(1): 47-58.
- Neilson, A. H. and R. A. Lewin. 1974. The uptake and utilization of organic carbon by algae: an essay in comparative biogeochemistry. *Phycologia* 13(3): 227-264.
- Nilkens, M., E. Kress, P. Lambrev, Y. Miloslavina, M. Müller, A. R. Holzwarth and P. Jahns. 2010. Identification of a slowly inducible zeaxanthin-dependent component of non-photochemical quenching of chlorophyll fluorescence generated under steady-state conditions in *Arabidopsis*. *Biochimica et Biophysica Acta (BBA) - Bioenergetics* 1797(4): 466-475.
- Orshansky, F. and N. Narkis. 1997. Characteristics of organics removal by PACT simultaneous adsorption and biodegradation. *Water Research* 31(3): 391-398.
- Papageorgiou, G. C. and Govindjee. 2014. Chapter 12: The Non-photochemical Quenching of the Electronically Excited State of Chlorophyll a in Plants: Definitions, Timelines, Viewpoints, Open Questions. In *Non-Photochemical Quenching and Energy Dissipation In Plants, Algae and Cyanobacteria*. Dordrecht: Springer.
- Papageorgiou, G. C. and Govindjee. 2011. Photosystem II fluorescence: Slow changes—Scaling from the past. *Journal of Photochemistry and Photobiology B: Biology* 104(1): 258-270.
- Park, H., K. Choo and C. Lee. 1999. Flux enhancement with powdered activated carbon addition in the membrane anaerobic bioreactor. *Separation Science and Technology* 34(14): 2781-2792.
- Peers, G., T. B. Truong, E. Ostendorf, A. Busch, D. Elrad, A. R. Grossman, M. Hippler and K. K. Niyogi. 2009. An ancient light-harvesting protein is critical for the regulation of algal photosynthesis. *Nature* 462(7272): 518-521.
- Perez-Garcia, O., F. M. E. Escalante, L. E. de-Bashan and Y. Bashan. 2011. Heterotrophic cultures of microalgae: Metabolism and potential products. *Water Research* 45(1): 11-36.
- Pirbazari, M., V. Ravindran, B. N. Badriyha and S. Kim. 1996. Hybrid membrane filtration process for leachate treatment. *Water Research* 30(11): 2691-2706.
- Pizarro, C., E. Kebede-Westhead and W. Mulbry. 2002. Nitrogen and phosphorus removal rates using small algal turfs grown with dairy manure. *Journal of Applied Phycology* 14(6): 469-473.

- Pizarro, C., W. Mulbry, D. Blersch and P. Kangas. 2006. An economic assessment of algal turf scrubber technology for treatment of dairy manure effluent. *Ecological Engineering* 26(4): 321-327.
- Prince, R. and H. Kheshgi. 2005. The photobiological production of hydrogen: Potential efficiency and effectiveness as a renewable fuel. *Critical Reviews in Microbiology* 31(1): 19-31.
- Rajeshwari, K. V., M. Balakrishnan, A. Kansal, K. Lata and V. V. N. Kishore. 2000. State-of-the-art of anaerobic digestion technology for industrial wastewater treatment. *Renewable and Sustainable Energy Reviews* 4(2): 135-156.
- Renou, S., J. G. Givaudan, S. Poulain, F. Dirassouyan and P. Moulin. 2008. Landfill leachate treatment: Review and opportunity. *Journal of Hazardous Materials* 150(3): 468-493.
- Richmond, A. 2004. *Handbook of Microalgal Culture : Biotechnology and Applied Phycology*. Ames, IA: Blackwell Science.
- Rodolfi, L., G. C. Zittelli, N. Bassi, G. Padovani, N. Biondi, G. Bonini and M. R. Tredici. 2009. Microalgae for oil: strain selection, induction of lipid synthesis and outdoor mass cultivation in a low-cost photobioreactor. *Biotechnology and Bioengineering* 102(1): 100-112.
- Ross, A. B., P. Biller, M. L. Kubacki, H. Li, A. Lea-Langton and J. M. Jones. 2010. Hydrothermal processing of microalgae using alkali and organic acids. *Fuel* 89(9): 2234-2243.
- Ruban, A. V., M. P. Johnson and C. D. Duffy. 2012. The photoprotective molecular switch in the photosystem II antenna. *Biochimica et Biophysica Acta (BBA)-Bioenergetics* 1817(1): 167-181.
- Safonova, E., K. V. Kvitko, M. I. Iankevitch, L. F. Surgko, I. A. Afti and W. Reisser. 2004. Biotreatment of industrial wastewater by selected algal-bacterial consortia. *Engineering in Life Sciences* 4(4): 347-353.
- Servos, M., D. Bennie, B. Burnison, A. Jurkovic, R. McInnis, T. Neheli, A. Schnell, P. Seto, S. Smyth and T. Ternes. 2005. Distribution of estrogens, 17 $\beta$ -estradiol and estrone, in Canadian municipal wastewater treatment plants. *Science of the Total Environment* 336(1): 155-170.
- Snyder, S. A., S. Adham, A. M. Redding, F. S. Cannon, J. DeCarolis, J. Oppenheimer, E. C. Wert and Y. Yoon. 2007. Role of membranes and activated carbon in the removal of endocrine disruptors and pharmaceuticals. *Desalination* 202(1): 156-181.
- Sooknah, R. D. and A. C. Wilkie. 2004. Nutrient removal by floating aquatic macrophytes cultured in anaerobically digested flushed dairy manure wastewater. *Ecological Engineering* 22(1): 27-42.

- Speitel Jr, G. E. and F. A. DiGiano. 1987. The bioregeneration of GAC used to treat micropollutants. *Journal of American Water Works Association* 79:64-73.
- Stewart, W. D. P. 1974. Heterotrophy of carbon. In *Algal Physiology and Biochemistry*, 989-1005. Berkeley: University of California Press.
- Suidan, M. T., C. E. Strubler, S. Kao and J. T. Pfeffer. 1983. Treatment of coal gasification wastewater with anaerobic filter technology. *Journal of Water Pollution Control Federation* 55: 1263-1270.
- Sundstrom, D. W., H. E. Klei, T. Tsui and S. Nayar. 1979. Response of biological reactors to the addition of powdered activated carbon. *Water Research* 13(12): 1225-1231.
- Tamer, E., M. A. Amin, E. T. Ossama, M. Bo and G. Benoit. 2006. Biological treatment of industrial wastes in a photobioreactor. *Water Science and Technology* 53(11): 117-125.
- Tarlan, E., F. B. Dilek and U. Yetis. 2002. Effectiveness of algae in the treatment of a wood-based pulp and paper industry wastewater. *Bioresource Technology* 84(1): 1-5.
- Tišler, T. and J. Zagorc-Končan. 1997. Comparative assessment of toxicity of phenol, formaldehyde, and industrial wastewater to aquatic organisms. *Water, Air, and Soil Pollution* 97(3-4): 315-322.
- Tokutsu, R. and J. Minagawa. 2013. Energy-dissipative supercomplex of photosystem II associated with LHCSR3 in *Chlamydomonas reinhardtii*. *Proceedings of the National Academy of Sciences of the United States of America* 110(24): 10016-10021.
- Tommaso, G., W. Chen, P. Li, L. Schideman and Y. Zhang. 2014. Chemical characterization and anaerobic biodegradability of hydrothermal liquefaction aqueous products from mixed-culture wastewater algae. *Bioresource Technology* 178:139-146.
- Toor, S. S., L. Rosendahl and A. Rudolf. 2011. Hydrothermal liquefaction of biomass: a review of subcritical water technologies. *Energy* 36(5): 2328-2342.
- Torri, C., L. Alba, C. Samori and D. Fabbri. 2012. Hydrothermal Treatment (HTT) of Microalgae: Detailed Molecular Characterization of HTT Oil in View of HTT Mechanism Elucidation. *Energy Fuels* 26(1): 658-671.
- Tyystjäarvi, E. 2013. Photoinhibition of Photosystem II. *International Review of Cell and Molecular Biology* 300:243-303.
- U.S. EPA. 2012. Title 40 - Protection of Environment, Chapter 1-Environmental protection agency, Subchapter N-Effluent guidelines and standards, Part 419-Petroleum refining point source category. Available at: <http://www.gpo.gov/fdsys/pkg/CFR-2012-title40-vol30/xml/CFR-2012-title40-vol30-part419.xml#seqnum419.50>. Accessed 1 May 2014.

- Valdez, P. J., M. C. Nelson, H. Y. Wang, X. N. Lin and P. E. Savage. 2012. Hydrothermal liquefaction of *Nannochloropsis* sp.: Systematic study of process variables and analysis of the product fractions. *Biomass and Bioenergy* 46: 317-331.
- Vinitnantharat, S., A. Baral, Y. Ishibashi and S. Ha. 2001. Quantitative bioregeneration of granular activated carbon loaded with phenol and 2, 4-dichlorophenol. *Environmental Technology* 22(3): 339-344.
- Walker, G. and L. Weatherley. 1999. Biological activated carbon treatment of industrial wastewater in stirred tank reactors. *Chemical Engineering Journal* 75(3): 201-206.
- Xiaojian, Z., W. Zhansheng and G. Xiasheng. 1991. Simple combination of biodegradation and carbon adsorption—the mechanism of the biological activated carbon process. *Water Research* 25(2): 165-172.
- Yu, G., Y. Zhang, L. Schideman, T. Funk and Z. Wang. 2011. Distributions of carbon and nitrogen in the products from hydrothermal liquefaction of low-lipid microalgae. *Energy Environmental Science* 4(11): 4587-4595.
- Zhang, L. 2010. Overview of recent advances in thermo-chemical conversion of biomass. *Energy Conversion and Management* 51(5): 969-982.
- Zhou, Y., L. Schideman, G. Yu and Y. Zhang. 2013. A synergistic combination of algal wastewater treatment and hydrothermal biofuel production maximized by nutrient and carbon recycling. *Energy and Environmental Science* 6(12): 3765-3779.
- Zimmo, O. R., R. M. Al-Sa'ed, N. P. van der Steen and H. J. Gijzen. 2002. Process performance assessment of algae-based and duckweed-based wastewater treatment systems. *Water Science and Technology* 45(1): 91-101.
- Zou, S., Y. Wu, M. Yang, C. Li and J. Tong. 2010. Bio-oil production from sub-and supercritical water liquefaction of microalgae *Dunaliella tertiolecta* and related properties. *Energy & Environmental Science* 3(8): 1073-1078.

## 2.7 Figures and Tables

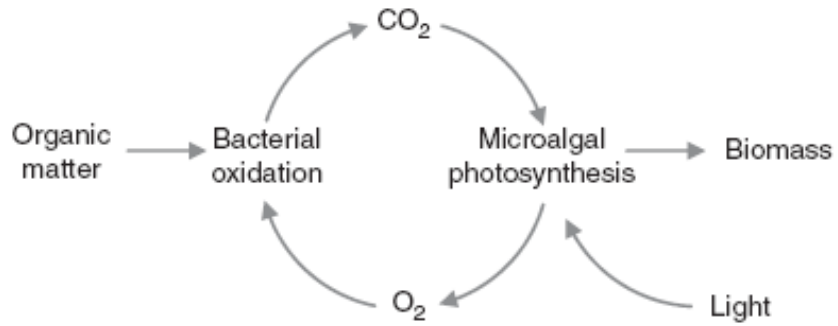
**Table 2-1. Organic removal by algae-bacteria based wastewater treatment system.**

Organic pollutants	Wastewater	Experimental system	Microorganisms	Removal efficiency	Reference
Color and organics	wood-based pulp and paper industry wastewater	1000 ml glass jar, batch experiment	Mixed culture of algae and bacteria	58% COD, 84% color and 80% AOX*	(Tarlan et al. 2002)
Color	pulping effluent	1000 ml glass jar	Mixed culture of algae and bacteria	80% color removal	(Dilek et al. 1999)
BOD	domestic wastewater	3 m*1 m*0.09 m pilot plant scale ponds	Mixed culture of algae and bacteria	85% BOD**	(Zimmo et al. 2002)
COD	Anaerobically digested flushed dairy manure	0.5 m length × 0.36 m width × 0.4 m height plastic container	Floating aquatic macrophytes (macroalage included here) and bacteria	80% COD*** removal	(Sooknah and Wilkie 2004)
Glucose	Oxidation pond water	250 ml flasks	<i>Scenedesmus obliquus</i> and bacteria	0.7 mol/mg(protein) per h	(Abeliovich and Weisman 1978)
Acetonitrile	mineral salt medium with acetonitrile at 1 g/l	600 ml Stirred Tank Reactor (STR)	<i>C. sorokiniana</i> and bacteria	2300 mg l <sup>-1</sup> d <sup>-1</sup>	(Muñoz et al. 2005)
Black oil	Black oil wastewater	100 l tank	<i>Chorella/Scenedesmus/Rhodococcus/Phormidium</i>	Oil spills 96%, Phenols 85% etc	(Safonova et al. 2004)
Phenanthrene	0.2L of silicone oil containing phenanth in 1.8L minimum slat medium	2 L STR with silicone oil at 10%	<i>C. sorokiniana</i> / <i>Pseudomonas migulae</i> and bacteria	8-36 mg l <sup>-1</sup> h <sup>-1</sup>	(Munoz et al. 2005)
Phenol	Coking factory wastewater	600 ml STR with NaHCO <sub>3</sub> at 8 g/L	<i>C. vulgaris</i> / <i>Alcaligenes</i> sp. and bacteria	90%	(Tamer et al. 2006)

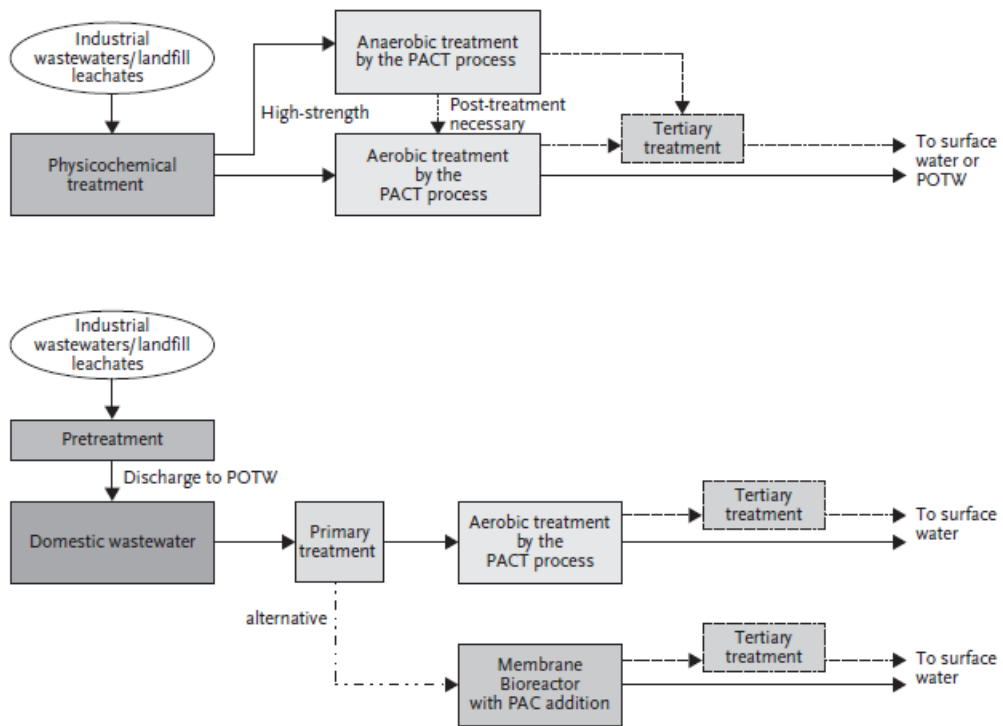
\*AOX: absorbable organic halides

\*\*BOD: biological oxygen demand

\*\*\*COD: chemical oxygen demand



**Figure 2-1. Principle of photosynthetic aeration in organic removal process (Muñoz and Guieysse).**



**Figure 2-2. Use of activated carbon in secondary treatment of wastewaters (Çeçen and Aktas 2011).**

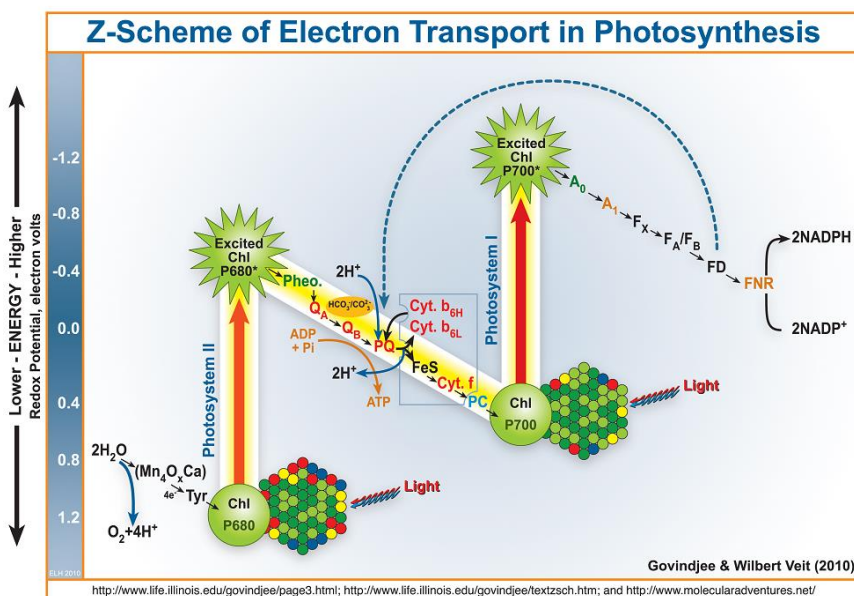
**Table 2-2. Summary of water quality of PHWW.**

Feedstock	HTL condition	pH	C	N	Inorganic N	P	References
<i>Spirulina platensis</i>	200-380°C, 0-120 min, 10-50% solid ratio	7.2-9.3	64,000-190,000mg/L COD 3.7-9.0 wt.%	1.22-3.95 wt.%			(Jena et al. 2011b)
<i>Spirulina platensis</i>	350°C, 60min, 20% solid ratio		3.92 wt.%	16,200 TN 1.84 wt.%	12,700 NH <sub>4</sub> <sup>+</sup> -N , 27 mg/L NO <sub>3</sub> <sup>-</sup> -N	795 mg/L P as PO <sub>4</sub> <sup>-</sup>	(Jena et al. 2011a)
<i>Chlorella</i>	260-300C, 30-90 min, 15-35% solid ratio		62,7000-104,000 mg/L COD	11,000-31,700 mg/L TN,		5,440 mg/L TP	(Gai et al. 2014)
<i>Chlorella</i> <i>Chlorogloeopsis</i> <i>Spirulina</i> <i>Chlorella</i> <i>Scenedesmus</i>	300-350°C	8.4-9.2	9,060-15,123 mg/L TOC	3,139-5,636 mg/L TN	4,785-6,295 mg/L NH <sub>4</sub> <sup>+</sup> -N, 192-508 NO <sub>3</sub> <sup>-</sup>	280-3,109 mg/L PO <sub>4</sub> <sup>-</sup>	(Biller et al. 2012)
<i>Nannocloropsis oculata</i>	200C, 40min, 20% solid ratio		134,800 mg/L COD, 45,700 mg/L TOC	9,650mg/L TN	1,343 mg/L NH <sub>4</sub> <sup>+</sup> -N 211 nitrate,	343 mg/L TP	(Du et al. 2012)
Wastewater algae			30,000 -70,000 mg/L COD	3,500-8,000 mg/L TN	1,800-4,500 mg/L NH <sub>4</sub> <sup>+</sup> -N		(Tommaso et al. 2014)
Pond algae	300°C, 30min, 20% solid ratio	7.89	85,253 mg/L COD 23,208 mg/L TOC	10,288 mg/L		1,558mg/L	(Zhou et al. 2013)
Mixed algal-bacterial biomass	300°C, 30min, 20% solid ratio	7.89	120,897 mg/L COD 39,432 mg/L TOC	20,342 mg/L	11,407mg/L NH <sub>4</sub> <sup>+</sup> -N		(Zhou et al. 2013)



**Table 2-3. Treatment standards for new sources from integrated subcategory of petroleum refining point source (U.S. EPA 2012).**

Pollutant or pollutant property	Standard of performance for new sources (for direct discharge) (mg/L)	Pretreatment Standard] (for discharge into a publicly owned treatment works) (mg/L)
BOD <sub>5</sub>	41.6	
TSS	28.1	
COD	295.0	
Oil and grease	12.6	100
Phenolic compounds	0.30	
Ammonia as N	23.4	1100
Sulfide	0.26	
Total chromium	0.64	
Hexavalent chromium	0.052	
pH	6-9	



**Figure 2-3. The electron transport pathway from water (H<sub>2</sub>O) to NADP+ (the Nicotinamide Adenine Dinucleotide Phosphate, oxidized form).**

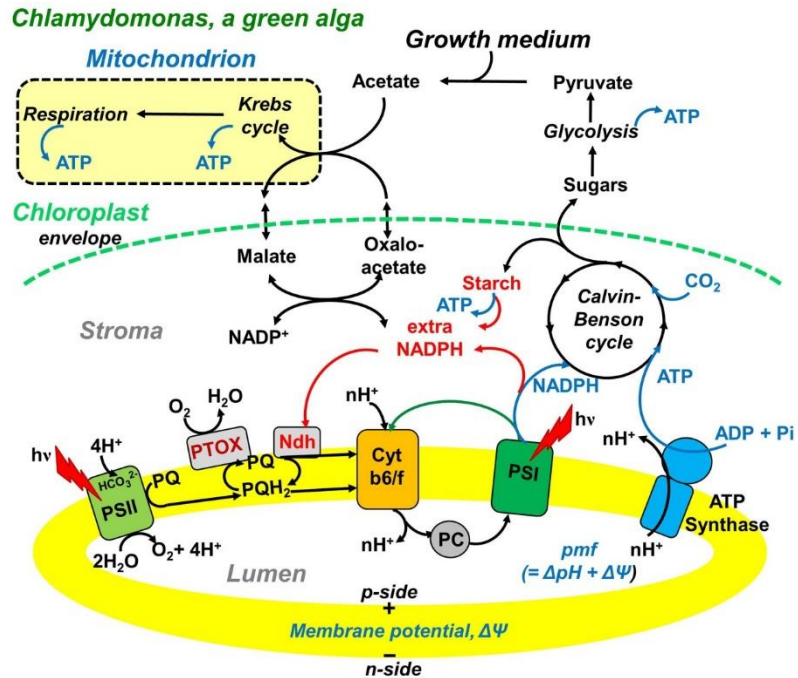


Figure 2-4. Electron transfer pathways and carbon assimilation in the chloroplast of a mixotrophically (acetate) grown *Chlamydomonas reinhardtii*, and their interaction with mitochondrion. Modified from (Alric 2010).

## CHAPTER 3

# AN INNOVATIVE BIOENERGY PRODUCTION SYSTEM WHICH COMBINES ALGAL WASTEWATER TREATMENT AND HYDROTHERMAL LIQUEFACTION

### 3.1 Introduction

A novel integrated waste-to-energy system that we refer to as Environment Enhancing Energy (E<sup>2</sup>-Energy) was proposed that integrates algal biomass production during wastewater treatment and hydrothermal liquefaction of that biomass into bio-crude oil. The objectives of this study are to experimentally confirm the feasibility of the “Key Steps” of E<sup>2</sup>-Energy as noted below, and then analyze overall mass balances and system impacts using a mathematical model that can simulate various application scenarios.

In the proposed E<sup>2</sup>-Energy system, as shown in Figure 3-1, wastewaters from a variety of sources (e.g., municipal, livestock, food processing) can be initially separated into a concentrated biosolids fraction and a dilute liquid fraction by common physicochemical processes (e.g., sedimentation, filtration). Mixed cultures of low-lipid, fast-growing algae and bacteria are then cultivated in a combination of the dilute liquid wastewater fraction and recycled PHWW (Key Step 1). As the algae and bacteria grow symbiotically, the wastewater is treated by providing removal of organics and nutrients (Key Step 2). Note that the energy input for aerobic breakdown of wastewater contaminants is reduced by the oxygen provided during algal photosynthesis. Subsequently, the mixed culture biomass is harvested, and combined with the concentrated biosolids separated from the initial wastewater. This mixture is then fed into a HTL reactor for biofuel production (Key Step 3). The HTL process also generates a CO<sub>2</sub>-rich gaseous product and strong wastewater with re-released organics/nutrients (Key Step 4), which is

recycled back to the algal-bacterial cultivation system for reuse. This recycling can repeat again and again over multiple cycles of algal growth, harvesting and biofuel conversion that leverages the nutrient content of wastewater to maximum bioenergy quantities, which can be many times the original wastewater energy content.

This process could potentially resolve the current major limitations to the economic feasibility of algal biofuels including the contamination of target high-oil algal cultures, high nutrient cost inputs, as well as the significant energy inputs for dewatering/extraction. This novel system maximizes biofuel potential from waste inputs by facilitating **multi-cycle nutrient reuse**, which amplifies waste nutrients through multiple cycles of algal biomass growth and nutrient recycling. Although DOE has identified the importance of using and recycling wastewater nutrients for algal biofuels, and several recent studies have investigated this concept using hydrothermal conversion, none of these studies showed how nutrient recycling could be incorporated into large-scale algal biofuel production. This study addresses these issues in pursuit of an optimized system integrating algal wastewater treatment and bioenergy production including original experimental data and process modeling that quantifies the mass balances for carbon, nitrogen, and total biomass. This analysis underscores the specific benefits of nutrient recycling and the national implications for sustainable biofuel production. Specifically, we will show that using waste organic biosolids from only three major sources (municipal wastewater, food waste, and livestock manure), it is possible to support the production of enough bio-crude oil to completely replace the current U.S. demand for petroleum imports. Thus, E<sup>2</sup>-Energy represents a major paradigm shift whereby wastewater treatment systems can become optimized producers of bioenergy feedstocks and improved water quality, while simultaneously providing a viable path to sustainable, carbon-neutral energy independence.

## 3.2 Materials and Methods

### 3.2.1 Experiments

#### 3.2.1.1 Step 1: Algae cultivation in different concentrations of PHWW

##### *Growth medium*

Cultivation medium was made from a combination of filtered municipal wastewater (WW) and PHWW from liquefaction of *Spirulina* (PHWW-*Spirulina*). The municipal WW was collected from the primary clarifier at a local WW treatment plant (Urbana-Champaign Sanitary District, UCSD) and filtered through 1.5 µm pore size glass fiber filter (Whatman 934-AH) before usage. PHWW-*Spirulina* was recovered from a pilot-scale continuous HTL test using the blue-green alga *Spirulina* as the feedstock (Zhou et al. 2011). The characteristics of PHWW-*Spirulina* and the filtered municipal WW are provided in Table 3-1, which summarizes all the sources PHWWs used in this study.

##### *Algal inoculum*

The inoculum of algae used in this study was a mixed algae culture that has been intermittently exposed to PHWW. The original seed was collected from the clarifier outlets at a local WW treatment plant (UCSD). Microscopic inspection of the original seed showed that it was mainly composed of single cell green algae including *Chlorella* spp., *Scenedesmus obliquus* and cyanobacteria (blue green algae). Several other algal species were also bio-augmented into the culture including *Chlorella protothecoides*, *Chlorella vulgaris*, *Botryococcus braunii*, *Nanochloropsis oculata*, *Spirulina platensis*, *Scenedemus dimorphus*, and *Chlamydomonas reinhardtii*. Heterotrophic bacteria also existed and no algae purification or isolation procedure was conducted to exclude bacteria from this culture. In order to obtain a PHWW-adapted culture, the mixed algal-bacterial culture was exposed to slowly increasing amounts of PHWW. After

several rounds of adaptation, microscopic observation showed that *Chlorella* spp. were the dominant species and this “PHWW-adapted culture” was maintained in municipal wastewater enriched with 0.5%-1% PHWW-Spirulina. The adaptation procedure and culture maintenance were both performed in 250 ml Pyrex flasks on a shaker table rotating at 150 rpm, 25 °C and a light intensity of 50  $\mu\text{mol photon m}^{-2} \text{s}^{-1}$ .

### ***Inhibition test***

PHWW-adapted algal culture (2 ml) samples were inoculated into 150 ml filtered municipal wastewater spiked with 0.5%, 1%, 2%, 5% and 10% PHWW-Spirulina in a 250 ml Pyrex flask. Flasks were placed on a shaker table rotating at a speed of 150 rpm with a light intensity of 50  $\mu\text{mol photon m}^{-2} \text{s}^{-1}$ . Chlorophyll concentration was measured each day and dry cell weight was measured at the end of the experiment (Day 10). Triplicate cultures for each condition were cultivated and the average values with standard deviations are reported.

### ***Biomass quantification***

Biomass was quantified by both dry cell weight and chlorophyll *a* content. Chlorophyll *a* concentration is an indication of autotrophic biomass (algae and cyanobacteria) while dry cell weight is the summation of the autotrophic and heterotrophic biomass. Dry cell weight was measured as total suspended solids (TSS) according to standard methods (Clesceri et al. 1999). Chlorophyll *a* concentration was extracted by methanol and measured according to the approach of Porra et al.(1989).

#### ***3.2.1.2 Step 2: Pollutant degradation when algae was cultivated in 1% PHWW-PBR***

### ***Pollutant degradation batch tests***

The removal of pollutants by PHWW-adapted algal-bacterial culture was determined using a mixture of 99% filtered municipal WW and 1% PHWW-PBR (see Table 3-1 for water

quality characteristics). The PHWW-PBR was produced in a batch HTL process using mixed algal-bacterial biomass from a PBR that was fed by 1% PHWW-Spirulina (Zhou et al. 2011). 10 ml of PHWW-adapted culture was seeded into a 2 L wide-base Pyrex flask containing 500 ml of medium that consisted of filtered municipal WW and 1% PHWW-PBR. The flasks were placed on a shaker table rotating at a speed of 150 rpm under light intensity of  $200 \mu\text{mol photon m}^{-2} \text{s}^{-1}$ . The headspace was filled with air enriched with 10% carbon dioxide and the headspace gas was refreshed every day during the experiment. Controls were cultivated under dark conditions to prevent photosynthetic growth and pollutant removal. Both the lighted batch reactors and dark controls were conducted in triplicate with average values and standard deviations reported.

#### ***Water quality analysis***

Water samples were first filtered using  $0.45 \mu\text{m}$  pore size syringe filters (Whatman paradisc-25 mm) to remove cells and particles. Then, soluble chemical oxygen demand (SCOD) was determined by visible light absorbance after dichromate digestion according to standard methods (Clesceri et al. 1999) with a HACH Model DR/2010 spectrophotometer. Total soluble nitrogen was measured using the HACH TNT Persulfate Digestion Method No. 10072. Ammonia nitrogen was determined according to HACH Nessler Method No. 8038. Total soluble phosphorous was measured using HACH PhoVer 3 Method No. 8190 with acid-persulfate digestion. TOC was measured as non-purgeable organic carbon according to standard methods (Clesceri et al. 1999).

#### ***3.2.1.3 Step 3: HTL test using algal biomass harvested from three different cultivation systems***

##### ***Mass algae cultivation as HTL feedstock***

In order to simulate different types of algal cultivation systems, several pilot-scale algal bioreactors were used to produce biomass for subsequent HTL testing. The three cultivation

systems used were carboy batch jars, an outdoor “open pond” batch, and a continuous-flow membrane PBR. Each system used PHWW-adapted algae culture as an inoculum. The carboys (three 18L jars) and continuous membrane PBR cultivation systems were fed by filtered municipal WW spiked with 1% PHWW-Spirulina, the outdoor open pond was grown using F/2 medium spiked with 0.01% PHWW-Manure (Zhou et al. 2011).

### ***Algal biomass composition analysis***

The crude protein of algal biomass was measured according to the methods of the Association of Official Analytical Chemists (AOAC 4.2.03). Lipid content was measured according to the Folch method (Folch et al. 1957). The carbon, hydrogen and nitrogen content of the algae were measured using a CE-440 CHN analyzer (Exeter Analytical, Inc., North Chelmsford, MA). Phosphorus content was measured by inductively coupled plasma mass spectroscopy (ICP-MS) (Sciex Elan DRC-e, Perkin Elmer, Norwalk, CT). Table 3-2 summarizes the characteristics of the algal biomass used.

### ***Hydrothermal liquefaction test***

Algal biomass harvested from open pond cultivation, carboys and PBR were adjusted to a moisture content of 80% and then subjected to HTL conditions (300 °C, 10-12 MPa) with a reaction time of 30 min to test the feasibility of converting them into bio- crude oil. The HTL experiments were performed according to previously reported methods (Yu et al. 2011) using a 100 ml completely mixed stainless steel reactor with a 70 ml operating volume. The product mixture was separated using a vacuum filter (Whatman No. 4 Filter Paper) into a water insoluble product and PHWW. Moisture content of the water insoluble product was determined by distillation according to ASTM Standard D95-99 (ASTM 2004a). Raw oil was defined as the water insoluble product after moisture removal and includes both oil and residual solids. The



residual solids fraction in the raw oil product was measured as the toluene insoluble portion after a Soxhlet extraction according to ASTM Standards D473-02 (ASTM 2004b) and D4072-98 (ASTM 2004c). The toluene soluble fraction is referred to as bio-crude oil. The mass of the gas product was calculated from the ideal gas law using the residual pressure after cooling down the reactor and assuming 100% CO<sub>2</sub> as the HTL gaseous product. PHWW yield was calculated by difference assuming the summation of all product yields is 100%.

The energy consumption ratio (ECR) has been used by several past researchers to compare the energy input for the HTL process with the energy output in the oil created by the process ( $E_{in}/E_{out}$ ). In order to better assess the overall energy balance of entire E<sup>2</sup>-Energy process, we added energy input terms for algal cultivation ( $E_{cul}$ ), algal harvesting ( $E_{har}$ ), and hydrotreatment upgrading of HTL oil ( $E_{upg}$ ) to make it a refinery-ready petroleum replacement. Since heating the reaction mixture is the predominant energy input for HTL, we neglected other minor HTL process energy inputs. Thus, the ECR was calculated according to the following equation, which was adapted from methods reported elsewhere (Biller and Ross 2011; Vardon et al. 2012),

$$ECR = \frac{E_{in}}{E_{out}} = \frac{E_{cul} + E_{har} + E_{HTL} + E_{upg}}{E_{out}}$$

$$= \frac{E'_{(cul+har)}(1 - W_i) + [W_i C_{pw} T + (1 - W_i) C_{ps} T](1 - R_h) + E_{upg}}{Y_{OIL}(HHV)(1 - W_i)R_c} \quad (3-1)$$

where  $W_i$  is the initial feedstock water content prior to conversion (20% in our case);  $T$  is the temperature increase required to reach conversion conditions (275 °C in our case);  $C_{pw}$  and  $C_{ps}$  are the specific heats of water and biomass, respectively (4.18 kJ/kg/ΔT and 1.25 kJ/kg/ΔT);  $R_h$  and  $R_c$  represent the efficiencies of heat recovery and combustion energy, respectively, which were both assumed to have moderate values of 0.7 (U.S. DOE 2008)  $Y_{OIL}$  is the bio-crude oil

yield fraction, and HHV (kJ/kg) is the higher heating value of the bio-crude oil that's calculated according to the Dulong formula (Brown et al. 2010; Zhou et al. 2010),

$$HHV(MJ \cdot kg^{-1}) = 0.3383 \cdot C + 1.422(H - \frac{O}{8}) \quad (3-2)$$

where C, H and O are the mass percentage of carbon, hydrogen and oxygen, respectively.

$E'_{(cul+har)}$  is the energy input for cultivating algae in open pond system and harvesting by flocculation followed by rotary press to produce an algal paste with a solids content of 20%. The value of  $E'_{(cul+har)}$  was estimated to be 1.5 MJ/kg based on the algal biofuels life-cycle analysis by Lardon et al.(2009).

ECR can be calculated with or without the upgrading energy term. Upgrading is most likely needed to obtain drop-in transportation fuels in current petroleum refineries, but may not be needed for heating oil, asphalt, or future refineries built for specifically for HTL oil feedstocks. The energy input for hydrotreatment upgrading includes energy input for steam heating and electricity, which has been estimated as 0.42 MJ/kg (Huo et al. 2008). Several recent studies have reported that the hydrogen for upgrading can be supplied by reforming the off-gas from the upgrading process without additional net energy input (National Research Council 2012; Sims 2011; Marker et al. 2010). Thus, no additional energy input was included in our ECR calculations for the hydrogen used to upgrade HTL oil. Our ECR calculations assumed that the product yield of upgrading is 85% and the HHV of upgraded oil is 40 MJ/kg (Marker 2005).

#### 3.2.1.4 Step 4: Elemental distribution analysis of HTL products

The elemental distribution of HTL products was measured to calculate how much of the organics and nutrients were re-released into different HTL products. The carbon, hydrogen and nitrogen content of HTL raw oil and solid residue were analyzed using a CHN analyzer (CE-440,

Exeter Analytical, Inc., North Chelmsford, Mass.); oxygen content was calculated by difference. Therefore, the calculated oxygen content is slightly larger than the true value because it accounts for the mass of the other minor elements. The elemental composition of the bio-crude oil product was calculated by difference between raw oil and solid residue. HTL gas samples were analyzed using a Varian CP-3800 Gas Chromatography as described previously (Yu et al. 2011).

### **3.2.2 Model development**

#### *3.2.2.1 Model Objectives*

In order to better understand the long-term steady-state impacts of nutrient and carbon recycling in the E<sup>2</sup>-Energy system, a mathematical mass balance model was developed to simulate a continuously operating system in terms of energy and material flows, as well as environmental impacts (wastewater treatment performance and greenhouse gas capture).

#### *3.2.2.2 Modeling Approach*

A mathematical model of the E<sup>2</sup>-Energy process was developed using STELLA<sup>®</sup> (Strongly Typed Lisp-Like Language) modelling platform (<http://www.iseesystems.com>). STELLA<sup>®</sup> facilitates the building of a model for dynamic systems by creating a pictorial diagram of the system and then assigning values and mathematical functions to various components of the system. The key features of STELLA<sup>®</sup> consist of the following four tools (Figure 3-2): (1) Stocks, which are the state variables for accumulation. They collect anything that flows into and out of them; (2) Flows, which are the exchange variables, control the arrival or exchanges of information between state variables; (3) Converters, are the auxiliary variables. These variables can be represented by constant values or by values dependent on other variables, curves, or functions of various categories; and (4) Connectors, which are used to connect modeling features, variables, and elements. STELLA has been widely used in biological,

ecological, and environmental sciences. An elaborate description of the STELLA package can be found in Isee Systems.

The approach taken in this analysis is to use the STELLA<sup>®</sup> software to model a multi-component mass balance for two scenarios of the E<sup>2</sup>-Energy system for a specific amount of influent municipal wastewater (10<sup>6</sup> L/day or 10<sup>3</sup> m<sup>3</sup>/day). One scenario uses “baseline” parameters that were obtained from the experimental results of this study, whereas the second scenario uses some “improved” parameters that were identified through sensitivity analysis (described later) and adjusted based on data reported elsewhere in the literature. The later scenario was used to investigate the potential to improve the overall system performance via optimization of individual system components. The final outputs of the model include mass flows, energy production, pollutant treatment efficiency and GHG emissions, which are then compared between the two scenarios and with the performance of conventional municipal wastewater systems and typical algal cultivation systems.

In this model, we simulate mass flow, carbon flow, and nitrogen flow, as they are all very important for understanding the process impacts. Mass flow of biosolids determines the energy production capacity of the E<sup>2</sup>-Energy system as biosolids is the feedstock of HTL that ultimately produces usable bioenergy. Carbon includes both organic carbon and inorganic CO<sub>2</sub> in this model. Organic carbon is perhaps the most important target pollutant in wastewater, and it is also the major form of energy in wastewater. Dissolved organic carbon in wastewater is converted to CO<sub>2</sub> and particulate organic carbon during heterotrophic biomass production. CO<sub>2</sub> is the only carbon source for autotrophic microbial growth, and it is also one of the most important GHGs. Both heterotrophic and autotrophic biomass is used as an HTL feedstock and thus the carbon flow determines the mass flow of the E<sup>2</sup>-Energy system. The key feature of E<sup>2</sup>-Energy is

multiple cycles of nutrient reuse to maximize biomass production. Nitrogen is also one of the most essential nutrients to support biological activity and various forms of nitrogen are also considered to be pollutants in wastewater. Therefore, nitrogen flow determines the biomass amplification ratios and would provide comparison criteria with other biofuel production systems. Other nutrients such as phosphorus are also going to be recycled in the E<sup>2</sup>-Energy system, and future modelling work is expected to study additional nutrients.

### 3.2.2.3 Model description

The E<sup>2</sup>-Energy model consists of three sub-models for mass, carbon and nitrogen, which are interrelated. Mass flow tracks the biosolids, which can be harvested for biofuel production. Carbon is tracked as both organic carbon and inorganic carbon (CO<sub>2</sub>). Organic carbon serves as both a target pollutant and a substrate for heterotrophic growth. Inorganic carbon is the sole carbon source for autotrophic growth and an important GHG. Nitrogen flow is also simulated to quantify the multi-cycle nutrient reuse feature of E<sup>2</sup>-Energy, which amplifies biomass production.

Each sub-model contains three major compartments, waste pretreatment (PT), algal-bacterial cultivation (AC) and hydrothermal liquefaction (HTL) as shown in Figure 3-1. The following bulletized list provides a general description of the model assumptions, formulations, and the transformation processes occurring within each compartment.

#### (1) For the PT compartment

- The incoming total nitrogen or carbon includes substrate nitrogen ( $S_{N_{INF}}^{PT}$ ) or carbon ( $S_{C_{INF}}^{PT}$ ) and nitrogen or carbon in suspended solids ( $SS_{INF}^{PT} \times f_N^{SS}$  or  $SS_{INF}^{PT} \times f_C^{SS}$ )
- Nitrogen or carbon removal in this stage is only achieved by suspended solid removal as primary sludge; no dissolved component was removed

## (2) For the AC compartment

- The incoming total nitrogen or carbon includes two parts: nitrogen or carbon in the PT effluent ( $TN_{EFF}^{PT}$  or  $TC_{EFF}^{PT}$ ) and the dissolved nitrogen or carbon in the recycled post-hydrothermal liquefaction wastewater (PHWW) ( $TN_{PHWW}$  or  $TC_{PHWW}$ )
- The suspended solids in PT effluent is hydrolyzed into soluble substrate to support biomass production; the particulate nitrogen or carbon contained in these suspended solids is released into the water as dissolved nitrogen or carbon
- Nitrogen removal is achieved by being taken up by microbes which include autotrophic microbes ( $X_{AUTO}^{AC}$ ) and heterotrophic microbes ( $X_{HETO}^{AC}$ ) (Mixotrophic biomass growth was very limited in our system and was neglected for simplicity)
- Nitrogen or carbon removal efficiency ( $RR_N^{AC}$  or  $RR_C^{AC}$ ) is decided by the nitrogen or carbon biodegradability of the two incoming streams ( $\alpha_N^{RW}, \alpha_N^{PHWW}$  or  $\alpha_C^{RW}, \alpha_C^{PHWW}$ )
- Heterotrophic biomass was defined as microbes that can only utilize organic carbon substrate as a carbon and energy source. Available organic carbon ( $TC_{INF}^{AC} \times RR_C^{AC}$ ) is the only limiting factor for heterotrophic biomass production\*. Heterotrophic microbes have priority in using available nitrogen since they generally grow faster than autotrophs ( $TN_{AUTO}^{AC} = TN_{BS}^{AC} - TN_{HETO}^{AC}$ ).
- Autotrophic biomass was defined as phototrophic microbes that utilize CO<sub>2</sub> as the only carbon source, and light as the only energy source in our model. Nitrogen availability is considered as the only limiting factor for autotrophic growth ( $X_{AUTO}^{AC} = Y_{AUTO}^{OBS} \times TN_{AUTO}^{AC}$ )\*.
- Autotrophic microbes utilize inorganic carbon from three resources: respiration from heterotrophic microbes (assuming 100% is captured by autotrophic microbes), recycled HTL gaseous product (mainly CO<sub>2</sub>), and CO<sub>2</sub> from ambient air or point source.

- Biomass containing removed nitrogen or carbon ( $TN_{BS}^{AC}$  or  $TC_{BS}^{AC}$ ) was harvested with an efficiency of  $RR_{SS}^{AC}$  and sent to HTL as feedstock

\*Only one limiting growth factor related to carbon or nitrogen is assumed for each kind of microorganism in this model, as the current model focuses more on the nutrient and carbon recycling potential rather than detailed biological activity.

### (3) For the HTL compartment

- The total incoming nitrogen, carbon, or solids includes the nitrogen, carbon, or solids in the primary sludge from PT ( $TN_{PS}^{PT}$ ,  $TC_{PS}^{PT}$  or  $TSS_{PS}^{PT}$ ) and that from biosolids harvested in AC ( $TN_{Harv}^{AC}$ ,  $TC_{Harv}^{AC}$  or  $TSS_{Harv}^{AC}$ )
- Nitrogen or carbon are released into different products during HTL and PHWW containing soluble nitrogen or carbon ( $TN_{PHWW}$  or  $TC_{PHWW}$ ) was recycled back to AC. The partitioning ratio ( $y_N^{OIL, PHWW, GAS \text{ or } RES}$  and  $y_C^{OIL, PHWW, GAS \text{ or } RES}$ ) only depends on temperature and pressure, but not feedstock composition.

Table 3-3 provides definitions of the model parameters and the values used in the two modeling scenarios (baseline and improved). The specific processes and equations governing transformations are shown in Table 3-4.

The nitrogen leveraging ratio ( $R_N$ ), carbon leveraging ratio ( $R_C$ ), and solids leveraging efficiency ( $R_S$ ) were defined and used to evaluate the performance and energy production capacity of the E<sup>2</sup>-Energy system. They were defined as the ratio of total nitrogen/carbon/suspended solids in the feedstocks flowing into the HTL compartment at steady state divided by the total nitrogen/carbon/suspended solids in the incoming waste flowing into the pretreatment compartment.

$$R_N = \frac{TN_{FEED}^{HTL}}{TN_{INF}^{PT}}, \quad R_C = \frac{TC_{FEED}^{HTL}}{TC_{INF}^{PT}}, \quad R_S = \frac{TSS_{FEED}^{HTL}}{TSS_{INF}^{PT}} \quad (3-3)$$

Note that the calculation of  $R_S$  focuses on suspended solids because that is the form of organic material that can be most readily harvested for bio-energy production, which makes  $R_S$  the best measure of bioenergy amplification.

Sensitivity analysis was conducted to understand how parameter variations affect system performance in terms of the nitrogen, carbon and solids leveraging ratios ( $R_N$ ,  $R_C$ ,  $R_S$ ) and to identify the parameters that are most critical for improving bioenergy production. Tested parameters included suspended solids removal in PT ( $RR_{SS}^{PT}$ ), biodegradability of nitrogen and carbon in PHWW ( $\alpha_N^{PHWW}$  and  $\alpha_C^{PHWW}$ ), product yield of PHWW ( $Y_{PHWW}$ ), nitrogen and carbon partitioning ratio into PHWW ( $y_N^{PHWW}$  and  $y_C^{PHWW}$ ), which were selected because of their potential for improvement, based on performance data reported by others. Note that the later three parameters would not change independently, because the summation of yields for all four HTL products must be equal to one in order to maintain conservation of mass. Thus, in the sensitivity analysis, when we increased or decreased the value of  $Y_{PHWW}$ ,  $y_N^{PHWW}$ ,  $y_C^{PHWW}$  by a certain percentage (e.g., 10%), we held the ratio of the other three HTL product yields constant, and the sum of all four product yields equal to one.

### 3.3 Results and Discussion

#### 3.3.1 Step 1: Biomass production in PHWW

Figure 3-3 shows the experimental results from batch cultivations of mixed algal-bacterial biomass in various dilutions of post-HTL wastewater (PHWW) mixed with the filtered municipal wastewater. We observed two different primary modes of biomass growth depending



on PHWW dosage: heterotroph dominant mode (cultures spiked with 2%, 5% and 10% PHWW) and autotroph dominant mode (cultures spiked with 0%, 0.5% and 1% PHWW). In the heterotroph dominant mode, the dry cell weight of cultures increased with PHWW dosage from 2% to 5% to 10% (see Figure 3-3). Actually, a linear relationship between the total organic content and biomass production was observed, where biomass production (mg/L dry wt.) =  $0.047 \times \text{COD (mg/L)}$ ,  $R^2=0.98$ . This makes sense because most of the organics in the medium (>98%) came from PHWW, and heterotrophic growth generally depends on the available organic substrate. The biomass in heterotroph dominant mode was predominantly heterotrophic microbes as shown by very low Chlorophyll *a* concentrations (see Figure 3-3B).

In contrast, cultures spiked with 0%, 0.5% and 1% PHWW were dominated by autotrophic microbes like algae and cyanobacteria. As shown in Figure 3-3, the final dry cell weight for these three cultures reached 318 mg/L, 541 mg/L and 146 mg/L, respectively. If we assume the same linear relationship between organic substrate and heterotrophic biomass production as noted above, then heterotrophic biomass would only account for 3 mg/L, 31 mg/L and 62 mg/L in cultures spiked with 0%, 0.5% and 1% PHWW, respectively. Thus, the autotrophic biomass production in these three cultures would account for 99%, 94% and 51% of total biomass production. Also, the higher Chlorophyll *a* concentration at low PHWW dosages (see Figure 3-3B) confirms more active autotrophic growth at low PHWW dosages.

The reason for the stark differences between the two biomass production modes can be explained by the idea that autotrophic and heterotrophic microbes in this system have a different response to PHWW. For autotrophic microbes like algae, there is a threshold concentration of PHWW, below which algal growth is enhanced; but above this threshold, algal growth is inhibited. As shown in Figure 3-3B, the final Chlorophyll *a* content of the cultures with 0.5%

PHWW is 47% higher than the culture without any PHWW spike. This increase in autotrophic production is likely due to additional nutrients provided by PHWW. Nitrogen and phosphorus concentrations in PHWW are more than 150 times greater than the filtered municipal wastewater (see Table 3-1). However, when PHWW concentration is above a certain threshold, the algal production is partially inhibited (i.e., culture with 1% PHWW in Figure 3-3B) or completely inhibited (cultures with 2%, 5% and 10%). In cultures spiked with 2%, 5% and 10% PHWW, algal cells were observed microscopically and found to be lysed open, which could be explained by toxic effects associated with high PHWW dosages.

Many compounds identified in PHWW could be inhibitory or toxic to algae, including ammonia and various organic compounds. For instance, 2% PHWW would contain 64 mg/L  $\text{NH}_4^+\text{-N}$  (Table 3-1), which is a level reported as toxic for several algae species (Abeliovich and Azov 1976; Kallqvist and Svenson 2003; Konig et al. 1987). Organic compounds such as phenol, toluene, propenal, allyl alcohol and benzene have been identified in PHWW and are known to be toxic to algal growth (Elliot 1993; Appleford 2005; Lu et al. 2008; Agrawal and Gupta 2009). However, concentrations of these organics in PHWW were not previously reported, and more research is needed to elucidate potential toxic effects on algae. In contrast to the autotrophs, heterotrophic microbes showed much less sensitivity to PHWW. If there are inhibitory effects of PHWW on heterotrophic microbes, they are outweighed by the positive effects of increasing organic substrate levels. As a result, no sudden decrease of heterotrophic biomass production was observed as PHWW dosage increased.

Although both of the biomass production modes can effectively produce biomass, the autotrophic dominant mode is more favorable for E<sup>2</sup>-Energy system. This is because only the autotrophic microbial growth can amplify the energy harvest from wastewater by growing new

photosynthetic biomass, which brings extra solar energy (and CO<sub>2</sub>) into the wastewater biosolids. In contrast, the heterotrophic microbial growth is only able to recover a portion of the existing energy in a wastewater. Therefore, it is preferable to keep the PHWW concentration low enough that it doesn't inhibit autotrophic microbial growth.

There is potential to increase the threshold PHWW concentration for autotrophic microbes via adaptation and species selection. These adaptive phenomena have already been observed as our PHWW-adapted mixed algal species, which, after long-term adaptation, can now grow well in medium spiked with 1% PHWW-Spirulina, but initially could not survive when the medium was spiked with 0.5% PHWW-Spirulina. Additionally, augmentation of cultures with algal species that have better tolerance of PHWW toxicity could also improve biomass production. For example, a wide range of ammonia toxicity has been reported for different algal species ranging from 0.35 mg/L to 250 mg/L (Keller et al. 1987; Tam and Wong 1996). Therefore, we expect that algal species with better tolerance of PHWW likely exist.

### **3.3.2 Step 2: Pollutant degradation in PHWW**

A second batch culture experiment was conducted in filtered municipal wastewater spiked with 1% PHWW-PBR to monitor the pollutant removal during biomass production. As shown in Figure 3-4B, phototrophic algae dominated the lighted cultures with Chlorophyll a increasing from 1 mg/L to 25 mg/L versus a negligible increase in the controls grown without light. Total biomass production also increased significantly, from 22 mg/L to 2500 mg/L. Assuming the heterotrophic bacteria had similar growth in lighted and dark cultures, the autotrophic algal biomass was about 14 times greater than the heterotrophic biomass production. This confirms the idea that encouraging autotrophic growth can increase overall biomass (and bioenergy) production.

The consortium of algae and bacteria growing in our wastewater medium effectively removed both organics and nutrients. The lighted cultures with algal growth showed enhanced nutrient removal, but the removal of organics was essentially equal in lighted and dark cultures. As shown in Figures 3-4C, D and E, the lighted cultures had good removal of total soluble nitrogen (TSN), ammonium nitrogen ( $\text{NH}_4^+\text{-N}$ ), and total soluble phosphorous (TSP)--86%, 100% and 95%, respectively. The dark controls had much lower nutrient removal efficiencies--18% for TSN and 38% for TSP, whereas  $\text{NH}_4^+\text{-N}$  actually increased 31%. The increase in ammonia likely resulted from the breakdown of organic nitrogen into ammonia.

Organics removal was similar in lighted cultures (63%) and dark controls (69%) (see Figure 3-4F). There was slightly over 30% residual SCOD even after a relatively long cultivation time (185 hours), which indicates the presence of recalcitrant or slowly-degrading organics. The residual TSN is likely to be nitrogen heteroatoms contained in these organic compounds. This topic will be studied and discussed in detail in Chapter 4.

Bacterial activity is important for both pollutant degradation and biomass production with the E<sup>2</sup>-Energy approach, even though they are typically considered a contamination problem in most other algal production systems. Bacteria can degrade organic pollutants that algae cannot utilize because only some algal species can conduct mixotrophic or heterotrophic metabolism, and the range of organics algae can digest is much narrower than for heterotrophic bacteria (Neilson and Lewin 1974). In addition, the consumption rate of organics by algae is generally slower than bacteria (Kamjunke et al. 2008; Lau et al. 1995). Microscopic observation of cultures grown in the dark showed that algal cell density was stagnant, indicating that active heterotrophic algae were scarce. In addition, since algal growth under lighted conditions did not enhance organic removal (Figure 3-4F), mixotrophic algae also were apparently rare. Thus,

almost all of the organics removal in both lighted and dark cultures can be attributed to heterotrophic bacteria.

A second benefit of the bacteria is their ability to transform nutrients to a form that algae are capable of utilizing. As shown in Table 3-1, approximately half of the nitrogen contained in PHWW-PBR was  $\text{NH}_4^+\text{-N}$ , and the other half was organic nitrogen, which autotrophic algae are unable to utilize directly. However, only 14% of TSN remained in the lighted culture and virtually zero  $\text{NH}_4^+\text{-N}$  (see Figures 3-4C, D). This could be explained by transformation of organic nitrogen into usable forms (e.g.,  $\text{NH}_4^+\text{-N}$ ) during bacterial degradation of nitrogenous organics. As shown in Figure 3-4D, the  $\text{NH}_4^+\text{-N}$  concentration in dark controls had a relatively fast increase in the first 68 hours, the same period when bacterial growth and SCOD removal occurred. Since bacterial growth also uses nitrogen and some could be converted into nitrite and nitrate, the total nitrogen release from degraded organics by bacteria was greater than the net increase of  $\text{NH}_4^+\text{-N}$  shown in Figures 3-4D. After bacterial growth became limited by the available organic substrates, unused ammonium was left in the dark cultures. In contrast, autotrophic algae in the lighted cultures continued to consume any released  $\text{NH}_4^+\text{-N}$  until it was gone at around 160 hours. Thus, autotrophic algal biomass production and total nutrient removal was enhanced by bacterial activity. This highlights the importance of algal-bacterial consortiums for E<sup>2</sup>-Energy systems and suggests that the balance of bacteria and algae could be further optimized to maximize pollutant removal and biomass production.

### **3.3.3 Step 3: HTL conversion of algal-bacterial biomass grown in wastewater**

Algal-bacterial biomass harvested from three wastewater bioreactor systems as described earlier were successfully converted into a self-separating bio-crude oil product via HTL at 300 °C and 30 minutes of reaction time. As shown in Figure 3-5, the biomass from the carboy had the

highest bio-crude oil yield (52.2%), followed by biomass from PBR (51.3%), and biomass from open pond had the lowest yield (37.9%). The initial lipid content of these feedstocks varied from 15-20%, highlighting that high-lipid algae are not necessary for biofuel production with HTL. Others have reported successful conversion of low-lipid algae species such as *Chlorella pyrenoidosa* (< 0.1% crude fat) (Yu 2012) and *Spirulina* (5% crude fat) (Vardon et al. 2011) with bio-crude oil yields ranging from 30%-50%. These studies suggested that protein was the primary source material for bio-crude oil production because it accounted for most of the feedstock mass. Considering the exceptionally high growth rates of some low-lipid algae, HTL of these algae into bio-crude oil is quite promising for large-scale algal biofuels. HTL can also convert bacteria and other types of biosolids into bio-crude oil. Several other studies have found that various wastewater sludges (primary, secondary and anaerobically digested) can all be converted into bio-crude oil by HTL with yields ranging from 25%–45% (Suzuki et al. 1988; Yokoyama et al. 1987; Dote et al. 1993; Itoh et al. 1994). Thus, in contrast to other algal biofuel production systems, E<sup>2</sup>-Energy can elegantly handle any bacterial contamination by also converting bacterial biomass into usable biofuels.

In our tests, there was a conspicuous difference in the appearance of the raw oil product from HTL of the open pond biomass, which was a highly-viscous, bitumen-like product that settled to the bottom of the aqueous phase. HTL oil from the carboy and PBR biomass had lower viscosity, density and was flowable at room temperature like crude petroleum. This difference may have resulted from the relatively high ash content (16.7%) of the open pond biomass, which can become mixed with the oil product. This kind of raw oil product could be fed to a biomass boiler, pyrolysis or gasification unit that can handle relatively high ash content feedstocks, or used as asphaltic binder.

Despite the differences in raw oil products described above, the elemental composition of the bio-crude oil product (i.e., the toluene soluble portion of raw oil) showed very similar properties for all three cultivation types (see Table 3-5). It is quite noteworthy that the HTL energy recovery into bio-crude oil was very high in all three cases-ranging from 82-88% of the energy content in the original feedstock. This is much higher than other conventional bioenergy processes such as anaerobic digestion of wastewater biosolids, which typically recovers only 25-60% of incoming energy content (Carrère et al. 2010). It is also better than algal biofuel schemes based on extracting lipids, which typically achieve 20-50% oil content in the algae (Chisti 2007).

The high heating values (HHVs) shown in Table 3-5 range from 32-38 MJ · kg<sup>-1</sup>, which is comparable to previously reported HHVs from HTL of microalgae (Biller and Ross 2011; Brown et al. 2010; Yu et al. 2011; Vardon et al. 2011). However, these values are lower than algal biodiesel (41 MJ · kg<sup>-1</sup>) (Amin 2009) and petroleum crude oil (45 MJ · kg<sup>-1</sup>) (Boundy et al. 2011), which is a result of higher nitrogen content (5-7%) and oxygen content (8-15%) in HTL bio-crude oil. Petroleum typically has less than 2% oxygen (Inoue et al. 1997) and less than 1% nitrogen (Speight 2010), while biodiesel from vegetable oil usually contains essentially no nitrogen and around 11% oxygen (U.S. DOE 2006). These HTL bio-oil products are heavy crudes that could be used for direct boiler firing and some types of turbines. If drop-in transportation fuels are desired, then HTL biocrude oil will likely require upgrading to remove nitrogen and oxygen through hydrotreating, which requires some additional energy input. This application of hydroprocessing is envisioned as being similar to hydrotreating of petroleum with similar system requirements, and some sources even suggest it is probably easier than to develop refining techniques for heavy crudes (Elliott 2007; Grange et al. 1996).

The Energy Consumption Ratio ( $ECR = E_{in}/E_{out}$ ) was used in this study to quantify the net energy balance of the entire E<sup>2</sup>-Energy process. An ECR below one indicates a positive energy balance because the energy output exceeds energy input. The ECR is between 0.22-0.30 without upgrading and 0.26-0.35 with upgrading as shown in Table 3-5 assuming a moderate heat recovery efficiency (0.7) (U.S. DOE 2008). This ECR is better than many other biofuel production processes. For instance, the corresponding ECR ( $E_{in}/E_{out}$ ) for corn ethanol is about 0.57 based on literature reported data (Wang et al. 2011). Algal biodiesel production via lipid extraction followed by either transesterification or hydrotreatment has been found to have an ECR value in the range of 0.75-4.0 depending on different cultivation and extraction methods (National Research Council 2012), (Lardon et al. 2009). The majority of energy savings for the HTL conversion route used in E<sup>2</sup>-Energy in comparison to the algal biodiesel route is in drying and extraction. The analysis here provides a preliminary estimation of the energy balance in the E<sup>2</sup>-Energy process that highlights the potential advantages of this novel approach. However, a more detailed LCA study is recommended in future studies as scalable and process-specific operating data becomes available.

Although economic analysis is very important, the process development for HTL and algal biofuels is still very immature and economic data are very limited. Data collection and validation of technical and economic system performance for an industry that has yet to be commercially realized is one of the biggest challenges for techno-economic analysis. A wide range of cost for microalgal biofuel has been reported, from \$0.17/L (Lundquist et al. 2010) to \$10.6/L (Rosenberg et al. 2011) depending on the production scenario and assumptions used. A very recent publication by Delure et al. estimated that the cost for HTL biocrude oil using algae as feedstock is about \$3.8/L (including feedstock production, conversion and upgrading through



hydrotreating) (Delrue et al. 2013). This cost could potentially be significantly reduced if a credit for the value of wastewater treatment is included. For instance, Lundquist (Lundquist et al. 2010) reported that the overall cost for algal biofuel production was reduced 93% (from \$2.6 to \$0.17/L) when including a wastewater treatment credit. Based on these two studies, we estimate that when wastewater treatment is synergistically integrated with HTL biofuel production, the cost has the potential to drop below \$0.40/L. This preliminary economic evaluation highlights the strong potential of the E<sup>2</sup>-Energy process, but also highlights the need for more comprehensive techno-economic analysis as additional relevant and scalable process performance data becomes available.

#### **3.3.4 Step 4: Nutrient re-release from the HTL process**

Figure 3-6 shows the elemental distribution of carbon and nitrogen in the four different products of HTL. Bio-crude oil and PHWW are the two biggest pools for carbon and nitrogen among the HTL products. Most of the nitrogen was released into the PHWW product (51% for open pond biomass and 64% for both carboy and PBR biomass). This confirms that there is a significant opportunity for nutrient recycling with HTL, because PHWW would be recycled back to algal cultivation in the E<sup>2</sup>-Energy process. Bio-crude oil was the second largest recipient of nitrogen, which was 28%, 32% and 35% for open pond biomass, carboy biomass and PBR biomass, respectively. Increasing the percentage of nitrogen released into PHWW increases the potential for biomass/biofuel amplification, and this percentage could be optimized via HTL reaction conditions, catalysts and/or feedstock pretreatment. For instance, past studies have reported that the ratio of nitrogen distributed into PHWW was a function of reaction temperature and could achieve 70%-90% when treating municipal sewage sludge, algae, and high protein feedstocks (Yu et al. 2011; Inoue et al. 1997; Dote et al. 1996). Catalysts like sodium carbonate

have also been shown to reduce the distribution of nitrogen to HTL oils (Biller and Ross 2011; Dote et al. 1996). Pretreatment could also potentially decrease the nitrogen partitioning into oil product by cleaving amine groups from proteins and removing them prior to HTL (Biller and Ross 2011; Inoue et al. 1997).

The biggest pool for carbon was the bio-crude oil product of HTL, which accounted for 54%, 67% and 71% of feedstock carbon for open pond, carboy and PBR cases, respectively. Gas was the smallest pool for carbon in all three cases, and it consisted of over 98% CO<sub>2</sub> with very small amounts of CO and CH<sub>4</sub>. This gas would also be recycled back into algae cultivation unit in the E<sup>2</sup>-Energy scheme. In this study, PHWW contained 15%-24% of the carbon (as shown in Figure 3-6), which is lower than previously reported values that ranged from 35%-55% (Biller and Ross 2011; Yu et al. 2011).

### **3.3.5 Model simulation of E<sup>2</sup>-Energy**

The experimental results provided above have confirmed the feasibility of the four main process steps in the proposed E<sup>2</sup>-Energy system, and the ability to reuse nutrients for multiple cycles of algae growth. Specifically, the experiments for Step 2 and Step 3 as described above completed two rounds of HTL conversion of algal biomass to crude oil followed by cultivation of algae in the HTL wastewater (note the PHWW used for pollutants degradation experiment in Step 2 was from HTL of algal biomass grown on PHWW-Spi described in Step 3). However, these stepwise results don't fully represent the effects of long-term internal recycling on the steady-state mass balances, bioenergy production, and other important process characteristics. Thus, we developed a mathematical process model of the integrated E<sup>2</sup>-Energy system using STELLA<sup>®</sup> modelling software created to investigate steady-state performance, provide sensitivity analysis, evaluate process improvements, and provide strategic guidance for life-cycle

analysis and other sustainability measures. The list of model parameters and values is presented in Table 3-3. Most of the parameter values came from the average values measured in the experiments of this study, but some were taken from the literature or assumed values as noted by the reference numbers.

A sensitivity analysis was conducted to understand how parameter variations affect system performance in terms of the nitrogen, carbon and solids leveraging ratios ( $R_N$ ,  $R_C$ ,  $R_S$ ) and to identify the parameters that are most critical for improving bioenergy production. This analysis revealed that the nitrogen biodegradable fraction for PHWW ( $\alpha_N^{PHWW}$ ) was the most sensitive parameter. Specifically, a 10% increase in  $\alpha_N^{PHWW}$  caused increases of 11.8% in  $R_N$ , 10.6% in  $R_C$  and 10.3% in  $R_S$ . The other high-impact factor for the system was the partitioning ratio of nitrogen into PHWW,  $y_N^{PHWW}$ , which caused 11.3%, 10.6%, and 10.1% increases in  $R_N$ ,  $R_C$  and  $R_S$  respectively when  $y_N^{PHWW}$  was increased 10%. Although the biodegradable fraction of carbon in PHWW,  $\alpha_C^{PHWW}$ , was not as sensitive as the two other parameters discussed above, it would likely be changed at the same time as  $\alpha_N^{PHWW}$  and has significant room for improvement.

As discussed earlier, optimized HTL process conditions, catalysts, and feedstock pretreatment could all potentially improve  $y_N^{PHWW}$ . Other previous studies have reported optimized values of  $y_N^{PHWW}$  ranging from 70%-90%, indicating significant potential for improving  $y_N^{PHWW}$  from our baseline value (0.6). Therefore, we choose a value of 0.8 for  $y_N^{PHWW}$  in our “improved” modelling scenario. Both  $\alpha_N^{PHWW}$  and  $\alpha_C^{PHWW}$  can potentially be improved by assembling specialized algal/bacterial consortia that can better breakdown recalcitrant compounds so that a higher percentage of carbon and nitrogen in PHWW can be converted into usable substrate for algae and bacterial growth. Also, pretreatment by ozonation is a widely used

method expected to make recalcitrant PHWW compounds more biodegradable. It has been reported that ozone treatment could convert more than 95% of the non-biodegradable organic carbon and more than 75% of non-biodegradable organic nitrogen into biodegradable compounds (Aparicio et al. 2007; Ikehata and El Din 2004). Thus, in modeling the “improved” condition, we assumed that 70% of non-biodegradable carbon and nitrogen could be converted into biodegradable material, resulting in “improved” values for  $\alpha_N^{PHWW}$  and  $\alpha_C^{PHWW}$  of 0.96 and 0.91, versus baseline values of 0.86 and 0.69, respectively.

The model results confirm that the E<sup>2</sup>-Energy system can indeed leverage nitrogen content in the incoming waste to support multiple cycles of algae and bacteria growth. The model mass balance results for the baseline and improved scenarios are shown in Figures 3-7A and B. The nitrogen leveraging ratio ( $R_N$ ) is 1.9 in the baseline scenario and 3.8 in the improved scenario under steady state conditions.  $R_N$  reflects the nutrient recycling efficiency of the system. It would be less than one in a typical algal cultivation system without nutrient recycling because only part of the soluble nitrogen would be used for biomass production. The U.S. Department of Energy (DOE) has identified multi-cycle nutrient reuse as a goal for algal biofuels because U.S. wastewater nutrient flows are insufficient to fully support the national need for renewable fuels with algae on the basis of single-use nutrients (U.S. DOE 2010). However, DOE did not identify the means of achieving multi-cycle nutrient reuse, and thus, the E<sup>2</sup>-Energy system fulfills a recognized need in providing a viable pathway to achieve this goal. Multi-cycle nutrient reuse is a powerful concept that amplifies carbon capture and bio-energy production. As shown in Figure 3-7, the carbon leveraging ratio ( $R_C$ ) would range from 4.0-8.0 for an E<sup>2</sup>-Energy system with baseline and improved scenario parameters, respectively. This occurs because photosynthesis would bring an extra 314 kg (baseline scenario) to 686 kg (improved scenario) of carbon into this

system in the form of CO<sub>2</sub> to produce algal biomass. In contrast,  $R_C$  would be less than one in a typical conventional wastewater bioenergy system without photosynthetic biomass production because only part of the incoming carbon will end up in the final biofuel product. The combined result of multi-cycle nutrient reuse and carbon fixation (by photosynthesis) is increased biomass production, which is reflected in the value of  $R_S$  showing that the total biosolids harvest would be 5.2-10.1 times of the original incoming wastewater biosolids for the baseline and improved scenarios, respectively. The amplification of wastewater derived biosolids as represented by  $R_S$  provides the most important measure of the E<sup>2</sup>-Energy system, because it shows how much more bioenergy can be produced via the concept of multi-cycle nutrient reuse.

The model results also showed that the toxic and inhibitory compounds in PHWW would not likely be a problem in real applications when treating municipal wastewater. The percentage of PHWW flowing into the algae cultivation process at steady-state will only be 0.48 % and 0.90% in the baseline scenario and improved scenario, respectively. This level of PHWW was shown to support robust growth of mixed algal-bacterial biomass in our batch tests. We have also successfully operated a continuous PBR fed by 1% PHWW-Spirulina for more than six months (see Chapter 4) and this operating condition did not exert any obvious negative effect on algae growth. Therefore, the need for dilution does not impose an additional water demand and can be cost-effectively accommodated at full-scale.

We estimate there is potential to replace most if not all of U.S. petroleum imports with HTL bio-crude oil produced from just wastewater inputs by using E<sup>2</sup>-Energy. To demonstrate this potential, we begin by noting that the domestic wastewater, animal manure, and landfilled food wastes in the United States contain more than 153 million dry tons collectable solids as shown in Table 3-6, which could potentially be used to produce bioenergy. By applying the E<sup>2</sup>-

Energy system to these various waste streams, the amount of biosolids produced in the baseline and improved scenarios would be between 0.80 to 1.55 billion dry tons. Subsequently, these biosolids can be converted using HTL into 0.38 to 0.73 billion tons of bio-crude oil per year. By way of comparison, the total U.S. oil demand was about 1.1 billion tons in 2011 of which about 0.5 billion tons was imported (U.S. EIA 2012).

E<sup>2</sup>-Energy also presents an advantageous paradigm shift for the wastewater treatment industry to become a significant net energy producer and achieve a net negative carbon footprint. In the past, wastewater technology has focused on cost-effective removal of aqueous pollutants rather than on energy efficiency. As a result, the wastewater industry commonly uses energy-intensive processes that account for approximately 3% of total U.S. electrical demand.(U.S. EPA 2006) 50-60% of this energy is used for mechanical aeration in activated sludge processes (WERF 2011). However, in algal based wastewater treatment systems, photosynthetic aeration by algae can greatly reduce the mechanical aeration demand. One company that provides algal wastewater treatment systems, Algae Wheel, has reported a 50% energy reduction for aeration of their algal wastewater treatment plants (Limcaco 2012). In addition, E<sup>2</sup>-Energy amplifies the energy harvest from wastewater by growing new biomass photosynthetically, which brings in extra solar energy (and CO<sub>2</sub>) to the wastewater biosolids. Considering both the reduced energy inputs and increased energy outputs, E<sup>2</sup>-Energy can help the wastewater industry to surpass the goals of carbon neutrality and net-zero energy wastewater treatment and instead become a significant net producer of renewable energy. In addition, algal-based treatment facilities can be less expensive to build and operate than conventional mechanical aeration facilities. For example, high-productivity algae ponds have a total cost that is estimated to cost up to 70% less than conventional activated sludge wastewater plants (Lundquist et al. 2010; U.S. EPA 2006).

Enhanced effluent quality would also be achieved during algal wastewater treatment, especially for nutrient removal (U.S. DOE 2010; Mata et al. 2010; Yang et al. 2011).

There are many changes needed to realize this paradigm shift, and one of the most significant is that the wastewater treatment enterprise would become more like an agricultural operation that optimizes growth of photosynthetic biomass using wastewater nutrients. This would require significantly more land than current wastewater treatment systems. However, it would reduce the total land requirements for biofuels as both DOE (2010) and National Research Council (2012) estimate that the areal productivity for algal biofuels can potentially be more than 10 times greater than current terrestrial crop based biofuels. For example, if the current land area of corn for ethanol production (1.3% of total U.S. land area (U.S. EIA 2012; USDA 2011)) is used for algal cultivation, the algal biofuel produced could be up to 55% of current U.S. petroleum consumption for transportation fuel usage (calculation based on values obtained from literature (National Research Council 2012)). Current corn ethanol production is providing less than 7% of the current U.S. transportation demand and needs arable land for corn production. In contrast, algae cultivation could be conducted on non-arable land areas like wastewater lagoons and stabilization ponds. In addition, proper planning can also help us to better utilize land resources. For example, one study showed that over 50% and 85% of the land around urban and rural wastewater treatment plants, respectively, could be potentially available for algal production (Fortier and Sturm 2012). Another study showed that focusing on locations along the Gulf Coast, southeaster seaboard, and Great Lakes could result in a 67% reduction in land use for algal biofuel production (Wigmosta et al. 2011).

### 3.4 Conclusions

This study investigated the novel E<sup>2</sup>-Energy system for algal biofuel production, which integrates algal biomass production during wastewater treatment and hydrothermal liquefaction of that biomass into bio-crude oil. A series of algal cultivation and hydrothermal liquefaction experiments were conducted to confirm the feasibility of the major process steps in the proposed system. This experimental work confirmed the ability to reuse nutrients multiple times for growing multiple rounds of algal biomass, thus amplifying the bioenergy that can be derived from waste sources. A mathematical model was then constructed to simulate the steady-state mass flows in this system and to guide the further system optimization. The E<sup>2</sup>-Energy process resolves the current major limitations to the economic feasibility of algal biofuels including the contamination of target high-oil algal cultures, high nutrient cost inputs, as well as the significant energy inputs for dewatering/extraction. The bioenergy potential of E<sup>2</sup>-Energy is tremendous because of the multi-cycle nutrient reuse feature, which amplifies the biomass and bioenergy potential of wastewater. We have shown that using waste organic biosolids from only three major sources (municipal wastewater, food waste, and livestock manure), could potentially support the production of enough bio-crude oil to completely replace the current U.S. demand for petroleum imports.

### 3.5 References

- Abeliovich, A. and Y. Azov. 1976. Toxicity of ammonia to algae in sewage oxidation ponds. *Applied and Environmental Microbiology* 31(6): 801-806.
- Agrawal, S. and S. Gupta. 2009. Survival and reproduction of some blue-green and green algae as affected by sewage water, fertilizer factory effluent, brassica oil, phenol, toluene and benzene. *Folia Microbiologica* 54(1): 67-73.
- Amin, S. 2009. Review on biofuel oil and gas production processes from microalgae. *Energy Conversion and Management* 50(7): 1834-1840.



- Aparicio, M. A., M. Eiroa, C. Kennes and M. C. Veiga. 2007. Combined post-ozonation and biological treatment of recalcitrant wastewater from a resin-producing factory. *Journal of Hazardous Materials* 143(1-2): 285-290.
- Appleford, J. M. 2005. Analyses of the products from the continuous hydrothermal conversion process to produce oil from swine manure. PhD diss. Champaign, IL: University of Illinois at Urbana-Champaign.
- ASTM. 2004a. Standard test method for water in petroleum products and bituminous materials by distillation. ASTM D95-99. West Conshohocken, PA.: Am. Soc. for Testing Materials.
- ASTM. 2004b. Standard test method for sediment in crude oils and fuel oils by the extraction. ASTM D473-02ASTM, West Conshohocken, PA.: Am. Soc. for Testing Materials.
- ASTM. 2004c.: Standard test method for toluene-insoluble (TI) content of tar and pitch. In *Annual Book of ASTM Standards*. ASTM D4072-98. West Conshohocken, PA.: Am. Soc. for Testing Materials.
- Biller, P. and A. B. Ross. 2011. Potential yields and properties of oil from the hydrothermal liquefaction of microalgae with different biochemical content. *Bioresource Technology* 102(1): 215-225.
- Boundy, B., S. Diegel W., L. Wright and S. Davis C. 2011. *Biomass Energy Data Book*. Oak Ridge, TN: U.S. Department of Energy.
- Brown, T., P. Duan and P. Savage. 2010. Hydrothermal Liquefaction and Gasification of *Nannochloropsis* sp. *Energy Fuels* 24(6): 3639-3646.
- Carrère, H., C. Dumas, A. Battimelli, D. J. Batstone, J. P. Delgenès, J. P. Steyer and I. Ferrer. 2010. Pretreatment methods to improve sludge anaerobic degradability: A review. *Journal of Hazardous Materials* 183(1-3): 1-15.
- Chisti, Y. 2007. Biodiesel from microalgae. *Biotechnology Advances* 25(3): 294-306.
- Clesceri, L. S., A. E. Greenberg and D. E. Andrew. 1999. *Standard Methods for the Examination of Water and Wastewater*. New York: American Public Health Association.
- Delrue, F., Y. Li-Beisson, P. -. Setier, C. Sahut, A. Roubaud, A. -. Froment and G. Peltier. 2013. Comparison of various microalgae liquid biofuel production pathways based on energetic, economic and environmental criteria. *Bioresource Technology* 136(0): 205-212.
- Dote, Y., S. Inoue, T. Ogi and S. Yokoyama. 1996. Studies on the direct liquefaction of protein-contained biomass: The distribution of nitrogen in the products. *Biomass and Bioenergy* 11(6): 491-498.

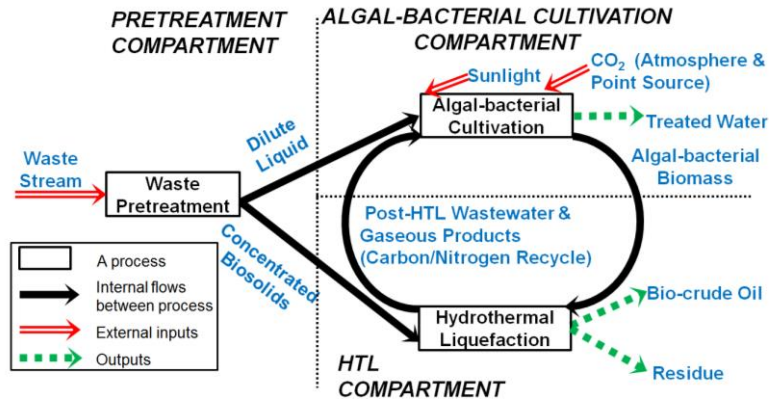
- Dote, Y., S. Yokoyama, T. Minowa, T. Masuta, K. Sato, S. Itoh and A. Suzuki. 1993. Thermochemical liquidization of dewatered sewage sludge. *Biomass and Bioenergy* 4(4): 243-248.
- Elliot, D. C. 1993. Evaluation of wastewater treatment requirements for thermochemical biomass liquefaction. In *Advances in Thermochemical Biomass Conversion*, 1299-1313. Netherlands: Springer.
- Elliott, D. 2007. Historical developments in hydroprocessing bio-oils. *Energy Fuels* 21(3): 1792-1815.
- Folch, J., M. Lees and G. Stanley. 1957. A simple method for the isolation and purification of total lipides from animal tissues. *Journal of Biological Chemistry* 226(1): 497-509.
- Fortier, M. P. and B. S. Sturm. 2012. Geographic analysis of the feasibility of collocating algal biomass production with wastewater treatment plants. *Environmental Science & Technology* 46(20): 11426-11434.
- Grange, P., E. Laurent, R. Maggi, A. Centeno and B. Delmon. 1996. Hydrotreatment of pyrolysis oils from biomass: reactivity of the various categories of oxygenated compounds and preliminary techno-economical study. *Catalysis Today* 29(4): 297-301.
- Huo, H., M. Wang, C. Bloyd and V. Putsche. 2008. Life-cycle assessment of energy use and greenhouse gas emissions of soybean-derived biodiesel and renewable fuels. *Environmental Science & Technology* 43(3): 750-756.
- Ikehata, K. and M. El Din. 2004. Degradation of recalcitrant surfactants in wastewater by ozonation and advanced oxidation processes: A review. *Ozone: Science Engineering* 26(4): 327-343.
- Inoue, S., S. Sawayama, Y. Dote and T. Ogi. 1997. Behaviour of nitrogen during liquefaction of dewatered sewage sludge. *Biomass & Bioenergy* 12(6): 473-475.
- Itoh, S., A. Suzuki, T. Nakamura and S. Yokoyama. 1994. Production of heavy oil from sewage-sludge by direct thermochemical liquefaction. *Desalination* 98(1-3): 127-133.
- Kallqvist, T. and A. Svenson. 2003. Assessment of ammonia toxicity in tests with the microalga, *Nephroselmis pyriformis*, Chlorophyta. *Water Research* 37(3): 477-484.
- Kamjunke, N., B. Köhler, N. Wannicke and J. Tittel. 2008. Algae as Competitors for Glucose with Heterotrophic Bacteria. *Journal of Phycology* 44(3): 616-623.
- Keller, M. D., R. C. Selvin, W. Claus and R. R. L. Guillard. 1987. Media for the culture of oceanic ultraphytoplankton. *J. Phycol.* 23(4): 633-638.
- Konig, A., H. W. Pearson and S. A. Silva. 1987. Ammonia Toxicity to Algal Growth in Waste Stabilization Ponds. *Water Science and Technology* 19(12): 115-122.

- Lardon, L., A. Hédias, B. Sialve, J. P. Steyer and O. Bernard. 2009. Life-cycle assessment of biodiesel production from microalgae. *Environmental Science & Technology* 43(17): 6475-6481.
- Lau, P. S., N. F. Y. Tam and Y. S. Wong. 1995. Effect of algal density on nutrient removal from primary settled waste-water. *Environmental Pollution* 89(1): 59-66.
- Limcaco, C. 2012. Personal communication about operational energy consumption of Algae Wheel full scale wastewater treatment plant in Reynolds, IN.
- Lu, G., C. Wang and X. Guo. 2008. Prediction of toxicity of phenols and anilines to algae by quantitative structure-activity relationship. *Biomedical and Environmental Sciences* 21(3): 193-196.
- Lundquist, T. J., I. C. Woertz, N. W. T. Quinn and J. R. Benemann. 2010. A realistic technology and engineering assessment of algae biofuel production. Berkeley, California Energy: Biosciences Institute.
- Marker, T., M. Linck and L. Felix. 2010. Integrated Hydropyrolysis and Hydroconversion (IH2) Process for Direct Production of Gasoline and Diesel Fuel from Biomass.
- Marker, T. 2005. *Opportunities for biorenewables in oil refineries*. DOEGO15085Final. Washington, D.C.: U.S. Department of Energy, Office of Energy Efficiency and Renewable Energy.
- Mata, T. M., A. A. Martins and N. S. Caetano. 2010. Microalgae for biodiesel production and other applications: A review. *Renewable & Sustainable Energy Reviews* 14(1): 217-232.
- National Research Council. 2012. Sustainable Development of Algal Biofuels. Washington, D.C.:The National Academic Press.
- Neilson, A. H. and R. A. Lewin. 1974. The uptake and utilization of organic carbon by algae: an essay in comparative biogeochemistry. *Phycologia* 13(3): 227-264.
- Rosenberg, J. N., A. Mathias, K. Korth, M. J. Betenbaugh and G. A. Oyler. 2011. Microalgal biomass production and carbon dioxide sequestration from an integrated ethanol biorefinery in Iowa: A technical appraisal and economic feasibility evaluation. *Biomass and Bioenergy* 35(9): 3865-3876.
- Sims, B. 2011. GTI signs licensing agreement with Shell Group subsidiary. Available at <http://biomassmagazine.com/articles/6748/gti-signs-licensing-agreement-with-shell-group-subsiary/?ref=brm>. Accessed 30 April 2013.
- Speight, J. G. 2010. *The Chemistry and Technology of Petroleum*. Boca Raton, FL: CRP press.
- Suzuki, A., T. Nakamura, S. Yokoyama, T. Ogi and K. Koguchi. 1988. Conversion of Sewage-Sludge to Heavy Oil by Direct Thermochemical Liquefaction. *Journal of Chemical Engineering of Japan* 21(3): 288-293.

- Tam, N. F. Y. and Y. S. Wong. 1996. Effect of ammonia concentrations on growth of *Chlorella vulgaris* and nitrogen removal from media. *Bioresource Technology* 57(1): 45-50.
- U.S. DOE. 2010. National algal biofuels technology roadmap. U.S. Department of Energy, Office of Energy Efficiency and Renewable Energy, Biomass Program.
- U.S. DOE. 2008. Waste Heat Recovery: Technology and Opportunities in U.S. Industry. U.S. Department of Energy, Industrial Technologies Program.
- U.S. DOE. 2006. Biodiesel handling and use guidelines, third edition. DOE/GO-102006-2358. Oak Ridge, TN: U.S. Department of Energy Office of Scientific and Technical Information
- U.S. EIA. 2012. Annual Energy Review 2011. DOE/EIA-0384(2011). Washington, D.C.: U.S. Energy Information Administration.
- U.S. EPA. 2006. Energy Conservation-Wastewater Management Factsheet. EPA 832-F-06-024. Washington, D.C.: U.S. Environmental Protection Agency, Office of Water.
- USDA. 2011. Agricultural Statistics 2011. Washington, D.C.:U.S. Department of Agriculture, National Agricultural Statistic Service.
- Vardon, D. R., B. K. Sharma, G. V. Blazina, K. Rajagopalan and T. J. Strathmann. 2012. Thermochemical conversion of raw and defatted algal biomass via hydrothermal liquefaction and slow pyrolysis. *Bioresource Technology* 109: 178-187.
- Vardon, D. R., B. K. Sharma, J. Scott, G. Yu, Z. Wang, L. Schideman, Y. Zhang and T. J. Strathmann. 2011. Chemical properties of biocrude oil from the hydrothermal liquefaction of *Spirulina* algae, swine manure, and digested anaerobic sludge. *Bioresource Technology* 102(17): 8295-8303.
- Wang, M. Q., J. Han, Z. Haq, W. E. Tyner, M. Wu and A. Elgowainy. 2011. Energy and greenhouse gas emission effects of corn and cellulosic ethanol with technology improvements and land use changes. *Biomass and Bioenergy* 35(5): 1885-1896.
- WERF. 2011. Energy production and efficiency research-the roadmap to net-zero energy. Alexandria, VA: Water Environmental Research Foundation.
- Wigmosta, M. S., A. M. Coleman, R. J. Skaggs, M. H. Huesemann and L. J. Lane. 2011. National microalgae biofuel production potential and resource demand. *Water Resources Research* 47: 1-13.
- Yang, J., M. Xue, X. Zhang, Q. Hu, M. Sommerfeld and Y. Chen. 2011. Life-cycle analysis on biodiesel production from microalgae: Water footprint and nutrients balance. *Bioresource Technology* 102 (1): 159-165.

- Yokoyama, S., A. Suzuki, M. Murakami, T. Ogi, K. Koguchi and E. Nakamura. 1987. Liquid fuel production from sewage-sludge by catalytic conversion using sodium-carbonate. *Fuel* 66(8): 1150-1155.
- Yu, G., Y. Zhang, L. C. Schideman, T. Funk and Z. Wang. 2011. Hydrothermal liquefaction of low lipid content microalgae into bio-crude oil. *Transactions of the ASABE* 54(1): 239-245.
- Yu, G. 2012. Hydrothermal liquefaction of low-lipid microalgae to produce bio-crude oil. PhD diss. Champaign, IL: University of Illinois at Urbana-Champaign.
- Yu, G., Y. Zhang, L. Schideman, T. Funk and Z. Wang. 2011. Distributions of carbon and nitrogen in the products from hydrothermal liquefaction of low-lipid microalgae. *Energy Environmental Science* 4(11): 4587-4595.
- Zhou, Y., L. C. Schideman, Y. Zhang and G. Yu. 2011. Environment-Enhancing Energy: A Novel Wastewater Treatment System that Maximizes Algal Biofuel Production and Minimizes Greenhouse Gas Emissions. In *Proc. of WEFTEC 2011*. Los Angeles, CA: Water Environment Federation.
- Zhou, D., L. Zhang, S. Zhang, H. Fu and J. Chen. 2010. Hydrothermal Liquefaction of Macroalgae *Enteromorpha prolifera* to Bio-oil. *Energy Fuels* 24(7): 4054-4061.

### 3.6 Figures and Tables



**Figure 3-1. Simplified schematic of the Environment-Enhancing Energy process for integrated wastewater treatment and biofuel production.**

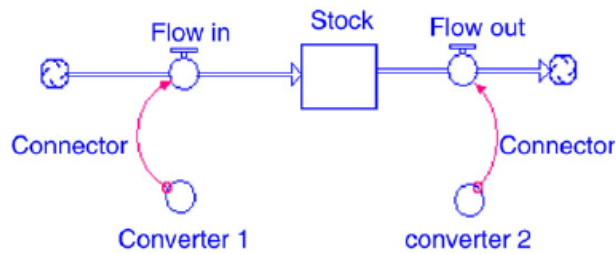
**Table 3-1. Chemical characteristics of PHWW and filtered municipal wastewater.**

Parameter (mg/L)	PHWW-Spirulina	PHWW-PBR	PHWW-Pond	PHWW-Carboy	PHWW-Manure <sup>d</sup>	Filtered Municipal WW
COD <sup>a</sup>	127,518±1,083	120,897±518	85,253±854	99,372±380	52,030	54
TOC <sup>b</sup>	41,136	39,432	23,208	34,964	NA	NA
NH <sub>4</sub> <sup>+</sup> -N <sup>c</sup>	3,230	11,407	NA	NA	NA	NA
Total nitrogen	5,482	20,342	10,288±167	17,307	5,355	33
Total phosphorus	1,865	1,558±62	NA	686±94	1,499	8
pH	7.5	7.89	7.89	7.89	5.6	NA
Usage of this water in this study	Step 1; Step 3	Step 2	Step 4	Step 4	Step 3	Step1-3

NA indicates values not measured. <sup>a</sup> COD= chemical oxygen demand; <sup>b</sup> TOC= total organic carbon; <sup>c</sup> Ammonia nitrogen; <sup>d</sup> This is a mixture of many PHWW from HTL using swine manure as feedstock under different process conditions (pressure and reaction time). Additional information about the PHWW from HTL using manure as feedstock is available in a previous publication (Appleford 2005)

**Table 3-2. Characteristics of harvested algal-bacterial biomass (dry matter basis).**

Parameter (%)	Cultivation systems		
	Outdoor open pond	Carboy batch jar	Photo-bioreactor
Volatile solid content	83.3	93.4	95.5
Ash content	16.7	6.6	4.5
Crude protein	36.7	NA	66.1
Acid Detergent Fiber	5.84	NA	<0.5
Lipid content	14.9±1.4	14.7±1.1	20.1±2.5
Carbon	46.2	49.8	51.1
Hydrogen	6.5	7.0	7.2
Nitrogen	6.2	9.8	10.1
Phosphorus	0.66	1.52	1.2



**Figure 3-2. A schematic diagram showing the four key features of STELLA: (1) stock, (2) flow, (3) converter, and (4) connector.**

**Table 3-3. Nomenclature, process parameter definitions and values used in the model.**

Parameters	Nomenclature	Symbols
Flow rate (L/day)		$Q$
Pretreatment		$PT$
Algal-bacterial cultivation		$AC$
Hydrothermal liquefaction		$HTL$
Influent/Effluent		$INF/EFF$
Substrate of carbon/nitrogen, as TOC/TN (mg/L)		$S_C/S_N$
Suspended solid (mg/L)		$SS$
Total nitrogen/carbon/suspended Solid (kg)		$TC/TN/TSS$
Primary sludge harvested in PT (kg)		$PS$
Biomass production (kg/d)		$X$
Heterotrophic/Autotrophic microbes		$HETE/AUTO$
Observed biomass yield (g SS/g Substrate)		$Y^{OBS}$
Biosolid (kg)		$BS$
HTL yield (g product/g dry feedstock)		$Y$
Weight of HTL products (kg)		$M$
Removal efficiency		$RR$
The gravimetric ratio of element $a$ in subject $b$		$f_a^b *$
Biodegradability of component $a$ in subject $b$		$\alpha_a^b *$
The partitioning ratio of element $a$ into HTL product $b$		$y_a^b *$

Note: Except for variables marked with an \*, superscripts indicate the process compartment (PT, AC or HTL), and subscripts describe the variable type. For example,  $TN_{INF}^{PT}$  means total nitrogen content in the influent of the pretreatment compartment, and  $RR_N^{AC}$  means the removal efficiency of nitrogen in the algal-bacterial cultivation compartment. Variables marked with an \* are ratios or efficiencies where superscripts (b) indicate the fraction/component of interest and subscripts (a) indicate the element or other variable type. For example,  $f_N^{SS}$  means the gravimetric ratio of nitrogen in suspended solids, whereas  $y_N^{OIL}$  means the partitioning ratio of nitrogen into HTL oil product.

Process parameter definitions and values		
Parameters		Value
<b>Pretreatment (PT)</b>		
Overall flow rate ( $Q$ )		1,000,000 L/d <sup>d</sup>
Suspended solid in influent of PT ( $SS_{INF}^{PT}$ )		210 mg/L (Asano 2007)
Soluble carbon in influent of PT ( $S_C^{PT}$ )		50 mg/L (Asano 2007)
Soluble nitrogen in influent of PT ( $S_N^{PT}$ )		35 mg/L (Asano 2007)
Suspended solids removal in PT ( $RR_{SS}^{PT}$ )		0.7 (Tchobanoglous et al. 1991)
Fraction of solid in primary sludge ( $f_{SPS}$ )		0.2 <sup>a</sup>
Fraction of carbon in primary sludge ( $f_C^{PS}$ )		0.39 (Smidt and Parravicini 2009)
Fraction of nitrogen in primary sludge ( $f_N^{PS}$ )		0.025 (Tchobanoglous et al. 1991)
Specific gravity of primary sludge ( $G_{PS}$ )		1.08 (Metcalf & Eddy et al. 2003)
Biodegradability of soluble carbon in raw waste ( $\alpha_C^{RW}$ )		0.9 <sup>d</sup>
Biodegradability of soluble nitrogen in raw waste ( $\alpha_N^{RW}$ )		0.9 <sup>d</sup>
<b>Algal-bacterial Cultivation (AC)</b>		
Solid content of biosolids sent to HTL ( $f_{BS}$ )		0.2 <sup>a</sup>
Observed heterotrophic biomass yield (kg biomass/kg TOC consumed) ( $Y_{HETE}^{OBS}$ )		0.85 <sup>a</sup>
Observed autotrophic biomass yield (kg biomass/kg TN consumed) ( $Y_{AUTO}^{OBS}$ )		12.5 <sup>a</sup>
Fraction of carbon in autotroph ( $f_C^{AUTO}$ )		0.5 <sup>a</sup>
Fraction of carbon in heterotroph ( $f_C^{HETE}$ )		0.5 <sup>a</sup>



**Table 3-3 (cont.)**

Parameters	Value
Fraction of nitrogen in heterotroph ( $f_N^{HETE}$ )	0.04 (Metcalf & Eddy et al. 2003)
Suspended solids harvesting in AC ( $RR_{SS}^{AC}$ )	0.99 (Metcalf & Eddy et al. 2003)
<b>Hydrothermal liquefaction (HTL)</b>	
Product yield of oil, PHWW, gas, residue ( $Y_{OIL}, Y_{PHWW}, Y_{RES}, Y_{GAS}$ )	0.47, 0.30, 0.18, 0.05 <sup>a,b</sup>
Carbon partitioning ratio into bio-crude oil, PHWW, gas and residue ( $y_C^{OIL}, y_C^{PHWW}, y_C^{RES}, y_C^{GAS}$ )	0.64, 0.22, 0.12, 0.03 <sup>a,b</sup>
Nitrogen partitioning ratio into bio-crude oil, PHWW, gas and residue ( $y_N^{OIL}, y_N^{PHWW}, y_N^{RES}, y_N^{GAS}$ )	Baseline: 0.31, 0.60, 0.09, 0 <sup>a,b</sup> Improved <sup>e</sup> : 0.155, 0.80, 0.045, 0 (Yu et al. 2011) <sup>c</sup>
Biodegradability of carbon in PHWW ( $\alpha_C^{PHWW}$ )	Baseline: 0.69 <sup>a</sup> ; Improved: 0.91 <sup>e</sup>
Biodegradability of nitrogen in PHWW ( $\alpha_N^{PHWW}$ )	Baseline: 0.86 <sup>a</sup> ; Improved: 0.96 <sup>e</sup>

<sup>a</sup> Values are obtained from experiments reported in this study.

<sup>b</sup> Values are averages of three HTL testing results.

<sup>c</sup> Parameters used were from results with processing *Chlorella* at 280 °C and a 60 min reaction time.

<sup>d</sup> Values were assumed based on experience.

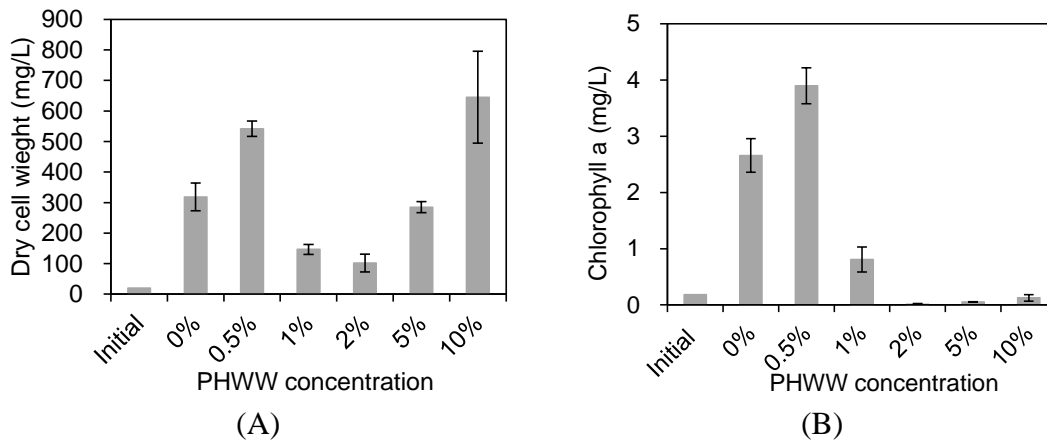
<sup>e</sup> Reasons for these values provided in the results and discussion section.

**Table 3-4. Governing equations used for the nitrogen sub-model of the E<sup>2</sup>-Energy system model.**

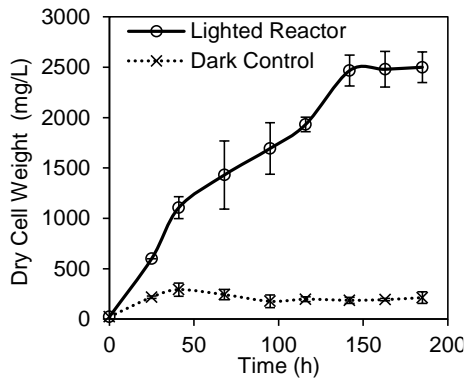
<b>Pretreatment (PT)</b>	
Inputs	<p>From incoming waste stream: <math>TSS, TC_{INF}^{PT}, TN_{INF}^{PT}, Q</math></p> $TN_{INF}^{PT} = (SS_{INF}^{PT} \times f_N^{SS} + S_{N_{INF}}^{PT}) \times Q$ $TC_{INF}^{PT} = (SS_{INF}^{PT} \times f_C^{SS} + S_{C_{INF}}^{PT}) \times Q$ $TSS_{INF}^{PT} = SS_{INF}^{PT} \times Q$
Processes	<ul style="list-style-type: none"> <li>Nitrogen removal through primary sludge settling (assuming no soluble nitrogen removal) <math display="block">SS_{EFF}^{PT} = SS_{INF}^{PT} \times (1 - RR_{SS}^{PT})</math> <math display="block">TSS_{PS}^{PT} = (SS_{INF}^{PT} - SS_{EFF}^{PT}) \times Q</math> <math display="block">TN_{PS}^{PT} = TSS_{PS}^{PT} \times f_N^{PS}</math> </li> <li>Carbon removal through primary sludge removal <math display="block">TC_{PS}^{PT} = TSS_{PS}^{PT} \times f_C^{PS}</math> </li> </ul>
Outputs	<p>To AC: <math>TSS_{EFF}^{PT}, TC_{EFF}^{PT}, TN_{EFF}^{PT}, Q_L</math></p> <p>To HTL: <math>TSS_{PS}^{PT}, TC_{PS}^{PT}, TN_{PS}^{PT}, Q_s</math></p>
<b>Algal-bacterial Cultivation (AC)</b>	
Inputs	<p>From PT: <math>TSS_{EFF}^{PT}, TC_{EFF}^{PT}, TN_{EFF}^{PT}, Q_L</math></p> <p>From HTL: <math>TC_{PHWW}, TC_{GAS}, TN_{PHWW}, Q_{PHWW}</math></p> <p>From atmosphere: <math>TC_{AUTO}^{CO_2\_Seq\_Atm}</math></p> $TN_{INF}^{AC} = TN_{EFF}^{PT} + TN_{PHWW}$ $TC_{INF}^{AC} = TC_{EFF}^{PT} + TC_{PHWW}$ $TSS_{INF}^{AC} = TSS_{EFF}^{PT}$
Processes	<ul style="list-style-type: none"> <li>Hydrolysis of residual suspended solids from PT <math display="block">TSS_{N_{INF}}^{AC} = TN_{INF}^{AC}</math> <math display="block">TS_{C_{INF}}^{AC} = TC_{EFF}^{PT} + TC_{PHWW}</math> </li> </ul>

**Table 3-4 (cont.)**

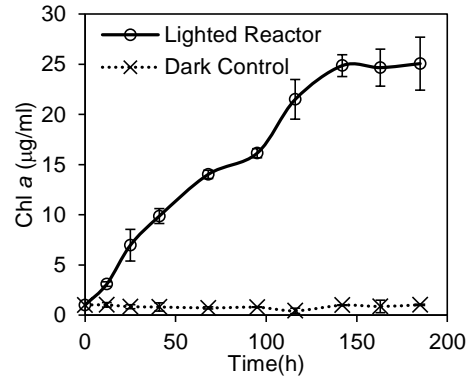
	<ul style="list-style-type: none"> <li>Soluble nitrogen removal by microbial uptake           <math display="block">TN_{BS}^{AC} = TSS_{N_{INF}}^{AC} \times RR_N^{AC}</math> </li> </ul>
	-Removal efficiency depends on nitrogen biodegradability of two incoming waste stream $RR_N^{AC} = \frac{TN_{EFF}^{PT} \times \alpha_N^{RW} + N_{PHWW}^{HTL} \times \alpha_N^{PHWW}}{TN_{EFF}^{PT} + TN_{PHWW}^{HTL}}$
	-Nitrogen utilization to support heterotrophic growth (heterotrophs have priority to use nitrogen) $X_{HETE}^{AC} = Y_{HETE}^{OBS} \times TC_{INF}^{AC} \times RR_C^{AC}$ $TN_{HETE}^{AC} = X_{HETE}^{AC} \times f_N^{HETE}$
	-Nitrogen utilization to support autotrophic growth $X_{AUTO}^{AC} = Y_{AUTO}^{OBS} \times TN_{AUTO}^{AC}$ $TN_{AUTO}^{AC} = TN_{BS}^{AC} - TN_{HETE}^{AC}$
	<ul style="list-style-type: none"> <li>Soluble carbon removal in the form of heterotrophic biomass</li> </ul>
	--Removal efficiency depends on nitrogen biodegradability of two incoming waste stream $RR_C^{AC} = \frac{TC_{EFF}^{PT} \times \alpha_C^{RW} + TC_{PHWW} \times \alpha_C^{PHWW}}{TC_{EFF}^{PT} + TC_{PHWW}}$
	--Carbon utilization to support heterotrophic growth $X_{HETO}^{AC} = Y_{HETO}^{OBS} \times TC_{INF}^{AC} \times RR_C^{AC}$
	--CO <sub>2</sub> emission from respiration of heterotrophic microbes $TC_{HETO}^{CO_2-RES} = TC_{INF}^{AC} \times RR_{SC}^{AC} - TC_{HETO}^{AC}$
	<ul style="list-style-type: none"> <li>CO<sub>2</sub> fixation from ambient air/point source to support autotrophic growth           <math display="block">TC_{AUTO}^{CO_2-Seq-Atm} = TC_{AUTO}^{AC} - TC_{HETO}^{CO_2-RES} - TC_{GAS}</math> <math display="block">TC_{AUTO}^{AC} = X_{AUTO}^{AC} \times f_C^{AUTO}</math> </li> </ul>
	<ul style="list-style-type: none"> <li>Biosolids increased in the form of biomass           <math display="block">TSS_{BS}^{AC} = (X_{HETO}^{AC} + X_{AUTO}^{AC})</math> </li> </ul>
	--Heterotrophic microbes growth $X_{HETO}^{AC} = Y_{HETO}^{OBS} \times TC_{INF}^{AC} \times RR_C^{AC}$
	--Autotrophic microbes growth $X_{AUTO}^{AC} = Y_{AUTO}^{OBS} \times TN_{AUTO}^{AC}$
	<ul style="list-style-type: none"> <li>Biomass harvesting           <math display="block">TN_{Harv}^{AC} = TN_{Harv}^{AC} \times RR_{SS}^{AC}</math> <math display="block">TSS_{Harv}^{AC} = TSS_{BS}^{AC} \times RR_{SS}^{AC}</math> <math display="block">TC_{Harv}^{AC} = TC_{BS}^{AC} \times RR_{SS}^{AC}</math> </li> </ul>
Outputs	To treated water: $TSS_{EFF}^{AC}, TC_{EFF}^{AC}, TN_{EFF}^{AC}, Q_{AC}$ To HTL: $TN_{Harv}^{AC}, TC_{Harv}^{AC}, TSS_{Harv}^{AC}$
<b>Hydrothermal liquefaction (HTL)</b>	
Inputs	From PT: $TSS_{PS}^{PT}, TC_{PS}^{PT}, TN_{PS}^{PT}, Q_s$ From AC: $TSS_{Harv}^{AC}, TC_{Harv}^{AC}, TN_{Harv}^{AC}$ $TSS_{FEED}^{HTL} = TSS_{Harv}^{AC} + TSS_{PS}^{PT}$ $TC_{FEED}^{HTL} = TC_{Harv}^{AC} + TC_{PS}^{PT}$ $TN_{FEED}^{HTL} = TN_{Harv}^{AC} + TN_{PS}^{PT}$
Processes	<ul style="list-style-type: none"> <li>Hydrothermal liquefaction: <math>M_{OIL, PHW, GAS \text{ or } RES} = TSS_{FEED}^{HTL} \times Y_{OIL, PHW, GAS \text{ or } RES}</math></li> <li>Nitrogen release into HTL product : <math>TN_{OIL, PHWW, GAS \text{ or } RES} = TN_{FEED}^{HTL} \times y_N^{OIL, PHWW, GAS \text{ or } RES}</math></li> <li>Carbon release into HTL product : <math>TC_{OIL, PHW, GAS \text{ or } RES} = TC_{BS}^{AC} \times y_C^{OIL, PHWW, GAS \text{ or } RES}</math></li> </ul>
Outputs	To biorude oil: $M_{OIL}, TC_{OIL}, TN_{OIL}$ To residue: $M_{RES}, TC_{RES}, TN_{RES}$ To PHWW: $M_{PHWW}, TC_{PHWW}, TN_{PHWW}, Q_{PHWW}$ To waste gas: $M_{GAS}, TC_{GAS}$



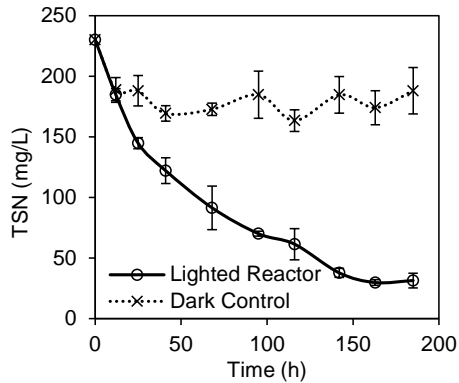
**Figure 3-3. Biomass production in filtered municipal wastewater spiked with various doses (0-10%) of post-HTL wastewater (PHWW-Spirulina) after 10 days of cultivation. (A) Total biomass production presented as dry cell weight. (B) Autotrophic biomass production presented as Chlorophyll *a* concentration. Error bars represent the standard deviation.**



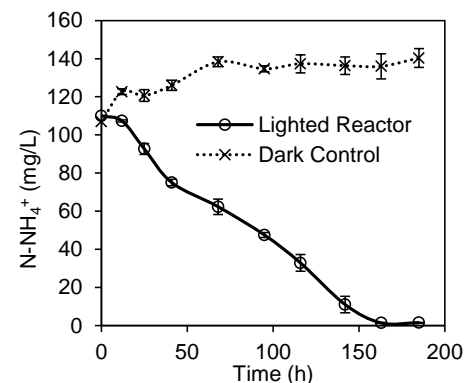
(A)



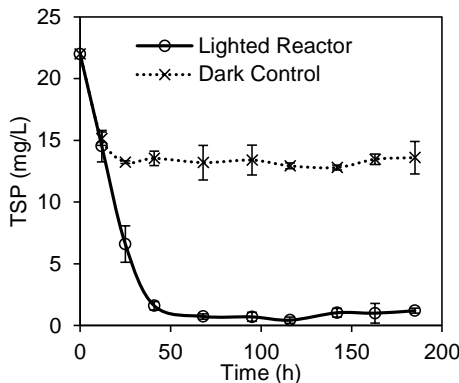
(B)



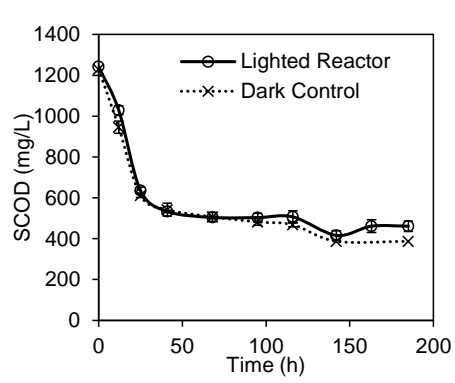
(C)



(D)



(E)



(F)

**Figure 3-4. Biomass production and pollutant degradation when algae were cultivated in municipal wastewater spiked with 1% PHWW-PBR. Error bar represent standard deviation. (A) Biomass production presented by dry cell weight. (B) Autotrophic biomass concentration presented by Chlorophyll a concentration. (C) Total soluble nitrogen removal. (D) Ammonia nitrogen removal. (E) Total soluble phosphorus removal. (F) Soluble chemical oxygen demand removal.**

**Table 3-5. Bio-crude oil characteristics and energy balance of E<sup>2</sup>-Energy system for processing 1 kg dry algae.**

		<b>Pond</b>	<b>Carboy</b>	<b>PBR</b>
Elemental Composition of Bio-crude oil	C(%)	77.4	70.4	75.5
	H(%)	9.4	8.2	9.4
	N(%)	5.2	6.6	7.1
	O(%)	8.1	14.7	8.0
Higher Heating Value (MJ*kg <sup>-1</sup> )	Feedstock	17.6	20.8	21.9
	Raw Oil	22.5	30.4	36.6
	Bio-crude Oil	38.1	32.9	37.5
Energy input for algal cultivation and harvesting (MJ) <sup>a</sup>			1.50	
Energy input for HTL (MJ) <sup>b</sup>			1.48	
Energy output (MJ) <sup>c</sup>		10.09	12.00	13.47
ECR		0.30	0.25	0.22
Energy Recovery		82%	82%	88%
Energy input for upgrading (MJ) <sup>d</sup>		0.16	0.22	0.22
Energy output after upgrading (MJ) <sup>e</sup>		9.01	12.42	12.21
ECR with upgrading		0.35	0.26	0.26

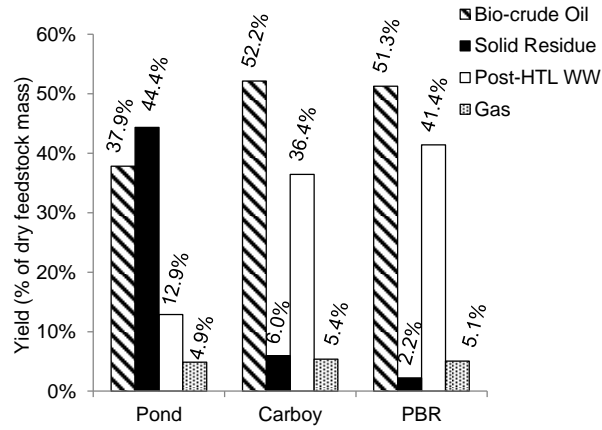
<sup>a</sup> In the proposed E<sup>2</sup>-Energy system, open pond cultivation is assumed, with an energy consumption of 1.5 MJ/kg dry algae for cultivation and harvesting to reach solid content of 20% described previously.

<sup>b</sup> Heat recovery is considered.

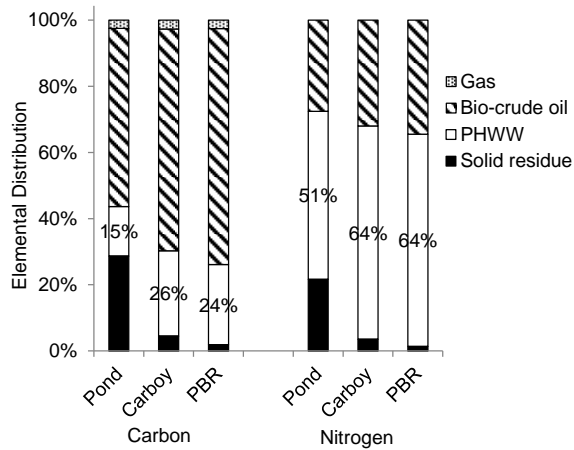
<sup>c</sup> Combustion efficiency is considered.

<sup>d</sup> The energy consumption for upgrading is assumed to be 0.42 MJ/kg oil processed.

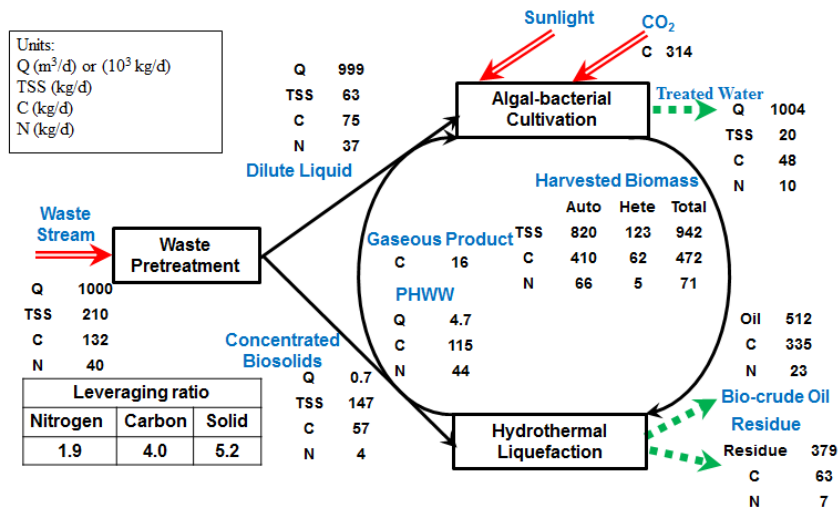
<sup>e</sup> The product yield of upgrading is assumed to be 85% and HHV of upgraded oil to be 40 MJ/kg.



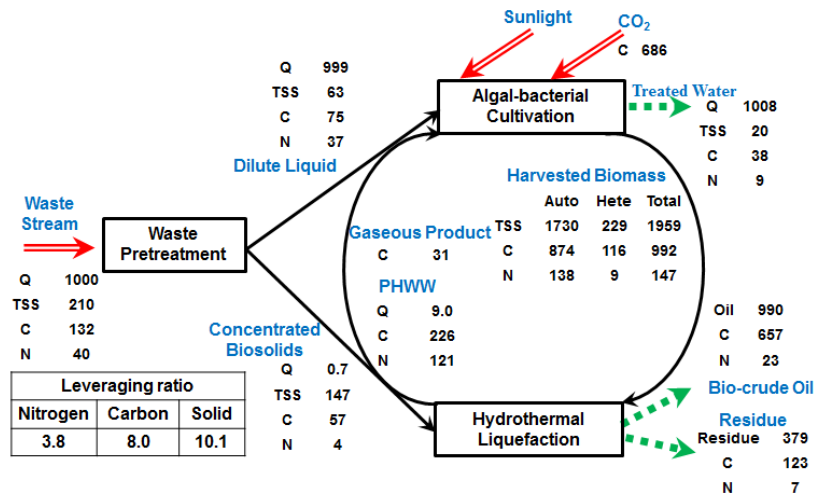
**Figure 3-5. HTL product yield using three kinds of algae feedstock from wastewater.**



**Figure 3-6. Elemental distribution of carbon and nitrogen in HTL products.**



(A)



(B)

**Figure 3-7. Multi-component mass balance for two scenarios of E<sup>2</sup>-Energy. (A) Baseline scenario-based on model parameters from this study. (B) Improved scenario based on model parameters reported in the literature that would improve net energy yield.**



**Table 3-6. Estimation of collectable biosolids in the U.S.**

<b>Sources</b>	<b>Quantity (million dry tons)</b>
Human waste(U.S. EPA, Office of Wastewater Management 2006)	8 <sup>a</sup>
Food scraps in municipal solid waste(U.S. EPA 2011)	10 <sup>b</sup>
Animal manure (USDA 2011; ASAE 2005; USDA 1995)	135 <sup>c</sup>
Total	153

<sup>a</sup> The 8 million tons here only includes outgoing biosolids from wastewater treatment plant (after aerobic and anaerobic digestion) rather than total initial incoming human waste. More biosolids than this quantity from human waste should be potentially available.

<sup>b</sup> Assuming moisture content of food scraps to be 70%.

<sup>c</sup> Current total animal manure production is estimated to be 235 dry tons/year according to the total US livestock herds(USDA 2011) and the average manure production rate(ASAE 2005) of different animals. The readily collectable portion of manure was estimated according to a USDA methodology(USDA 1995).

## CHAPTER 4

### ADSORBENT AMENDED HYBRID PHOTOBIOREACTOR FOR ENHANCED ALGAL WASTEWATER TREATMENT

#### 4.1 Introduction

Mass cultivation of algae in wastewater treatment systems offers some of the best potential for sustainable biofuels because wastewater provides a significant source of low-cost nutrients and water needed for algae cultivation. At the same time, this integration also provides unique opportunity for conventional wastewater treatment including: 1) photosynthetic aeration resulting from the symbiotic relationship between algae and bacteria, which can reduce the energy input for aeration; 2) improved nutrient removal can be achieved while avoiding some the extra costs commonly associated with conventional biological nutrient removal systems. Despite this potential, one challenge currently limiting algal wastewater treatment is that algae are generally more sensitive to toxic compounds than bacteria. As a result, algal-based wastewater treatment systems may be more susceptible to upset and performance failure, compared to conventional activated sludge and biological nutrient removal processes, which are dominated by bacteria. In addition, all biological treatment systems face challenges from recalcitrant, inhibitory and toxic contaminants present in various wastewater streams. These chemicals may exert deleterious impacts on human health and natural ecosystems if not removed prior to environmental discharge. They can also cause upsets in biological treatment systems that make them less reliable. An example of these kinds of challenges was observed in the previous chapters when using an algal-bacterial system to treat the post-hydrothermal liquefaction wastewater. To meet increasingly stringent discharge standards, enhancements to algal wastewater treatment technologies are needed to ensure consistent treatment efficiency.

One promising method to address these issues is to integrate adsorbents into algal treatment systems, such as activated carbon and ion exchange resins. Adsorption processes can passively remove a broad spectrum of chemicals from water with negligible energy inputs, and they generally only require seconds or minutes of contact time with the water, which is significantly faster than the net rates of biological processes (Metcalf & Eddy et al. 2003). Therefore, adsorbents can provide fast physicochemical capture of slowly-degrading and toxic compounds to accommodate the time needed for biological removal. Adsorbents can improve effluent quality by maintaining consistently lower effluent concentrations of organics, and then slowly release the organics as they are taken up by the microbes. Moreover, the adsorption process is much less sensitive to upset and natural variations in operating conditions, and can temporarily store organic substrates while microbes are adapting to changed conditions. Thus, adsorbents provide benefits such as buffering against shock loadings, toxic compounds, and fluctuations in biological performance due to temperature, pH, sunlight intensity, etc. This will improve reactor stability and effluent water quality, which is obviously important for wastewater treatment applications.

Previous results showed that mixed algal-bacterial systems can quickly uptake most of the organic carbon released into PHWW, but a sizeable fraction (10-30%) of these organics is not quickly assimilated and may be recalcitrant to biological degradation. In this chapter, we investigate an innovative algal wastewater treatment system, a hybrid adsorption membrane photobioreactor using granular adsorbents to enhance treatment of PHWW that contains both toxic and recalcitrant compounds. The objectives of this study are to: 1) evaluate the long term operation of this photobioreactor and investigate the effects of key parameters including loading

rate, hydraulic and solid retention time on reactor performance; 2) investigate the effect of incorporating adsorbents into the algal photobioreactor on reactor performance.

## **4.2 Materials and Methods**

### **4.2.1 Adsorption batch test**

Adsorption isotherm experiments were conducted to determine the feasibility of adsorptive treatment with activated carbon for enhancing the PBR effluent quality by the mechanism of abiotic physicochemical adsorption. Two adsorption batch isotherm tests were performed. The first test used DARCO ULTRA 100 PAC for treating effluent from the PBR when influent was 1% PHWW+99% municipal wastewater, HRT=5 days and SRT=20 days without GAC added (Phase I, Stage 1). Effluent was filtered through 0.45  $\mu\text{m}$  filter paper to remove any particles and cells in order to minimize biological activity. The test was performed in 250 ml Erlenmeyer flasks with 100 ml PBR effluent. Different doses of PAC were added to the PBR effluent and contacted for 14 days at 4  $^{\circ}\text{C}$  on an orbital shaker operating at 150 rpm before the final analysis. Calgon FILTRASORB<sup>®</sup>400 GAC (Calgon Carbon Corporation, Pittsburgh, PA, USA) was used for the other adsorption test treating PBR effluent when the influent was 4% PHWW+96% municipal wastewater, HRT=5 days and SRT=20 days without GAC added. For this batch isotherm test, the GAC was ground into small particles that made it similar in size to PAC. The second adsorption batch isotherm test was conducted with a similar procedure as described above, except the containers were 150 ml serum bottles with 100 ml PBR effluent and shaken at room temperature for 100 days before the final analysis.

The Freundlich isotherm equation was used as an empirical model to fit the isotherm data. The equation is expressed as  $q_e = K_f C_e^{1/n}$ , where  $q_e$  represents the amount adsorbed per amount of adsorbent at the equilibrium (mg adsorbate/g activated carbon),  $C_e$  represents the equilibrium

liquid phase concentrations (mg adsorbate /L water), and  $K_f$  and  $n$  are empirical fitting parameters that depend on the adsorbate and adsorbent.  $K_f$  is the Freundlich capacity factor (mg adsorbate/g activated carbon)  $\times$  (L water/mg adsorbate)<sup>1/n</sup>, and  $n$  is the Freundlich intensity parameter.

#### 4.2.2 Continuous flow photobioreactor

A mixed algal-bacterial culture that was adapted to PHWW as described previously (Chapter 3) was inoculated into a 10 L continuous flow PBR. The original seed was collected from the primary clarifier outlets at a local wastewater treatment plant (Urbana-Champaign Sanitary District). During the development of this culture, various algal species were bio-augmented into the culture including *Chlorella protothecoides*, *Chlorella vulgaris*, *Botryococcus braunii*, *Nanochloropsis oculata*, *Spirulina platensis*, *Scenedesmus dimorphus*, and *Chlamydomonas reinhardtii*.

A polyvinylidene difluoride (PVDF) hollow fiber ultrafiltration membrane module (ZW-1000 Jr, GE-Zenon) was placed in the center of the reactor, which has a nominal pore size of 0.04  $\mu\text{m}$  and membrane area of approximately 1  $\text{m}^2$  as shown in Figure 4-1A. Two peristaltic pumps were used to deliver influent and withdraw effluent through the membrane module with a hydraulic retention time of 5 days. Light was provided by eight 22 W fluorescent lights installed around the bioreactor. The light intensity at the center of the empty reactor was between 200-250  $\mu\text{mol photon m}^{-2} \text{s}^{-1}$ . Air was provided through a diffuser at the bottom of the reactor at a flow rate of 4 LPM. The influent was a mixture of PHWW-Spirulina and filtered municipal WW. Algal biomass was removed regularly to obtain a certain solids retention time, which was varied over the course of the study.

The entire reactor operation was divided into four phases, as shown in Table 4-1. The objectives of each phase are summarized below:

Phase I: study the effect of GAC on removing refractory/slow-degrading compounds;

Phase II: study the effect of loading rate on reactor performance without GAC;

Phase III: study the effect of SRT on reactor performance without GAC;

Phase IV: study the effect of GAC on enhancing reactor performance under adverse environmental conditions (high loading rate and low SRT).

Steady-state conditions were assumed to have been reached when three consecutive effluent samples had fairly stable water quality characteristics. Following this, samples were drawn every other day for a least 10 samples before switching to another condition.

#### **4.2.3 Water quality analysis**

COD, total dissolved nitrogen (TDN), ammonia nitrogen ( $\text{NH}_4^+\text{-N}$ ), and total dissolved phosphorus (TDP) was measured as described in the previous chapter. In addition, nitrate+nitrite ( $\text{NO}_3^-\text{-N}+\text{NO}_2^-\text{-N}$ ) was determined according to HACH Cadmium Reduction Method No. 8171.

#### **4.2.4 GC-MS analysis**

The chemical composition of water samples was analyzed using GC-MS (Agilent 7890A GC-5975C MS, Agilent Technologies, Santa Clara, CA) equipped with flame ionization detector (FID) and a 15 m ZB-WAX column with 0.25 mm inner diameter and 0.25  $\mu\text{m}$  film thickness (Phenomenex, Torrance, CA, USA). The injection temperature was set to be 250°C, MSD transfer line was 250 °C, and the ion source was 230 °C. The spectra of all chromatogram peaks were evaluated using the HP chem station (Agilent, Palo Alto, CA, USA) and AMDIS (NIST, Gaithersburg, MD, USA) programs and compared with electron impact mass spectrum from

NIST Mass Spectral Database (NIST08) and W8N08 library (John Wiley & Sons, Inc.). An internal standard (3-methylbutanoic acid, 0.1  $\mu\text{M}$ ) was used to normalize all data and facilitate comparison between samples.

#### **4.2.5 Chinese Hamster Ovary (CHO) Cell Chronic Cytotoxicity Assay**

Four water samples from Phase I operation were tested for cytotoxicity: the influent of the PBR, effluent during Stage 1, effluent during Stage 2 for the first 15 days, and the effluent during Stage 2 from the following 15 days. Organic compounds in these four water samples were first extracted and concentrated using an EPA's standard method for extracting organic disinfection byproducts using XAD-2 and XAD-8 resins (Richardson 2011).

The cytotoxicity assay used Chinese hamster ovary (CHO) cell line AS52, clone 11-4-8. CHO cells were maintained in Ham's F12 medium which contains 5% fetal bovine serum (FBS), 1% antibiotics (100 U/mL sodium penicillin G, 100  $\mu\text{g}/\text{mL}$  streptomycin sulfate, 0.25  $\mu\text{g}/\text{mL}$  amphotericin B in 0.85% saline), and 1% glutamine at 37  $^{\circ}\text{C}$  in a humidified atmosphere of 5%  $\text{CO}_2$ . CHO cell chronic cytotoxicity assay measures the reduction in the cell density of mammalian CHO cells as a function of the concentration of the extracted organics from each sample. The test was conducted on flat-bottom 96-well microplates. Extracted organics in DMSO were diluted with F12+FBS medium to achieve target concentration/dilution factor. 10 different concentrations of each tested samples were used, and 8-16 replicates of each concentration were analyzed. The final cell density was monitored at 72 hours, which is around 3 cell cycles. A concentration-response curve was generated for each sample and a regression analysis was conducted with each curve. The  $\text{LC}_{50}$  values were calculated from the regression analysis and represent the sample concentration factor that induced a 50% reduction in cell density as compared to the concurrent negative controls. This assay were repeated at least 2

times for each tested sample. This assay has been used to evaluate both individual compounds and complex mixtures, and additional details for this assay and the statistical analysis were described previously (Plewa et al. 2002; Plewa et al. 2012).

### **4.3 Results and Discussion**

#### **4.3.1 Algal-bacterial consortium**

After being inoculated in the PBR, the biomass in the reactor started to form small flocs, with a size around a couple of mm, as shown in Figure 4-1B. Microscopic examination of the algal-bacterial floc indicates a mixed population of algae, bacteria, free-swimming and stalked protozoa, and rotifers. After a couple of months of operation, the major algae species were identified including common wastewater algae *Scenedesmus dimorphus*, *Chlorella spp.*; filamentous cyanobacterium *Oscillatoria*; and multiple *diatoms* as shown in Figure 4-1C. Algae was shown to be the dominant biomass compared bacteria.

#### **4.3.2 Recalcitrant compound analysis**

Our GC-MS analysis of the effluent from the photobioreactor with 1% PHWW as influent without GAC added found that many of the recalcitrant or slow-degrading compounds contain ring structures and nitrogen heteroatoms, some of which are shown in Table 4-2. The formation of these compounds was likely related to cross reactions with proteins and carbohydrates (Torri et al. 2012). Recent studies have identified nitrogenous organics resulting from HTL treatment of algal feedstocks, such as amino-phenol, 2-piperidione, 2-pyrrolidinone, pyridina and its derivatives, and piperidinone and its derivatives (Torri et al. 2012; Pham 2014; Jena et al. 2011; Anastasakis and Ross 2011). Potential removal methods include adsorption, ozone, hydrothermal catalytic gasification and/or second-stage biological treatment with adapted or specialized microbes.



### 4.3.3 Adsorption batch test

When treating effluent from PBR with 1% PHWW as influent, the addition of GAC did result in considerable removal of recalcitrant COD, with highest removal efficiency of 91%, as shown in Figure 4-2A,. When the GAC dosage was 1g/L, the COD is already at a relatively low level (59 mg/L). Additional GAC dosage above 1g/L did not result in significantly increased removal of COD. When treating effluent from the PBR with a higher influent organic concentration (4% PHWW), the activated carbon still showed good physicochemical adsorption ability in removing residual organic compounds, as shown in Figure 4-3A. The highest removal efficiency 84% happened at a dosage of 25 g/L. Actually when the dosage was 5g/L and 10g/L, the removal efficiency was already fairly high, 67% and 74% respectively.

It is noteworthy that in both cases, even at very high activated carbon dosage, like 15g/L or 20 g/L, there was still about 10% residual COD, indicating the existence of recalcitrant/slow-degrading and non-absorbable organic compounds in wastewater effluent. Although activated carbon is well known for removing various organics from water, there are some low affinity pollutants that are hard to remove. Two sources could potentially contribute to the 10% non-adsorbable COD. One group is the chemicals that originally exists in PHWW. For example, PHWW contains many compounds similar to those found in petroleum, many of which have been reported to have a low affinity to activated carbon. Giusti et al (1974) reported that when using high dosage of PAC (5 g/L) to treat representative petrochemicals including adorability was quite variable, with the lowest to be only 3.6%. The other group that may have contributed to the 10% COD residue is the product from biological degradation of large molecules that originally exist in PHWW. As we can see in later section where we analyzed the 4% PHWW influent and effluent using GC-MS (Table 4-4), some low molecular weight compounds like

isopropanol and acetonitrile that come from the breakdown of larger molecules were observed in the effluent. The concentration of these compounds was higher in the effluent than the influent, and they also showed poor absorbability to activated carbon as we can see from both the batch test results (Table 4-4) and literature (Giusti et al. 1974).

The adsorption isotherm data were fitted to the Freundlich isotherm equation. The typical graphical representations of the linearized plots are shown in Figures 4-3 and 4-4 for adsorption of COD, inorganic nitrogen ( $\text{NH}_4^+\text{-N}$ ,  $\text{NO}_3^-\text{-N}+\text{NO}_2^-\text{-N}$ ) and TN on activated carbon. The Freundlich constants determined from the slopes and intercepts of the respective plot are summarized in Table 4-3. As we can see, in both cases, the COD fit the Freundlich isotherm fairly well, with relatively high correlation coefficients of 0.86 and 0.97, respectively. The  $K_f$  values (0.14 and 0.028 respectively), are both low, indicating a low capacity for recalcitrant/slow-degrading compound to both types of activated carbon, although the PAC showed better capacity than GAC. For example, benzene is reported to need high quantities for routine water treatment, it has  $K_f$  values ranged from 1.0-26.8 for PAC and from 0.73 to 26 for GAC (Faust and Aly 1987). Just as a comparison, readily adsorbed compounds like 1,2-dichlorobenzene can have  $K_f$  values ranging from 89 to 360 for PAC, and 300 for GAC. Therefore, the  $K_f$  in our case are very low. Petrochemicals, which contains many similar compounds as what we have in PHWW, have been reported to also show a low affinity to activated carbon compared to many other organic compounds. For example, ethylacetate showed  $K$  as low as 0.04 (Giusti et al. 1974).

Activated carbon is not capable of adsorbing inorganic nitrogen effectively from the PBR effluent, as shown in Figure 4-2E for nitrate and nitrite, and Figure 4-3E for ammonia. Even at very high dosage of activated carbon 15 g/L and 25 g/L in each case, the removal efficiency is

only 29% and 18%. This is because activated carbon is dominated by nonpolar surfaces, and therefore they do not have significant adsorption capacity for polar (ionic) compounds like ammonium, nitrate and nitrite (Faust and Aly 1987). This is also confirmed by the Freundlich isotherm fitting results. The  $K_f$  for  $\text{NO}_3^-$ -N+ $\text{NO}_2^-$ -N and  $\text{NH}_4^+$ -N on activated carbon is very low, almost close to 0, indicating the adsorption of inorganic nitrogen is extremely unfavorable and activated carbon is not effectively treatment for removing them through physicochemical adsorption. Total nitrogen showed very similar situation with inorganic nitrogen removal using activated carbon, indicated by extremely small  $K_f$  as see in Table 4-2.

To summarize, when treating PBR effluent using activated carbon, both PAC and GAC proved to be effective in removing recalcitrant/slow-degrading organic compounds (with up to 91% removal efficiency), although the affinity of these compounds to activated carbon is relatively low compared to other organic compounds. However, activated carbon is not capable of removing inorganic nitrogen nor total nitrogen effectively indicated by both low removal efficiencies and extremely low affinity.

#### **4.3.4 Phase I operation: the effect of GAC with low loading rate**

##### *4.3.4.1 Organics removal with and without GAC*

Figure 4-4A shows the organics removal in the PBR over 200 days of operation. Before the addition of the GAC (Stage 1), COD removal efficiency was fairly stable at around  $73 \pm 4\%$ , and the effluent COD hovered around 300 mg/L. This is slightly lower than other conventional biological treatment processes for municipal wastewater (i.e., activated sludge), which normally removes 80-85% COD from wastewater (Metcalf & Eddy et al. 2003). Our previous studies with PHWW also found that there was always a sizeable fraction (~30%) of organics in PHWW that were not readily assimilated by microorganisms, and this occurred regardless of how PHWW

was treated— in a batch test with more than 7 days of biodegradation, or in a continuously operating PBR with shorter hydraulic retention time of 2 days (Zhou et al. 2011; Zhou et al. 2013). This effluent COD concentration without GAC (~300 mg/L COD) would meet the discharge limits established for petroleum refining point sources (388 mg/L COD, for the integrated subcategory), but it is above the limit for the petrochemicals subcategory (210 mg/L) (U.S. EPA, Effluent Guidelines: Petroleum Refining). These two benchmarks are considered to be reasonable targets for the wastewater from a process that produces a renewable alternative to standard petroleum crude oil. However, to meet more stringent discharge standards, including those commonly used for large-scale municipal wastewater treatment, additional treatment strategies need to be considered, such as incorporating adsorbents, which can enhance removal of residual organic compounds. The effluent during Stage 1 was sent for GC-MS analysis and our initial analysis found that many of the slow-degrading compounds contain ring structures and nitrogen heteroatoms as discussed before (section 4.3.2)

The addition of GAC to the PBR improved the COD removal. When the GAC was first added on day 65, the effluent COD showed a quick reduction from 300 mg/L down to 90 mg/L over several days, which is primarily credited to the physicochemical adsorption of recalcitrant organics. Then as the GAC became loaded, the average COD in the effluent increased up to 100-120 mg/L, which was maintained throughout Stage 2 and corresponded to an overall COD removal efficiency of 91%. Around 60% of the previously slow-degrading/recalcitrant compounds were removed with the addition of GAC to the PBR. Physicochemical adsorption certainly contributed significantly to the COD reduction, as proved by the batch test result discussed above. It is also possible that more biological degradation of these slow-degrading compounds occurred because these compounds were held in the reactor for an extended period

via adsorption on the GAC (Metcalf & Eddy et al. 2003). Note that there was incomplete removal of COD even immediately after the addition of a large quantity of GAC (200 g dosed into 10 L reactor): the lowest COD value observed was 83 mg/L. This result is consistent with what we saw in the batch adsorption test, indicating that there is a portion (~10%) of slow-degrading and non-absorbable organic compounds in PHWW. This COD level in effluent certainly meets the EPA standard if categorized as effluent from petroleum refining, and could be discharged into surface water.

#### 4.3.4.2 *Enhanced ammonia oxidation facilitated by GAC addition*

Ammonia is one of the biggest concerns for wastewater discharge. As shown in Figure 4-4B, during Stage 1 without GAC, the ammonia level in the effluent was 80-100 mg/L, corresponding to an average ammonia removal efficiency of 26%. After the addition of GAC, the ammonia dropped quickly to almost zero (within 4 days). This extremely low level maintained for more than 2 months all throughout Stage 2. As is well known, activated carbon typically has nonpolar surfaces that do not provide any significant adsorption capacity for ammonia, nor for the breakdown products of nitrate and nitrite. Therefore, physicochemical adsorption mechanisms would not have significant direct effect on ammonia removal in this study like it did with COD removal.

The comparison of ammonia ( $\text{NH}_4^+\text{-N}$ ) and nitrate+nitrite ( $\text{NO}_3^-\text{-N}+\text{NO}_2\text{-N}$ ) profiles in Figure 4-4B indicates that the enhanced ammonia oxidation processes greatly contributed to the increased ammonia removal. As shown in Figure 4-4B, there was almost no  $\text{NO}_3^-\text{-N}+\text{NO}_2\text{-N}$  in the effluent during Stage 1. As the GAC was added on day 65, there was a sudden spike in nitrate+nitrite levels that corresponded to a dramatic decrease of ammonia level. After the spike,  $\text{NO}_3^-\text{-N}+\text{NO}_2\text{-N}$  decreased slowly until it reached a steady level around 80 mg/L, which stayed

throughout the entire operation. The big spike of the  $\text{NO}_3^-$ -N+ $\text{NO}_2^-$ -N, which even exceeded the level of incoming nitrogen, is most likely related to the pattern of algal utilization of nitrogen source. Studies showed that algal cells grown in the presence of excess ammonium cannot utilize nitrate; and only if the supply of ammonium is inadequate (in the low  $\mu\text{M}$  range) they start to develop capability to utilize nitrate (Flynn 1991). As we can see in Figure 4-4, it is not until a couple of days after the addition of GAC that the  $\text{NH}_4^+$ -N level dropped from very high level to relatively low level (low  $\mu\text{M}$  range). During this couple of days, even nitrate kept being produced from ammonia oxidation process, they are not being consumed by the algae, which is dominant biomass in our reactor, until the algae “sensed” the very low extracellular  $\text{NH}_4^+$ -N level and started to “learn” how to use nitrate. During this period, the nitrate accumulated and resulted in big spike.

The most likely reason for such sudden improvement is that GAC removed some ammonia oxidation inhibitors. Ammonia oxidizing organisms are sensitive organisms and extremely susceptible to a wide variety of inhibitors (Metcalf & Eddy et al. 2003). A variety of organic and inorganic agents can inhibit the growth and action of these organisms. Inhibitors noted in previous studies include aromatic compounds like phenol (Lauchnor and Semprini 2013), and a diverse group of heterocyclic N compounds like pyrrole, pyridine, and indole (McCarty 1999) are also commonly identified in liquefaction wastewater from conversion of algae like *Spirulina* and other biomass (Elliott 1993; Pham et al. 2013). It was actually found in our preliminary result (see section 4.3.2) that many of the slow-degrading/recalcitrant compounds in Stage 1 effluent contains aromatic ring structures and nitrogen heteroatoms. High concentrations of ammonia itself can also be inhibitory to ammonia oxidizing organisms (Metcalf & Eddy et al. 2003). Given that GAC showed good physicochemical adsorption

capacity of the recalcitrant organic compounds (both in batch test and continuous operation), we anticipate that the sudden enhancement of ammonia oxidation is mainly a result of the removal of organic inhibitors by GAC.

It is worth mentioning that during the long term operation, biofilms may start to develop on GAC media that could further improve ammonia oxidation (Lee et al. 2002). GAC has been reported as an ideal support media for slow-growing and sensitive microbes, which can improve the biodegradation of toxic or recalcitrant compounds in wastewater (Van Agteren et al. 1998). These biofilm processes normally require a relatively long time to develop, and therefore should not have had such a sudden effect (within 3-4 days) on the inorganic nitrogen level as observed in this study. However, during the longer term operation, for example, like later in Stage 2 operation, this may be an important factor contributing to sustained ammonia removal.

The enhanced activity of ammonia oxidizing microbes may have also contributed to the enhanced removal of slow-degrading/recalcitrant organic compounds. A general characteristic of ammonia oxidizing microbes is a broad substrate range, including alkanes up to C<sub>16</sub>, alkenes, halocarbons, and various aromatic and heterocyclic compounds (McCarty 1999; Hyman et al. 1988). There is even interest in the use of these microorganisms for bioremediation of chlorinated hydrocarbons in the environment, thereby taking advantage of the broad spectrum of alternative substrates that can be used by ammonia oxidizing microbes. What is interesting is that high ammonia concentrations will decrease the oxidation rates of many alternative organic substrates (McCarty 1999). Therefore, as the ammonia level decreased in the PBR, the oxidation of various organic compounds by ammonia oxidizing microbes is expected to increase, which likely contributed to the enhanced removal of “recalcitrant” organics that began in Stage 2.

#### 4.3.4.3 *GAC facilitated long term microbial community activity/composition change*

The addition of GAC not only enhanced the removal of pollutants because of physicochemical adsorption, but it also had a long-term effect on pollutants removal by causing changes in the suspended microbial community change that favored the degradation of recalcitrant compounds and ammonia. As shown in Figures 4-4A and B during Stage 3, even after the GAC was removed, the COD and  $\text{NH}_4^+\text{-N}$  removal efficiencies still maintained high: 92% COD removal and almost 100%  $\text{NH}_4^+\text{-N}$  removal. Only biological activity from the suspended growing microbes (rather than any biofilms developed on the GAC) can account for the pollutants removal after GAC was removed during Stage 3. Thus, the suspended microbial community activity or composition was obviously different compared to that during Stage 1. This community composition change most likely already occurred during Stage 2, initiated by the addition of GAC. Many slow-degrading/recalcitrant compounds are actually degradable at low concentration but are inhibitory to the microbes at high concentration (Van Agteren et al. 1998). When the initial adsorption process of GAC helped to decrease toxic substrate level, the previously inhibited microbes had a chance to grow and degrade these substrates. As the microbes kept developing, the microbial community eventually became robust enough to keep up the rate of degradation with the feeding rate of these substrates. Thus, the level of these potentially inhibitory substrates could always be maintained below inhibitory concentrations in the reactor. In this case, GAC served as a rapid physicochemical sink for inhibitory or toxic substrates that allowed the microbes to survive and thrive.

Actually, the suspended microbial community must have already developed well enough during the end of Stage 2 before GAC was removed. Under this circumstance, simultaneous adsorption and biodegradation of inhibitory substrate must have occurred, resulting in continuous



bioregeneration of the GAC in-situ (Aktas and Ferhan 2007). During this process, as the inhibitory substrates in aqueous phase are degraded, those adsorbed on GAC would be slowly desorbed and released to be subsequently degraded by the microbes. Thus, the GAC is being continuously regenerated through biological activity. Bioregeneration of GAC has been reported and discussed in several previous studies including the aerobic biodegradation of phenolic compounds (Lee and Lim 2005) and aromatic compounds (De Jonge et al. 1996). When successful bioregeneration happens, the GAC adsorption process still provides benefit of buffering against shock loadings, toxic compounds, and fluctuations in biological performance due to temperature, pH, etc. Thus, the entire process would be much less sensitive to upset and natural variations in the operating conditions because GAC can temporarily store substrates while microbes are adapting to changing conditions. This will improve reactor stability and effluent water quality, which is important for wastewater treatment (Aktas and Ferhan 2007). Continuous bioregeneration of GAC is also a valuable process from an economic perspective because it would decrease the need to periodically replace or thermally regenerate the activated carbon. This resolves the issue that high dosage of GAC would be needed if the pollutants are removed only by the mechanisms of physicochemical adsorption and no inexpensive regeneration method is available. The bioregeneration observed in this study definitely benefits the proposed treatment process and makes it more applicable for large-scale operations by providing a cost-effective regeneration method.

One other thing worth pointing out is that the “recalcitrant/slow degrading compounds” may not actually be “recalcitrant”. Some changes in microbial activity could easily turn them into biodegradable compounds as observed in Stage 3. However, there was still about 10% residual COD in the effluent during Stages 2 and 3, which might be very similar to the residue

organics in the isotherm batch tests. These compounds could potentially be the “real” recalcitrant/slow degrading and also potentially non-absorbable.

#### 4.3.4.4 Cytotoxicity test result

Organic matter in wastewater effluents have often been cited as one of the biggest concerns for human and environmental health (Shon et al. 2006). As a proposed wastewater treatment scheme that will eventually discharge effluent into various surface waters, it is important to not only evaluate the ability of this hybrid PBR in removing pollutants, but also to evaluate the potential hazards for human and environmental health of its effluent. Therefore, the CHO mammalian cytotoxicity assay was used here to evaluate the relative cytotoxicity removal of the treatment process. Figure 4-5A compares the concentration-response curves for organics extracted from wastewater samples before and after treatment with PBR and GAC (8-16 replicated experiments were averaged and plotted). The concentration factor refers to the number of folds of concentration of the isolated organic material as compared to the original wastewater sample. The data in Figure 4-5A was used to do regression analysis and to calculate the  $LC_{50}$  (the dosage that results in a 50% reduction of cell density compared to the negative control). As demonstrated in Figure 4-5A, the toxicity of the wastewater was reduced after biological treatment, and the presence of GAC in the PBR helped to further enhance toxicity removal. Specifically, the  $LC_{50}$  concentration factor values of the influent, effluent without GAC, effluent with GAC for the first 15 days, and effluent with GAC for the second 15 days were  $4.8\times$ ,  $8\times$ ,  $11.7\times$  and  $12.7\times$ , respectively. Pham used the same assay and found that the  $LC_{50}$  of the secondary effluent from a local wastewater treatment plant was about  $4\times$  (Pham 2014).

Figure 4-5B represents the cytotoxicity index values of the tested wastewater samples (the cytotoxicity index value was determined as  $(LC_{50})^{-1}(\times 10^3)$ , where a larger value represents

greater toxic potency). The cytotoxicity index value of reactor influent reduced 40% after PBR treatment without GAC. It was previously reported that after secondary treatment (biological treatment), the effluent from a conventional wastewater treatment plant was only 30% less toxic than the influent when the same CHO cell assay was used (Pham 2014). While it is a little bit surprising that conventional wastewater treatment scheme only removed 30% of the cytotoxicity from wastewater, this comparison also shows that our proposed algal-bacterial treatment scheme is completely capable of removing cytotoxicity and even outperform the most widely used wastewater treatment scheme.

The addition of GAC helped to enhance the removal of cytotoxicity to 59%, as shown in Figure 4-5B. The comparison between COD and cytotoxicity removal indicates that the recalcitrant and non-absorbable organics tends to contribute more to the cytotoxicity: the 30% unremoved COD (after biological treatment during Stage 1) corresponds to 60% of the cytotoxicity, and the 10% unremoved COD (after biological and physicochemical treatment during Stage 2) that is both non-biodegradable and non-absorbable corresponds to more than 40% of the cytotoxicity. Although as discussed before, the cytotoxicity of our current effluent already reached a decent level, further study is recommended to characterize these residual compounds. Effective removal methods will be needed if there is serious concern of these compounds to aquatic ecosystems and human health because of long-term accumulation in the environment. Potential methods include other adsorption (resins), ozonation, wet-air oxidation and/or second-stage biological treatment with adapted or specialized microbes.

### **4.3.5 Phase II operation: the effect of loading rate**

#### *4.3.5.1 Organic removal*

The main objective of this phase's operation is to investigate the effect of loading rate on reactor performance (pollutants removal and algal biomass production). It needs to be pointed out that although loading rate is commonly presented as kg COD/m<sup>2</sup>/day (which depends on the area of the reactor), since we don't think it is fair to calculate organic loading rates based on the cross section of our cylindrical vertical reactor, we used PHWW percentage to represent the relative organic loading rate most of the times in this section.

Figures 4-6 shows the COD, ammonia nitrogen, total nitrogen, and biomass concentration at 4 different loading rates: 1%, 2%, 3% and 4% PHWW. Figure 4-7 summarizes the reactor performance under different loading rates during the steady state portion. The COD removal efficiency was between 73-93%, which was fairly good compared to other similar algal-bacterial based wastewater treatment systems. For instance, Aziz (1992) reported COD removals of 80% or less when treating domestic wastewater and piggery wastewater, which generally contain less toxic compounds and more biodegradable compounds than the PHWW used in this study. Godos (2009) reported 76±11% COD removal efficiency and HRT of 10 days during long-term operation of high rate algal ponds for treating piggery wastewater with influent COD concentration of 4346 ± 1848 mg/L, which had a similar COD as our 4% PHWW influent. Under aerobic conditions, organic removal is related to many factors, including the composition of functional microbes, dissolved oxygen level (DO), organic loading rate, hydraulic retention time, solid retention time, etc. (Metcalf & Eddy et al. 2003). The advantageous microbial community with enhanced degradation of recalcitrant compounds might have contributed significantly to the good removal efficiency in this study, as discussed in the Phase I results.

Besides biotic factors, a relatively high aeration rate might have also contributed to the better COD removal efficiency in our study.

The organic removal rate in general showed positive relationship with organic loading rate, as shown in Figure 4-7B, indicating that no significant inhibition of aerobic degradation existed. However, the percent removal efficiency showed a slight decrease as the loading rate increased, from 93% under conditions of 1% PHWW, to 86% under 2% PHWW, to 80% under 3% PHWW, to 79% under 4% PHWW. One possible explanation is that higher organic loading rates created adverse environment. As the loading rate kept increasing, toxic organic compounds level started to increase in the reactor, to the level that may causes slight inhibition on the degradation of these compounds in our case. It is common that excessive loading rate can be detrimental to the survival of both algae and bacteria (Metcalf & Eddy et al. 2003; Mayo and Noike 1994). Another possibility is that as the loading rate increased, the oxygen supply did not catch up with the increasing demand for oxygen.

#### 4.3.5.2 Nitrogen removal

Ammonia nitrogen removal efficiency decreased significantly as the loading rates increased, from 99% to 68%, and to 50% eventually, as shown in Figures 4-6 and 4-7. There are mainly two mechanisms for ammonia removal: biological assimilation into biomass and biological ammonia oxidation (into nitrite/nitrate). Both mechanisms might have been affected as the loading rate increased. As discussed in previous chapter, high PHWW concentration has inhibitory effect to algae, resulting in slower or even stopped algal growth. Higher concentrations of PHWW in the influent caused more inhibition to algal growth, resulting in decreased assimilation rate of ammonia. However, since the biomass concentration did not show any obvious change, the decrease in ammonia assimilation is not likely to be the main cause. The

other explanation is the impaired ability of ammonia oxidizing microbes to convert ammonia into nitrate, caused by increased inhibition to ammonia oxidizer.

Total nitrogen removal efficiency kept at the similar level, around 30% as shown in Figure 4-7. Compared to organics, there is still much space for improvement in nitrogen removal. The TN in the effluent currently consists of two dominant parts, organic nitrogen (~50%), and inorganic nitrogen. The inorganic nitrogen assimilation rate could be enhanced by optimizing the reactor operation, e.g., decrease the solid retention time to allow more nutrient uptake. The improvement of the degradation of the organic nitrogen into inorganic nitrogen will need to be further investigated.

#### 4.3.5.3 GC-MS analysis results

When the loading rate was 4% PHWW, GC-MS was used to analyze the removal of individual organic compounds. As shown in Figure 4-8, many of the peaks in the original influent disappeared after the treatment. The identified compounds and their quantities (relative integrated signal) are summarized in Table 4-4. Many of the organic acids, like acetic acid, propanoic acid, butanoic acid are readily degradable by bacterial, and can also be utilized by algae to support mixotrophic or heterotrophic growth (Perez-Garcia et al. 2011). We note that many of the detected aromatic compounds such as 3-Pyridinol, N-methylglutarimide, as well as nitrogen heterocyclic compounds such as 2-Piperidinone, Cycloglycyl valine also were well removed during treatment.

Isopropanol and acetonitrile are the only two detected compounds that showed an increase in the effluent compared to the influent. Acetonitrile is the simplest organic nitrile, and its increase suggests that more complicated organonitriles have been degraded during the PBR treatment. Organonitriles represent a class of extremely toxic compounds (and priority

pollutants) that affect many different living organisms, including human beings, and are known to be highly carcinogenic and mutagenic, and are hard to degrade (Li et al. 2007). While the increase in acetonitrile indicates that the potentially more toxic organonitroles have been degraded, it also highlights that acetonitrile degradation is a rate limiting step. Isopropanol is also known to be toxic to both aquatic species and human beings (Lilius et al. 1995). Both of these two compounds also have poor GAC adsorbability, as shown in Table 4-4, even at very high GAC dosage of 25 g/L.

#### **4.3.6 Phase III operation: the effect of SRT and HRT**

HRT was only varied during reactor start up in phase I. During the reactor startup (day 0-50), various HRT ranging from 2-10 days, and SRT ranging from 20 days to infinite were used. COD removal was consistently between 60-70%, even though removal of other nutrients showed much more significant variability. This is probably because organic removal was mainly due to heterotrophic bacterial activity, and HRT and SRT values tested here, as well as other operation parameters (e.g., aeration rate) were within the range to obtain good organic removal. In Chapter 3, we have demonstrated that in batch tests the organic (COD) removal efficiency was not affected by the photoautotrophic microbial activity, and most of the organics removal could be achieved within the first 24 hours of treatment. Both of these results indicate that if COD removal is the only treatment goal, then there is still space to further decrease HRT (5 days) of the current operation, which is fairly long compared to the typical HRT used in conventional wastewater treatment plant (6-8 hours for secondary biological aeration tank).

Variations in SRT had a significant impact on ammonia removal and biomass concentration. Figure 4-9 shows the concentration of pollutants as well as biomass concentration when SRT changed from 20 days to 15 days, and to 10days. When SRT changed to 15 days,

there was no significant change of COD, ammonia nitrogen, or total nitrogen. As expected, the biomass concentration decreased. Our previous experience, as well as later experiment with the PBR indicates that 15 days' SRT under such operation condition is feasible and won't result in the complete wash out of biomass.

However, the PBR showed pretty obvious response when SRT was changed from 15 days to 10 days. Several days after the change, the ammonia nitrogen in the effluent started to increase, and quickly approached the influent level (Figure 4-9). Although the other parameters did not show a significant change, the failure of the ammonia oxidation is considered a major failure of the reactor performance. At the same time, the color of the biomass started to change: from dark green to light yellowish green, indicating an unhealthy condition for the microbes. Based on both the treatment failure in ammonia removal and deteriorating biomass, the SRT was switched back to 15 days. However, the ammonia nitrogen in the influent kept increasing, and the reactor turned to yellow completely indicating the significant loss of active photosynthetic algal biomass.

TN level showed a slight decrease in the effluent when SRT decreased to 10 days. While the average TN in the effluent was  $530 \pm 21$  mg/L when SRT was 15 days, the TN dropped to  $415 \pm 15$  mg/L when the SRT was 10 days. This is expected, since the main mechanism of the TN removal here is biomass assimilation and subsequent biomass harvesting. Thus, when SRT is decreased, more biomass is harvested, and more TN is removed. Although a short SRT of 10 days temporarily promoted nutrient removal, it also lead to failure of the reactor in other aspects, and thus this is not a good long-term strategy.

The reactor failure is most likely caused by the washout of ammonia oxidizing microbes in the reactor under short SRT (10 days). With conventional nitrification in activated sludge



processes, the effectiveness of ammonia oxidizing is controlled by maintaining a suitable SRT, and for municipal wastewater systems, a typical nitrification SRT is between 8-20 days (Celenza 1999). In our case, 10 days appears to already be outside the favorable SRT range. The failure in ammonia oxidation also had a negative impact on algae, which is known to be sensitive to high ammonia concentrations: the chlorophyll concentration dropped from 70 mg/L when the SRT was 20 days to only 15 mg/L at the end of the 10 day SRT operation.

The reactor failure was not corrected by simply changing the SRT back to 15 days, a condition that has been proven acceptable. With this change, the ammonia level remained high and biomass kept deteriorating. Therefore, it was decided that the reactor should be run in batch mode for a period of time to recover from the failure.

#### **4.3.7 Phase IV operation: the effect of GAC under high loading rate**

During Phase I, adding GAC to the PBR showed several advantages including (1) reduction of refractory pollutants, (2) better ammonia removal. We want to further investigate on the third perspective: how GAC help PBR to improve system stability, especially under relative adverse conditions. Based on our reasoning of reactor failure during phase III (the wash out of ammonia oxidizing microbes), we made the hypothesis that GAC can improve the system stability by developing biofilm on its surface allowing for stable operation even during adverse SRT condition. In order to investigate on the long term effect of GAC, GAC was added before we created the same failure condition (switching SRT from 20 days to 15 days, and then to 10 days). As we can see in Figures 4-9A and B, again the addition of GAC resulted in enhanced COD and ammonia removal, which is consistent with what we've seen in Phase I operation. Biomass concentration showed an increase after the addition of GAC, as shown in Figure 4-9D,

probably due to mitigated inhibition from the reduction in both toxic organic compounds and ammonia.

After stabilizing the reactor making sure it was operating normally and the biomass was healthy again, we started to recreate the condition that lead to previous failure on day 545. As shown in Figure 4-9, after the SRT was changed to 10 days (on day 568), ammonia showed an initial increase and then quickly stabilized at around 120 mg/L. The COD, as expected, did not show any obvious change. Biomass also showed a decrease, as anticipated based on the previous effect of reducing SRT. However, the biomass during Phase IV operations, maintained a healthy status as indicated by maintaining a dark green color as well as microscopic examination of the biomass. By comparing the ammonia level and biomass condition with the corresponding situation during Phase III, it is obvious that GAC enhanced the PBR stability by preventing the failure caused by short SRT. This can be explained by nitrifiers that colonized the GAC, and were kept within the reactor and functioning well for ammonia oxidizing. This effect may not be obvious during periods with low loading rates and long SRTs, but is crucial with high loading rates or short SRTs.

In order to confirm the effect of GAC on reactor stability under adverse conditions, the GAC was removed at day 602. The ammonia concentration showed a quick increase right away, and at the same time, the biomass started to turn yellow, as observed during the Phase III failure. The concentration of biomass showed a sharp decrease too, reaching the lowest point (<500 mg/L) during the entire PBR operation. At this point, we can make the conclusion that, the removal of GAC resulted in reactor failure again.

To summarize the Phase IV operation, when the condition that leads to previous performance failure was recreated, the existence of GAC helped the microbes to survive well in the reactor rather than being washed out, resulting in stable performance of the reactor.

#### 4.4 Conclusions

A PBR that incorporated hollow-fiber membranes and GAC was developed and operated over 800 days to monitor the long-term performance when treating a combination of municipal wastewater and PHWW, as well as to evaluate the effect of activated carbon on improving effluent quality and stabilizing reactor performance. During operation covering a range of operating conditions (15-20 days SRT, 1% to 4% PHWW loading rate, with and without GAC), the PBR supported stable and efficient removal of organic carbon (79%-93% COD) and nitrogen (50%-99%  $\text{NH}_4^+$ , and 27%-30% TN). Increasing PHWW loading rates generally reduced the removal of COD and  $\text{NH}_4^+$ . SRT below 15 days lead to reactor failure without GAC present. The addition of GAC facilitated stable PBR performance with shorter SRTs and higher PHWW loading rates. GAC also improved COD removal from 70% to over 90%, improved  $\text{NH}_4^+$  removal from 26% to 100%, and improved cytotoxicity removal of the combined wastewater from 40% to 60%.

#### 4.5 References

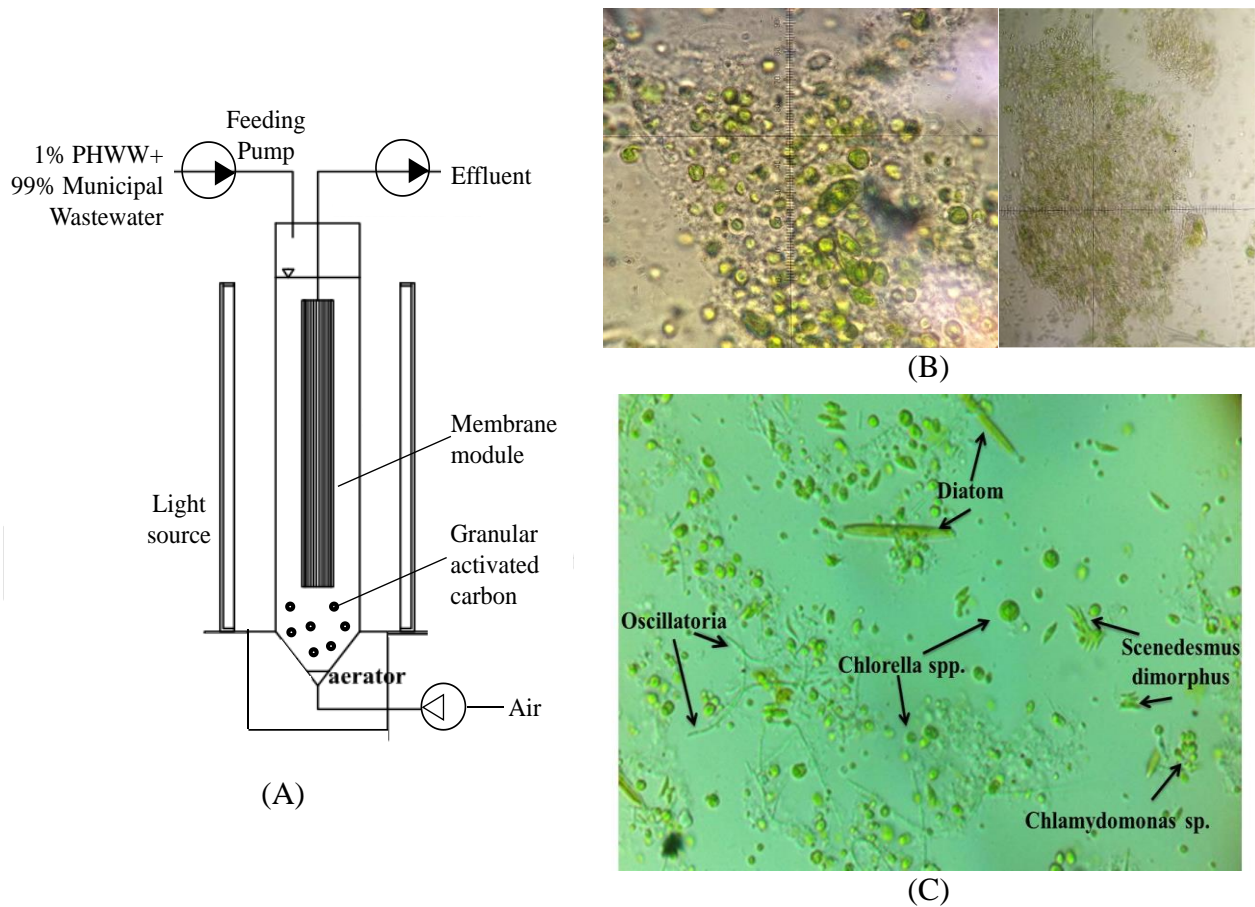
- Aktas, Ö. and Ç. Ferhan. 2007. Bioregeneration of activated carbon: a review. *International Biodeterioration & Biodegradation* 59(4): 257-272.
- Anastasakis, K. and A. B. Ross. 2011. Hydrothermal liquefaction of the brown macro-alga *Laminaria Saccharina*: Effect of reaction conditions on product distribution and composition. *Bioresource Technology* 102(7): 4876-4883.
- Aziz, M. A. and W. J. Ng. 1992. Feasibility of wastewater treatment using the activated-algae process. *Bioresource Technology* 40(3): 205-208.

- Celenza, G. 1999. *Industrial Waste Treatment Process Engineering: Biological Processes, Volume 2*. Lancaster, PA: CRC Press.
- De Jonge, R. J., A. M. Breure and J. G. Van Andel. 1996. Bioregeneration of powdered activated carbon (PAC) loaded with aromatic compound. *Water Research* 30(4): 875-882.
- Elliott, D. C. 1993. Evaluation of wastewater treatment requirements for thermochemical biomass liquefaction. In *Advances in Thermochemical Biomass Conversion*, 1299-1313. Netherlands: Springer.
- Faust, S. D. and O. M. Aly. 1987. *Adsorption Processes for Water Treatment*. Butterworth London.
- Flynn, K. 1991. Algal carbon–nitrogen metabolism: a biochemical basis for modelling the interactions between nitrate and ammonium uptake. *Journal of Plankton Research* 13(2): 373-387.
- Giusti, D., R. Conway and C. Lawson. 1974. Activated carbon adsorption of petrochemicals. *Journal of Water Pollution Control Federation* 100: 947-965.
- Godos, I. d., S. Blanco, P. A. Garc ía-Encina, E. Becares and R. Muñoz. 2009. Long-term operation of high rate algal ponds for the bioremediation of piggery wastewaters at high loading rates. *Bioresource Technology* 100(19): 4332-4339.
- Hyman, M. R., I. B. Murton and D. J. Arp. 1988. Interaction of Ammonia Monooxygenase from *Nitrosomonas europaea* with Alkanes, Alkenes, and Alkynes. *Applied and Environmental Microbiology* 54(12): 3187-3190.
- Jena, U., K. C. Das and J. R. Kastner. 2011. Effect of operating conditions of thermochemical liquefaction on biocrude production from *Spirulina platensis*. *Bioresource Technology* 102(10): 6221-6229.
- Lauchnor, E. G. and L. Semprini. 2013. Inhibition of phenol on the rates of ammonia oxidation by *Nitrosomonas europaea* grown under batch, continuous fed, and biofilm conditions. *Water Research* 47(13): 4692-4700.
- Lee, H. S., S. J. Park and T. I. Yoon. 2002. Wastewater treatment in a hybrid biological reactor using powdered minerals: effects of organic loading rates on COD removal and nitrification. *Process Biochemistry* 38(1): 81-88.
- Lee, K. M. and P. E. Lim. 2005. Bioregeneration of powdered activated carbon in the treatment of alkyl-substituted phenolic compounds in simultaneous adsorption and biodegradation processes. *Chemosphere* 58(4): 407-416.

- Li, T., J. Liu, R. Bai, D. Ohandja and F. Wong. 2007. Biodegradation of organonitriles by adapted activated sludge consortium with acetonitrile-degrading microorganisms. *Water Research* 41(15): 3465-3473.
- Lilius, H., T. H ästbacka and B. Isomaa. 1995. A comparison of the toxicity of 30 reference chemicals to *Daphnia Magna* and *Daphnia Pulex*. *Environmental Toxicology and Chemistry* 14(12): 2085-2088.
- Mayo, A. W. and T. Noike. 1994. Effect of glucose loading on the growth behavior of *Chlorella vulgaris* and heterotrophic bacteria in mixed culture. *Water Research* 28(5): 1001-1008.
- McCarty, G. 1999. Modes of action of nitrification inhibitors. *Biology and Fertility of Soils* 29(1): 1-9.
- Metcalf & Eddy, G. Tchobanoglous, F. L. Burton and H. D. Stensel. 2003. *Wastewater Engineering: Treatment and Reuse*. 4th ed. Boston: McGraw-Hill.
- Perez-Garcia, O., F. M. E. Escalante, L. E. de-Bashan and Y. Bashan. 2011. Heterotrophic cultures of microalgae: Metabolism and potential products. *Water Research* 45(1): 11-36.
- Pham, M. 2014. Characterizing the effects of hydrothermal processes on bioactive compounds in wastewater bioenergy systems. PhD diss. University of Illinois at Urbana-Champaign.
- Pham, M., L. Schideman, J. Scott, N. Rajagopalan and M. Plewa. 2013. Chemical and biological characterization of wastewater generated from hydrothermal liquefaction of spirulina. *Environmental science technology* 47(4): 2131-8.
- Plewa, M. J., Y. Kargalioglu, D. Vanker, R. A. Minear and E. D. Wagner. 2002. Mammalian cell cytotoxicity and genotoxicity analysis of drinking water disinfection by-products. *Environmental and Molecular Mutagenesis* 40(2): 134-142.
- Plewa, M. J., E. D. Wagner, D. H. Metz, R. Kashinkunti, K. J. Jamriska and M. Meyer. 2012. Differential toxicity of drinking water disinfected with combinations of ultraviolet radiation and chlorine. *Environmental Science & Technology* 46(14): 7811-7817.
- Richardson, S. D. 2011. XAD resin extraction of disinfectant byproducts drinking water. *RSB-003.1*. Athens, GA,: Environmental Protection Agency.
- Shon, H. K., S. Vigneswaran and S. A. Snyder. 2006. Effluent organic matter (EfOM) in wastewater: Constituents, effects, and treatment. *Critical Reviews in Environmental Science & Technology* 36(4): 327-374.
- Torri, C., L. Alba, C. Samori and D. Fabbri. 2012. Hydrothermal Treatment (HTT) of Microalgae: Detailed Molecular Characterization of HTT Oil in View of HTT Mechanism Elucidation. *Energy Fuels* 26(1): 658-671.

- Van Agteren, M. H., S. Keuning and D. Janssen. 1998. *Handbook on Biodegradation and Biological Treatment of Hazardous Organic Compounds*. Netherlands: Springer.
- Zhou, Y., L. Schideman, G. Yu and Y. Zhang. 2013. A synergistic combination of algal wastewater treatment and hydrothermal biofuel production maximized by nutrient and carbon recycling. *Energy and Environmental Science* 6(12): 3765-3779.
- Zhou, Y., L. C. Schideman, Y. Zhang, G. Yu, Z. Wang and M. Pham. 2011. Resolving Bottlenecks in Current Algal Wastewater Treatment Paradigms: A Synergistic Combination of Low-Lipid Algal Wastewater Treatment and Hydrothermal Liquefaction for Large-Scale Biofuel Production. In *Proceeding of Energy and Water 2011: Efficiency, Generation, Management, and Climate Impacts*, 347-361. Chicago, IL: Water Environment Federation.

## 4.6 Figures and Tables

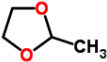
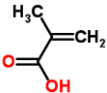
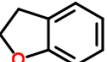
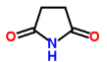
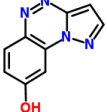
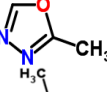
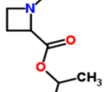



**Figure 4-1. Continuous flow hollow fiber membrane photobioreactor set up. (A) reactor configuration; (B) algal-bacterial flocs; (C) individual algal cells inside algal bioreactor.**

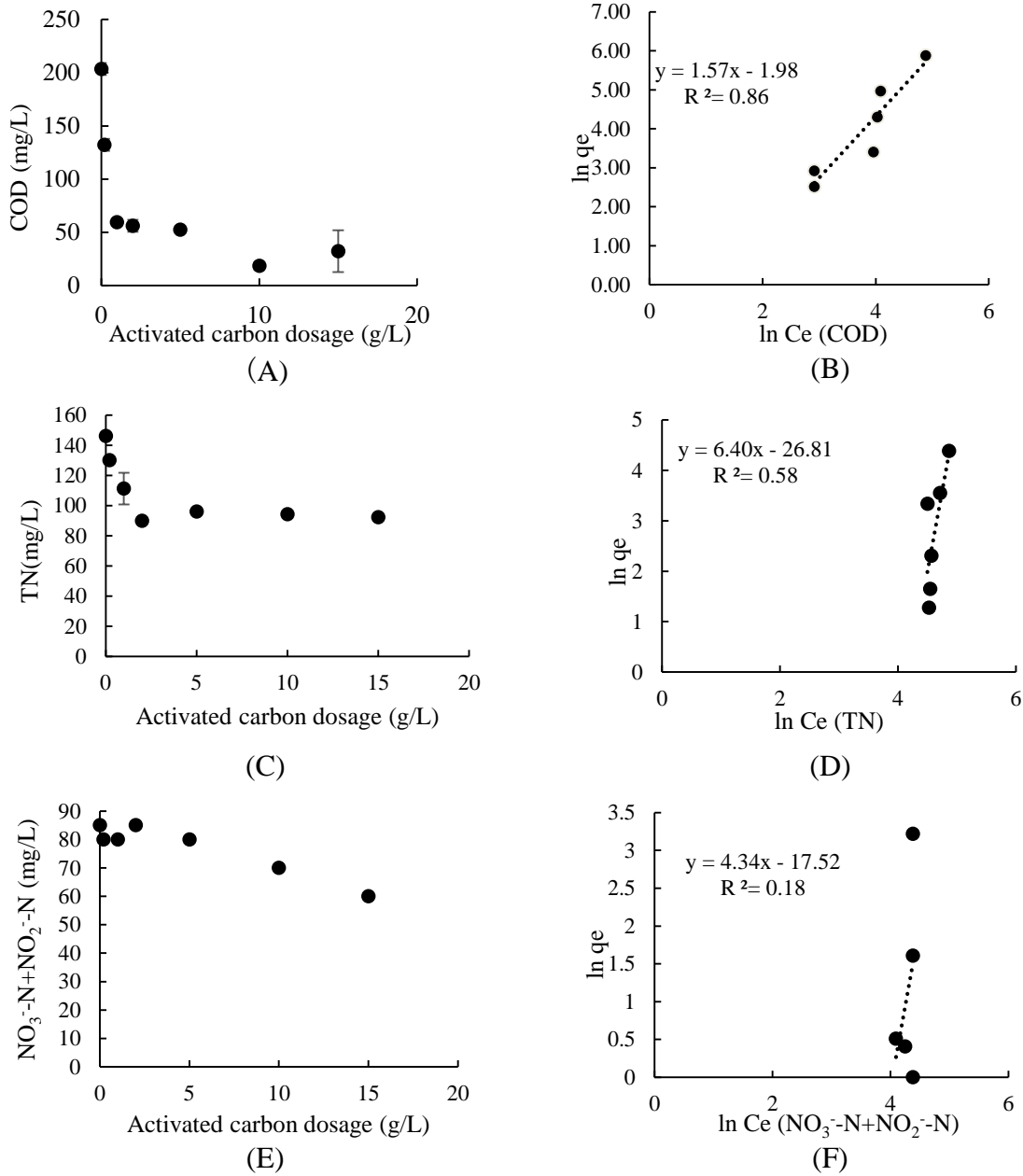
**Table 4-1. Four phases of reactor operation.**

Phase	I	II	III	IV
Feed	1% PHWW	1%, 2%, 3%, 4% PHWW	4% PHWW	4-5% PHWW
SRT	20 days	20days	10, 15 and 20 days	10, 15 and 20 days
HRT			5 days	
GAC	With (200 g)	without	without	With (200 g)

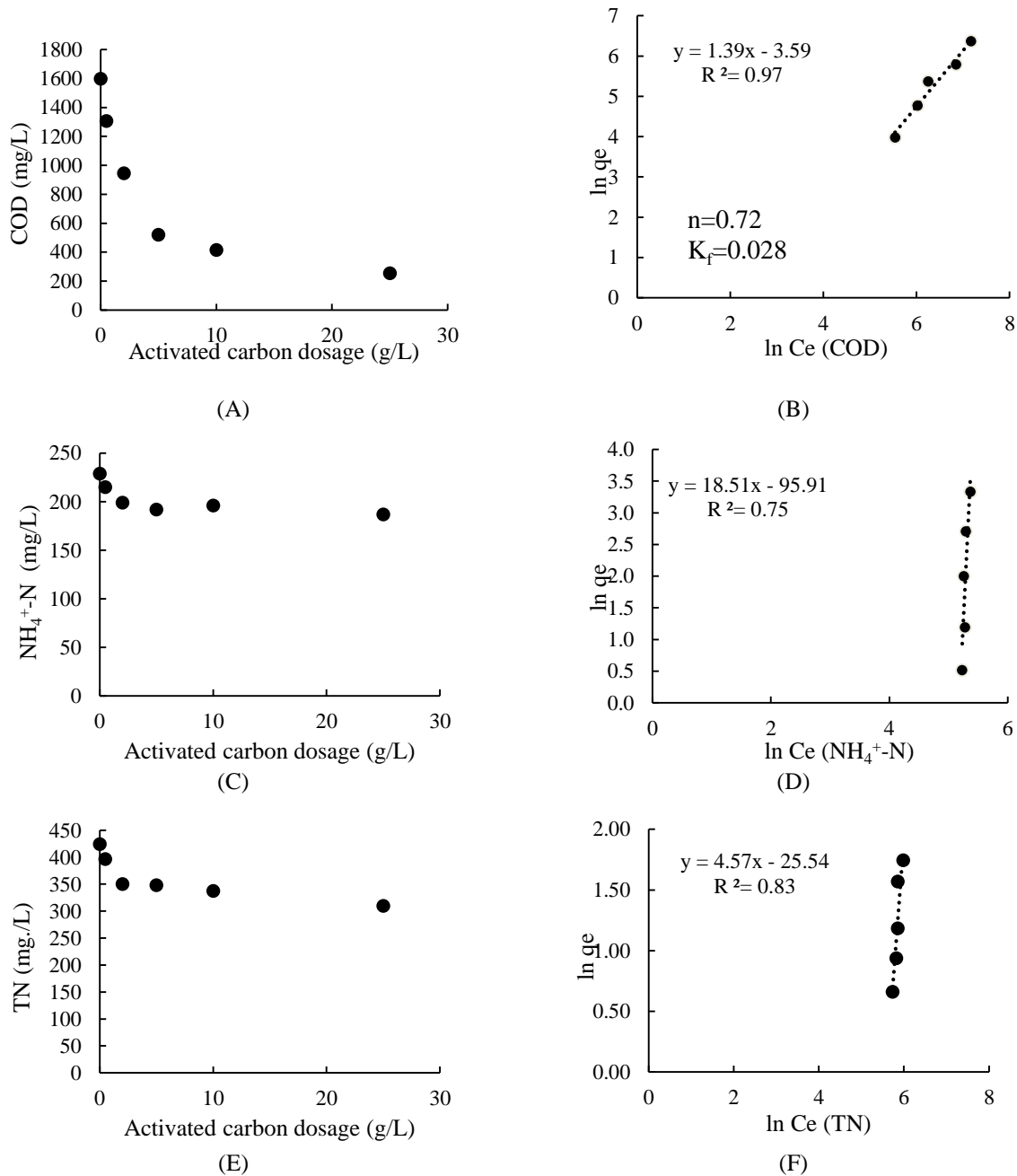
**Table 4-2. Identified recalcitrant/slow-degrading compounds in PRB effluent using 1% PHWW as influent.**

No	Name	Formula	Structure
1	1,3-Dioxolane, 2-methyl	C <sub>4</sub> H <sub>8</sub> O <sub>2</sub>	
2	2-Propenoic acid, 2-methyl-	C <sub>4</sub> H <sub>6</sub> O <sub>2</sub>	
3	Benzofuran, 2,3-dihydro-	C <sub>8</sub> H <sub>8</sub> O	
4	2,5-Pyrrolidinedione	C <sub>4</sub> H <sub>5</sub> NO <sub>2</sub>	
5	Pyrazolo[5,1-c][1,2,4]benzotriazin-8-ol	C <sub>9</sub> H <sub>6</sub> N <sub>4</sub> O	
6	2-Methyl[1,3,4]oxadiazole	C <sub>3</sub> H <sub>4</sub> N <sub>2</sub> O	
7	N-Ethyl-2-isopropoxycarbonylazetidone	C <sub>9</sub> H <sub>17</sub> NO <sub>2</sub>	
8	1-Pyrrolid-2-one, N-carbamoyl-	C <sub>5</sub> H <sub>8</sub> N <sub>2</sub> O <sub>2</sub>	





**Figure 4-2. Activated carbon adsorption batch test results when treating photobioreactor (PBR) effluent with 1% post-hydrothermal liquefaction wastewater (PHWW) as PBR influent. (A)(C)(E) The removal of chemical oxygen demand (COD), ammonia nitrogen (NH<sub>4</sub><sup>+</sup>-N) and total nitrogen (TN). (B)(D)(F) Freundlich adsorption isotherm of COD, TN and NO<sub>3</sub><sup>-</sup>-N+NO<sub>2</sub><sup>-</sup>-N.**



**Figure 4-3. Activated carbon adsorption batch test results when treating photobioreactor (PBR) effluent with 4% post-hydrothermal liquefaction wastewater as PBR influent. (A)(C)(E) The removal of chemical oxygen demand (COD), ammonia nitrogen (NH<sub>4</sub><sup>+</sup>-N) and total nitrogen (TN). (B)(D)(F) Freundlich adsorption isotherm of COD, TN and NO<sub>3</sub><sup>-</sup>-N+NO<sub>2</sub><sup>-</sup>-N.**

**Table 4-3. Freundlich isotherm parameters for adsorption of pollutants onto activated carbon.**

Water sample	Activated carbon	Pollutants	n	K <sub>f</sub>	R <sup>2</sup>
PBR effluent when the influent is 1% PHWW	ULTRA DARCO 100 PAC	COD	0.64	0.14	0.86
		NO <sub>3</sub> <sup>-</sup> -N+NO <sub>2</sub> <sup>-</sup> -N	0.23	2.5E-8	0.18
		TN	0.16	2.3E-12	0.58
PBR effluent when the influent is 4% PHWW	Calgon 400 GAC	COD	0.72	0.028	0.97
		NH <sub>4</sub> <sup>+</sup> -N	0.05	2E-42	0.75
		TN	0.22	8E-12	0.83

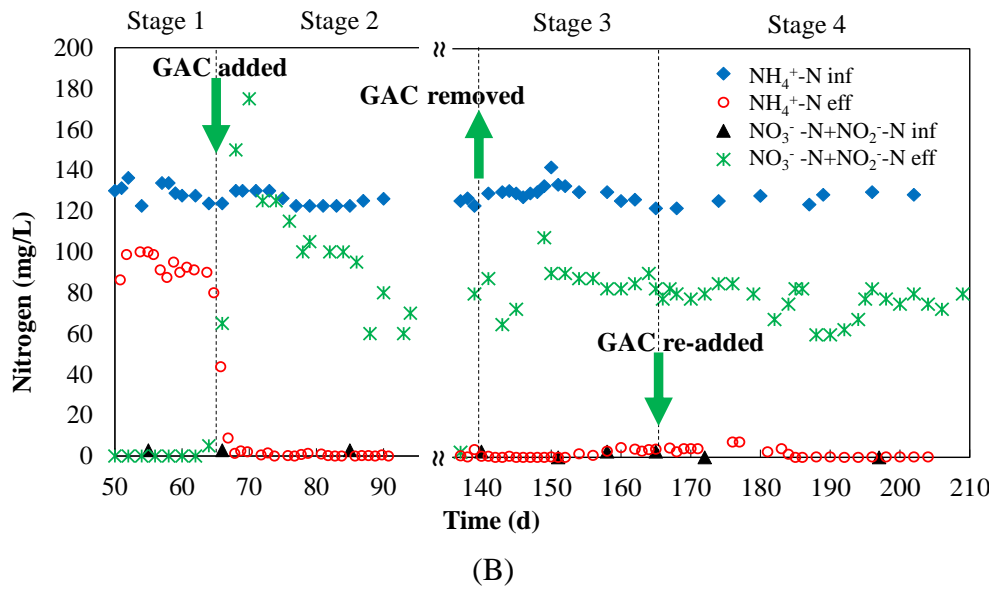
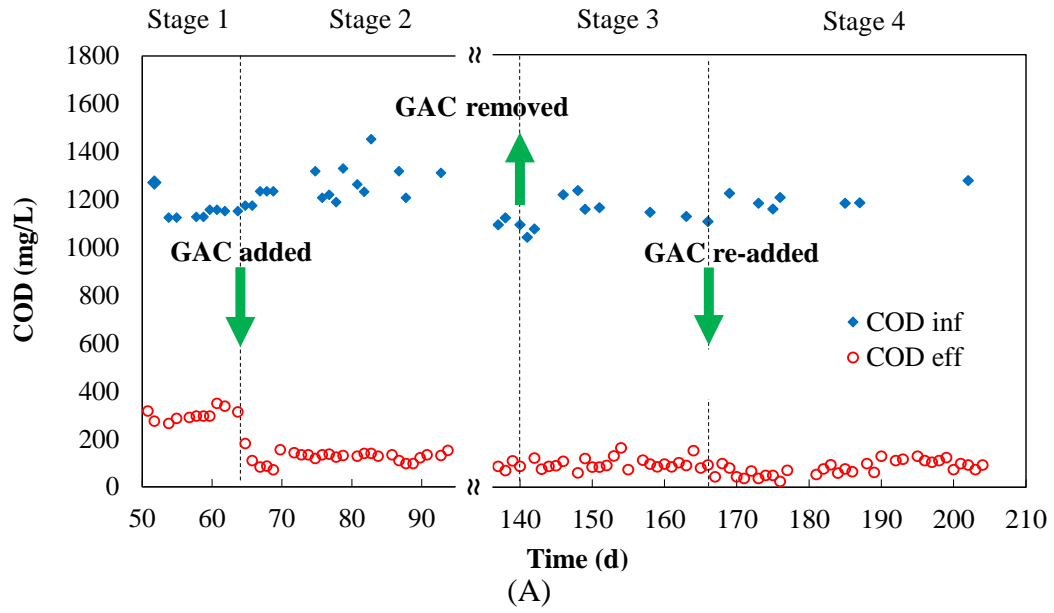
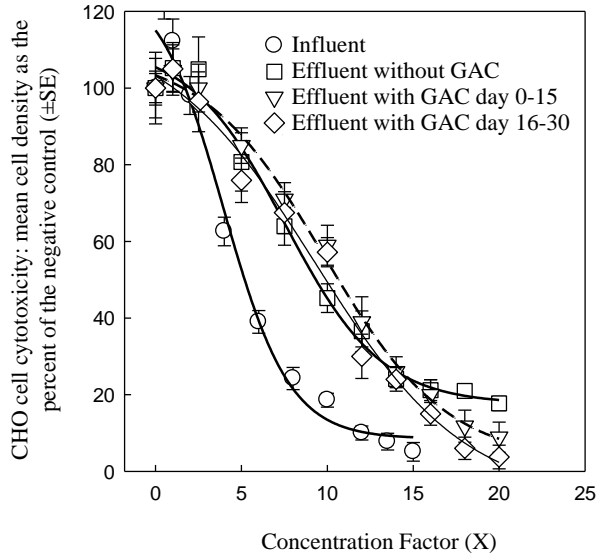
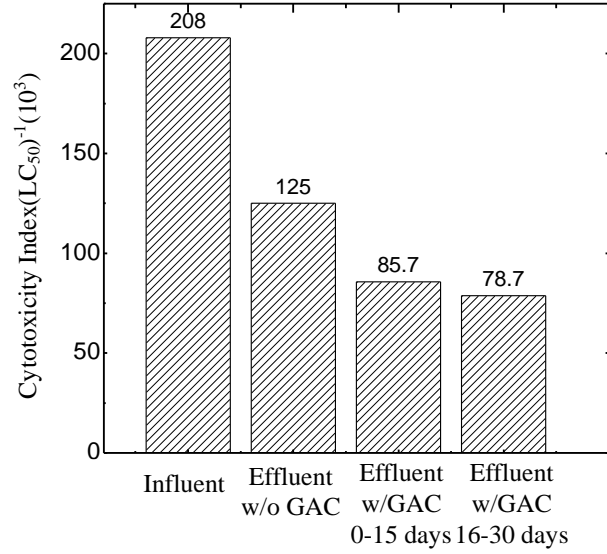


Figure 4-4. The effect of GAC on COD removal (A) and inorganic nitrogen removal (B) during Phase I operation.

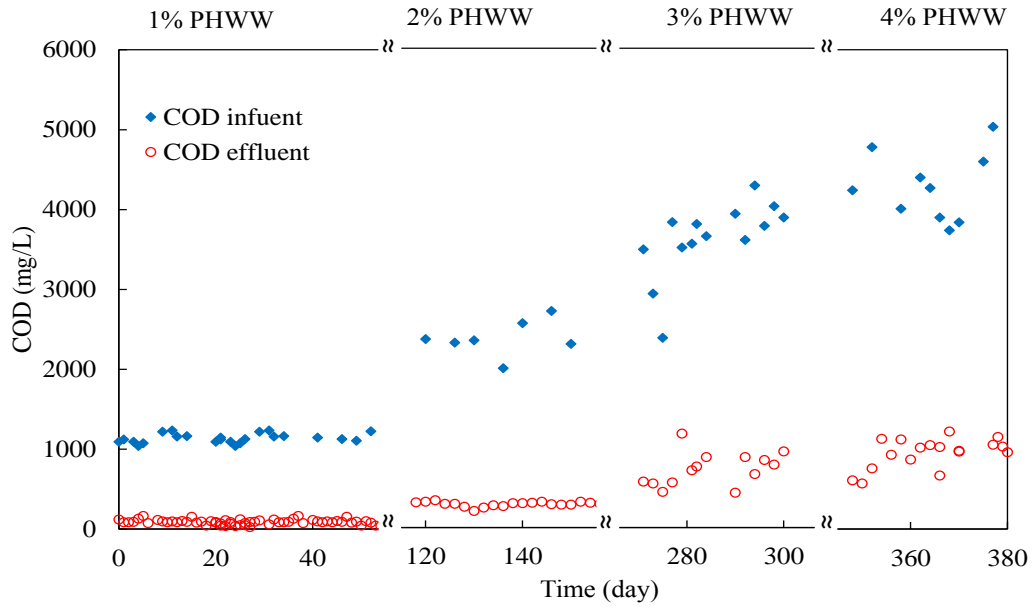


(A)

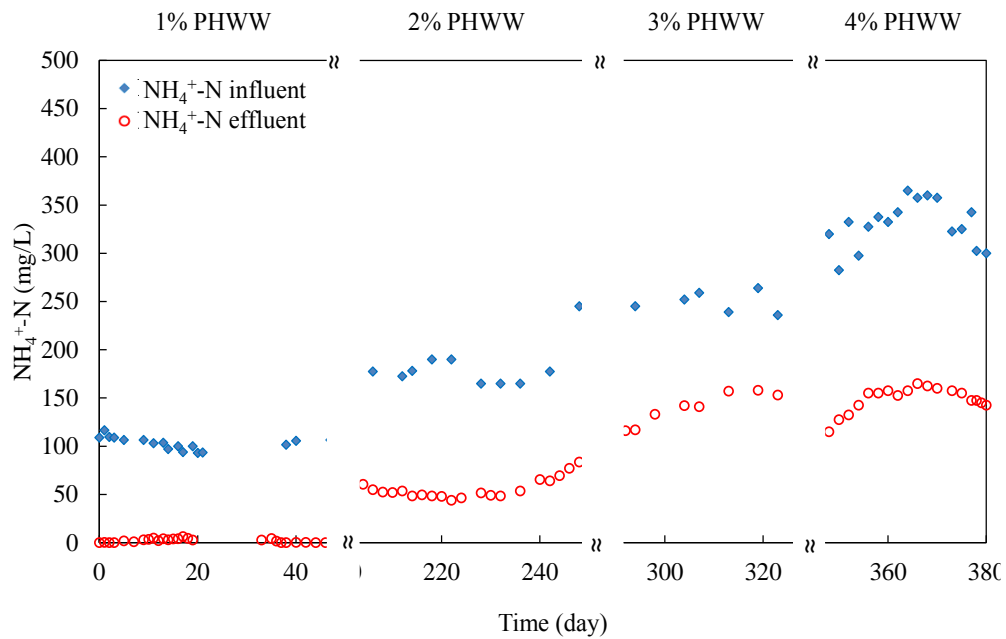


(B)

**Figure 4-5. Cytotoxicity test results of the wastewater before and after photobioreactor treatment during Phase I operation. (A) CHO cytotoxicity concentration response curves for organic extract from 1% *Spirulina* post-hydrothermal liquefaction wastewater (PHWW) and 99% municipal wastewater before and after treatment with algal bioreactor and GAC. Their response at each concentrating factor was generated from 8-16 independent clones of CHO cells. (B) Comparison of the CHO cell cytotoxicity index values for PHWW before and after treatment with algal bioreactor and GAC. Index values are expressed in dimensionless units.**

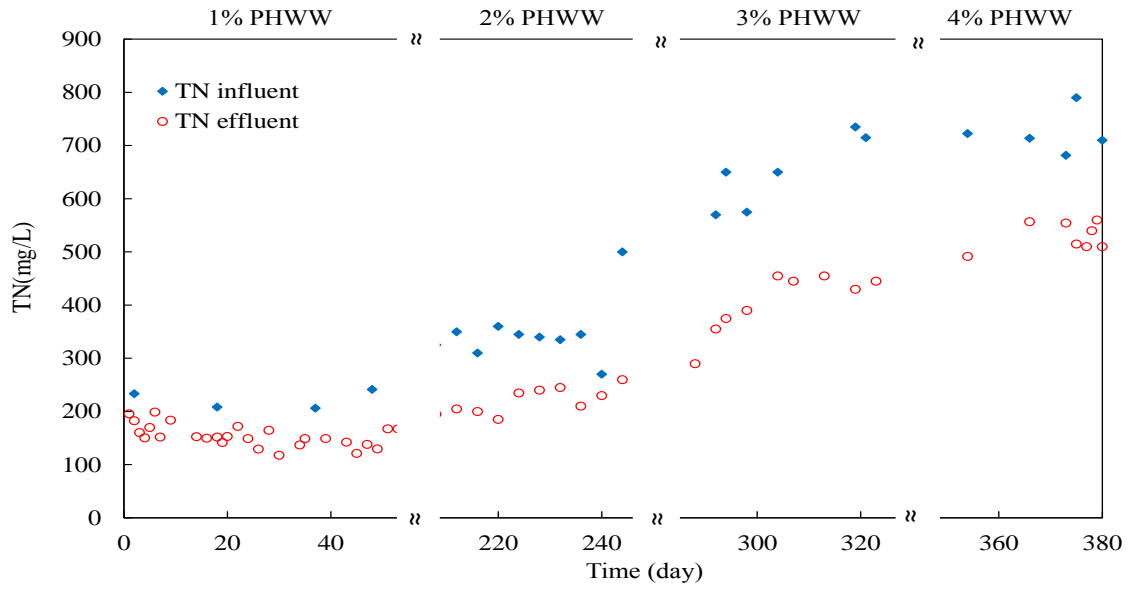


(A)

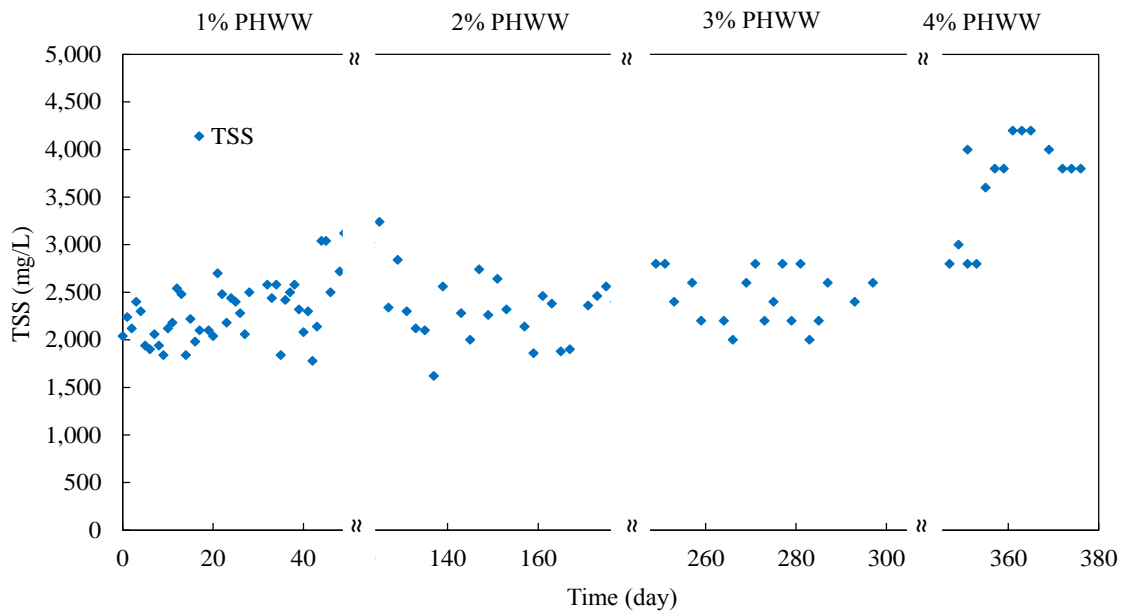


(B)

**Figure 4-6. Phase II operation: (A) COD, (B) ammonia nitrogen, (C) total dissolved nitrogen, (D) total suspended solid (TSS).**

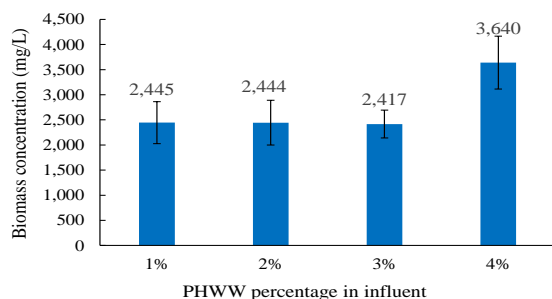
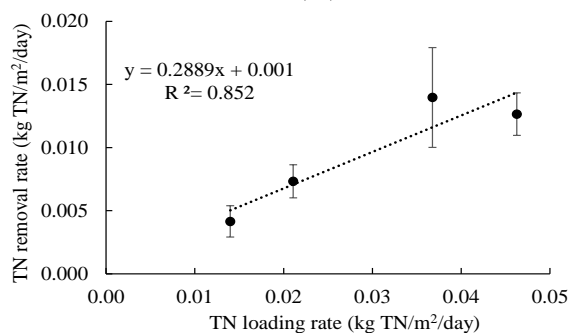
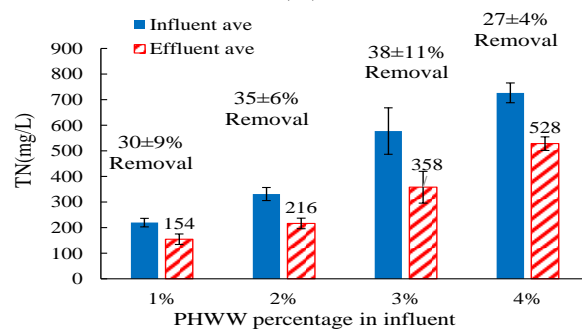
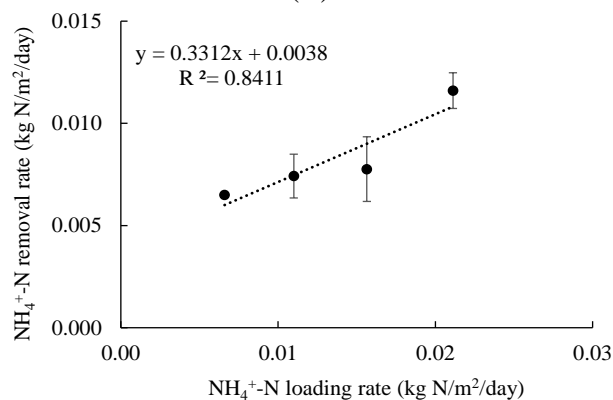
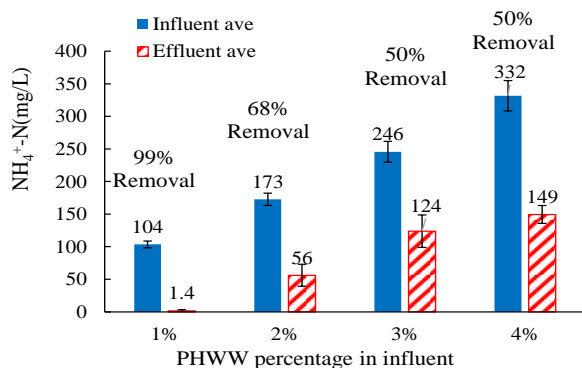
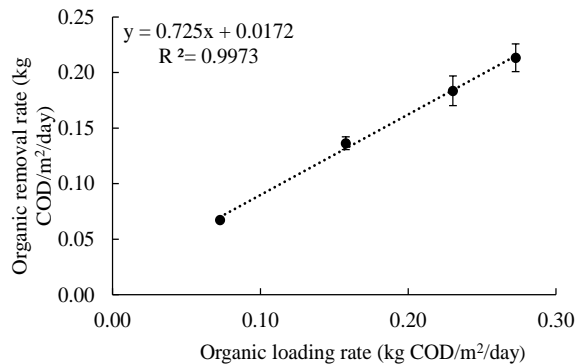
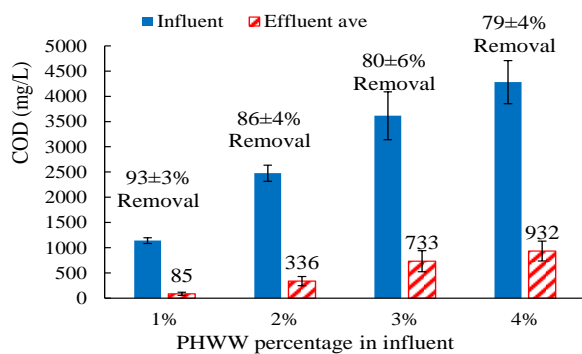


(C)



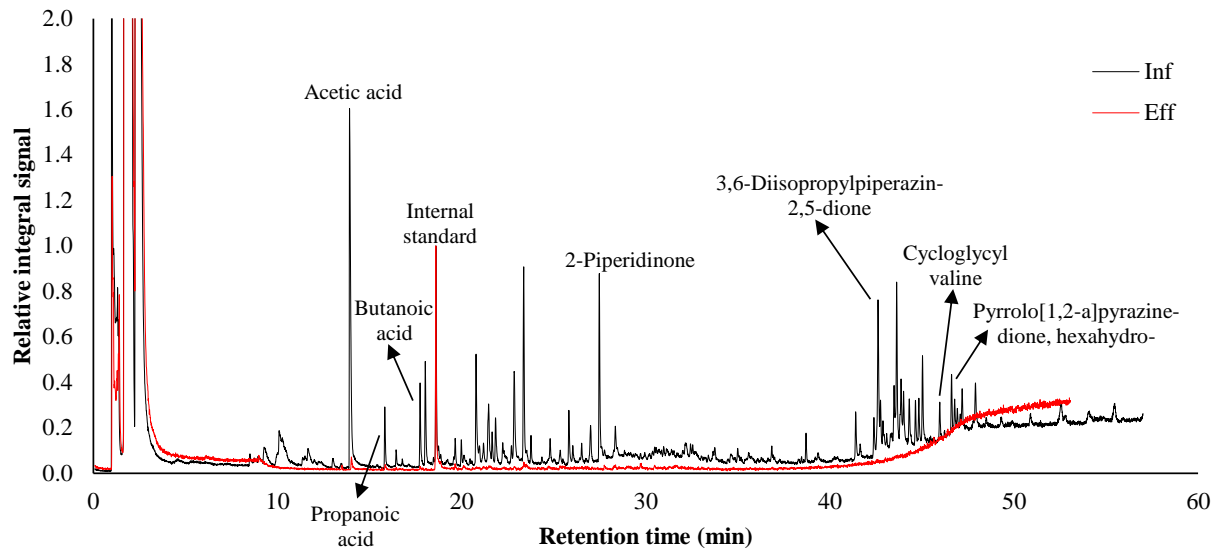
(D)

Figure 4-6 (cont.)



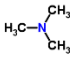
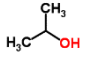
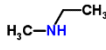
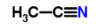
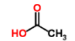
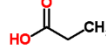

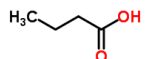
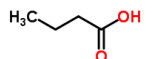
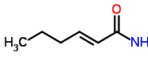
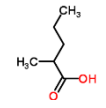
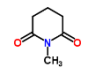
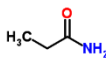
**Figure 4-7. Calculated average levels of pollutants and their corresponding removal rates: (A)(B) for COD, (C)(D) for NH<sub>4</sub><sup>+</sup>-N, and (E)(F) for TN. (E) during phase II operation under 4 different loading rates.**



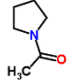
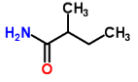
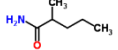
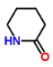
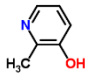
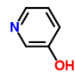
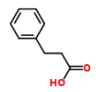
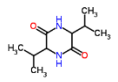
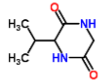
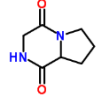


**Figure 4-8. GC-MS spectra of influent and effluent of the photobioreactor when having 4% PHWW as influent.**

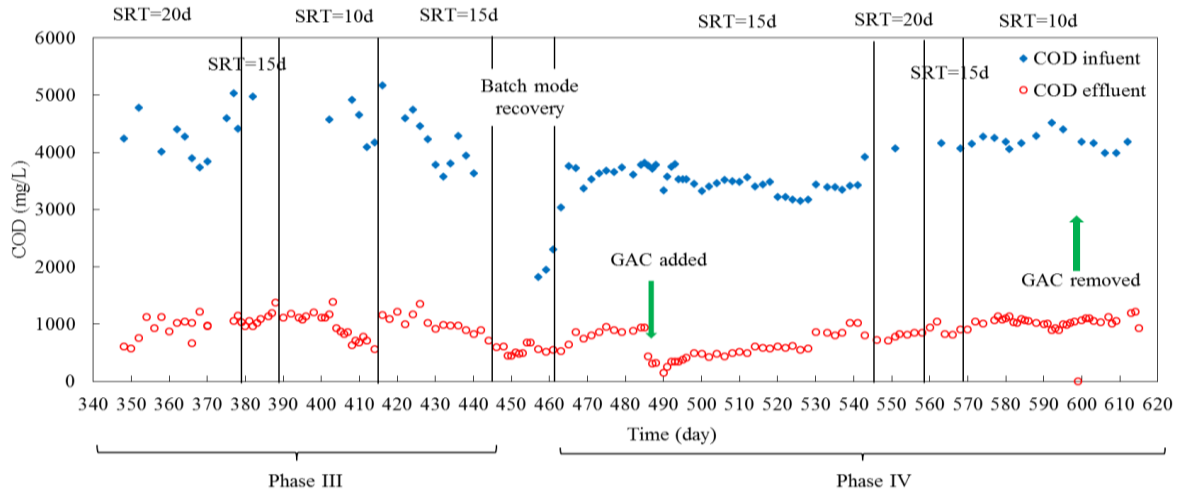
**Table 4-4. Detected organic compounds during GC-MS analysis for influent and effluent of photobioreactor.**

Name	Retention Time (min)	Relative Integrated Signal					Structure
		Influent (4% PHWW)	Effluent 1 (SRT=20days)	Effluent 2 (SRT=10days)	5 g/L GAC	25 g/L GAC	
Trimethylamine	1.23	0.01	N.D.	N.D.	N.D.	N.D.	
Isopropanol	1.68	36.52	86.34	73.29	67.93	58.83	
Ethyl-N-methylamine	1.99	0.19	N.D.	N.D.	N.D.	N.D.	
Acetonitrile	2.30	32.82	79.84	72.08	69.33	60.88	
Acetic acid	13.91	2.09	0.07	0.37	0.16	0.1	
Propanoic acid	15.83	0.26	0.03	0.06	0.05	0.04	
N-methylpropanoic acid	16.46	0.05	N.D.	0.01	0.01	0.01	
Butanoic acid	17.74	0.33	0.01	0.02	0.03	0.02	
Butanoic acid, 3-methyl- (internal standard)	18.61	1	1	1	1	1	
N-hexenamide	19.14	N.D.	N.D.	0.01	N.D.	N.D.	
Pentanoic acid, methyl-	21.43	0.17	N.D.	N.D.	N.D.	N.D.	
N-methylglutarimide	21.47	0.19	N.D.	N.D.	N.D.	N.D.	
Propanamide	21.66	0.12	N.D.	N.D.	N.D.	N.D.	

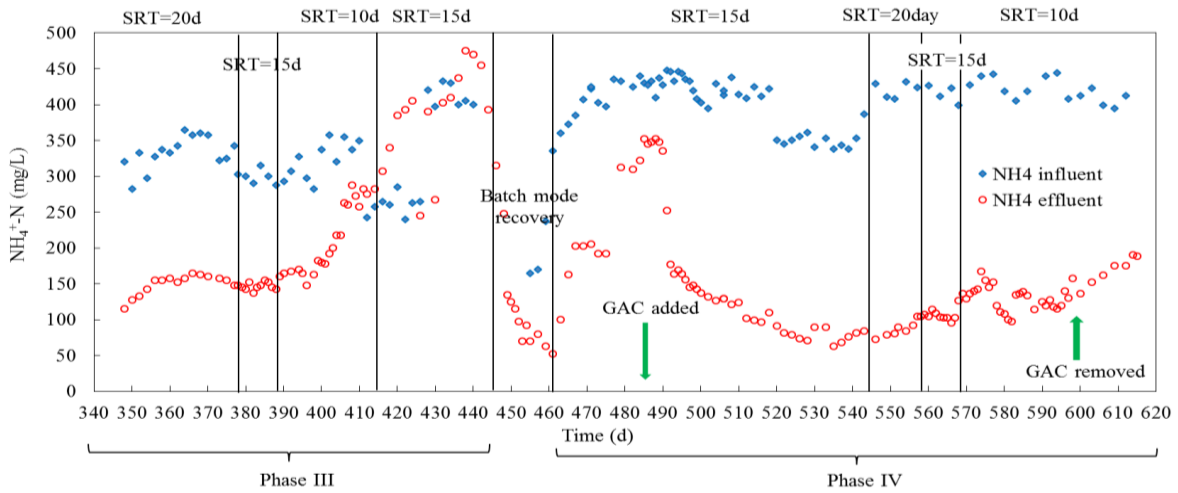
**Table4-4 (cont.)**

Name	Retention Time (min)	Relative Integrated Signal					Structure
		Influent (4% PHWW)	Effluent 1 (SRT=20days)	Effluent 2 (SRT=10days)	5g/L GAC	25g/L GAC	
Pyrrolidine, acetyl-	21.86	0.22	N.D.	0.01	N.D.	N.D.	
Butanamide, methyl-	23.77	0.10	N.D.	N.D.	N.D.	N.D.	
Pentanamide, methyl-	26.52	0.05	N.D.	N.D.	N.D.	N.D.	
2-Piperidinone	27.48	0.83	N.D.	N.D.	N.D.	N.D.	
3-Pyridinol, methyl-	32.13	0.02	N.D.	N.D.	N.D.	N.D.	
3-Pyridinol	32.43	0.06	N.D.	N.D.	N.D.	N.D.	
Benzenepropanoic acid	35.59	0.03	N.D.	N.D.	N.D.	N.D.	
3,6-Diisopropylpiperazin-2,5-dione	42.41	0.13	N.D.	N.D.	N.D.	N.D.	
Acetamido-3-ethyloctane	44.03	0.12	N.D.	N.D.	N.D.	N.D.	
Cycloglycyl valine	45.95	0.07	N.D.	N.D.	N.D.	N.D.	
Pyrrolo[1,2-a]pyrazine-dione, hexahydro-	46.61	0.23	N.D.	N.D.	N.D.	N.D.	

N.D. indicates not detected.

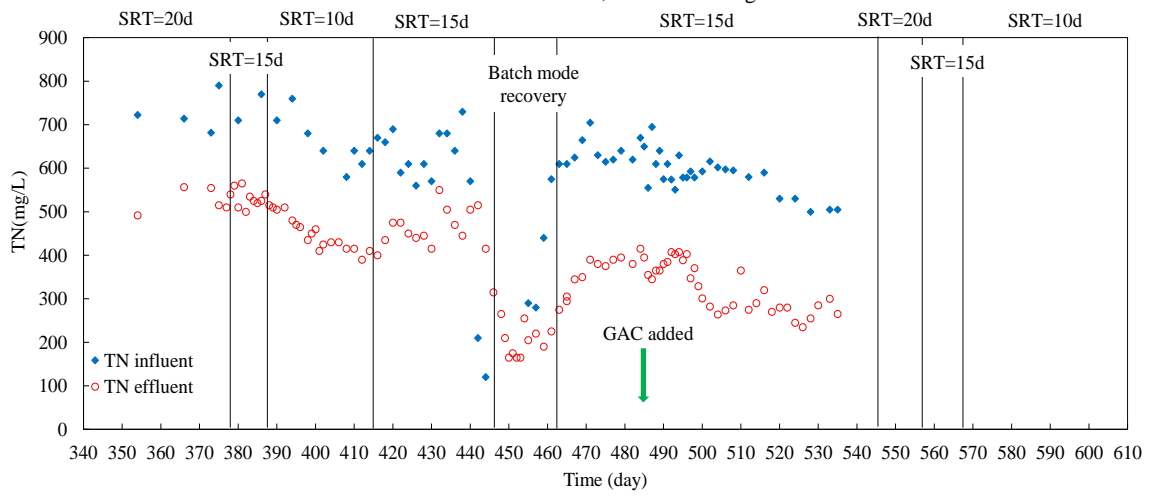


(A)

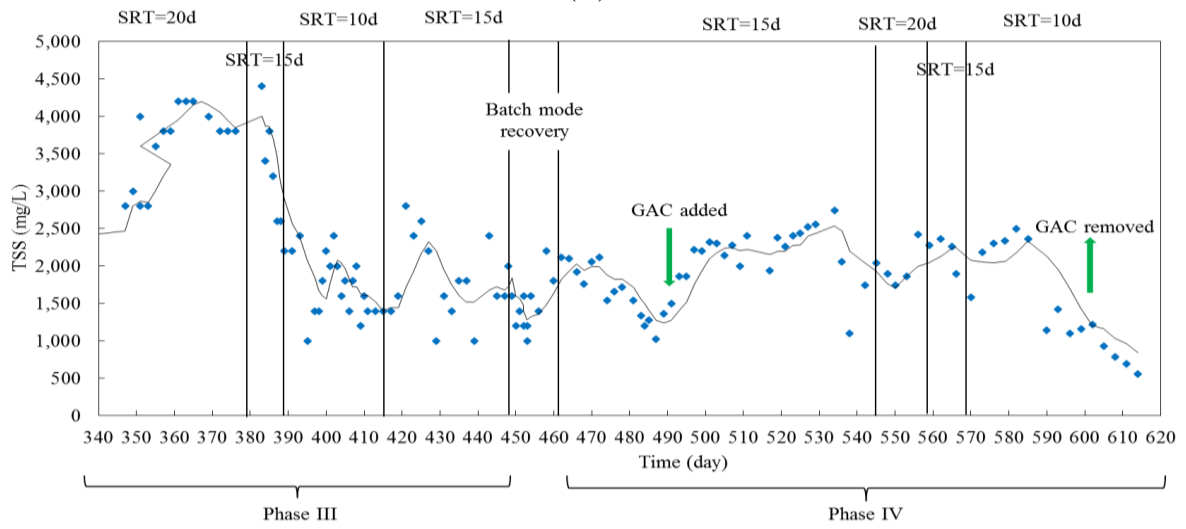


(B)

**Figure 4-9. Phase III and Phase IV operation: (A) COD, (B)  $\text{NH}_4^+\text{-N}$ , (C) total nitrogen (TN) and (D) biomass (indicated as total suspended solid, TSS).**



(C)



(D)

Figure 4-9 (cont.)

## CHAPTER 5

# ANAEROBIC TREATMENT OF AQUEOUS PRODUCT OF HYDROTHERMAL LIQUEFACTION TO INCREASE CARBON EFFICIENCY DURING BIOFUEL PRODUCTION

### 5.1 Introduction

HTL is a promising thermochemical process for converting wet biomass and organic waste into biocrude oil for fuel or other applications (Toor et al. 2011) with a net positive energy balance. It uses elevated temperatures (200 – 400 °C) and pressures (10-15 MPa) to convert organic solids in the feedstock into four products: (1) biocrude oil, (2) bio-char solid residue, (3) carbon dioxide-rich gas, and (4) an aqueous PHWW. The HTL process offers several advantages compared to other chemical or thermochemical fuel production processes, such as transesterification or pyrolysis, including the ability to use of a wide variety of low-lipid feedstocks (e.g., livestock manure, wastewater sludge, and fast-growing, low-lipid algae), shorter processing times, and a lower energy consumption for feedstock dewatering/drying (Toor et al. 2011; Ocfemia et al. 2006; Suzuki et al. 1988; Yu 2012).

Despite all the advantages of HTL, several issues have limited its development beyond lab scale, one of which is limited carbon efficiencies. That is, HTL cannot convert all the organics in the feedstock into biocrude oil, leaving behind an aqueous product with high concentrations of potentially valuable organics and nutrients: up to 40% of the carbon and 80% of the nutrients from the feedstock is released into PHWW (Yu et al. 2011). While several previous studies have focused on increasing the oil yield and minimizing carbon release into the aqueous product through HTL process optimization (pressure, temperature, retention time etc.), relatively little attention has been paid to carbon recovery from PHWW. The U.S. DOE has highlighted the importance of carbon recovery in biofuel production as exemplified by their

recently initiated CHASE program (Carbon, Hydrogen, and Separation Efficiencies in Bio-Oil Conversion Pathways). This program seeks to develop technologies that make better use of PHWW and other thermochemical process sidestreams to improve the overall carbon efficiency and commercial viability of these bio-oil conversion processes. Although some recent studies have investigated resource recovery from sidestreams of thermochemical conversion processes, the main focus has been on nutrient recovery rather than carbon recovery (Jena et al. 2011; Biller et al., 2012).

AD is the most widely used method for carbon/energy recovery from wet organic wastes. Besides the advantages of low cost of implementation and operation, low sludge production, etc., one of the most attractive features of AD for treating PHWW is the potential to utilize the biogas as a renewable fuel. When synergistically integrated with hydrothermal liquefaction and algal cultivation, the AD of PHWW could help facilitate carbon recovery from the atmosphere and multi-cycle nutrient reuse, maximizing bioenergy production from waste streams (this is discussed in detail in Section 5.3.4.). However, PHWW has also been reported to be toxic to both mammalian cells (Pham et al. 2013) and microorganisms (Zhou 2010). Many compounds identified in PHWW could potentially be inhibitory or toxic to AD processes, including ammonia and various organic compounds. These inhibitory effects could potentially be mitigated through dilution or the addition of adsorptive medium, such as activated carbon. The use of activated carbon in AD processes in wastewater treatment systems has been reported to improve process stability, counteract inhibition (caused by toxic compounds), enhance removal efficiencies of recalcitrant and toxic pollutants, and provide immobilization of anaerobic microbes (Çeçen and Aktas, 2011). Therefore, the objective of this study is to investigate the feasibility of removing organics from PHWW via AD and the addition of activated carbon, in

order to improve effluent water quality and increase the overall energy and carbon efficiency of the HTL process.

## **5.2 Material and Methods**

### **5.2.1 PHWW and anaerobic inoculum**

The PHWW used in this study was a mixture of PHWW from HTL of swine manure under different process conditions (pressure and reaction time). Characteristics of the PHWW are provided in Table 5-1. A characterization of water quality parameters for PHWW resulting from swine manure conversions under different HTL operating conditions was reported previously in detail by Appleford (2005). Mesophilic anaerobic inoculum was collected from a full-scale anaerobic digester operating at the Urbana-Champaign Sanitary District, and was used within 2 hours after collection. Characteristics of the anaerobic inoculum is also provided in Table 5-1.

### **5.2.2 Anaerobic batch test design and set-up**

Batch anaerobic tests were conducted to investigate 1) the anaerobic digestibility of PHWW, and 2) the effect of adsorptive medium on the anaerobic digestion of PHWW. Mesophilic batch digestion experiments were carried out at 37 °C in an incubation chamber. As shown in Table 5-2, reactors were loaded with a range of PHWW concentrations from 3.3% to 66.7%. The PHWW was diluted into the supernatant of the anaerobic inoculum, which provided a growth medium suitable for the anaerobic culture. The supernatant was obtained after centrifuging the inoculum sludge at 4000 rpm for 20 min. PAC (Norit DARCO Ultra 100) was added to four of the reactors. All the reactors were sealed with rubber septa and caps. The headspace of the reactors was purged with N<sub>2</sub> gas for 10 minutes to ensure anaerobic conditions. All of the reactors were manually mixed once a day for 30 seconds prior to measuring biogas



volume. Control batch reactors containing only inoculum and sludge supernatant were also prepared.

### **5.2.3 Measurements and calculations**

Biogas production was regularly monitored using a water displacement column and flask filled with deionized water acidified to pH 2 using H<sub>2</sub>SO<sub>4</sub>. Cumulative biogas production was normalized by subtracting biogas production from the control reactors and dividing by COD of the PHWW substrate added. The methane (CH<sub>4</sub>) concentration of the biogas in the reactors' headspace was analyzed using a Varian CP-3600 gas chromatograph (GC) equipped with a thermal conductivity detector as described previously (Zhou 2010). Filtered (0.45 μm pore size Nylon filter) water samples before and after digestion were analyzed for COD by visible light absorbance after dichromate digestion, according to standard methods (Clesceri et al. 1999). Two types of biogas production yields (ml biogas/mg COD<sub>added/removed</sub>) were calculated, by dividing the cumulative biogas production rate by either the COD added into the reactor or removed from the reactor (the COD removal from the control reactors was also “subtracted out”).

## **5.3 Results and Discussion**

### **5.3.1 Biogas production**

Figure 5-1A shows cumulative biogas production from the anaerobic batch test with PHWW concentrations ranging from 3.3% to 66.7%. The response of the anaerobic digestion process to different PHWW concentrations was quite variable. At low concentrations of PHWW (3.3% and 6.7%), biogas production started promptly after the test began and steadily increased for about 25 days. At the end of the digestion period (65 days), these two reactors reached a biogas yield of about 0.32 ml/mg COD<sub>added</sub>, respectively. Biogas samples from these two reactors were collected near the end of the steady biogas production phase (day 27) and GC analysis

showed that high quality biogas was produced with a methane content above 70% (Figure 5-1B). Assuming the overall methane content is about 60-70% of the total biogas production (Metcalf & Eddy et al., 2003), this gives us an energy recovery ratio of 49-57% from PHWW.

Under higher PHWW concentrations (13.3% and 26.7%), a lag phase of biogas production was observed. As shown in Figure 5-1A, after about 8 days of negligible biogas production in the 13.3% PHWW condition and 35 days in the 26.7% PHWW condition, biogas production rose sharply and resulted in a final biogas yield of 0.35 ml/mg COD<sub>add</sub> and 0.11 ml/mg COD<sub>add</sub>, respectively, at the end of the 65 day digestion period. Since both of these biogas production curves were still increasing at the end of the test, the maximum biogas production potential of these two conditions is very likely to be higher than the highest value achieved during this study. Biogas samples from these conditions were collected and analyzed for methane content on Day 44, which was the early stage of steady biogas production for both. As shown in Figure 5-1B, methane content in the 13.3% PHWW condition was 78%, while methane content in the 26.7% PHWW condition was much lower at 58%. However, since the biogas was sampled at a very early stage in the case of the 26.7% PHWW condition, it is quite possible that the methane content would increase to a level similar to the conditions with lower PHWW concentrations.

For the highest PHWW concentrations tested, 33.3% and 66.7%, complete inhibition of the anaerobic digestion process was observed, indicated by almost no biogas production during the entire 65 day digestion period, as well as low methane content (sampled at day 27), as shown in Figure 5-1.

The batch test results show that PHWW concentrations at or above 13.3% inhibited AD and resulted in an extended biogas production lag phase and eventual failure of the AD process

with little to no biogas production. Several factors may have contributed to the observed inhibition. Ammonia is one possibility since the PHWW contained high levels of  $\text{NH}_4^+\text{-N}$  (3.57 g/L). A wide range of inhibiting ammonium concentrations for anaerobic digestion has been reported; 1.7 g/L to 14 g/L  $\text{NH}_4^+\text{-N}$  has been reported to cause a 50% reduction in methane production (Chen 2008). In this study, reactors with 26.7%, 33.3%, and 66.7% PHWW in all showed fairly high  $\text{NH}_4^+\text{-N}$  levels, (~1.7 g/L, 1.9 g/L and 2.7 g/L  $\text{NH}_4^+\text{-N}$ , respectively), which could have partially contributed to the inhibition of the PHWW. However, given that complete inhibition of biogas production occurred at a relatively low ammonia level of 1.9 g/L, it would suggest that other significant inhibitory effects may have also been present. Similarly, the significant lag phase observed in the 13.3% and 26.7% PHWW conditions, which corresponded to ammonia levels of 1.4 and 1.7 g/L, respectively, suggests that other factors played a significant role in the inhibition of AD.

The low pH of PHWW may be a possible factor contributing the inhibition of AD of PHWW. A pH range of 6.5 to 8.2 is generally considered suitable for successful anaerobic digestion processes (Speece 1983). Initial pH in 66.7% PHWW condition was 5.82 (shown in Table 5-2) and the complete inhibition in this test was definitely contributed significantly by the low pH. Although the pH in the 33.3% PHWW condition (pH=6.67) was within the range of feasible anaerobic digestion, it is just barely above 6.5 and we suspect this pH have partially contributed to the inhibition of anaerobic digestion.

Toxic organic compounds may have contributed significantly to the inhibition observed in experimental conditions with high PHWW concentrations. A variety of organic compounds were identified in the PHWW from swine manure conversion including sugars, isosorbide, indole, 3-amonio-phenol, 2-cyclopenten-1-one, carboxylic acids, ketones, alcohols, various

cyclic hydrocarbons, and many nitrogen-containing compounds such as amides, azines and pyrroles (Appleford 2005). Many of these compounds are toxic to anaerobic digestion processes, including phenol and nitrophenols (Borja et al. 1997), alcohols (Demirer and Speece 1998), carboxylic acid (Stergar et al. 2003) and various cyclic compounds such as benzene and nitrobenzene (Bhattacharya et al. 1996), pyridine and its derivatives (Wu and Huang 1998). However, many factors can influence the toxicity during anaerobic digestion process, including toxicant concentration (inhibition concentration ranges vary widely for specific toxicants), biomass concentration, toxicant exposure time, cell age, feeding pattern, acclimation, and temperature (Chen 2008). In order to identify the specific toxicants that contributed to inhibition during anaerobic digestion of PHWW in this study, further investigations needed, including characterization of the organic compounds in PHWW, and a series of toxicology studies for each individual compound and mixtures of compounds.

Compared to tissue cells or other microorganisms, anaerobic microbes seem to be relatively tolerant of the mixture of chemical compounds found in PHWW. Zhou et al. reported that 5% of the same PHWW as was used in this study would completely inhibit algal growth (Zhou 2010). Other research has found that organic components extracted from 7.5% PHWW from algal biomass conversion resulted in a 50% reduction in mammalian cell growth, and in this case the toxicity of the extracted PHWW only accounted for 10~20% of the toxicity of full strength PHWW (Pham et al. 2013; Pham 2013). Under certain concentrations of PHWW, the presence of the relatively long lag phase followed by significant biogas production indicates the ability of inhibited anaerobic microorganisms to adapt and acclimate to the toxic compounds in PHWW. Reversibility of toxic effects is commonly noted during anaerobic processes (Chen 2008). It is expected that long-term adaptation would reduce the lag phase of biogas production

and eventually allow anaerobic digestion to proceed more quickly under higher concentrations of PHWW. Even more importantly, anaerobic microbes can breakdown many toxic compounds including a variety of polycyclic aromatic hydrocarbons and nitrogen heterocyclic compounds, such as phenol, phenol derivatives, picoline, and pyridine (Rabus 1995; Carmona 2009), which have been reported to cause toxicity in PHWW. Therefore, it is likely that the inhibitory effects of PHWW will gradually decrease as the anaerobic digestion process proceeds. This highlights the benefit of anaerobic digestion as a potential detoxification step for PHWW treatment. For instance, cultivating algae in PHWW offers significant potential advantages for nutrient recycling and bioenergy production. However, algae is more sensitive to the toxicity of PHWW than anaerobic microbes. Therefore, anaerobic digestion could be an advantageous pretreatment step to reduce the toxicity of PHWW before sending PHWW for use in algal cultivation.

### **5.3.2 The effect of activated carbon on the anaerobic digestion of PHWW**

One way to enhance anaerobic digestion of PHWW is to use an adsorptive media to sequester potentially toxic compounds and thereby mitigate potential inhibition effects. Results from this study showed that activated carbon can indeed accelerate biogas production, reduce the lag phase, and facilitate successful digestion under higher concentrations of PHWW. Figure 5-2 compares batch test biogas production and methane content from anaerobic digestion of PHWW with and without the addition of PAC. In conditions with a relatively low concentration of PHWW (6.7%), no obvious inhibition effect was observed in terms of a lag phase prior to biogas production. However, the addition of PAC did slightly increase the rate of biogas production, as indicated by a steeper slope in the cumulative biogas production curve shown in Figure 5-2A. The methane content of the biogas from digestion of 6.7% PHWW was not significantly affected

by the addition of PAC; both conditions showed a high methane content of 77% and 78%, respectively, at Day 27 (Figure 5-2B).

At a higher PHWW concentration of 26.7%, AD without PAC incurred a 35-day lag phase prior to biogas production. However, the addition of PAC resulted a reduced lag phase of only 23 days. Methane content in the condition with PAC was also higher (68%) compared to the condition without PAC (58%), which is likely related to the shortened lag phase. (Both of the biogas samples were taken on Day 44, which was the earlier stage of biogas production for the condition without PAC.) At an even higher PHWW concentration of 33.3%, almost no biogas production occurred without PAC. The addition of PAC mitigated the complete inhibition of AD and biogas production commenced after a 34-day lag phase. Methane content in the 33.3% PHWW condition with PAC continued to increase, from 34% on Day 27, to 43% on Day 34, and 64% on Day 47. This corresponded to the time period during which cumulative biogas production was increasing steadily as well. The resulting biogas production and methane content confirmed that successful anaerobic digestion of 33.3% PHWW was achieved through the addition of PAC. However, addition of PAC was not able to benefit AD of 66.7% PHWW during this test period.

As discussed previously, low pH, high ammonia levels, and toxic organic compounds in the PHWW may have all contributed to the inhibition of anaerobic digestion. However, in determining the mechanism by which the addition of PAC was able to alleviate the inhibiting effects of PHWW, it was found that addition of PAC had a very limited effect on pH and ammonia levels. Less than a 5% change in these two parameters was observed during the first week of testing when almost all of the physical adsorption would have taken place. Thus, the process enhancement resulting from addition of PAC was most likely a result of a reduction in

toxic organic compounds in the aqueous phase. Activated carbon is well known for its ability to adsorb a wide range of organic compounds, including toxic compounds identified in PHWW such as indole, alcohols, ketons, various cyclic hydrocarbons, and many nitrogenous organic compounds (e.g., amides, azines, pyrroles, amino-phenol, and pyridine and its derivatives) (Pham et al. 2013; Appleford 2005). Pham et al. (2013) found that the treatment of PHWW by activated carbon can greatly reduce the cytotoxicity to mammalian cells. In anaerobic digestion of coal gasification wastewater, which shares some similar chemical compounds with PHWW (various aromatic compounds and nitrogen containing compounds, including pyridine, methyl-, dimethyl-, and ethyl-substituted pyridines), Suidan et al. (Suidan et al. 1983) reported that the presence of granular activated carbon served to sequester the inhibitory and non-biodegradable components of the wastewater and permit the breakdown of degradable compounds during anaerobic digestion.

There are several possible mechanisms for the reduction of organic toxic compounds in the presented study. The reduction may be a result of pure physical adsorption of toxic compounds. The adsorption process generally requires only minutes to days to achieve equilibrium depending on the adsorbent chosen, which is significantly faster than the net rates for anaerobic digestion. Thus, PAC serves as a rapid physico-chemical sink for inhibitory or toxic substrates allowing the microbes to survive within an otherwise adverse environment. It is also possible that simultaneous adsorption and biodegradation of toxic compounds occurred (Aktaş and Çeçen, 2007) resulting in continuous bioregeneration of the adsorbent in-situ. In this case, the activated carbon serves as a buffer, where the initial adsorption process helps to decrease toxic compound levels, and thereby enhances microbial growth and survival. As the remaining aqueous phase toxic compounds are degraded, adsorbed compounds slowly desorb

and are re-released into the aqueous phase. Microbes then have an opportunity to degrade the released compounds without experience the inhibitory effects. Bioregeneration of activated carbon has been reported and discussed in several previous studies including anaerobic digestion of coal gasification wastewater (Suidan et al. 1983) and the aerobic biodegradation of phenolic compounds (Lee and Lim 2005) and aromatic compounds (De Jonge et al. 1996).

Bioregeneration is a very valuable process since it can decrease the need to periodically replace or thermally regenerate the activated carbon. This process is dependent on many factors including biodegradability, absorbability, and desorbability of the adsorbed compounds, as well as the characteristics of the activated carbon, and process configurations (Aktaş and Çeçen, 2007).

### **5.3.3 Total organic matter removal**

Biogas production in the conditions with 3.3%, 6.7% and 13.3% PHWW, which achieved nearly plateaued levels, were tested for total dissolved organic matter removal. Results showed that 50%, 55%, and 45% of organic matter was removed, respectively, as indicated by COD concentrations. The PHWW had been reported to have limited biodegradability in a previous study as well although under aerobic condition (Zhou 2010). Further research is needed to characterize the residual un-digested compounds and develop effective methods to remove them. Potential methods include adsorption (with activated carbon or resins), ozone oxidation, and/or a second stage biological treatment with aerobic or other specialized microbial cultures.

Based on the rate of cumulative biogas production and total organic removal, calculations indicated that the conditions with 3.3%, 6.7% and 13.3% PHWW had biogas production efficiencies of 0.49, 0.50, and 0.50 ml biogas /mg COD<sub>removed</sub>, respectively. Given that the methane content for all of these conditions at a single time point during the steady state biogas



production was above 70% (Figure 5-1B), indicating successful and efficient anaerobic digestion, we assume the overall methane production to be around 60-70% of the total biogas produced (Metcalf & Eddy et al., 2003) (cumulative methane production was not measured in this study). In this case, anaerobic digestion of these three conditions resulted in a methane yield of around 0.3-0.35 ml methane/ mg COD<sub>removed</sub>. This estimated methane yield proves to be decent compared to anaerobic digestion of other types of high strength industrial wastewater which has been reported to be 0.25-0.35 ml methane/mg COD<sub>removed</sub> (Ersahin et al., 2011). This comparison highlights that PHWW is a suitable feedstock for AD processes, and through AD successful and efficient carbon/energy recovery from PHWW can be achieved.

#### **5.3.4 Integration of anaerobic digestion with the hydrothermal liquefaction process**

Anaerobic digestion could provide multiple benefits when synergistically integrated with HTL. First, the overall carbon efficiency and energy production of HTL could be increased by recovering organic carbon from PHWW in the form of methane rich biogas. Successful anaerobic digestion could recover 49-57% energy from PHWW (as discussed in section 3.1), which can increase the bioenergy production efficiency of HTL from 40-65% (Gai et al., 2014) to up to 80%. In addition, anaerobic digestion could potentially function as a pre-treatment step before sending PHWW for algal cultivation to facilitate nutrient recycling and recovery. PHWW contains up to 80% nutrient (e.g., nitrogen) (Yu et al., 2011) from feedstock providing great potential for nutrient recycling and addition biomass production if sent for algae cultivation (Jena et al., 2011; Biller et al., 2012). However, PHWW has been shown to be toxic to algae most likely because of various organic compounds and ammonia nitrogen etc.(Pham et al., 2013; Zhou et al., 2013). Anaerobic microbes have been widely reported to breakdown many toxic compounds including a variety of polycyclic aromatic hydrocarbons and nitrogen heterocyclic

compounds, such as phenol, phenol derivatives, picoline, and pyridine (Rabus, 1995; Carmona, 2009), which have been reported to cause toxicity in PHWW. And our study has shown that ~50% of the organic content in PHWW could be removed through AD. Therefore, it might be advantageous to use AD as a detoxification step of PHWW before sending it for algal biomass production algal cultivation facilitating nutrient recovery and even more bioenergy production of HTL (Zhou et al., 2013).

#### **5.4 Conclusions**

This study investigated the feasibility of recovering carbon/energy from PHWW through AD. Results showed that AD was successful when treating appropriate concentrations of PHWW ( $\leq 6.7\%$ ), which yielded  $\sim 0.5$  ml biogas/mg  $\text{COD}_{\text{removed}}$  and organic removal efficiencies of  $\sim 50\%$ . Higher PHWW concentrations ( $\geq 13.3\%$ ) showed an inhibitory effect on AD with delayed, reduced, or even no biogas production. Activated carbon mitigated the inhibition by shortening the lag phase of biogas production and allowing AD to occur at higher concentrations of PHWW (up to 33.3%). Thus, AD is a feasible and advantageous process for carbon/energy recovery from PHWW.

#### **5.5 References**

- Aktas, Ö. and Ç. Ferhan. 2007. Bioregeneration of activated carbon: a review. *International Biodeterioration & Biodegradation* 59(4): 257-272.
- Appleford, J. M. 2005. Analyses of the products from the continuous hydrothermal conversion process to produce oil from swine manure. PhD diss. Champaign, IL: University of Illinois at Urbana-Champaign.
- Bhattacharya, S. K., M. Qu and R. L. Madura. 1996. Effects of nitrobenzene and zinc on acetate utilizing methanogens. *Water Research* 30(12): 3099-3105.

- Billar, P., A. B. Ross, S. C. Skill, A. Lea-Langton, B. Balasundaram, C. Hall, R. Riley and C. A. Llewellyn. 2012. Nutrient recycling of aqueous phase for microalgae cultivation from the hydrothermal liquefaction process. *Algal Research* 1(1): 70-76.
- Borja, R., J. Alba and C. J. Banks. 1997. Impact of the main phenolic compounds of olive mill wastewater (OMW) on the kinetics of acetoclastic methanogenesis. *Process Biochemistry* 32(2): 121-133.
- Carmona, M. 2009. Anaerobic catabolism of aromatic compounds: A genetic and genomic view. *Microbiology and Molecular Biology Reviews* 73(1): 71-133.
- Çeçen, F. and Ö. Aktas. 2011. *Activated Carbon for Water and Wastewater Treatment: Integration of Adsorption and Biological Treatment*. Hoboken, NJ: John Wiley & Sons.
- Chen, Y. 2008. Inhibition of anaerobic digestion process: A review. *Bioresource Technology* 99(10): 4044-4064.
- Clesceri, L. S., A. E. Greenberg and D. E. Andrew. 1999. *Standard Methods for the Examination of Water and Wastewater*. New York: American Public Health Association.
- De Jonge, R. J., A. M. Breure and J. G. Van An del. 1996. Bioregeneration of powdered activated carbon (PAC) loaded with aromatic compound. *Water Research* 30(4): 875-882.
- Demirer, G. N. and R. E. Speece. 1998. Anaerobic biotransformation of four 3-carbon compounds (acrolein, acrylic acid, allyl alcohol and n-propanol) in UASB reactors. *Water Research* 32(3): 747-759.
- Ersahin, M. E., H. Ozgun, R. K. Dereli and I. Ozturk. 2011. Anaerobic treatment of industrial effluents: an overview of applications. *Waste Water-Treatment and Reutilization* 121:1233-1237
- Gai, C., Y. Zhang, W. Chen, P. Zhang and Y. Dong. 2014. Energy and nutrient recovery efficiencies in biocrude oil produced via hydrothermal liquefaction of *Chlorella pyrenoidosa*. *RSC Advances* 4(33): 16958-16967.
- Jena, U., N. Vaidyanathan, S. Chinnasamy and K. C. Das. 2011. Evaluation of microalgae cultivation using recovered aqueous co-product from thermochemical liquefaction of algal biomass. *Bioresource Technology* 102(3): 3380-3387.
- Lee, K. M. and P. E. Lim. 2005. Bioregeneration of powdered activated carbon in the treatment of alkyl-substituted phenolic compounds in simultaneous adsorption and biodegradation processes. *Chemosphere* 58(4): 407-416.
- Metcalf & Eddy, G. Tchobanoglous, F. L. Burton and H. D. Stensel. 2003. *Wastewater Engineering: Treatment and Reuse*. 4th ed. Boston: McGraw-Hill.

- Ocfemia, K. S., Y. Zhang and T. Funk. 2006. Hydrothermal processing of swine manure to oil using a continuous reactor system: Effects of operating parameters on oil yield and quality. *Transactions of the ASABE* 49(6): 1897-1904.
- Pham, M. 2013. Personal communication with Mai Pham about the cytotoxicity testing method.
- Pham, M., L. Schideman, J. Scott, N. Rajagopalan and M. Plewa. 2013. Chemical and biological characterization of wastewater generated from hydrothermal liquefaction of spirulina. *Environmental science technology* 47(4): 131-138.
- Rabus, R. 1995. Anaerobic degradation of ethylbenzene and other aromatic hydrocarbons by new denitrifying bacteria. *Archives of Microbiology* 163(2): 96-103.
- Speece, R. E. 1983. Anaerobic biotechnology for industrial wastewater treatment. *Environmental Science & Technology* 17(9): 416A-427A.
- Stergar, V., J. Zagorc-Konan and A. Zgajnar-Gotvanj. 2003. Laboratory scale and pilot plant study on treatment of toxic wastewater from the petrochemical industry by UASB reactors. *Water Science & Technology* 48(8): 97-102.
- Suidan, M. T., C. E. Strubler, S. Kao and J. T. Pfeffer. 1983. Treatment of coal gasification wastewater with anaerobic filter technology. *Journal of Water Pollution Control Federation* 55: 1263-1270.
- Suzuki, A., T. Nakamura, S. Yokoyama, T. Ogi and K. Koguchi. 1988. Conversion of Sewage-Sludge to Heavy Oil by Direct Thermochemical Liquefaction. *Journal of Chemical Engineering of Japan* 21(3): 288-293.
- Toor, S. S., L. Rosendahl and A. Rudolf. 2011. Hydrothermal liquefaction of biomass: a review of subcritical water technologies. *Energy* 36(5): 2328-2342.
- Wu, C. and H. Huang. 1998. Toxicity and anaerobic biodegradability of pyridine and its derivatives under sulfidogenic conditions. *Chemosphere* 36(10): 2345-2357.
- Yu, G. 2012. Hydrothermal liquefaction of low-lipid microalgae to produce bio-crude oil. PhD diss. Champaign, IL: University of Illinois at Urbana-Champaign.
- Yu, G., Y. Zhang, L. Schideman, T. Funk and Z. Wang. 2011. Distributions of carbon and nitrogen in the products from hydrothermal liquefaction of low-lipid microalgae. *Energy Environmental Science* 4(11): 4587-4595.
- Zhou, Y. 2010. Improving algal biofuel production through nutrient recycling and characterization of photosynthetic anomalies in mutant algae species. MS thesis. Urbana, IL: University of Illinois at Urbana-Champaign.

Zhou, Y., L. Schideman, G. Yu and Y. Zhang. 2013. A synergistic combination of algal wastewater treatment and hydrothermal biofuel production maximized by nutrient and carbon recycling. *Energy and Environmental Science* 6(12): 3765-3779.

## 5.6 Figures and Tables

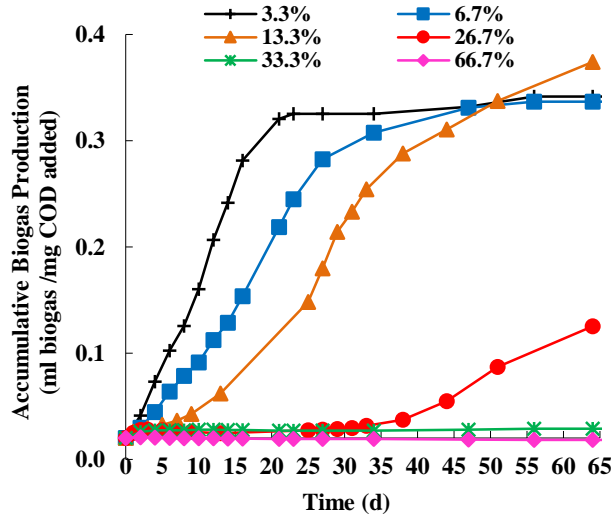
**Table 5-1. Characteristics of post-hydrothermal liquefaction wastewater (PHWW), supernatant of centrifuged sludge, and anaerobic sludge inoculum.**

Parameter	PHWW	Supernatant of centrifuged sludge	Anaerobic sludge inoculum
COD (mg/L)	52,030	1,356	18,100
NH <sub>4</sub> <sup>+</sup> -N (mg/L)	3,570	1,075	--
Total nitrogen(mg/L)	5,355	--	--
Total phosphorus(mg/L)	1,001	215	--
pH	5.60	7.75	--
Solid content (mg/L)	--	--	29,500
Suspended solid (mg/L)	--	--	28,350

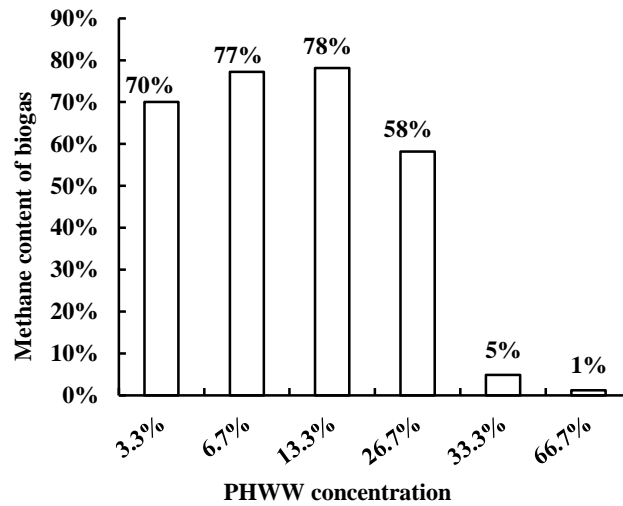
**Table 5-2. Batch experiment set-up for anaerobic digestion of post-hydrothermal liquefaction wastewater (PHWW).**

ID	PHWW (of liquid volume)	Supernatant of centrifuged sludge (of liquid volume)	Sludge inoculum (of liquid volume)	PAC dosage (g/L)	Initial pH
control	0%	96.7%	3%		7.92
control*	0%	80.0%	20%		8.12
3.3%	3.3%	93.3%	3%		7.67
6.7%	6.7%	90.0%	3%		7.41
13.3%*	13.3%	66.7%	20%		7.43
26.7%*	26.7%	53.3%	20%		6.86
33.3%	33.3%	63.3%	3%		6.64
66.7%	66.7%	30.0%	3%		5.72
6.7%+PAC	6.7%	90.0%	3%	1.4	7.41
26.7%+PAC*	26.7%	53.3%	20%	2.4	6.86
33.3%+PAC	33.3%	63.3%	3%	1.4	6.50
66.7%+PAC	66.7%	30.0%	3%	1.4	5.82

\* These four tests were conducted in 120 ml serum bottles with 100ml operational/liquid volume while all the other tests were conducted in 200ml serum bottles with 150ml operational/liquid volume. In addition, these four tests had larger amount of inoculum (inoculum was 20% of total operational volume versus 3% in the other tests).

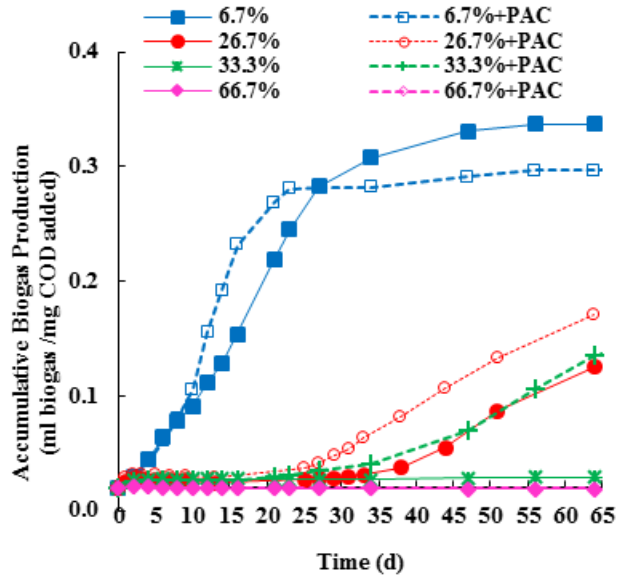


(A)

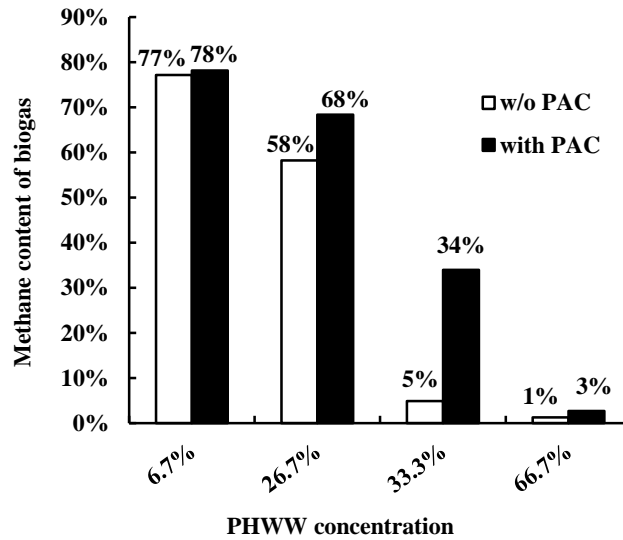


(B)

**Figure 5-1. Biogas production and methane content of biogas in batch anaerobic digestion reactors (A) Cumulative biogas production for a 65-day incubation period containing various concentrations (3.3%-66.7%) of post-hydrothermal liquefaction wastewater (PHWW); (B) Methane content of biogas sampled during exponential increase phase of biogas production (13.3% and 26.7% tests were sampled at day 44, all the other tests were sampled at day 27).**



(A)



(B)

**Figure 5-2. Comparison of biogas production and methane content for batch anaerobic digestion tests with and without the addition of powdered activated carbon (PAC): (A) cumulative biogas production; (B) methane content of biogas produced (26.7% post-hydrothermal liquefaction wastewater (PHWW) tests were sampled on Day 44. All other tests were sampled on Day 27.**



## CHAPTER 6

# EFFECT OF HTL OPERATING CONDITIONS AND WATER QUALITY ON THE INHIBITION CHARACTERISTICS OF POST HYDROTHERMAL LIQUEFACTION WASTEWATER

### 6.1 Introduction

Despite the significant potential of the novel E<sup>2</sup>-Energy system for significantly increasing the bioenergy harvested from wastewater as discussed in the previous chapter, one potentially limiting issue is the inhibitory effect of PHWW on algal growth. This inhibitory effect is important because it can constrain the beneficial reuse of PHWW to support algal production, which is crucial for maximizing bioenergy production for a given amount of nutrient/organic input to the system. In order to achieve the goal of utilizing PHWW efficiently, several levels of understanding of the inhibitory characteristics of PHWW are needed. First, what is the composition of PHWW? The answer to this question can help to identify the components of PHWW that can be “food” to support biomass production and the components that are potential toxins that inhibit algal or bacterial growth. It can also help to identify potential detoxification measurements. Second, what factors affect the inhibitory characteristics of PHWW? This includes an understanding of how the HTL operating conditions and other factors affect the PHWW composition and subsequent inhibitory effects. It will also be useful to investigate whether there is any relationship between some commonly used water quality parameters and PHWW inhibition, so that we can have a quick “diagnosis” of the PHWW inhibition. Third, how can we integrate the information to best utilize PHWW? Can we manipulate the HTL operating conditions to minimize the inhibition? Is it possible to produce PHWW that contains the best nutrients and organics to support algal biomass production and the least toxic compounds that inhibit algal growth? Can we optimize the HTL operating conditions

to provide a suitable balance of energy recovery, oil quality, and inhibitory effects on algae growth?

There are relatively few studies that elucidate the aqueous phase product because biomass liquefaction technology, especially using algae as feedstock, is a relatively young topic of research, and the initial focus of most research has been on the oil product as a liquid fuel alternative. Much of the information about the aqueous phase from HTL has only been addressed as a tangential issue in most articles and studies. Only in the last couple of years, several research groups have started to investigate the properties of PHWW in depth, as well as considering the potential to utilize and recover resources from PHWW, which is the most abundant product of HTL.

Scattered and limited information are available regarding the composition of PHWW, as well as the toxic and non-toxic components of PHWW. The organic compounds detected in PHWW can be categorized into three major groups: oxygen-containing compounds (carboxylic acids, alcohols and ketones), cyclic hydrocarbons and nitrogenous organic compounds (Elliot 1993; Appleford 2005). PHWW also contains various nutrients including nitrogen (ammonia and organic forms), phosphorus, and various micronutrients. While some of the PHWW compounds could be food or nutrients to support algal and bacterial growth, like acetate and ammonia, many of the components could also be toxic, such as various cyclic hydrocarbons and nitrogenous organic compounds. However, until now, there is only one detailed study that investigated on the toxicity of PHWW compounds, which focused on nitrogenous organic compounds, and it found that these compounds only accounted for a small fraction of the overall toxicity of PHWW. Therefore, the composition of PHWW is a relatively immature topic of research, not to mention

the understanding of what components could potentially be used for microbial food and what components would most likely lead to toxicity to algal growth.

Until now, there is no study investigating how HTL operating conditions affect the algal inhibition characteristics of PHWW. However, there have been lots of studies investigating how HTL operating conditions affect oil product. Although there is definitely some relationships between these two products because they are formed in close contact to each other, these two products can be very different. The components in these two phases may also come from completely different sources and reactions. For example, one study concluded that the products in the aqueous phase primarily come directly from the algal biomass, and compounds that originally partitioned into the biocrude oil fraction that get converted into aqueous-phase products account for only a small amount of the material (Valdez et al. 2012). In addition, partitioning will also affect the content in each phase. The biocrude oil produced is a hydrophobic phase with primarily hydrophobic components, whereas the aqueous phase contains more hydrophilic components.

A few recent studies made some progress toward deepening our understanding of how HTL operating conditions affect general PHWW quality, including pH, COD, TN, TP,  $\text{NH}_4^+\text{-N}$ , etc., and found that the tested water quality parameters of PHWW were strongly affected by HTL operating condition (Jena et al. 2011b; Gai et al. 2014b). These data provide useful insights because the organic content and nutrients in PHWW can be an important resource to support algal cultivation that is both cost-effective and environmentally friendly. Indeed, several studies found that the algal growth/inhibition was closely related to the water quality parameters (Biller et al. 2012; Du et al. 2012; Jena et al. 2011a). However, the commonly used water quality parameters could only provide indirect information when it comes to the case of evaluating the

inhibitory effects of PHWW. This is because some of these parameters represent a broad spectrum of compounds, some of which are beneficial to algal growth while some others can be inhibitory (Zhou et al. 2013; Pham 2014; Pham et al. 2013). In other words, the water quality parameters probably have a complex relationship with the inhibition characteristics of PHWW. Therefore, even though data on the effects of HTL operating condition on these water quality parameters are available, they may not be easily translated into accurate predictions of the inhibitory effects.

In order to fill the knowledge gaps, this study directly investigates and quantifies the relationship between HTL operating conditions, PHWW water quality, and the inhibition of algal growth by PHWW. We also conducted detailed chemical composition analysis of the most toxic and least inhibitory PHWW samples to provide information on the specific chemicals commonly found in PHWW to provide additional insight on the inhibitory effects of PHWW.

## **6.2 Materials and Methods**

### **6.2.1 HTL feedstock**

*Chlorella pyrenoidasa* powder was purchased from a health-food store. The elemental and molecular composition of the powdered algae are summarized in Table 6-1.

### **6.2.2 HTL experiment**

HTL experiments were carried out in 100 mL stainless steel cylindrical reactors (Model 4593, Parr Instrument Co, Moline, IL). Three replicates for each reaction condition were conducted. During each test, 70 g feedstock slurries with different solids ratio (15%, 25%, 35%) were first loaded into the reactor. After the reactor was sealed, the reactor was purged with pure nitrogen gas three times. The reactor was then pressurized again by pure nitrogen gas to 0.69 MPa. The reactor was then heated by an electric heater with a heating rate of around 6 °C/min.

The internal stirring rate was set at 300 rpm for mixing. After the target reaction temperature was reached, it was maintained for a certain retention time. Finally, the reactor was cooled down to room temperature by flowing tap water through the cooling coil (about an hour). The recovery procedure of the HTL products was shown in Figure 6-1. The gas in the reactor was first sampled using a Tedlar® gas sampling bag through a control valve, then analyzed by a gas chromatography (Varian CP-3800). Afterwards, the reactor was opened and the remaining mixture was separated. Raw oil products were separated from the aqueous phase by filtration. The solid residue fraction of the raw oil products was obtained via Soxhlet extraction using the solvent of toluene. The toluene soluble fraction of the raw oil product was defined as the bio-crude oils.

### **6.2.3 Algal growth-inhibition assay**

#### *6.2.3.1 Algal strains and culture media*

Stock cultures of *Chlorella vulgaris* (UTEX 398) was obtained from UTEX Culture Collection of Algae, Texas. It was maintained routinely on both liquid and agar plates under room light conditions at ~25 °C by regular sub-culturing. The medium used was Bold's Basal Medium (BBM) which contained the following (mg/L): NaNO<sub>3</sub>, 250; KH<sub>2</sub>PO<sub>4</sub>, 175; CaCl<sub>2</sub>·2H<sub>2</sub>O, 25; MgSO<sub>4</sub>·7H<sub>2</sub>O, 75; K<sub>2</sub>HPO<sub>4</sub>, 75; NaCl, 25; EDTA, 50; FeSO<sub>4</sub>·7H<sub>2</sub>O, 4.98; H<sub>3</sub>BO<sub>3</sub>, 11.42; ZnSO<sub>4</sub>·7H<sub>2</sub>O, 8.82; NaMoO<sub>4</sub>·2H<sub>2</sub>O, 0.72; CoCl<sub>2</sub>·6H<sub>2</sub>O, 0.38; MnCl<sub>2</sub>·4H<sub>2</sub>O, 1.44; CuSO<sub>4</sub>·5H<sub>2</sub>O, 1.57; thiamine, 10; biotine, 0.1; vitamin B12, 0.01. The cultures were subject to routine microscopic examination to ensure the purity of the cultures. Prior to each experiment, colonies from the agar plates were used to inoculate stock cultures made in 250 ml Erlenmeyer flasks with 50 ml of liquid TAP medium (without Bacto agar) that were mixed on an orbital shaker at 24 °C under 20 μmol photons m<sup>-2</sup> s<sup>-1</sup> of PAR provided by fluorescent lamps. An

inoculum culture in test medium was prepared 48 hours before the inhibition test to ensure that algal cells in exponentially growing phase were used as inoculum for the algal growth-inhibition tests.

#### 6.2.3.2 *Algal growth-inhibition assay in 24-well plates*

Algal growth inhibition assay were performed according to EPA standard test method 1003.0 (Weber et al. 2002) (a short-term method that uses green algae for estimating the chronic toxicity of effluents and receiving waters to freshwater organisms) and other published methods (Eisentraeger et al. 2003) that's in accordance with the standard ISO 8692 and OECD 201.

Tests were performed in 24-well plates (Krystal 24 Well Black TC Plate) with a total liquid volume of 2ml. Each plate contained four growth controls near the samples with the lowest concentration to avoid cross contamination. PHWW were assayed from low to high concentrations with 2 replicate cultures per concentration. 2-3 plates were prepared for each PHWW to provide 4-6 replicates of each test concentration and 8-12 replicates of the control. Algal inoculum stock solution (50  $\mu$ l) was put into each well to achieve an initial concentration of  $8 \times 10^4$  cell/ml. The microplate was then covered with microplate lid which contains condensation rings to avoid cross contamination and sealed with Parafilm. Plates were placed on a shaker table under continuous illumination of 200  $\mu$ mol photons  $m^{-2} s^{-1}$  of PAR. Inhibition tests were terminated after 72 hours of exposure to tested water. Algal cell density was quantified using Tecan® 200 PRO microplate reader (Männedorf, Switzerland) by reading the fluorescence excitation wavelength of 488 nm and emission at 680 nm.

Algal average growth rate during the 72 hours is calculated according to the following equation:

$$\mu_{i-j} = \frac{\ln X_i - \ln X_j}{t_i - t_j} \quad (6-1)$$

where  $\mu_{i-j}$  is the average specific growth rate between time i and j;  $X_i$  is the biomass concentration at time i;  $X_j$  is the biomass concentration at time j;  $t_i$  is the time of  $i^{\text{th}}$  biomass measurement after beginning of exposure;  $t_j$  is the time of  $j^{\text{th}}$  biomass measurement after beginning of exposure.

The percent inhibition of growth rate for each concentration was calculated from the equation below

$$I_{\mu} = \frac{\mu_c - \mu_{\tau}}{\mu_c} \times 100 \quad (6-2)$$

where:  $I_{\mu}$  is the percent inhibition in average specific growth rate;  $\mu_c$  is the mean value for average specific growth rate ( $\mu$ ) in the control group;  $\mu_{\tau}$  is the average specific growth rate for the treatment replicate.

4-6 replicates were analyzed for each water sample concentration and the experiments were repeated at least 2 times. A concentration-response curve was generated for each sample and a regression analysis was conducted with each curve using the dosage response equation. The  $IC_{50}$  values were calculated from the regression analysis and represent the sample concentration that induced a 50% reduction in growth rate as compared to the concurrent controls.

#### **6.2.4 Response surface methodology**

Three effective operating variables, reaction temperature (T), solids ratio (SR), and retention time (RT) were chosen to be experimentally studied. The design of experiment method is used to design the experiments in such a way to analyze the effect of parameters while using a minimum number of experiments and also to evaluate the interaction between the effective operating parameters. The response surface methodology (RSM) is a technique accompanied by

DOE methods used for modeling and analysis of problems where a desired output variable (response) is influenced by several independent variables. Based on the results of preliminary single factor experiments (Yu et al., 2012), the levels of three operating parameters were determined in the range of 260-300 °C, 30-90 mins and 15-35 wt.% for reaction temperature, retention time and solids ratio, respectively. The response variable is the IC<sub>50</sub>, as described in the section above. A face-centered central composite design (FCCCD) was employed to design the experiment. The detailed experimental design is shown in Table 6-2.

Second-order polynomial regression equation was used to fit response surface models based on the experimental results, which is expressed as the following

$$y = \beta_0 + \sum_{i=1}^k \beta_i x_i + \sum_{i=1}^k \beta_{ii} x_i^2 + \sum_{i=1}^{k-1} \sum_{j=i+1}^k \beta_{ij} x_i x_j + \varepsilon \quad (6-3)$$

where  $y$  is the response variable;  $\beta_0$  is the interception coefficient;  $\beta_i$  is the first order quadratic model coefficient;  $\beta_{ii}$  is the second order quadratic model coefficient;  $\beta_{ij}$  is the linear model coefficient for the interaction between independent variables  $i$  and  $j$ ;  $\varepsilon$  is the fitting error,  $x_i$  and  $x_j$  are the coded independent variables. Because the operating variables have different scales, the variables were normalized to the interval  $[-1,1]$  before the polynomial regression was applied.

The normalization was performed according to the following equation

$$x_{coded,i} = \frac{2x_{actual,i} - x_{actual,max} - x_{actual,min}}{x_{actual,max} - x_{actual,min}} \quad (6-4)$$

where  $x_{actual}$  and  $x_{coded}$  are the actual and coded forms of the independent variable. Statistical tests were performed to evaluate the precision of the empirical second-order polynomial correlation.

It is worth mentioning that these correlations are not recommended for use as pure predictions; more elaborate models are needed for this purpose. In the present work, they were



used for evaluating the effective variables and their interactions as well as finereading the optimized conditions.

### **6.2.5 GC-MS analysis**

The chemical compositions of selected wastewater samples were analyzed using GC-MS (Agilent 7890A GC-5975C MS, Agilent Technologies, Santa Clara, CA) equipped with flame ionization detector (FID) and 15 m ZB-WAX column with 0.25 mm inner diameter and 0.25  $\mu\text{m}$  film thickness (Phenomenex, Torrance, CA, USA). The injection temperature was set to 250  $^{\circ}\text{C}$ , MSD transfer line to be 250  $^{\circ}\text{C}$ , and the ion source to be 230  $^{\circ}\text{C}$ . The spectra of all chromatogram peaks was evaluated using the HP chem station (Agilent, Palo Alto, CA, USA) and AMDIS (NIST, Gaithersburg, MD, USA) programs and compared with electron impact mass spectrum from NIST Mass Spectrial Database (NIST08) and W8N08 library (John Wiley & Sons, Inc.). Internal standard (3-methylbutanoic acid, 0.1  $\mu\text{M}$ ) was used to normalize all data to allow comparison between samples.

## **6.3 Results and Discussion**

### **6.3.1 Inhibition of PHWW on algal growth**

Figure 6-2 shows the concentration response curves for algal growth on PHWW generated from HTL conversion of 15%, 25%, and 35% solids ratio at different reaction temperatures and retention times. These plots show average inhibition data points of each PHWW concentration for 8-10 independent microplate algal cultures, and standard error is indicated as the error bar.  $\text{IC}_{50}$  is calculated as the concentration that induced a 50% reduction in growth rate as compared to the control, and the  $\text{IC}_{50}$  values are summarized in Table 6-3. To directly compare the inhibition effect of each PHWW sample, an inhibition index was also calculated. The inhibition index is determined as  $(\text{IC}_{50})^{-1} \times 100$ , where a larger value represents

greater inhibition. Results showed that the inhibition effect of PHWW varied significantly among the 15 tested HTL operating conditions, and the  $IC_{50}$  values varied from 0.34-1.90% of the PHWW. The two most inhibitory PHWW samples were produced under conditions of 300°C, 90min, 35% solids ratio (#8), and 280°C, 90min, 25% solids ratio (#12), which had  $IC_{50}$  values of 0.35% and 0.34%, respectively. The least inhibitory PHWW sample was produced under HTL conditions of 260°C, 30min, 15% solids ratio (#1), which had an  $IC_{50}$  value of 1.90%. We note that both the most toxic and least toxic PHWWs were generated at the extreme ends of the operating conditions. The lowest inhibitory concentration of each PHWW sample is also shown in Table 6-3, which describes lowest concentration in the algal growth inhibition response curves that induced a statistically significant amount of inhibition as compared to the control. In general, the more inhibitory the PHWW is (lower  $IC_{50}$  value is), the smaller the value of the lowest inhibitory concentration.

Although this study is focused more on the inhibitory effects of PHWW (higher PHWW concentration points), there were often a couple of data points that showed algal growth enhancement at relatively lower PHWW concentration points. These data provide valuable information generated from the concentration response curves regarding the range of PHWW concentrations that can improve total algal growth. As shown in Figure 6-2, when the PHWW is highly diluted, algal growth was generally enhanced, as indicated by negative inhibition values. Table 6-3 also summarizes the maximum growth rate increase observed with each PHWW sample and the corresponding concentration of PHWW. Our data showed that the greatest growth enhancement occurred with 0.05%-0.2% PHWW, which resulted in up to a 15% increase in growth rate, which is a significant enhancement to total biomass production. For example, for algae with a doubling time of 1 day, this growth rate increase could lead to a 50% increase in

overall biomass production during a three day growth period, and more than 100% increase over a five day growth period. This biomass production improvement was also observed in our previous study (Chapter 3): when the PHWW-Spirulina was spiked into municipal wastewater, the overall biomass (algae+bacteria) production increased by up to 60%, and the algal biomass productivity increased by up to 47%. The growth enhancement likely resulted from nutrients like ammonia nitrogen in PHWW, as well as certain organic substrates, such as acetate, which is known to support heterotrophic and mixotrophic algal growth (Perez-Garcia et al. 2011).

### **6.3.2 Model fitting and statistical analysis**

The  $IC_{50}$  values generated from the algal inhibition test were used to fit the response surface model described earlier. The precision of the empirical second-order polynomial correlation was evaluated using analysis of variance (ANOVA), which was developed to interpret the results of systems where several factors can vary simultaneously and influence the parameter of interest,  $IC_{50}$  in this case. Statistically, three tests are required to evaluate the reliability of the model: the test of significance of terms, the R-squared test, and the lack of fit test. Table 6-4 shows the corresponding results of these three tests.

The test of significance of the model and terms are evaluated by the p-value. The p-values for our model were less than 0.05 (Table 6-4), which means the surface response model is statistically significant at the 95% confidence level. The R-squared test was applied to evaluate how well a model can predict the experimental results. Both the R-squared value (0.9517) and adjusted R-squared (0.9083) showed acceptable values ( $\geq 0.8$ ), which confirms a reasonable fit of the experimental data by the model. This indicates that all the  $IC_{50}$  values obtained in this study can be accurately estimated using second-order polynomial regression equations. The adequate precision parameter measures the signal to noise ratio, and a value greater than 4 is

desirable. Our value was 19, indicating the noise of the experiment is small enough that it won't exert a significant influence on the response variable. The lack-of-fit test was used to evaluate the probability of the model failing to predict the experimental values due to systematic errors or other overlooked factors. According to our result, our p-value of lack of fit is very small ( $<0.0001$ ), which indicates that our response surface model would not be reliable to predict the inhibition effect of PHWW for HTL operating conditions outside of our tested range. Multiple reasons could be contributing to this situation. For example, there might be factors that influence the inhibition effect significantly that were not included in the experimental design. It is also possible that the second order polynomial model, which is the most commonly used regression model, is not appropriate for our case. In any case, the developed surface response model is still valid and precise for the range of operating conditions and the experimental setup tested herein, giving that the test of significance and the coefficient of the determination test showed pretty good results. Therefore this model is useful for studying the relative influence of the effective variables and their interactions, making predictions of the system performance, and finding the optimal operating conditions for the system under study.

Based on the ANOVA results, the developed model is given below

$$\begin{aligned}
 IC_{50} = & 4.293 \times 10^{-3} - 2.120 \times 10^{-3} \times X_T - 1.68 \times 10^{-3} \times X_{RT} - 2.611 \times 10^{-3} \times X_{SR} + 1.338 \times 10^{-3} \times X_T \\
 & \times X_{RT} + 5.875 \times 10^{-4} \times X_T \times X_{SR} + 8.875 \times 10^{-4} \times X_{RT} \times X_{SR} + 6.164 \times 10^{-4} \times X_T^2 + 6.162 \times 10^{-4} \times X_{RT}^2 \\
 & + 2.871 \times 10^{-3} \times X_{SR}^2
 \end{aligned} \quad (6-4)$$

where  $X_T$ ,  $X_{RT}$ , and  $X_{SR}$  represent reaction temperature, retention time, and total solids ratio, respectively.

### 6.3.3 Effect of HTL operating condition on PHWW inhibition

#### 6.3.3.1 Effect of solids ratio

Our data showed that as solids ratio increased from 15% to 25%, PHWW inhibition of algae increased significantly, and then it decreased slightly as solids ratio increased from 25% to 35%. As shown in Figure 6-3A, at fixed reaction temperature of 280 °C and retention time of 60 min, the  $IC_{50}$  value decreased by more than half from 0.92% to 0.44% (i.e., inhibition increased more than two-fold) when solids ratio increased from 15% to 25%. The overall trends in  $IC_{50}$  values, can be seen in more detail in the response surfaces plotted in Figure 6-3B: the surfaces of 15% and 25% solids ratio are clearly separated, which indicates a relatively big change in  $IC_{50}$ . This result is not surprising because the higher the solids ratio is, the more materials that participate in the reaction, and the more substances end up in the aqueous phase. The substances in PHWW come from two main sources: the biomass that dissolved into aqueous phase, reacted, and remained; and the part that came from intimate contact with oil phase formed during the HTL reaction. Both of these components increase as the solids ratio increase. Many studies found that the organic content and nutrient content in aqueous product increased as the solids ratio increased (Jena et al. 2011b; Gai et al. 2014b). As discussed in previous chapter, the toxic organic compounds and ammonia in PHWW can contribute significantly to the inhibition of algal growth on PHWW. Higher amounts of dissolved substances in the aqueous PHWW product indicates a potentially higher level of toxic compounds, resulting in more inhibitory effects on algal growth.

As shown in Figure 6-3A, when the solids ratio increased from 25% to 35%, there was actually a very slight decrease of inhibition (increase in  $IC_{50}$  value), but the difference is not statistically significant and these values should be considered to be functionally the same. This

can be seen more clearly in the response surfaces in Figure 6-3B: the surfaces of 15% and 25% solids ratio are clearly separated, while the surfaces of 25% and 35% solids ratio are very close together with even overlapping. The minimum change of  $IC_{50}$  when solids ratio further increased to 35% may be related to the dissolution capacity of various compounds. Many compounds might have already reached or have been very close to the maximum solubility at the solids ratio of 25%, and further increase in solids ratio would not significantly increase the soluble content in PHWW. For example, Gai et al. (2014b) found that COD in PHWW increased dramatically as solids ratio increased from 15% to 25%, and had very slight increase from 25% to 35%. Thus, the lower dissolution efficiency of substances as the solids ratio increased from 25% to 35% might have resulted in very small change in inhibitory effect.

#### 6.3.3.2 *Effect of reaction temperature*

Figures 6-3C, D illustrate the effect of reaction temperature on PHWW inhibition. Experimental results showed that higher reaction temperatures generally resulted in a higher level of inhibition on algal growth by PHWW (lower  $IC_{50}$  values). For example, as shown in Figure 6-3C, at fixed retention time of 60 min and solids ratio of 25%, the  $IC_{50}$  value first decreased from 0.53% to 0.44%, and then to 0.42% (inhibition kept increasing) as reaction temperature increased from 260 °C to 280 °C, and to 300 °C. This is also true for other sets of experimental data (Table 6-3) although only two levels of comparison (HTL conditions with two different reaction temperatures, at a fixed solids ratio and retention time) are available for other conditions. The effect of reaction temperature can be seen more clearly in the response surfaces in Figure 6-3D, the  $IC_{50}$  value kept decreasing as the reaction temperature increased from 260 °C to 300 °C all throughout the tested range.

Many inhibitory compounds have been reported to show increased level in PHWW as reaction temperature increases. One example would be ammonia nitrogen, which mainly comes from the decomposition of protein and is well known to be toxic to many aquatic organisms. Both Inoue et al. (1997) and Valdez et al. (2012) found that the increase of reaction temperature resulted in increased ammonia nitrogen concentration and total nitrogen in the aqueous product of HTL. Phenol is another example that is well known for its toxicity to many microorganisms including algae (Tišler and Zagorc-Končan 1997), and it is normally formed via ring closure by two or more smaller molecules under relatively high temperatures (Kruse et al. 2005; Biller and Ross 2011). Tommaso et al. (2014) reported that the phenol content kept increasing from 0.21% to 8.44% as the HTL reaction temperature increased from 260 °C to 320 °C. Another example is nitrogen-heterocyclic compounds, the formation of which is related to cross-reactions with proteins and carbohydrates. They have been shown to be toxic to algal growth (Pham et al. 2013), and were found to increase as the reaction temperature increased (Tommaso et al. 2014).

#### 6.3.3.3 *Effect of reaction time*

Our data showed that longer retention time generally resulted in PHWW that is more inhibitory to algal growth. For example, as shown in Figure 6-3E, at a given solids ratio of 25% and given reaction temperature of 280 °C, the  $IC_{50}$  decreased from 0.61% to 0.44%, and to 0.34% as retention time increased from 30 min to 60 min, and to 90 min, respectively. This was also true for other sets of experimental data (Table 6-3) with two levels of comparison (i.e., HTL conditions with two different retention times, at a fixed solids ratio and reaction temperature). The response surface in Figure 6-3F also confirmed this trend, although at low solids ratio and high temperature this effect is very minimal.

### 6.3.4 Correlation between water quality and inhibition of PHWW

In order to investigate whether there is any relationship between water quality parameters and the inhibition of PHWW, a Pearson correlation analysis was used, which is a common technique for exploring the relationship (linear) between 2 variables. As shown in Table 6-5, among several tested water quality parameters, COD, TN, ammonia nitrogen concentration showed a significant linear relationship with the PHWW inhibition ( $IC_{50}$ ), which is indicated by p values below 0.05. Among these three parameters, ammonia nitrogen has the highest absolute value of the correlation coefficient, followed by total nitrogen and COD. Ammonia is well known for its toxicity to algae. It has been reported to inhibit photosynthesis, carbon assimilation and thus overall algal growth with concentration around the level of 20 mg or even 20  $\mu$ g (mM or even  $\mu$ M range) (Abeliovich and Azov 1976; Azov and Goldman 1982; Kallqvist and Svenson 2003). Free ammonia was found to be the predominant toxic form in the ammonium/water system, and the specific toxicity of ammonia ( $EC_{50}$ , 24h exposure) can be as low as 2.34  $\mu$ M (32.8  $\mu$ g ammonia nitrogen/L) (Kallqvist and Svenson 2003). Ammonium ion, although less toxic than free ammonia, can still inhibit algal photosynthesis and growth. Since ammonia nitrogen is a measurement of a single compound, it is not surprising that its relationship with the PHWW inhibition is more direct and obvious, compared to other parameters like TN and COD that represent a broad range of compounds. Although TN also showed a moderate negative linear relationship with  $IC_{50}$  values of PHWW, this can be credited to the ammonia nitrogen, which is about half of the TN. The rest of TN is organic nitrogen, which did not show a significant relationship with the inhibition (Table 6-5).

COD also showed a moderate negative linear relationship with  $IC_{50}$  values, which means there is a tendency that increasing COD is correlated with higher algal inhibition by PHWW.



Many of the detected organic compounds in PHWW are found to be toxic to algae growth as discussed previously. It is worth noting that unlike ammonia nitrogen, COD is a parameter that represents a broad spectrum of compounds. While some of the organics are toxic to algae, others are not, such as a variety of simple organic acids, which can even promote algal growth. The more complex nature of COD is likely a reason for the lower correlation coefficient compared to that of ammonia nitrogen.

### **6.3.5 GC-MS analysis**

The most toxic (#8: 300 °C, 90 min, 35% solids ratio) and least toxic (#1: 260 °C, 30 min, 15% solids ratio) PHWW samples were subject to GC-MS analysis to elucidate and compare the chemical composition. The NIST mass spectral databased was used to identify the main peaks in the total ion chromatograms of PHWW. As shown in Figure 6-4, the major chemical components are categorized into groups, such as short chain acid (C2-C4), fatty acid and its derivatives, straight amine derivatives, N,O-heterocyclic compounds, aromatic carboxylic acid, and straight chain oxygenates. The primary chemical compounds and their relative quantities are listed in Table 6-6. It is worth mentioning that saturated and unsaturated hydrocarbons were barely found in the aqueous samples, but they are one of the main components detected in biocrude oils (Gai et al. 2014a). This again demonstrates that the oil and aqueous phase products of HTL are very different and additional characterization of the aqueous phase products is justified.

It is clear that the N,O-heterocyclic compounds make up a large portion of the chemical composition in PHWW, followed by straight amine derivatives and straight oxygenates. Although #1 PHWW (the least toxic) showed slightly higher quantity of N,O-heterocyclic compounds, #8 PHWW (the most toxic) was observed to have more heterocyclic species with

methyl groups and additional ring structures such as 1-acetyl-Pyrrolidine-, 1,3-Dioxolane-2-methyl-, 1-(1-oxopropyl)-Pyrrolidine, 1-ethyl-2,5-Pyrrolidinedione, 1-Methyl-2,5-Pyrrolidinedione-, Pyrrolo[1,2-a]pyrazine-1,4-dione, hexahydro-3-(2-methylpropyl)-. It has been reported that hydrocarbon-ring addition and methyl substitution could cause a linear toxicity increase, coupled with an increase in resistance to biological degradation (Schultz et al. 1978; Schultz et al. 1980). #8 was also observed to have more aromatic carboxylic acids, such as benzeneacetic acid. Various alicyclic carboxylic acids have been reported to be toxic to algae and microbes (Fiorentino et al. 2003; Frank et al. 2008). Straight chain oxygenates are generally easy to be utilized by microbes (Atlas 1991), and thus it is not surprising that they were observed to be significantly higher in the #1 PHWW (least toxic) than in the PHWW #8 sample (most toxic).

### **6.3.6 Advantageous HTL operating conditions**

One important objective of this study is to provide guidance on HTL operating conditions to produce PHWW suitable for algal growth and to maximize the energy production of the entire E<sup>2</sup>-Energy system. Besides inhibition, many factors should be taken into consideration, such as the energy recovery (ER) efficiency of the HTL process, the quality of the oil (e.g., heating value and nitrogen content), carbon and nitrogen recovery ratio etc. Here, we consider high energy recovery to be the primary criteria, and aim for PHWW that has a relatively mild inhibitory effect on algal growth with some other parameters also considered. We created an objective function which is the rank of the energy recovery \* rank of the IC<sub>50</sub>, with the results of 15 samples shown in Figure 6-5. With this objective function, a lower number is preferred, and Figure 6-5 shows that sample #11 showed the best result because it had a relatively high energy recovery (66.1%, 3<sup>rd</sup> highest energy recovery) and a relatively low inhibitory effect on algal

growth ( $IC_{50}$  0.92%, 3<sup>rd</sup> least inhibitory PHWW). This condition also resulted in fairly good biocrude oil yield (3<sup>rd</sup> highest), and the good quality oil in terms of high heating value (6<sup>th</sup> highest) and low nitrogen recovery (4<sup>th</sup> lowest) of biocrude oil (Gai et al. 2014a). Although #12 also showed some promise in terms of a low objective function value in Figure 6-5, we can see that a 5% increase in energy recovery is accompanied by 48% decrease in  $IC_{50}$  (almost one fold increase in inhibitory effect) compared to #11 (see Table 6-3). The #1 condition, was the third best scenario according to our objective function. Unfortunately it also showed the least heating value of biocrude oil among all 15 samples (Gai et al. 2014a) and therefore is not recommended. Overall, the condition of 280 °C, 60 min, and 15% solids ratio was judged to be the most favorable HTL operating condition because it gave an advantageous balance of fairly high energy recovery, oil yield and quality, and a lower inhibitory effect of PHWW on algal growth.

#### **6.4 Conclusions**

An algal-growth inhibition assay and response surface methodology were developed and used to study how HTL operating conditions affect the inhibition of algae by PHWW. The  $IC_{50}$  values (concentration that induces 50% reduction in cell growth rate) of 15 PHWW samples generated under various HTL operating conditions (260-300 °C, 30-90 min, 15-35% solids ratio) ranged from 0.34%-1.9%. As solids ratio increased from 15% to 25%, PHWW inhibition of algae increased significantly, and then it decreased slightly as solids ratio increased from 25% to 35%. PHWW inhibition also generally increased as temperature and retention time increased. GC-MS analysis revealed chemical compound differences between the most toxic and least toxic PHWW regarding the content of N, O heterocyclic compounds and straight chain oxygenates etc. COD,  $NH_4^+$ , and TN were all found to have moderate correlation with the PHWW inhibition. 280 °C, 60 min, and 15% solids ratio is recommended as the most favorable HTL operating

conditions that yield relatively high energy recovery (66.1%), and relatively low PHWW inhibition effects on algal growth (IC<sub>50</sub> of 0.92%).

## 6.5 References

- Abeliovich, A. and Y. Azov. 1976. Toxicity of ammonia to algae in sewage oxidation ponds. *Applied and Environmental Microbiology* 31(6): 801-806.
- Appleford, J. M. 2005. Analyses of the products from the continuous hydrothermal conversion process to produce oil from swine manure. PhD diss. Champaign, IL: University of Illinois at Urbana-Champaign.
- Atlas, R. M. 1991. Microbial hydrocarbon degradation-bioremediation of oil spills. *Journal of Chemical Technology & Biotechnology* 52(2): 149-156.
- Azov, Y. and J. C. Goldman. 1982. Free Ammonia Inhibition of Algal Photosynthesis in Intensive Cultures. *Applied and Environmental Microbiology* 43(4): 735-739.
- Biller, P. and A. B. Ross. 2011. Potential yields and properties of oil from the hydrothermal liquefaction of microalgae with different biochemical content. *Bioresource Technology* 102(1): 215-225.
- Biller, P., A. B. Ross, S. C. Skill, A. Lea-Langton, B. Balasundaram, C. Hall, R. Riley and C. A. Llewellyn. 2012. Nutrient recycling of aqueous phase for microalgae cultivation from the hydrothermal liquefaction process. *Algal Research* 1(1): 70-76.
- Du, Z., B. Hu, A. Shi, A. Ma, X. Cheng, Y. Chen, P. Liu, Y. Lin and X. R. Roger. 2012. Cultivation of a microalga *Chlorella vulgaris* using recycled aqueous phase nutrients from hydrothermal carbonization process. *Bioresource Technology* 126: 354-357.
- Eisentraeger, A., W. Dott, J. Klein and S. Hahn. 2003. Comparative studies on algal toxicity testing using fluorometric microplate and Erlenmeyer flask growth-inhibition assays. *Ecotoxicology and Environmental Safety* 54(3): 346-354.
- Elliot, D. C. 1993. Evaluation of wastewater treatment requirements for thermochemical biomass liquefaction. In *Advances in Thermochemical Biomass Conversion*, 1299-1313. Netherlands: Springer.
- Fiorentino, A., A. Gentili, M. Isidori, P. Monaco, A. Nardelli, A. Parrella and F. Temussi. 2003. Environmental effects caused by olive mill wastewaters: toxicity comparison of low-molecular-weight phenol components. *Journal of Agricultural and Food Chemistry* 51(4): 1005-1009.

- Frank, R. A., K. Fischer, R. Kavanagh, B. K. Burnison, G. Arsenault, J. V. Headley, K. M. Peru, G. V. D. Kraak and K. R. Solomon. 2008. Effect of carboxylic acid content on the acute toxicity of oil sands naphthenic acids. *Environmental Science & Technology* 43(2): 266-271.
- Gai, C., Y. Zhang, W. Chen, P. Zhang and Y. Dong. 2014a. Energy and nutrient recovery efficiencies in biocrude oil produced via hydrothermal liquefaction of *Chlorella pyrenoidosa*. *RSC Advances* 4(33): 16958-16967.
- Gai, C., Y. Zhang, W. Chen, Y. Zhou, L. Schideman, P. Zhang, G. Tommaso, C. Kuo and Y. Dong. 2014b. Characterization of aqueous phase from the hydrothermal liquefaction of *Chlorella Pyrenoidosa*. *Bioresource Technologies* 184: 328-335.
- Jena, U., N. Vaidyanathan, S. Chinnasamy and K. C. Das. 2011a. Evaluation of microalgae cultivation using recovered aqueous co-product from thermochemical liquefaction of algal biomass. *Bioresource Technology* 102(3): 3380-3387.
- Jena, U., K. C. Das and J. R. Kastner. 2011b. Effect of operating conditions of thermochemical liquefaction on biocrude production from *Spirulina platensis*. *Bioresource Technology* 102(10): 6221-6229.
- Kallqvist, T. and A. Svenson. 2003. Assessment of ammonia toxicity in tests with the microalga, *Nephroselmis pyriformis*, Chlorophyta. *Water Research* 37(3): 477-484.
- Kruse, A., A. Krupka, V. Schwarzkopf, C. Gamard and T. Henningsen. 2005. Influence of Proteins on the Hydrothermal Gasification and Liquefaction of Biomass. 1. Comparison of Different Feedstocks. *Industrial & Engineering Chemistry Research* 44(9): 3013-3020.
- Perez-Garcia, O., F. M. E. Escalante, L. E. de-Bashan and Y. Bashan. 2011. Heterotrophic cultures of microalgae: Metabolism and potential products. *Water Research* 45(1): 11-36.
- Pham, M. 2014. Characterizing the effects of hydrothermal processes on bioactive compounds in wastewater bioenergy systems. PhD diss. University of Illinois at Urbana-Champaign.
- Pham, M., L. Schideman, J. Scott, N. Rajagopalan and M. Plewa. 2013. Chemical and biological characterization of wastewater generated from hydrothermal liquefaction of spirulina. *Environmental science technology* 47(4): 2131-2138.
- Schultz, T. W., M. Cajina-Quezada and J. N. Dumont. 1980. Structure-toxicity relationships of selected nitrogenous heterocyclic compounds. *Archives of Environmental Contamination and Toxicology* 9(5): 591-598.
- Schultz, T. W., L. M. Kyte and J. N. Dumont. 1978. Structure-toxicity correlations of organic contaminants in aqueous coal-conversion effluents. *Archives of Environmental Contamination and Toxicology* 7(1): 457-463.

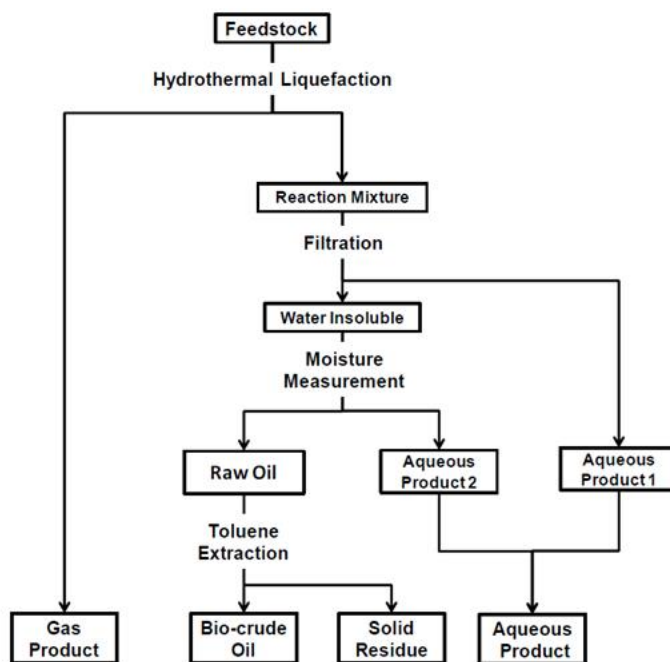
- Tišler, T. and J. Zagorc-Končan. 1997. Comparative assessment of toxicity of phenol, formaldehyde, and industrial wastewater to aquatic organisms. *Water, Air, and Soil Pollution* 97(3-4): 315-322.
- Tommaso, G., W. Chen, P. Li, L. Schideman and Y. Zhang. 2014. Chemical Characterization and Anaerobic Biodegradability of Hydrothermal Liquefaction Aqueous Products from Mixed-culture Wastewater Algae. *Bioresource Technology* 178: 139-146..
- Valdez, P. J., M. C. Nelson, H. Y. Wang, X. N. Lin and P. E. Savage. 2012. Hydrothermal liquefaction of *Nannochloropsis* sp.: Systematic study of process variables and analysis of the product fractions. *Biomass and Bioenergy* 46: 317-331.
- Weber, C. I., W. Peltier, T. Norberg-King, W. Horning and F. Kessler. 2002. Methods for Measuring the Acute Toxicity of Effluent and Receiving Waters to Freshwater and Marine Organisms. Washington D.C.: U.S. EPA.
- Zhou, Y., L. Schideman, G. Yu and Y. Zhang. 2013. A synergistic combination of algal wastewater treatment and hydrothermal biofuel production maximized by nutrient and carbon recycling. *Energy and Environmental Science* 6 (12): 3765-3779.

## 6.6 Figures and Tables

**Table 6-1. Characteristics of *C. pyrenoidosa* powder (Yu et al. 2011).**

Properties	<i>C. pyrenoidosa</i>
Moisture content (wt %) <sup>a</sup>	6.3
Dry solid content (wt %) <sup>a</sup>	93.7
Volatile solid content	94.4
Ash content	5.6
Crude protein	71.3
Crude fat	0.1
Acid detergent fiber	0.5
Neutral detergent fiber	1.0
Lignin	0.2
Non-fibrous carbohydrate <sup>b</sup>	22.0
<b>Elemental composition</b>	
C	51.4
H	6.6
N	11.1
O <sup>b</sup>	30.9

<sup>a</sup>On a total weight basis (other values use a dry weight basis); <sup>b</sup>Calculated by difference

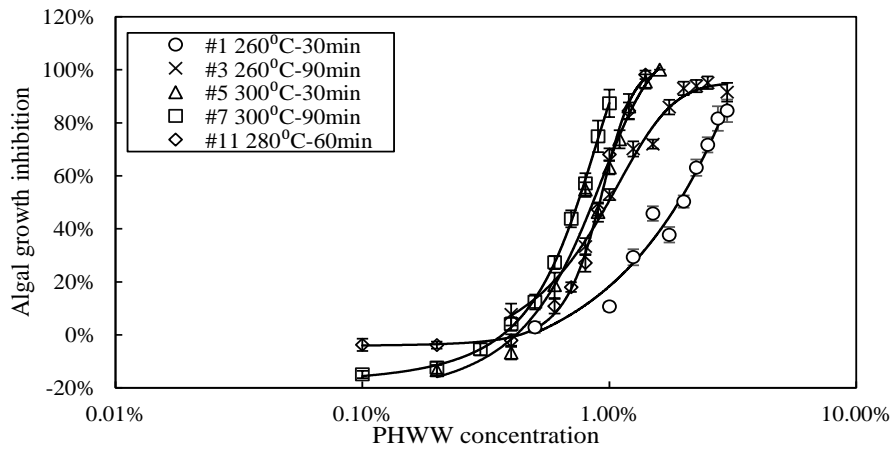


**Figure 6-1. Recovery procedures for products from a hydrothermal liquefaction process (Yu et al. 2011).**

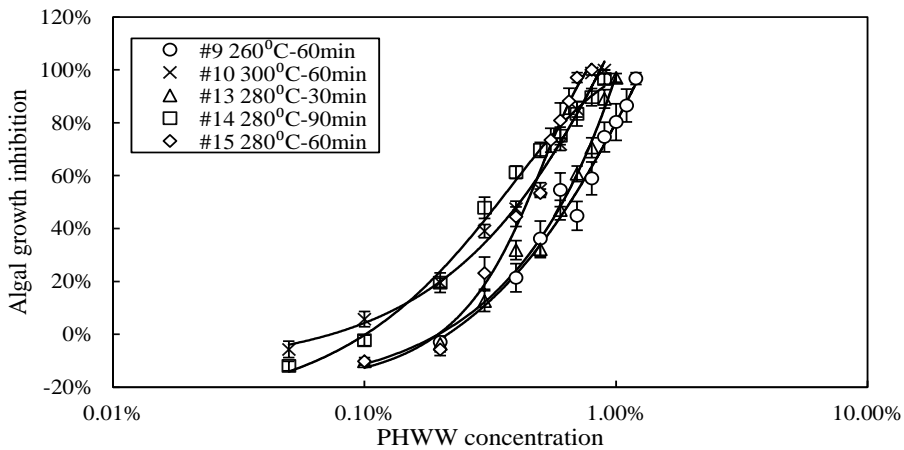
**Table 6-2. Design of experiment and water quality parameters (Pham 2014; Gai et al. 2014b; Gai et al. 2014a).**

Run no.	Point type	Reaction Temperature( °C)	Retention time (min)	Total solids ratio (wt.%)	Energy Recovery (%)	COD (g/L) ±SD	TN (g/L) ±SD	TP (g/L) ±SD	NH <sub>4</sub> <sup>+</sup> -N (g/L) ±SD
1	Factorial	260 (-1)	30 (-1)	15 (-1)	49.8	82.1±3.92	11.7±0.5	11.1±0.52	3.8±0.07
2	Factorial	260 (-1)	30 (-1)	35 (+1)	36.9	95.9±3.79	26.8±1.05	18.9±0.92	6.1±0.09
3	Factorial	260 (-1)	90 (+1)	15 (-1)	41.5	82.3±3.11	16.7±0.7	5.44±0.26	3.4±0.10
4	Factorial	260 (-1)	90 (+1)	35 (+1)	38.1	98.3±4.41	31.7±1.35	14.5±0.69	10.8±0.09
5	Factorial	300 (+1)	30 (-1)	15 (-1)	57.1	69.4±2.96	14.5±0.6	6.02±0.28	6.4±0.09
6	Factorial	300 (+1)	30 (-1)	35 (+1)	61.3	100±4.09	25.3±0.7	12.4±0.54	14.8±0.30
7	Factorial	300 (+1)	90 (+1)	15 (-1)	48.2	62.7±2.95	11.0±0.31	6.84±0.32	6.0±0.01
8	Factorial	300 (+1)	90 (+1)	35 (+1)	64.6	98.7±3.96	22.7±0.66	14.8±0.53	14.0±0.23
9	Axial	260 (-1)	60 (0)	25 (0)	47.5	97.6±4.57	19.8±0.71	8.16±0.37	7.6±0.09
10	Axial	300 (+1)	60 (0)	25 (0)	67.9	94.5±4.35	16.3±0.60	7.26±0.36	6.7±0.04
11	Axial	280 (0)	60 (0)	15 (-1)	66.1	84.2±3.88	13.6±0.50	5.56±0.26	3.0±0.10
12	Axial	280 (0)	60 (0)	35 (+1)	69.5	102±4.73	27.9±0.92	14.3±0.66	12.6±0.10
13	Axial	280 (0)	30 (-1)	25 (0)	50.8	100±2.91	18.8±0.76	15.0±0.70	9.4±0.03
14	Axial	280 (0)	90 (+1)	25 (0)	50.9	98.0±4.00	20.1±0.85	14.5±0.69	8.8±0.21
15	Center	280 (0)	60 (0)	25 (0)	64.3	101±3.95	18.9±0.70	9.94±0.48	8.2±0.06
16	Center	280 (0)	60 (0)	25 (0)	65.0	101±3.96	19.8±0.80	10.4±0.51	
17	Center	280 (0)	60 (0)	25 (0)	64.7	99.7±4.01	19.3±0.55	10.2±0.50	
18	Center	280 (0)	60 (0)	25 (0)	63.9	102±3.94	18.5±0.60	9.85±0.48	
19	Center	280 (0)	60 (0)	25 (0)	67.6	102±3.59	18.3±0.55	9.67±0.47	
20	Center	280 (0)	60 (0)	25 (0)	66.7	104±4.57	18.9±0.85	9.45±0.46	

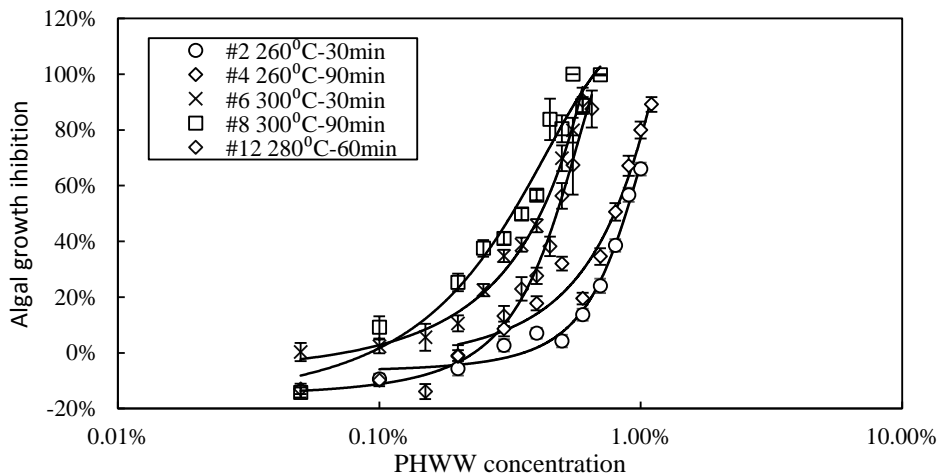




(A)



(B)



(C)

**Figure 6-2. Comparison of the algal inhibition concentration response curve for wastewater generated under different reaction temperature and retention times using feedstock of different solid content: (A) 15% solid content, (B) 25% solid content, (C) 35% solids content.**

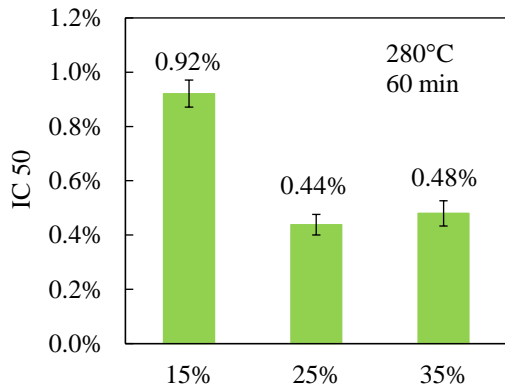
**Table 6-3. Parameters generated from concentration response curve of PHWW algal growth inhibition test.**

#	Reaction Temp. ( °C)	Reaction time (min)	Solid Ratio (%)	R <sup>2</sup>	Lowest inhib. Conc. (%)	IC <sub>50</sub> (%)±SE	Inhib. index	ANOVA test statistic	Growth Enhancement	
									Conc. (%)	Growth rate increase
1	260	30	15	0.95	1	1.90±0.43	53	$F_{10,119}=135.2, P\leq 0.0001$	--	--
2	260	30	35	0.98	0.4	0.91±0.05.	110	$F_{10,95}=154.2, P\leq 0.0001$	0.1	9.4%
3	260	90	15	0.98	0.4	0.97±0.018	103	$F_{10,119}=240.8, P\leq 0.0001$	--	--
4	260	90	35	0.95	0.3	0.62±0.014	161	$F_{10,119}=172.4, P\leq 0.0001$	0.2	1%
5	300	30	15	0.97	0.6	0.86±0.021	116	$F_{10,95}=222.1, P\leq 0.0001$	0.2	13.4
6	300	30	35	0.99	0.15	0.41±0.015	244	$F_{10,119}=34.5, P\leq 0.0001$	--	--
7	300	90	15	0.99	0.5	0.75±0.022	133	$F_{10,119}=132.2, P\leq 0.0001$	0.1	14.9%
8	300	90	35	0.95	0.1	0.35±0.01	286	$F_{10,119}=53.6, P\leq 0.0001$	0.05	14.2%
9	260	60	25	0.96	0.4	0.53±0.028	189	$F_{10,95}=52.36, P\leq 0.0001$	0.2	2.9%
10	300	60	25	0.99	0.1	0.42±0.011	238	$F_{10,119}=296.1, P\leq 0.0001$	0.05	5.7%
11	280	60	15	0.98	0.6	0.92±0.016	109	$F_{10,119}=294.8, P\leq 0.0001$	0.2	3.8%
12	280	60	35	0.98	0.3	0.48±0.015	208	$F_{10,119}=86.0, P\leq 0.0001$	0.15	13.9%
13	280	30	25	0.99	0.3	0.61±0.02	164	$F_{10,119}=179.2, P\leq 0.0001$	0.1	10.2%
14	280	90	25	0.99	0.2	0.34±0.01	294	$F_{10,95}=237.7, P\leq 0.0001$	0.05	12%
15	280	60	25	0.98	0.3	0.44±0.013	227	$F_{10,95}=158.4, P\leq 0.0001$	0.1	10.3%

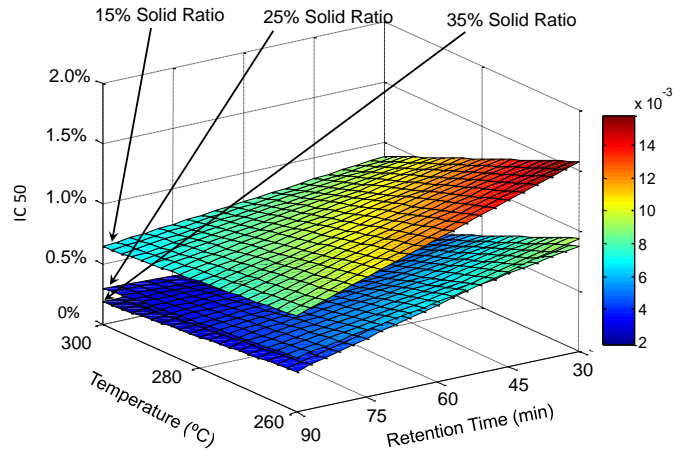
The lowest inhibition concentration was the lowest concentration of the tested PHWW in the concentration response curves that induced a significant amount of inhibition as compared to the control. R<sup>2</sup> is the coefficient of determination for the regression analysis upon which the IC<sub>50</sub> value was calculated. The IC<sub>50</sub> is the sample concentration that induced a 50% growth rate reduction of the control. The SE of the IC<sub>50</sub> was derived as the averaged SE of multiple IC<sub>50</sub> values determined from regression analysis for 8-10 concentration-response curves.

**Table 6-4. ANOVA evaluation of the IC50 of post-hydrothermal liquefaction wastewater.**

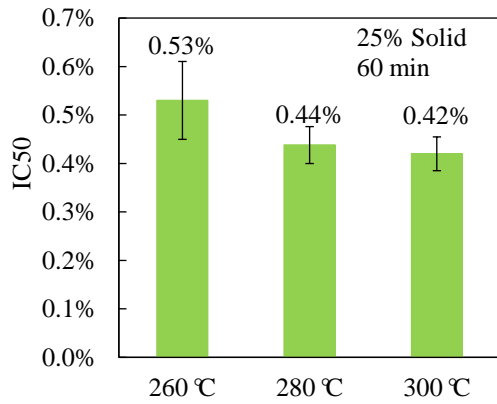
<b>Factor</b>	<b>Sum of squares</b>	<b>p value for F test</b>
Model	2.333E-4	<0.0001
X <sub>T</sub>	4.494E-5	0.0001
X <sub>RT</sub>	2.822E-5	0.0006
X <sub>SR</sub>	6.817E-5	<0.0001
X <sup>2</sup> <sub>T</sub>	1.431E-5	0.3695
X <sup>2</sup> <sub>RT</sub>	2.761E-6	0.3695
X <sup>2</sup> <sub>SR</sub>	6.301E-6	0.0014
X <sub>T</sub> X <sub>RT</sub>	1.045E-6	0.0059
X <sub>T</sub> X <sub>SR</sub>	1.045E-6	0.1576
X <sub>RT</sub> X <sub>SR</sub>	2.267E-5	0.0437
Residual	1.183E-5	
Lack-of-fit	1.173E-5	<0.0001
R squared	0.9517	
Adjusted R <sup>2</sup>	0.9083	
Adequate precision	19.283	



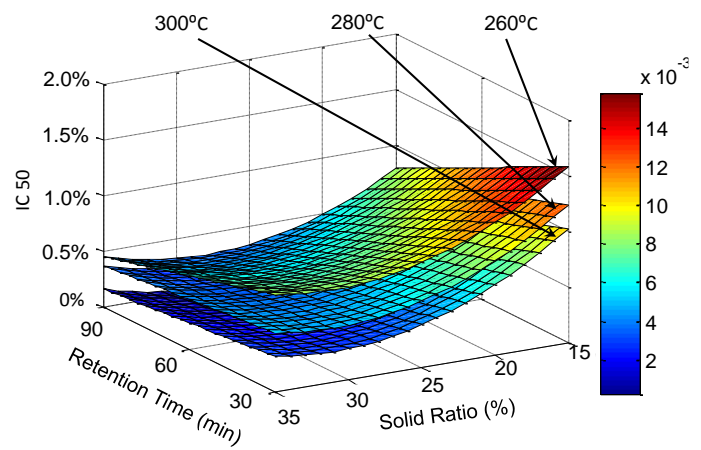
(A)



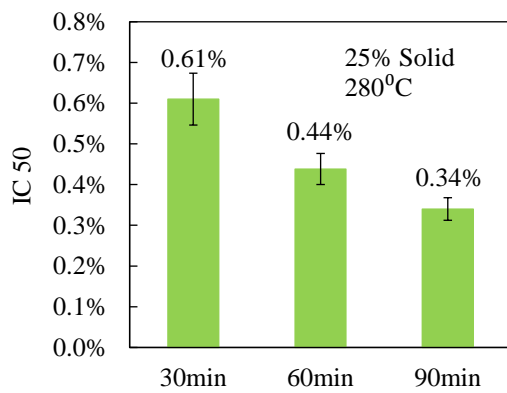
(B)



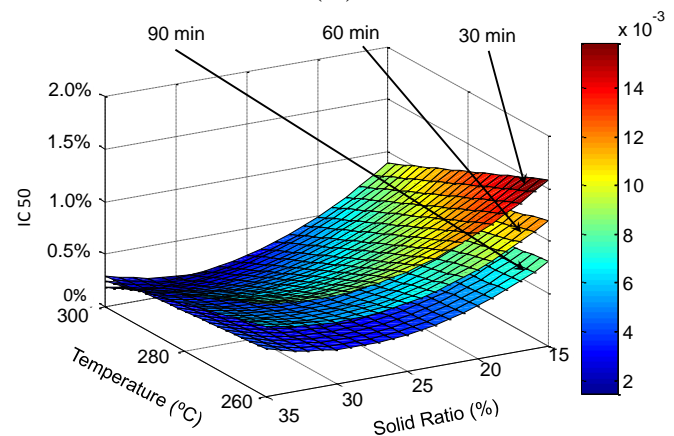
(C)



(D)



(E)



(F)

**Figure 6-3. The effect of hydrothermal liquefaction conditions, including solids content (A and B), reaction temperature (C and D), and retention times (E and F) on algal growth inhibition.**

**Table 6-5. Correlation between PHWW water quality parameters and inhibition.**

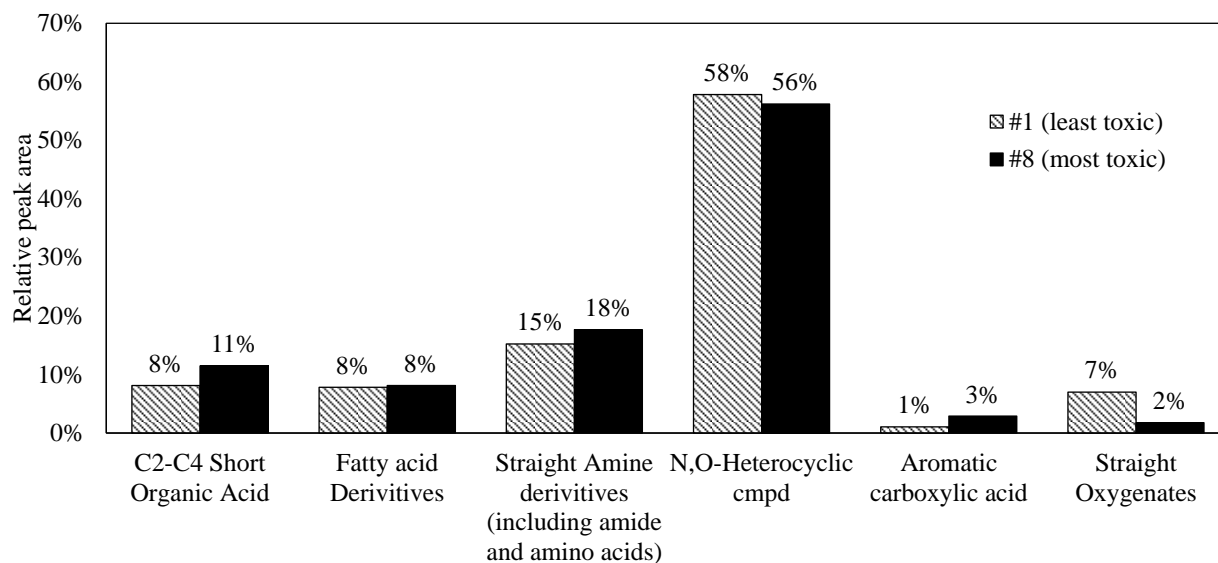
HTL related parameters	IC 50 of PHWW	
	Correlation Coefficient (r)	P value
<b>COD concentration (g/L)</b>	<b>-0.5636</b>	<b>0.0299</b>
<b>Total nitrogen concentration (g/L)</b>	<b>-0.6060</b>	<b>0.0166</b>
<b>Ammonia nitrogen concentration (g/L)</b>	<b>-0.6565</b>	<b>0.0079</b>
Organic nitrogen concentration (g/L)	-0.4441	0.0973
Total phosphorous (g/L)	-0.5130	0.0505

**Table 6-6. GC-MS analysis results of water samples.**

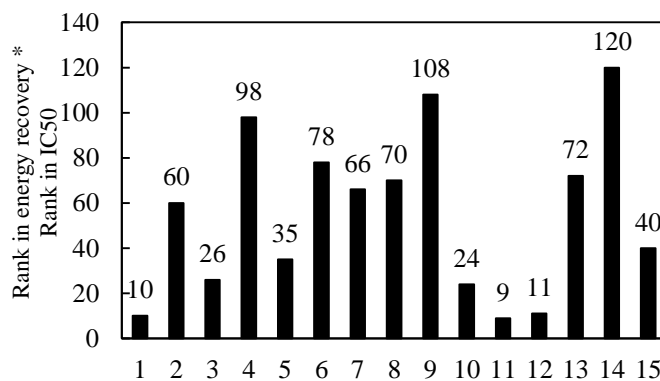
Name	RT	Relative integrated signal		
		#1 (least toxic)	#8 (most toxic)	#8/#1
Trimethylamine	1.08	0.25	0.01	4%
Acetaldehyde	1.29	0.23	N.D.	0%
2-Butanone	1.55	N.D.	0.03	INF
Isopropyl Alcohol	1.66	4.15	0.85	20%
Acetonitrile	2.25	3.25	0.72	22%
1-Propanamine, Dimethyl-	2.35	N.D.	0.27	INF
Piperidine, Dimethyl-	3.27	0.29	N.D.	0%
N-ethylpyrrolidine	3.28	0.32	N.D.	0%
Hygrine	6.81	0.23	0.01	4%
Pyrazine, methyl	8.11	0.67	0.25	37%
Pyrazine, dimethyl	9.68	0.34	0.14	41%
Acetic acid	13.54	2.35	2.86	122%
Propanoic acid	15.66	1.29	1.76	136%
2-methylpropanoic acid	16.34	0.2	0.29	145%
Butanoic acid	17.71	0.43	0.4	93%
1,3-Dioxolane, 2-methyl-	17.95	0.52	2.88	554%
Butanoic acid, 3-methyl- (Internal Standard)	18.6	1	1	100%
Acetamide, N-methyl-	18.11	N.D.	0.92	INF
Acetamide, N-butyl-	20.02	N.D.	0.77	INF
Acetamide	20.76	1.46	2.83	194%
Pentanoic acid, 4-methyl-	21.44	0.83	0.49	59%
Propanamide	21.61	0.47	1.35	287%
Pyrrolidine, 1-acetyl-	21.81	0.29	1.64	566%
N-(3-Methylbutyl)acetamide	22.26	N.D.	0.43	INF
Pyrrolidine, 1-(1-oxopropyl)-	22.46	N.D.	0.17	INF
2,5-Pyrrolidinedione, 1-ethyl-	22.82	N.D.	0.76	INF
2-tetradecanone, 14-(5-hydroxy-6-methyl-2-piperidinyl)	22.86	N.D.	0.03	INF
2,5-pyrrolidinedione, 1-methyl	23.31	0.37	0.92	249%
N-methylhexanamide	23.57	N.D.	0.3	INF
Butanamide, 3-methyl	23.73	0.37	0.66	178%

**Table 6-6 (cont.)**

Name	RT	Relative integrated signal		
		#1 (least toxic)	#8(most toxic)	#8/#1
2-pyrrolidinone	25.78	1.14	3.52	309%
N-ethyl-n-methylamine	26.01	0.29	N.D.	0%
Pentanamide, 4-methyl-	26.49	0.37	0.63	170%
2-Piperidinone	27.44	2.03	4.45	219%
Caprolactam	28.31	0.55	1.33	242%
Glycerin	30.93	4.91	4.11	84%
3-Cyclopentylcyclopentan-1-one	32.02	0.32	0.01	3%
3-Pyridinol, 6-methyl-	32.16	0.96	0.44	46%
3-Pyridinol	32.44	1.32	0.68	52%
Benzeneacetic acid	34.65	0.3	0.41	137%
Benzenepropanoic acid	35.57	0.36	1.04	289%
2,4,5-Trihydroxypyrimidine	42.7	2.75	N.D.	0%
3,6-Diisopropylpiperazin-2,5-dione	42.99	2.71	0.32	12%
Pyrrolo[1,2-a]pyrazine-1,4-dione, hexahydro-3-(2-methylpropyl)-	43.41	0.99	1.48	149%
5H, 10-H-Dipyrrolo [1,2-A: 1',2'-D] Pyrazine-5-10-dione, octahydro-	43.52	N.D.	1.65	INF
2H-Octahydropyrido[1,2-a]pyrazin-1-one	43.67	5.23	0.04	1%
N-(3-Ethyl-3-octanyl)acetamide	43.95	3.11	0.05	2%
1,4-Dioxaspiro[4.5]decane-6-carboxylic acid, dimethylamide	44.35	2.38	0.14	6%
2,5-Piperazinedione, 3,6-bis(2-methylpropyl)-	44.47	0.67	0.03	4%
Cycloglycylvaline	46.01	1.82	N.D.	0%
2(3H)-Furanone, 5-Hexyldihydro	46.26	0.89	N.D.	0%
Pyrrolo[1,2-a]pyrazine-1,4-dione, hexahydro-	46.63	2.71	N.D.	0%
2-Piperidinemethanol,-ethyl	46.82	N.D.	1.32	INF
DL-Threonine, N-glycyl-	46.94	0.95	N.D.	0%
Pyrrolidin-2-one, 5-pentyl-	47.12	N.D.	0.98	INF
2-Tetradecanone, 14-(5-hydroxy-6-methyl-2-piperidinyl)-,[2R-(2,5,6)]	47.23	2.04	N.D.	0%
2-Pyrrolidinecarboxylic acid-5-oxo-, ethyl ester	47.4	N.D.	0.26	INF
1-[2-Pyrrolidinylethyl]-3-methyl-3-(N-methylcarbamoyl) Triazene)	47.91	0.81	0.04	5%
Pidolic Acid	49.85	2.81	1.93	69%
DL-Proline, 5-oxo-	49.82	N.D.	2.12	INF
1-(4-Chloro-2-methyl-phenoxy)-3-(2-methyl-piperidin-1-yl)-propan-2-ol	51.97	0.81	0.01	1%
DL-Proline, 5-oxo-, methyl ester	52.74	N.D.	0.89	INF
2-(O-Tolylazo)naphthalene	54.21	0.34	N.D.	0%



**Figure 6-4. GC-MS analysis of the most toxic and least toxic PHWW samples.**



**Figure 6-5. The selection of advantageous condition for both biocrude oil and PHWW production.**

## CHAPTER 7

### CHARACTERIZATION OF CHLAMYDOMONAS REINHARDTII MUTANT STRAINS WITH IMPROVED PHOTOSYNTHETIC EFFICIENCY UNDER LIGHT-LIMITED CONDITIONS

#### 7.1 Introduction

Algae represent a promising new source of feedstock for the production of various renewable liquid biofuels (Chisti 2007; Sayre 2010) or hydrogen (Ghirardi et al. 2000; Ghirardi 2013; Dubini 2014) with a low carbon footprint. Their diverse metabolic capability also makes algae a unique and versatile “crop” to produce various food ingredients, nutraceuticals, pharmaceuticals and animal feed (Trentacoste et al. 2014). Algae have several key advantages, including higher growth rates than terrestrial plants, the ability to grow on marginal lands and in low quality water sources, as well as the ability to uptake excess nutrients in eutrophic waters (U.S. DOE 2010). Despite these significant advantages, the promise of algae for clean energy resources remains largely unfulfilled due to several practical bottlenecks in the production process. One important issue for the success of large-scale algal biomass production is maximizing their light utilization efficiency (Sheehan et al. 1998; Williams and Laurens 2010; Ogbonna and Tanaka 2000). Due to rapid light attenuation in dense algal cultures that results from light absorption and scattering, significant spatial heterogeneity of light intensities occurs inside most photobioreactors. Cells at the surface can be damaged by excess light (through photoinhibition) (Adir et al. 2003) and lose absorbed radiant energy to heat dissipation. In contrast, cells located deeper in the culture may experience light limitation that would decrease cell growth.

Genetic and molecular studies have led to the development of strains that can tolerate high light and have better growth under high irradiance. For example, truncated antenna in algae



can help improve light utilization efficiency by decreasing light absorption by the top layer cells, and enable light to penetrate deeper into the cultures (Melis 2009; Polle et al. 2002; Polle et al. 2003; Beckmann et al. 2009; Kosourov et al. 2011; Perrine et al. 2012). On the other hand, developing algal strains that can make maximum use of low light conditions is also advantageous because there are likely to be low irradiance and dark areas in large-scale photobioreactor systems. Thus, algae with improved light utilization efficiency and enhanced biomass production under low irradiance could thus be beneficial for improving overall algal production.

We present here our results on photosynthetic characterization of three different strains of *Chlamydomonas reinhardtii*, a photoautotrophic green alga that can be also grown mixotrophically in acetate-supplemented media, such as tris-acetate-phosphate (TAP). These algae remain green and retain normally developed chloroplasts under various growth conditions, due to their ability to use different reduced carbon sources, such as endogenous starch accumulated in the chloroplast during exposure to light, or exogenous organic carbon compounds like acetate, assimilated in the cytosol. This metabolic flexibility is due to a strong interaction between photosynthetic and non-photosynthetic carbon metabolisms. For an overview of the molecular biology of *Chlamydomonas*, see Rochaix et al. (eds.) (Rochaix et al. 1998).

A spontaneous “mutant” strain of *Chlamydomonas reinhardtii*, which we refer to as “IM” (for “immortal”), was discovered, in our laboratory, and exhibits improved biomass production under low light intensity. The IM strain was obtained from a culture of the previously described knock-out *ptx2* mutant of *C. reinhardtii* (KO), which has defects in both phototaxis and photoshock responses related to impairment of light-induced flagellar currents (Pazour et al. 1995). The IM strain arose spontaneously after a long-term storage of KO cells, on a selective medium, in dim room light. In this study, we have investigated and compared the biophysical

and biochemical characteristics of the IM strain, its progenitor, KO, and its wild-type, WT, when grown under different light intensities, to better characterize the special features of the IM cells. By elucidating the distinctive characteristics of the IM and KO mutants, we provide useful insights on potential ways to improve practical algal biofuel production systems.

## **7.2 Materials and Methods**

### **7.2.1 Algal strains and culture media**

The WT strain used was *Chlamydomonas reinhardtii* CC124. Pazour et al. (Pazour et al. 1995) had previously constructed a KO mutant of *Chlamydomonas reinhardtii* by insertional mutagenesis of the WT, which was totally deficient in light-induced flagellar currents. This KO strain is the progenitor of the spontaneous IM strain used in this study, which was discovered, in our laboratory, from a discarded KO culture that had a single surviving colony. “IM” appeared, in a sealed petri dish with selective agar medium, after a long period of storage under low and intermittent room light (Zhou et al. 2012)<sup>1</sup>.

All three strains of *Chlamydomonas reinhardtii* were maintained under room light conditions ( $\sim 30 \mu\text{mol photons m}^{-2} \text{s}^{-1}$ ), at  $\sim 25 \text{ }^\circ\text{C}$ , and on Tris–acetate–phosphate (TAP) agar culture medium plates (20 mM Tris; 17.4 mM acetate; 7 mM  $\text{NH}_4\text{Cl}$ ; 0.4 mM  $\text{MgSO}_4$ ; 0.3 mM  $\text{CaCl}_2$ ; 1 mM phosphate buffer; 1 ml/L Hutner’s trace metal solution; 15 g/L Bacto agar). Prior to each experiment, colonies from the agar plates were used to inoculate stock cultures made in 250 ml Erlenmeyer flasks with 50 ml of liquid TAP medium (without Bacto agar) that were

---

<sup>1</sup> A preliminary report on the “IM” mutant was first presented by Zhou et al. (Zhou et al. 2012) at the 15th International Conference on Photosynthesis in Beijing, China

mixed on an orbital shaker at 24 °C under 20  $\mu\text{mol photons m}^{-2} \text{ s}^{-1}$  of photosynthetically PAR provided by fluorescent lamps.

### **7.2.2 Algal growth curves under different light intensities**

WT, KO and IM cells were grown in TAP medium at three different light intensities:  $10 \pm 1$ ,  $20 \pm 2$  and  $640 \pm 5 \mu\text{mol photons m}^{-2} \text{ s}^{-1}$ , where the average and standard deviation of these light intensities were determined by measurements at least 9 positions covering the locations of various culture flasks on the shaker table. For the lowest light intensity experiments, light was produced by two 25 W fluorescent lamps. Four 25 W fluorescent lamps were placed on top of a shaker table to produce a light intensity of  $20 \mu\text{mol photons m}^{-2} \text{ s}^{-1}$ . For the highest light intensity, six 42 W compact fluorescent bulbs were placed directly over each culture flask. Culture flask positions were also rotated regularly to minimize any differences in light intensity. For growth rate experiments, cultivation of each algal strain was initiated in duplicate with a starting cell density of 10,000 cells/ml. Cell growth was measured as dry cell weight, and duplicate measurements of samples from each culture flask were averaged to determine the growth curves for each strain and each lighting condition. Dry cell weight was measured as total suspended solids according to standard methods (Clesceri et al. 1999).

### **7.2.3 Photosynthetic oxygen evolution measurements**

Rates of oxygen evolution, for WT, KO and IM cells, were measured using a Clark-type oxygen electrode (Hansatech Instruments). Algae were cultivated in TAP medium under light intensity of  $60 \mu\text{mol photon m}^{-2} \text{ s}^{-1}$ . Cells in the exponential growth phase (48 hours after inoculation) were used for these tests. Chlorophyll (Chl) concentration of samples was adjusted to 15  $\mu\text{g/ml}$ , and then the samples were suspended in 20 mM HEPES buffer (pH 7.4) before oxygen evolution measurements. Rates of oxygen evolution were measured as a function of

increasing light intensity using red LED light (peak intensity at 650 nm): 0, 20, 200, 400, 600 and 800  $\mu\text{mol photons m}^{-2}\text{s}^{-1}$ , with each light intensity being maintained for 2 min during oxygen measurements. Three separate cultures of each strain were used for this experiment, and duplicate measurements were made for each culture replicate; thus, oxygen evolution data are presented as the average of six measurements ( $n = 6$ ). Oxygen evolution rates were then normalized based on Chl concentrations, and reported as  $\mu\text{mol O}_2 \text{ mg Chl}^{-1} \text{ h}^{-1}$ .

#### **7.2.4 Chlorophyll a fluorescence transient measurements**

Chl *a* fluorescence transients were measured at room temperature ( $\sim 21^\circ\text{C}$ ) with a Handy PEA (Plant Efficiency Analyzer, Hansatech Instruments) by using a saturating excitation light ( $\lambda$ , 650 nm) of 3,000  $\mu\text{mol photons m}^{-2}\text{s}^{-1}$  for 300 s. A Corning RG9 cut-off filter was placed before the photodetector to avoid measuring excitation wavelengths at 650 nm, and to measure Chl fluorescence beyond 690 nm. The algal cultures used in these experiments were grown at either 20  $\mu\text{mol photons m}^{-2}\text{s}^{-1}$  (low light) or 640  $\mu\text{mol photons m}^{-2}\text{s}^{-1}$  (high light), and samples were taken from the exponential growth phase (48 hours after inoculation). Before fluorescence measurements, cell suspensions were placed in flasks, with stirring, under room illumination ( $\sim 30 \mu\text{mol photons m}^{-2}\text{s}^{-1}$ ). Three separate culture replicates of each strain were used for these experiments, and triplicate measurements were made for each culture replicate ( $n = 9$ ). All algal samples were adjusted to have a Chl concentration of 15  $\mu\text{g/ml}$  before measurements. These samples, suspended in TAP medium, were dark adapted for 6 min prior to measurement of the fast (up to 1 second) fluorescence transients (labeled as OJIP transients, see below), which were analyzed according to methods described in earlier publications (Strasser et al. 2000; Strasser et al. 2004; Stirbet and Govindjee 2011; Tsimilli-Michael and Strasser 2008). A number of fluorescence parameters were evaluated based on fluorescence values measured at specific times

on the OJIP curves, where O (origin) is the initial minimum fluorescence, which is followed by a rise to inflection points J and I, and then finally to the peak P (Govindjee 1995). Six fluorescence values were used in this analysis:  $F_o$ , at 0.02 ms;  $F(0.1)$ , at 0.1 ms;  $F(0.3)$ , at 0.3 ms;  $F_J$ , at 2 ms;  $F_I$ , at 30 ms; and  $F_m$  (the maximum fluorescence), at the P level (Strasser et al. 2000).

### **7.2.5 Measurement of non-photochemical quenching of the excited state of chlorophyll**

A Pulse Amplitude Modulation (PAM) portable fluorometer (PAM-2100, Walz), in saturating pulse (SP)-mode, was used for the evaluation of chlorophyll fluorescence parameters associated with the slow (up to minutes) fluorescence induction. Chl *a* fluorescence was measured at room temperature ( $\sim 21$  °C), with a weak modulated measuring light ( $\sim 0.1$   $\mu\text{mol photons m}^{-2} \text{ s}^{-1}$ ;  $\lambda = 650$  nm, modulated at 0.6 kHz). As noted above, Chl concentration in each sample was 15  $\mu\text{g/ml}$  before measurement. Cells of all three strains, IM, KO and WT (each suspended in TAP medium) were placed in a chamber designed for PAM fluorescence measurements of liquid cultures, with automatic stirring to prevent settling.

The following protocol was used for PAM measurements: (1) *Chlamydomonas* cells were first dark adapted for 5 min; (2) the minimum level of fluorescence,  $F_o$ , was then measured, after which a saturating light pulse ( $8,000$   $\mu\text{mol photons m}^{-2} \text{ s}^{-1}$ ;  $\lambda = 665$  nm, modulation frequency of 20 kHz) was applied, leading to an increase of fluorescence yield up to its maximum value ( $F_m$ ); (3) after  $\sim 40$  s of darkness, an actinic light source ( $\sim 600$   $\mu\text{mol photons m}^{-2} \text{ s}^{-1}$ ;  $\lambda = 665$  nm) was turned on for 5 minutes, during which a repeated pulses of saturating light (at  $\sim 20$  s intervals) were applied; at each light pulse, the fluorescence increased to a value  $F_m'$  (maximum fluorescence in light); and (4) the actinic light was turned off, and another train of saturating light pulses at  $\sim 20$  s or longer intervals was applied for 15 min.

NPQ of the excited state of chlorophyll was calculated according to the following equation (Oxborough and Baker 1997):  $NPQ = (F_m - F_m')/F_m'$ , where,  $F_m'$  is the maximum fluorescence in light, and  $F_m$  is the maximum fluorescence in the dark adapted sample. Three independent cultures of WT, KO and IM cells were used for these experiments, and triplicate measurements were made for each independent culture (n=9).

### **7.2.6 Metabolite profile analysis**

Metabolite profiling of the IM and WT algal strains during exponential growth phase was conducted according to methods described in earlier publications (Fiehn et al. 2000; Lisec et al. 2006; Rupassara 2008). Algal cells, collected during the exponential growth phase under low light ( $20 \mu\text{mol photons m}^{-2} \text{s}^{-1}$ ) and high light ( $640 \mu\text{mol photons m}^{-2} \text{s}^{-1}$ ), were first lyophilized, and then metabolites were extracted from 25 mg of dried and homogenized cells, using 0.7 ml of ~100% methanol. The extraction mixtures were shaken on a VSM-3 shaker (Pro Lab Plus Series, Pro Scientific Inc.) for 5 min, incubated at  $67 \text{ }^\circ\text{C}$  for 5 min, vortex mixed and then centrifuged at 13,000 rpm for 3 min. Supernatants were collected and kept at  $-20 \text{ }^\circ\text{C}$ , and the pellets were extracted a second time following the same procedure, except that the solvent used was 70% methanol (adjusted to  $\sim\text{pH} = 6.0$  with 0.1 M HCl) and the extraction mixtures were incubated at  $45 \text{ }^\circ\text{C}$  for 5 min. Supernatants, obtained after a second extraction, were added to the first extracts and stored at  $-20 \text{ }^\circ\text{C}$ . The pellets were extracted in the same manner a third time using 0.6 ml chloroform and incubation at  $45 \text{ }^\circ\text{C}$ , and these extracts were added to the previous extracts, and then the combined extracts were vacuum-dried, using a Savant SpeedVac. The dried extracts were stored at  $-20 \text{ }^\circ\text{C}$  until derivatization was performed. These dried extracts were then added to an internal standard ( $10 \text{ mg mL}^{-1}$  of hentriacontanoic acid in  $10 \mu\text{L}$  of pyridine), and vacuum dried. The metabolites were then derivatized using methoxyamine hydrochloride, followed by

trimethylsilylation with N-Methyl-N-(trimethylsilyl) trifluoroacetamide (final volume, 150  $\mu\text{L}$ ) and analyzed by GC-MS, as described previously (Rupassara 2008). ChemStation and Amdis software were used for data acquisition and deconvolution of the chromatographic peaks. Subsequently, extracted metabolites were identified by comparing their mass spectra with those available in several mass spectral libraries (NIST05, Golm Metabolome Database; <http://gmd.mpimp-golm.mpg.de/>; and personal libraries). Information on the amount of metabolites in different samples was based on their relative abundance compared with the internal standards. Because all samples were prepared using the same amount of biomass, extraction solvents and internal standard, the results are normalized based on dry cell weight and can be directly compared.

## **7.3 Results**

### **7.3.1 Cell growth under different light conditions**

Figure 7-1 shows growth curves for each of the three *Chlamydomonas* strains used in this study in terms of dry cell weight, which includes data for two low light intensities (10 and 20  $\mu\text{mol photons m}^{-2} \text{ s}^{-1}$ ) and one for a high (saturating) light intensity (640  $\mu\text{mol photons m}^{-2} \text{ s}^{-1}$ ).

With a light intensity of 10  $\mu\text{mol photons m}^{-2} \text{ s}^{-1}$ , all three *Chlamydomonas* strains reached their maximum dry cell weight at 144 h of growth. At this time, the IM strain had maximum dry cell weight of 433 mg/L, which was 27% higher than that of the WT cells; however, KO and WT cells had an almost identical maximum dry cell weight (Figure 7-1A). At a light intensity of 20  $\mu\text{mol photons m}^{-2} \text{ s}^{-1}$  (Figure 7-1B), the IM strain still showed slightly higher maximum biomass production compared to other strains, but the advantage was reduced. Specifically, the IM cells had a maximum dry cell weight of 545 mg/L after 170 hours of growth, which was 5% higher than the maximum dry cell weight of WT cells (520 mg/L after 119 hours).

This difference was statistically significant (p value of 0.0377 in two tailed t-test). Finally, under our high light condition ( $640 \mu\text{mol photons m}^{-2} \text{s}^{-1}$ ), all the samples (the IM, KO and WT cells) showed very similar (no statistically significant difference) maximum biomass production after 147 hours, as shown in Figure 7-1C.

### 7.3.2 Oxygen Evolution

Figure 7-2 shows net photosynthetic  $\text{O}_2$  evolution rates ( $P_n$ ) as a function of light intensity ( $P_n$ -E curves) for WT, KO and IM cells of *C. reinhardtii* grown under  $60 \mu\text{mol photons m}^{-2} \text{s}^{-1}$ . The KO and IM cells showed significantly higher net  $\text{O}_2$  evolution rates than the WT cells (see Table 7-1). The highest light intensity used in our experiment ( $800 \mu\text{mol photons m}^{-2} \text{s}^{-1}$ ) resulted in maximum net  $\text{O}_2$  evolution rates per chlorophyll ( $P_{\text{max}}$ ), which were approximately 1.5 times higher in KO and IM cells than in WT cells.

Further, our measurements showed that KO and IM cells have 1.6 to 1.4 times higher dark respiration rates than the WT cells (Table 7-1). As a general rule, the greater the metabolic activity of a photosynthetic organ or tissue, the higher its respiration rate (Keller 2010). Therefore, the KO and IM cells are very likely to have more active metabolism than the WT cells.

### 7.3.3 Chlorophyll a fluorescence transient

#### 7.3.3.1 *The fast (up to a second) chlorophyll a fluorescence transient*

Photosynthetic capacity is usually determined by measuring the rate of  $\text{CO}_2$  assimilation or  $\text{O}_2$  evolution, but it can also be predicted using Chl *a* fluorescence induction data, which is a rapid, noninvasive, sensitive, and accurate technique that is being currently used in a large number of studies (Govindjee 1995; Maxwell and Johnson 2000; Papageorgiou and Govindjee 2004; Baker 2008; Kalaji et al. 2012). Here we measured Chl *a* fluorescence transients under saturating light ( $\lambda$ , 650 nm;  $3,000 \mu\text{mol photons m}^{-2} \text{s}^{-1}$ ) that allowed us to characterize PSII



activity; our results for KO and IM cells show some similarities, but also some differences, in comparison to those for WT cells, grown under both low and high light conditions, as discussed below.

The fast (up to 1 s) Chl *a* fluorescence transients, shown in Figures 7-3A and B, were normalized both at O ( $F_o$ ) and P ( $F_m$ ) levels to obtain the relative variable fluorescence,  $V(t) = (F(t) - F_o)/(F_m - F_o)$ ; this double normalization allows us to compare fluorescence transients measured in different samples (Strasser et al. 2004). Figure 7-3A shows that, when grown under low light ( $20 \mu\text{mol photons m}^{-2} \text{s}^{-1}$ ), the fast fluorescence induction curves of all three *Chlamydomonas* strains (i.e., WT, KO and IM) show three characteristic phases, O-J, J-I, and I-P (Strasser and Govindjee 1991). These OJIP curves have quite similar shapes in all three samples, with only a slightly steeper J-I rise and a slightly higher I level (~5-10%) in the curves for IM cells. In order to highlight these differences, relative variable fluorescence of the WT cells was subtracted from that of the IM and KO cells (Strasser et al. 2007) and shown in Figure 7-3C. Indeed, the curve (IM – WT) shows a clear difference in the I-band.

For samples grown under high light ( $640 \mu\text{mol photons m}^{-2} \text{s}^{-1}$ ), the J step in all Chl *a* fluorescence curves is no longer discernible, while the I and P steps are still clearly seen (see Figure 7-3B). Differences between the fluorescence transients of *Chlamydomonas* strains grown under high light (see Figure 7-3D) were more noticeable than between those grown under low light, both before and after normalization. In particular, the fluorescence transients measured in KO cells showed a less steep O-I fluorescence rise and a lower I level (~15-20%) than in WT and IM cells. The reduced O-I fluorescence rise for KO cells probably reflects a smaller PSII antenna size (Strasser et al. 2004). The lower I level for KO is likely related to a faster electron

flow from  $Q_A^-$  to PSI acceptors due to an increased PSI/PSII ratio or a larger PSI antenna size (Strasser et al. 2004; Oukarroum et al. 2009; Ceppi et al. 2012).

Although many fluorescence parameters have been defined for the analysis of the OJIP transient in the literature (Stirbet and Govindjee 2011; Baker 2008; Yusuf et al. 2010), we present here only a few of the key fluorescence parameters commonly used for the characterization of photosynthetic samples (see Table 7-2).

### 7.3.3.2 *Minimum ( $F_o$ ), Maximum ( $F_m$ ), and Variable ( $F_v$ ) fluorescence*

Both the initial fluorescence ( $F_o$ ) and maximum fluorescence ( $F_m$ ) had relatively close values in the IM and KO strains grown under low light ( $20 \mu\text{mol photons m}^{-2} \text{s}^{-1}$ ), and the differences between the WT cells and the two mutants were less than 12.5% for  $F_o$ , and less than 16% for  $F_m$  (see Table 7-2). Therefore, the  $F_v/F_m$  ratios (where  $F_v = (F_m - F_o)$  is the maximum variable fluorescence) were also very similar (i.e.,  $\sim 0.78$ ) for all *Chlamydomonas* strains grown under low light. The  $F_v/F_m$  ratio is widely used in photosynthetic studies as a proxy for the maximum efficiency of PSII photochemistry (Butler and Kitajima 1975); for rationale of its use, see Govindjee (Govindjee 2004). A higher  $F_v/F_m$  value (i.e.,  $> 0.76$ ) was correlated with higher photosynthetic performance (Govindjee 1995), but only in the presence of similar  $\text{CO}_2$  levels, and in the absence of alternative electron sinks. Even though we found that IM and KO cells had a slightly higher maximum efficiency of PSII photochemistry compared to WT cells (i.e., +1.2% and +1.9%, respectively), the difference between WT and KO cells for this parameter was not a statistically significant difference according to the t-test, which had a p value of 0.2751. However, the difference between the WT and the IM was statistically significant with a p value of 0.0022.

In contrast,  $F_o$  and  $F_m$  measured in samples grown under high light showed much greater differences between the strains (see Table 7-2). The KO strain had a very low  $F_o$ , which was the lowest among the three strains, while the two other strains had higher  $F_o$  values. The  $F_o$  value in KO strain grown under high light was also lower (-24%) than those measured in low light grown cells, while the  $F_o$  values of WT and IM strains grown under high light were higher than those in low light grown cells (i.e., +74% and +37% for WT and IM strains, respectively). However, the slopes of the initial O-J fluorescence rise (see  $dV/dt_o$  values in Table 7-2) in WT and IM cells were higher than in the KO cells. Further, the increased apparent  $F_o$  value, observed in our data, is probably the result of a partial reduction of  $Q_A$  even after the dark adaptation period, due to a partial reduced PQ-pool (Stirbet et al. 2014). We note that the  $F_m$  values were much lower in cells grown in high light than for cells grown under low light (see Table 7-2), especially in the KO strain, which had the lowest  $F_o$  and  $F_m$  values. This can be attributed to a lower PSII excitation cross section (Strasser et al. 2004) in the KO strain, which may be related to a State 1 to State 2 transition (high to low fluorescence), taking place as a strategy to cope with high light (Allorent et al. 2013). In all *Chlamydomonas* cells grown under high light, the maximum quantum yield of PSII photochemistry had lower values (less than 0.62; see Table 7-2). Our data are in agreement with results obtained in other studies with *Chlamydomonas* grown at different light intensities, which also showed a reduction of  $F_v/F_m$  in high light compared to that in low light (Bonente et al. 2012). The low  $F_v/F_m$  values measured in WT and IM cells (i.e., 0.4 and 0.57, respectively) may be partially due to a high apparent  $F_o$  value, as mentioned above.

#### 7.3.3.3 *The ratios of $F_v$ to $F_o$ , and of $F_o$ to $F_m$*

The ratio  $F_v/F_o$ , a parameter also used as an indicator of potential PSII photochemistry and  $CO_2$  fixation capacity, was also higher in KO (+6.7%) and IM (+8.9%) cells than in WT

cells for samples grown under low light. These results suggest that differences in photosynthetic carbon metabolism, besides that of acetate assimilation, may have also contributed to the advantage in biomass production of the IM strain compared to WT and KO strains, observed in the growth experiments done under low light conditions.

Another important parameter is the ratio  $F_o/F_m$ , which is a measure of the efficiency of energy de-excitation in PSII, as  $F_o/F_m = k_N/(k_N + k_P)$ , where  $k_N$  is the global rate constant of all non-photochemical de-excitation processes for Chl *a* in PSII antenna (which includes fluorescence, heat and energy transfer to another PSII or PSI); and  $k_P$  is the rate constant for photochemical de-excitation at the PSII reaction center level (Strasser et al. 2004). This parameter had fairly similar values in all samples grown under low light, but was slightly higher in the IM and KO cells (see Table 7-2). For cells grown under high light,  $F_o/F_m$  ratios were significantly higher than in the same cells cultured under low light; however, in WT and IM cells these values are probably overestimated due to a higher apparent  $F_o$ , as mentioned above.

#### 7.3.3.4 *The slow phase of chlorophyll a fluorescence transient (from 1 s to 300 s)*

After the OJIP phase, Chl *a* fluorescence declines to a semi-steady state “S” level, and this is followed by a rise to an M (maximum) level followed by a decline to a terminal steady state level, T (Papageorgiou and Govindjee 1968b; Papageorgiou and Govindjee 1968a). Figure 7-4 shows our fluorescence data for the three *Chlamydomonas* strains (grown under low light) during the SMT phase, which is in the range of minutes. We note that the IM strain did not show a S-M fluorescence rise, in contrast to the KO and WT strains; this suggests that the IM strain has a reduced capacity to go from a low fluorescence state (State 2) to a high fluorescence state (State 1) (see Discussion section). This conclusion is based on the observations of Kaňa et al. (Kaňa et al. 2012) on the absence of the S to M fluorescence rise in a *Synechocystis* mutant (Rpa

C<sup>-</sup>) that is locked in State 1, and those of Kodru et al. (2013) on drastically reduced S-M rise in the *stt7* mutant of *C. reinhardtii*, which was also locked in State 1 (Depege et al. 2003). Further research is needed to fully understand the implications of this observation.

#### 7.3.3.5 *Non-photochemical quenching analysis*

NPQ of the excited state of Chl *a* is a process that down-regulates excitation pressure in the photosynthetic apparatus by increasing de-excitation, as heat, of the singlet excited state of Chl *a* (see Demmig-Adams et al 2014; Demmig-Adams et al 2006), in parallel with a decrease in Chl *a* fluorescence yield. We present and discuss here results on the kinetics of NPQ induction and its relaxation, as obtained by using a PAM instrument (Walz) for the three different *Chlamydomonas* strains grown both under low light (20  $\mu\text{mol photons m}^{-2} \text{s}^{-1}$ ; Figure 7-5A) and high light (640  $\mu\text{mol photons m}^{-2} \text{s}^{-1}$ ; Figure 7-5B). Our data show that the maximum fluorescence values ( $F_m$ ,  $F_m'$ ) in samples grown under low light, were significantly higher than those grown under high light. This agrees with the fluorescence results presented in Table 7-2, obtained with a HandyPea instrument (Hansatech).

As shown in Figure 7-5C, WT cells, grown under low light conditions, had biphasic NPQ induction kinetics, with the first phase characterized by a fast NPQ increase that reached a maximum, and then slightly decreased to a plateau in the second phase after approximately 100 s of illumination with actinic light. On the other hand, IM and KO mutant cells had NPQ that increased steadily through the actinic illumination period, but at a slower rate initially than the WT cells. At the end of the illumination period, NPQ in the IM cells had a significantly higher value than in both the WT and KO cells. After the actinic light was turned off, to our surprise, the NPQ continued to increase in all samples (but to a much lesser extent in the IM cells), and NPQ reached maximum values at 80 s, 200 s and 400 s for IM, KO and WT cells, respectively

(see Figure 7-5C). The WT cells reached the highest NPQ value, but it was close to maximum NPQ level for the IM cells. During the NPQ relaxation process that followed, the most dramatic difference between these samples was that NPQ in the IM cells decreased much faster, and reached a much lower value than in the KO and WT cells. For all three strains, the fluorescence recovery was still not complete at the end of the measurement, indicating that the cells were somewhat photoinhibited, and/or some other NPQ process characterized by slow dark recovery was present (Brooks et al. 2013), but the IM cells had significantly better dark NPQ recovery than the WT and KO strains.

The NPQ kinetics for *Chlamydomonas* cells grown under high light (Figure 7-5D) showed similar biphasic NPQ induction patterns in all the three strains, with a rapid NPQ increase, followed by a plateau, but here the KO strain reached a higher NPQ value than the IM and WT strains. We note however that here also the NPQ in the WT strain decreased transiently after 100 s actinic illumination. After the actinic light was turned off, the NPQ in WT and KO continued to increase for 50 s and 150 s, respectively (see Figure 7-5D), but it did not increase in IM cell. After reaching the peak, NPQ gradually relaxed in all three strains, but only in IM cells, it recovered completely during the dark (relaxation) period.

#### **7.3.4 Metabolite profiling**

Since differences in cellular activity other than photosynthesis were suspected of being affected in IM cells, we performed metabolite profiling analysis to obtain insight into the complex regulatory processes and to better understand the reasons behind the higher biomass production in the IM cells grown under low light. The metabolite profiling revealed some potentially advantageous differences in IM cells over WT cells under both low and high light conditions. Figure 7-6 shows a comparison of the relative quantities of some selected metabolites

produced in WT and IM cells during the exponential growth phase under both low light conditions ( $20 \mu\text{mol photons m}^{-2} \text{s}^{-1}$ ) and high light conditions ( $640 \mu\text{mol photons m}^{-2} \text{s}^{-1}$ ).

First, the IM cells grown under low light showed increased quantities of several important metabolites related to carbon metabolism. For instance, under low light ( $20 \mu\text{mol photons m}^{-2} \text{s}^{-1}$ ), IM cells had higher amounts of key sugars including ribose, fructose, maltotriose and glucose than WT cells (1.3-11.5 fold higher). In addition, IM had more sugar phosphates such as fructose-6-phosphate and mannose-phosphate (2.4 and 7.2 fold higher than WT, data not shown). However, under high light ( $640 \mu\text{mol photons m}^{-2} \text{s}^{-1}$ ), these sugars and sugar phosphates were at much lower levels in the IM cells (0.2 - 1.2 fold) compared to the WT cells, as shown in Figure 7-6A.

Under low light, IM cells also had much higher levels of key organic acids than the WT cells, such as glyceric acid, gluconic acid and malic acid (3.0-24.1 fold higher); however, under high light, these metabolites were at much lower levels (0.3-0.9 fold) compared with the WT cells, as shown in Figure 7-6A. Since these sugars and organic acids are either photosynthetic products or intermediates during carbon metabolism (López-Bucio et al. 2000) that are closely related to energy production in photosynthesis, we suggest that the high level of these key sugars and acids in IM cells under low light conditions could be related to the advantageous biomass production of IM cells observed under low light conditions (see Figure 7-1).

Another interesting observation is that, when cultivated under high light conditions, IM cells showed much higher levels of important compounds involved in oxidative stress protection compared to WT cells. These compounds include osmolytes, antioxidants (mannitol (Stoop et al. 1996; Voegelé et al. 2005), inositol (Loewus and Murthy 2000; Valluru and Van den Ende 2011),  $\beta$ -tocopherol (Sirikhachornkit et al. 2009; Maeda and Della. 2007)) and sterols

(stigmasterol (Schaller 2003), campesterol (Schaller 2003), and beta-sitosterol (Divi and Krishna 2009; Benveniste 2004)), all of which have protective functions against various environmental stresses. We postulate that the up-regulation of these protective compounds in IM cells could be a metabolic response to compensate for the defects of phototaxis and photoshock response in IM cells, which were, perhaps, inherited from the parent KO mutant, which has known phototaxis defects. Although we did not genetically confirm whether this specific phototaxis defect is conserved also in IM or not, the likelihood of the *ptx2* defect on phototaxis being conserved in IM is very high. This is because the integration of exogenous DNA in *Chlamydomonas* by insertional mutagenesis (as used to create KO) is usually associated with deletion of part of the chromosome at the site of insertion; thus, it is very unlikely that any subsequent mutation of event would restore the deleted gene in its original form. These protective compounds may have helped the IM cells to maintain their photosynthetic capacity and may have contributed to its higher rate of O<sub>2</sub> evolution under high light conditions. Some other potentially beneficial metabolites found to be up-regulated in IM cells include plant hormones like salicylic acid (Hayat et al. 2010; Vicente and Plasencia 2011) and gibberellic acid (Kadioglu 1992), which have been previously reported to increase photosynthetic efficiencies and promote growth in many algal species including *Chlorella vulgaris* and *Chlamydomonas reinhardtii* (Czerpak et al. 2002; Ismail et al. 2011).

## **7.4 Discussion**

### **7.4.1 Cell growth under different light intensities**

As seen in Figure 7-1, and as expected, all of the strains had a lower maximum biomass production when grown in low light (10-20  $\mu\text{mol photons m}^{-2} \text{s}^{-1}$ ), compared to high light (640  $\mu\text{mol photons m}^{-2} \text{s}^{-1}$ ) growth conditions. This is obvious because of more energy input, without



any significant amount of photoinhibition (Boyle and Morgan 2009). Further, Ballottari et al. (2007) have shown that high light conditions results in more Rubisco (ribulose- 1,5-bisphosphate carboxylase/oxygenase), the key enzyme of the Calvin-Benson cycle, than at low light. Moreover, when *Chlamydomonas reinhardtii* cells are grown autotrophically, under high light, a decrease in the ratio of PSI/PSII (due to a decrease in PSI), and an increase in Cyt *b6/f* and ATP synthase is observed (Bonente et al. 2012). For *C. reinhardtii* grown in mixotrophic conditions, both photosynthetic assimilation of inorganic carbon and heterotrophic assimilation of acetate contribute to biomass production. However, the ability of acetate to induce isocitrate lyase, the key glyoxylate cycle enzyme necessary for its utilization, is attenuated in the presence of light and inorganic carbon (Heifetz et al. 2000), so that acetate assimilation contributes to biomass production mainly under low irradiance. Therefore, it is possible that higher acetate assimilation in the IM strain was one of the reasons that led to increased biomass production for the IM strain in comparison to WT and KO strains grown under low light conditions . In view of the overall goal of our study, i.e., the perspective of large-scale algal biofuel production, growth of algae in the presence of organic carbon is highly important. For example, cultivation of algae in wastewater has been considered as one of the most promising pathways to efficiently and economically produce algal biofuels (U.S. DOE 2010; National Research Council 2012), and most wastewaters contain significant amounts of organic carbon. Therefore, we considered it important to characterize the special strains of algae grown under mixotrophic conditions since it supports the goal of using wastewater in large-scale algal cultivations.

#### **7.4.2 Oxygen evolution**

We note that results of oxygen measurements, as presented in Figure 7-2, cannot be exactly correlated with the growth data in Figure 7-1 because the algae were cultured under

different light conditions (60 versus 10-20  $\mu\text{mol photons m}^{-2} \text{s}^{-1}$ ). Moreover, rates of  $\text{O}_2$  evolution cannot always be strictly correlated with growth rates or biomass productivity in *Chlamydomonas* mutants, as already shown in several previous studies (Perrine et al. 2012; Forster et al. 1999; Lardans et al. 1998). Even so, oxygen evolution is an important product of photosynthesis, and our results show significant differences for both IM and KO cells in comparison to the WT cells, as was consistently observed when cells were exposed to a wide range of light intensity levels during these tests.

### **7.4.3 Fluorescence based measurements**

#### *7.4.3.1 The fast chlorophyll fluorescence transient*

*C. reinhardtii* cells, grown under low light (20  $\mu\text{mol photons m}^{-2} \text{s}^{-1}$ ), showed quite similar fast Chl fluorescence transient curves (Figure 7-3A) among the three strains, and therefore fluorescence parameters also had similar values (see Table 7-2). Results showed that the IM strain, had a slightly higher I level (Figures 7-3A and C). Usually, the J-I phase is correlated with the redox status of the PQ-pool, which typically has 6-12 PQ molecules per PSII that shuttle electrons between PSII and PSI via cytochrome b6/f (Kirchhoff et al. 2000; Stirbet and Govindjee 2012) (see a discussion of the evolution of the Z-scheme of electron transport by Govindjee and Björn (2012)). The increased I level observed in the IM cells, compared to KO and WT cells, suggests a potentially slower oxidation rate of plastoquinol ( $\text{PQH}_2$ ) by PSI due possibly to a decreased PSI/PSII ratio in the IM cells (Stirbet et al. 2014; Oukarroum et al. 2009; Ceppi et al. 2012). Further, the IM strain showed higher  $F_v/F_m$  and  $F_v/F_o$  ratios compared to WT and KO strains, which may indicate a slightly better photosynthetic capacity ( $\text{CO}_2$  fixation), in agreement with the results obtained in growth curves (Figure 7-1B). However, we suggest that processes other than photosynthesis must have contributed to the increased growth performance

observed in the IM mutant cells grown under a light intensity of  $10 \mu\text{mol photons m}^{-2} \text{ s}^{-1}$  (see Figure 7-1A).

In samples grown under high light ( $640 \mu\text{mol photons m}^{-2} \text{ s}^{-1}$ ), we observed clear differences in fast Chl fluorescence transient curves (Figures 7-3B and D), and their respective fluorescence parameters (Table 7-2). All these samples had lower  $F_m$ ,  $F_v/F_m$ ,  $F_v/F_o$ , and OJ rise initial slopes, compared to those grown under low light, which may be partially due to photoinhibition. However, for KO cells, the initial slope of the OJ rise, as well as both  $F_o$  and  $F_m$  had much lower values than in any other sample, which indicates a low PSII excitation cross section (Strasser et al. 2000) and low fluorescence state; thus we suggest that this sample had a state 1 to state 2 transition (high to low fluorescence) in darkness, which has also been observed under similar conditions by Allorent et al.(2013).

#### 7.4.3.2 *The slow Chlorophyll fluorescence transient. SM rise and state changes*

Kaňa et al. have proposed that the S to M fluorescence rise observed under certain conditions in the slow (seconds to minutes) Chl fluorescence transient may be used to evaluate regulatory mechanisms such as state changes in cyanobacteria (Kaňa et al. 2012); see Kodru et al. (2013) for the same conclusion in *Chlamydomonas*. We note that state changes (i.e, State 1 ↔ State 2) are regulatory mechanisms that optimize photosynthesis by adjusting the amount of excitation energy delivered by antenna pigments to PSII and PSI reaction centers under changing light regimes and/or metabolic needs (Minagawa 2011; Murata 1969; Bonaventura and Myers 1969; Papageorgiou and Govindjee 2011; Rochaix 2002). In *Chlamydomonas*, state changes are different than in plants because they can involve detachment of a higher proportion of LHCII trimers from the PSII antenna (70-80% versus 10-15% in plants, see Delosme et al. (1996)). However, only ~10% of these are actually incorporated in PSI antenna, and the rest form arrays

that quench the Chl *a* excited state (Nagy et al. 2014; Ünlü et al. 2014). Therefore, in *Chlamydomonas*, the State 1 to State 2 transition seems to play an important role as a short term (minutes) protection under high light conditions, which may compensate for the much slower (hours) NPQ response in these algae than in plants (Allorent et al. 2013; Ünlü et al. 2014; Rochaix 2014). Furthermore, state changes in *Chlamydomonas* were also found to coincide with changes in the ratio between cyclic and linear electron flow, and thus, the ATP/ADP ratio in cells (Rochaix 2002; Takahashi et al. 2013).

In our research, we found that the SM rise in the slow Chl fluorescence transient of the IM cells is missing, and hypothesize that, just as in *RpaC<sup>-</sup>* mutant of *Synechocystis* PCC6803 (Kaňa et al. 2012) and *stt7* mutant of *C. reinhardtii* (Kodru et al. 2013) (as mentioned earlier), the IM strain has a reduced capacity to perform state changes, even if other processes may also contribute to the SM phase (see a discussion in Stirbet et al. (Stirbet et al. 2014)) This hypothesis is also supported by the results on NPQ kinetics in *Chlamydomonas* cells as discussed below.

#### 7.4.3.3 *Non-photochemical quenching kinetics*

Several types of NPQ have been identified (Muller et al. 2001), each one characterized by a particular kinetic behavior: pH-dependent (qE) (Nilkens et al. 2010; Jahns and Holzwarth 2012; Ruban et al. 2012), state change-dependent (qT) (Minagawa 2011), and photoinhibition-dependent (qI) (Tyystjärvi 2013). Although we note that qT in most plants is not a true NPQ process because it does not involve changes in the rate constants of the de-excitation processes of singlet excited Chl *a*, but rather only changes in the antenna size of the two photosystems (Minagawa 2011; Papageorgiou and Govindjee 2011). However, in *Chlamydomonas*, during state 1 to state 2 transition, part of mobile phosphorylated LHCII trimers were shown to form

arrays in the membrane, in which non photochemical quenching (of qE type) takes place (Iwai et al. 2010; Papageorgiou and Govindjee 2014 (in press)), as mentioned above.

The qE quenching is the most rapid component of NPQ and is triggered by a pH gradient ( $\Delta$  pH) that builds-up across the thylakoid membrane. Therefore, qE is affected by all processes that influence  $\Delta$  pH, including ATP synthase activity, the linear and PSI-dependent cyclic electron transport flow, and ATP and NADPH consumption by the Calvin–Benson cycle (see Figure 2-4). However, in contrast to higher plants, qE in *Chlamydomonas* is not dependent on the presence of PsbS (Bonente et al. 2008), but on other proteins, such as Light-Harvesting Complex Stress-Related proteins (e.g., LhcSR1 and LhcSR3), which can sense pH changes and, unlike PsbS, can also bind pigments (Chl *a* and *b*, violaxanthin, zeaxanthin, and lutein) (Bonente et al. 2011; Tokutsu and Minagawa 2013; Peers et al. 2009).

The results of PAM experiments showed complex NPQ kinetics, both in samples grown under low light and high light conditions (Figures 7-5C and D). Specifically, our results showed that among the three strains of *C. reinhardtii* cells, grown in low light, IM had the highest qE component. Indeed, the NPQ developed by the IM cells at the end of the illumination with actinic light was twice as high as NPQ in WT and KO strains (Figure 7-5C), and IM had a faster and more complete recovery in darkness. Surprisingly, we also observed that after the actinic light was switched off, the NPQ continued to increase for 1-2 min in all these samples, before dark relaxation took place. However, in IM cells the NPQ increase finished much sooner and was very small compared to that in the WT and KO cells, which more than doubled their NPQ values reached during actinic illumination (see Figure 7-5C). An explanation of higher NPQ in WT and KO cells, than in IM cells, may be due to superimposition of an effect of state transitions, as noted by Allorent et al. (2013). They have also observed an NPQ increase during

the dark relaxation period in WT cells of *C. reinhardtii*, which they have correlated with an increase in LHCII phosphorylation, and thus to a State 1 to State 2 transition. Further, as shown in Figure 7-5C, the IM cells attained a lower NPQ level than WT and KO, which may imply that they were better protected against photoinhibition.

In cells grown under high light, KO reached a higher NPQ level during actinic illumination than WT and IM cells. However, in all likelihood, a large part of this NPQ in WT and KO cells was not of the qE type since their dark relaxation was only partial, and we know that qE is fully reversible in darkness; in contrast, the NPQ recovered completely in the IM cells. Since qE is dependent on the accumulation of LhcSR proteins, these results suggest that *Chlamydomonas* cells grown under high light conditions have higher levels of LhcSR proteins than those grown under low light, which offers a higher degree of photoprotection (Nagy et al. 2014; Tokutsu and Minagawa 2013). Other explanations are also possible for higher NPQ (that is lower fluorescence), such as quenching by higher  $[H^+]$  due to increased  $\Delta$  pH. In our work, we also observed a transient NPQ increase after the actinic light was turned off, but it was much smaller than in samples grown in low light, and mainly in the WT cells. The fact that the NPQ increase during the dark relaxation period was much lower in IM cells (both in cells grown in low and high light conditions; see Figures 7-5C and D) supports our idea that IM cells have reduced state transition capacity in comparison to WT and KO cells.

It is important to note that in WT cells grown in high light (and to a lesser extent for cells grown in low light), fluorescence showed a transient increase after ~100 s actinic illumination (Figure 7-5), similar (even if smaller) to the SM rise. Such a transient fluorescence increase was also reported by Allorent et al. (2013) during actinic illumination in WT *Chlamydomonas* cells that were initially in State 2; this fluorescence increase was assigned to a State 2 to State 1

transition, because it was absent in the *stt7-9* mutant (locked in state 1); further, the phosphorylation level of LHCII was shown to decrease upon illumination. Since this transient fluorescence recovery, and the SM rise observed, are related phenomena, our results, as well as those presented by Allorent et al. (2013) strongly support our hypothesis that SM rise in the OJIPSMT transient reflects a State 2 to State 1 change.

In summary, results of our NPQ kinetics experiments suggest that WT cells do undergo a State 2 to State 1 transition during actinic illumination, and a State 2 to State 1 transition after the actinic light is switched off. As compared to WT and KO, IM cells have a higher qE component for NPQ; this is especially true when cells are grown under low light, and are characterized by fast recovery of NPQ in darkness. Further, these IM cells are apparently much more protected against photoinhibition (especially when grown under high light), but are less capable of undergoing state transitions, compared to WT and KO cells.

#### **7.4.4 Metabolite profiling**

The metabolite profiling results of the IM strain showed some advantages over the WT strain in terms of metabolites related to carbon metabolism when grown under low light conditions. Under high light conditions, the IM advantages changed to enhanced production of metabolites that mitigate oxidative stress. However, the signaling and regulatory mechanisms of the IM strain mutation leading to these potentially beneficial alterations in carbon metabolism and stress responses are unclear. In addition, it is unknown at this time whether these metabolite effects are a result of the knocked-out gene in the KO parent strain, or if they are a result of further mutations in the IM strain. Further molecular studies are necessary to identify the genetic basis of the differences observed in this study. In addition, global gene expression patterns, when

available, would provide useful information for linking the function of the metabolic network with gene expression.

All our data on growth rate, Chlorophyll *a* florescence transient analysis, and O<sub>2</sub> evolution rates suggest that the IM cells are more efficient than the WT cells in terms of light utilization and biomass production when grown under low light, which is potentially a very valuable feature for algal biofuel production. Mass algal production involves optically dense cultures, where most of the cultivation reactor space is likely to be light limited, which would normally result in reduced or arrested cell growth. For example, one previous study with dense cultures (1 g/L), found that 80-95% of the light path was severely light limited (Williams and Laurens 2010). In cases where light is limiting, it would likely be advantageous to use algal strains, such as the IM cells reported here, that have improved biomass production under low light conditions. The reason we did not observe an obvious advantage of IM cells in our growth experiment with much higher light intensity (640 μmol photons m<sup>-2</sup> s<sup>-1</sup>) is likely due to the very short light path we used (~10 mm), which would have little or no light limited area. This feature may also make the IM strain a good candidate for cultivation systems that usually experience light limitations, especially outdoor algae cultivation systems that depend on natural light and experience highly dynamic incident photon irradiance conditions as a result of variations in solar elevation, cloud cover, and even rain. Low light requirements for photosynthesis also allow a longer period of biomass production and therefore an improved overall biomass production.

It is interesting that although both KO and IM cells show more efficient light utilization and higher O<sub>2</sub> evolution rate than WT cells, only IM cells showed an obvious advantage in biomass production under low light conditions. Generally, oxygen evolution rate can be used as an indicator of photosynthetic capacity because oxidation of water provides the primary source



of reducing equivalent (water derived electron and protons) and, ultimately ATP, which is used later for the conversion of CO<sub>2</sub> into biomass (Ferreira et al. 2004). Therefore, high O<sub>2</sub> evolution rates would normally be correlated with high photoautotrophic biomass production in algal cells. However, when some other metabolic process downstream of the light reactions (e.g., dark reactions, starch synthesis or cell division) is the limiting step, the O<sub>2</sub> evolution rate may not directly or accurately reflect the growth rate/biomass productivity. Several other studies (Perrine et al. 2012; Forster et al. 1999; Lardans et al. 1998) have reported *Chlamydomonas reinhardtii* mutants with reduced or increased O<sub>2</sub> evolution rate but unaffected biomass growth compared to wild type cells. It is quite possible that the differences between the two mutant strains (KO and IM) and the WT are not related to their photosynthetic activity only, but also to processes involved in other cellular processes such as acetate assimilation, regulation of cell division, and starch synthesis because the IM cells display better cell growth primarily under low light, and during the exponential growth phase, when the cell division rate and biomass production rate is high. These unique attributes are promising and suggest that further molecular, physiological and metabolic studies on these mutants are justified to help better elucidate these distinctive characteristics. Ultimately, metabolic and genetic engineering could be used to transfer the desirable features of our *Chlamydomonas* mutant into other algae species to improve the efficiency of algal biofuel production systems (Hong et al. 2014; Dubini and Ghirardi 2014). The improved photosynthetic efficiency could also be used to enhance productivity of other algal biochemical manufacturing platforms (such as recombinant proteins, antioxidants, hormones) for industrial, nutritional and medical uses (Rasala and Mayfield 2014; Guarnieri and Pienkos 2014).

## 7.5 Conclusions

We have discovered that a spontaneous mutant (that we refer to as IM) of the green alga *Chlamydomonas reinhardtii* exhibits certain unique biophysical and biochemical characteristics, which are potentially advantageous for biofuel production systems in comparison to its progenitor KO strain and WT cells. IM cells have increased biomass production (5%-27% higher) under low light intensities (10-20  $\mu\text{mol photons m}^{-2} \text{s}^{-1}$ ), but they do not show any productivity advantages under high light conditions (640  $\mu\text{mol photons m}^{-2} \text{s}^{-1}$ ). Both IM and KO cells grown under 60  $\mu\text{mol photons m}^{-2} \text{s}^{-1}$  also showed approximately 1.5 fold increase in  $\text{O}_2$  evolution rate over a large range of light intensities (20-800  $\mu\text{mol photons m}^{-2} \text{s}^{-1}$ ) as compared to WT cells. Chlorophyll *a* fluorescence measurements indicate that the IM cells grown under low light intensity (20  $\mu\text{mol photons m}^{-2} \text{s}^{-1}$ ) are less able to undergo state changes, and they can develop a higher pH-dependent non-photochemical quenching of the Chl *a* excited states (qE) than the WT and KO cells. Overall, these results indicate that IM cells are more efficient in light utilization and biomass production under low light, which is potentially a valuable feature for large-scale algal biofuel production, where light-limiting reactor conditions are expected. Additionally, in comparison to WT cells, metabolite profiling analysis showed that the IM cells had higher concentrations of important soluble carbohydrates and organic acids that are closely related to carbon metabolism when cultivated under low light. Under high light, IM did not have increased carbon metabolites, but higher levels of metabolites that can protect against oxidative damage.

## 7.6 References

- Adir, N., H. Zer, S. Shochat and I. Ohad. 2003. Photoinhibition - a historical perspective. *Photosynthesis Research* 76(1-3): 343-370.
- Allorent, G., R. Tokutsu, T. Roach, G. Peers, P. Cardol, J. Girard-Bascou, D. Seigneurin-Berny, D. Petroutsos, M. Kuntz, C. Breyton, F. Franck, F. A. Wollman, K. K. Niyogi, A. Krieger-Liszkay, J. Minagawa and G. Finazzi. 2013. A dual strategy to cope with high light in *Chlamydomonas reinhardtii*. *The Plant Cell* 25(2): 545-557.
- Alric, J. 2010. Cyclic electron flow around photosystem I in unicellular green algae. *Photosynthesis Research* 106(1-2): 47-56.
- Baker, N. R. 2008. Chlorophyll fluorescence: A probe of photosynthesis in vivo. *Annual Review of Plant Biology* 59: 89-113.
- Ballottari, M., L. Dall'Osto, T. Morosinotto and R. Bassi. 2007. Contrasting behavior of higher plant photosystem I and II antenna systems during acclimation. *The Journal of Biological Chemistry* 282(12): 8947-8958.
- Beckmann, J., F. Lehr, G. Finazzi, B. Hankamer, C. Posten and L. Wobbe. 2009. Improvement of light to biomass conversion by de-regulation of light-harvesting protein translation in *Chlamydomonas reinhardtii*. *Journal of Biotechnology* 142(1): 70-77.
- Benveniste, P. 2004. Biosynthesis and accumulation of sterols. *Annual Review of Plant Biology* 55: 29-57.
- Bonaventura, C. and J. Myers. 1969. Fluorescence and oxygen evolution from *Chlorella pyrenoidosa*. *Biochimica et Biophysica Acta (BBA)-Bioenergetics* 189(3): 366-383.
- Bonente, G., M. Ballottari, T. B. Truong, T. Morosinotto, T. K. Ahn, G. R. Fleming, K. K. Niyogi and R. Bassi. 2011. Analysis of LhcSR3, a protein essential for feedback de-excitation in the green alga *Chlamydomonas reinhardtii*. *PLoS Biology* 9(1): e1000577.
- Bonente, G., F. Passarini, S. Cazzaniga, C. Mancone, M. C. Buia, M. Tripodi, R. Bassi and S. Caffarri. 2008. The Occurrence of the psbS Gene Product in *Chlamydomonas reinhardtii* and in Other Photosynthetic Organisms and Its Correlation with Energy Quenching. *Photochemistry and Photobiology* 84(6): 1359-1370.
- Bonente, G., S. Pippa, S. Castellano, R. Bassi and M. Ballottari. 2012. Acclimation of *Chlamydomonas reinhardtii* to different growth irradiances. *The Journal of Biological Chemistry* 287(8): 5833-5847.
- Boyle, N. R. and J. A. Morgan. 2009. Flux balance analysis of primary metabolism in *Chlamydomonas reinhardtii*. *BMC Systems Biology* 3(1): 4-10.
- Brooks, M. D., E. J. Sylak-Glassman, G. R. Fleming and K. K. Niyogi. 2013. A thioredoxin-like/beta-propeller protein maintains the efficiency of light harvesting in Arabidopsis.

- Proceedings of the National Academy of Sciences of the United States of America* 110(29): 2733-2740.
- Butler, W. L. and M. Kitajima. 1975. Fluorescence quenching in photosystem II of chloroplasts. *Biochimica et Biophysica Acta (BBA)-Bioenergetics* 376(1): 116-125.
- Ceppi, M. G., A. Oukarroum, N. Çi çek, R. J. Strasser and G. Schansker. 2012. The IP amplitude of the fluorescence rise OJIP is sensitive to changes in the photosystem I content of leaves: a study on plants exposed to magnesium and sulfate deficiencies, drought stress and salt stress. *Physiologia Plantarum* 144(3): 277-288.
- Chisti, Y. 2007. Biodiesel from microalgae. *Biotechnology Advances* 25(3): 294-306.
- Clesceri, L. S., A. E. Greenberg and D. E. Andrew. 1999. *Standard Methods for the Examination of Water and Wastewater*. New York: American Public Health Association.
- Czerpak, R., A. Bajguz, M. Gromek, G. Kozłowska and I. Nowak. 2002. Activity of salicylic acid on the growth and biochemism of *Chlorella vulgaris* Beijerinck. *Acta Physiologiae Plantarum* 24(1): 45-52.
- Delosme, R., J. Olive and F. Wollman. 1996. Changes in light energy distribution upon state transitions: an in vivo photoacoustic study of the wild type and photosynthesis mutants from *Chlamydomonas reinhardtii*. *Biochimica et Biophysica Acta (BBA)-Bioenergetics* 1273(2): 150-158.
- Demmig-Adams, B., G. Garab, W. Adams III and Govindjee. 2014. *Non-Photochemical Quenching and Energy Dissipation In Plants, Algae and Cyanobacteria*. Dordrecht: Springer.
- Demmig-Adams, B., W. Adams III and A. K. Mattoo. 2006. *Photoprotection, Photoinhibition, Gene Regulation, and Environment*. Dordrecht: Springer.
- Depege, N., S. Bellafiore and J. D. Rochaix. 2003. Role of chloroplast protein kinase Stt7 in LHCII phosphorylation and state transition in *Chlamydomonas*. *Science (New York, N.Y.)* 299(5612): 1572-1575.
- Divi, U. K. and P. Krishna. 2009. Brassinosteroid: a biotechnological target for enhancing crop yield and stress tolerance. *New Biotechnology* 26(3-4): 131-136.
- Dubini, A. and M. L. Ghirardi. 2014. Engineering photosynthetic organisms for the production of biohydrogen. *Photosynthesis Research* 123(3): 241-253.
- Ferreira, K. N., T. M. Iverson, K. Maghlaoui, J. Barber and S. Iwata. 2004. Architecture of the photosynthetic oxygen-evolving center. *Science* 303(5665): 1831-1838.
- Fiehn, O., J. Kopka, R. Trethewey and L. Willmitzer. 2000. Identification of uncommon plant metabolites based on calculation of elemental compositions using gas chromatography and quadrupole mass spectrometry. *Analytical Chemistry* 72(15): 3573-3580.

- Forster, B., C. B. Osmond, J. E. Boynton and N. W. Gillham. 1999. Mutants of *Chlamydomonas reinhardtii* resistant to very high light. *Journal of Photochemistry and Photobiology. B, Biology* 48(2-3): 127-135.
- Ghirardi, M. L. 2013. Photobiological H<sub>2</sub> Production: Theoretical Maximum Light Conversion Efficiency and Strategies to Achieve It. *ECS Transactions* 50(49): 47-50.
- Ghirardi, M. L., L. Zhang, J. W. Lee, T. Flynn, M. Seibert, E. Greenbaum and A. Melis. 2000. Microalgae: a green source of renewable H<sub>2</sub>. *Trends in Biotechnology* 18(12): 506-511.
- Govindjee. 2004. Chlorophyll a fluorescence: a bit of basics and history. In *Chlorophyll a Fluorescence: A Signature of Photosynthesis*. Dordrecht: Springer.
- Govindjee. 1995. Sixty-three years since Kautsky: Chlorophyll a fluorescence. *Australian Journal of Plant Physiology* 22(2): 131-160.
- Govindjee and L. O. Björn. 2012. Dissecting oxygenic photosynthesis: The evolution of the “Z”-scheme for thylakoid reactions. In *Photosynthesis: Overviews on Recent Progress & Future Perspective*. New Delhi, India: I K International Publishing House.
- Guarnieri, M. T. and P. T. Pienkos. 2014. Algal omics: unlocking bioproduct diversity in algae cell factories. *Photosynthesis Research. Photosynthesis Research* 123(3): 321-329.
- Hayat, Q., S. Hayat, M. Irfan and A. Ahmad. 2010. Effect of exogenous salicylic acid under changing environment: A review. *Environmental and Experimental Botany* 68(1): 14-25.
- Heifetz, P. B., B. Forster, C. B. Osmond, L. J. Giles and J. E. Boynton. 2000. Effects of acetate on facultative autotrophy in *Chlamydomonas reinhardtii* assessed by photosynthetic measurements and stable isotope analyses. *Plant Physiology* 122(4): 1439-1445.
- Hoefnagel, M. H., O. K. Atkin and J. T. Wiskich. 1998. Interdependence between chloroplasts and mitochondria in the light and the dark. *Biochimica et Biophysica Acta (BBA)-Bioenergetics* 1366(3): 235-255.
- Hong, J. W., S. Jo and H. Yoon. 2014. Research and development for algae-based technologies in Korea: a review of algae biofuel production. *Photosynthesis Research* 123(3): 261-272.
- Ismail, A. M., M. A. Abou Alhamd, H. R. M. Galal and F. A. Nasr-Eldeen. 2011. Modification of photosynthetic pigments, osmotic solutes and ions accumulation in chlorella vulgaris and wheat Cv. Sds-1 seedlings under the influence of NaCl with salicylic acids. *Research Journal of Botany* 6(3): 100-111.
- Iwai, M., M. Yokono, N. Inada and J. Minagawa. 2010. Live-cell imaging of photosystem II antenna dissociation during state transitions. *Proceedings of the National Academy of Sciences of the United States of America* 107(5): 2337-2342.

- Jahns, P. and A. R. Holzwarth. 2012. The role of the xanthophyll cycle and of lutein in photoprotection of photosystem II. *Biochimica et Biophysica Acta (BBA)-Bioenergetics* 1817(1): 182-193.
- Kadioglu, A. 1992. The effects of gibberellic acid on photosynthetic pigments and oxygen evolution in *Chlamydomonas* and *Anacystis*. *Biologia Plantarum* 34(1-2): 163-166.
- Kalaji, H. M., V. Goltsev, K. Bosa, S. I. Allakhverdiev, R. J. Strasser and Govindjee. 2012. Experimental in vivo measurements of light emission in plants: A perspective dedicated to David Walker. *Photosynthesis Research* 114(2): 69-96.
- Kaňa, R., E. Kotabová, O. Komárek, B. Šedivá, G. C. Papageorgiou, Govindjee and O. Prášil. 2012. The slow S to M fluorescence rise in cyanobacteria is due to a state 2 to state 1 transition. *Biochimica et Biophysica Acta (BBA)-Bioenergetics* 1817(8): 1237-1247.
- Keller, M. 2010. Photosynthesis and Respiration. In *The Science of Grapevines: Anatomy and Physiology*. San Diego: Academic Press.
- Kirchhoff, H., S. Horstmann and E. Weis. 2000. Control of the photosynthetic electron transport by PQ diffusion microdomains in thylakoids of higher plants. *Biochimica et Biophysica Acta (BBA)-Bioenergetics* 1459(1): 148-168.
- Kodru, S., S. Nellaepalli, T. Malavath, E. Devadasu and R. Subramanyam. 2013. Does the slow S to M rise of chlorophyll a fluorescence induction reflect transition from state 2 to state 1 in the green alga *Chlamydomonas reinhardtii*? Abstract of Poster #146. St. Louis, MO: 16th International Congress on Photosynthesis Research.
- Kosourov, S. N., M. L. Ghirardi and M. Seibert. 2011. A truncated antenna mutant of *Chlamydomonas reinhardtii* can produce more hydrogen than the parental strain. *International Journal of Hydrogen Energy* 36(3): 2044-2048.
- Lardans, A., B. Forster, O. Prasil, P. Falkowski and V. Sobolev. 1998. Biophysical, biochemical, and physiological characterization of *Chlamydomonas reinhardtii* mutants with amino acid substitutions at the Ala(251) residue in the D1 protein that result in varying levels of photosynthetic competence. *Journal of Biological Chemistry* 273(18): 11082-11091.
- Lisec, J., N. Schauer, J. Kopka, L. Willmitzer and A. Fernie. 2006. Gas chromatography mass spectrometry-based metabolite profiling in plants. *Nature Protocols* 1(1): 387-396.
- Loewus, F. A. and P. P. N. Murthy. 2000. Myo-Inositol metabolism in plants. *Plant Science* 150(1): 1-19.
- López-Bucio, J., M. F. Nieto-Jacobo, V. Ramírez-Rodríguez and L. Herrera-Estrella. 2000. Organic acid metabolism in plants: from adaptive physiology to transgenic varieties for cultivation in extreme soils. *Plant Science* 160(1): 1-13.
- Maeda, H. and D. Della. 2007. Tocopherol functions in photosynthetic organisms. *Current Opinion in Plant Biology* 10(3): 260-265.

- Maxwell, K. and G. Johnson. 2000. Chlorophyll fluorescence - a practical guide. *Journal of Experimental Botany* 51(345): 659-668.
- Melis, A. 2009. Solar energy conversion efficiencies in photosynthesis: Minimizing the chlorophyll antennae to maximize efficiency. *Plant Science* 177(4): 272-280.
- Minagawa, J. 2011. State transitions-The molecular remodeling of photosynthetic supercomplexes that controls energy flow in the chloroplast. *Biochimica et Biophysica Acta (BBA)-Bioenergetics* 1807(8): 897-905.
- Muller, P., X. Li and K. Niyogi. 2001. Non-photochemical quenching. A response to excess light energy. *Plant Physiology* 125(4): 1558-1566.
- Murata, N. 1969. Control of excitation transfer in photosynthesis I. Light-induced change of chlorophyll a fluorescence in *Porphyridium cruentum*. *BBA - Bioenergetics* 172(2): 242-251.
- Mus, F., L. Cournac, V. Cardellini, A. Caruana and G. Peltier. 2005. Inhibitor studies on non-photochemical plastoquinone reduction and H<sub>2</sub> photoproduction in *Chlamydomonas reinhardtii*. *Biochimica et Biophysica Acta (BBA)-Bioenergetics* 1708(3): 322-332.
- Nagy, G., R. Unnep, O. Zsiros, R. Tokutsu, K. Takizawa, L. Porcar, L. Moyet, D. Petroustos, G. Garab, G. Finazzi and J. Minagawa. 2014. Chloroplast remodeling during state transitions in *Chlamydomonas reinhardtii* as revealed by noninvasive techniques in vivo. *Proceedings of the National Academy of Sciences of the United States of America* 111(13): 5042-5047.
- National Research Council. 2012. Sustainable Development of Algal Biofuels. Washington, D.C.: The National Academic Press.
- Nilkens, M., E. Kress, P. Lambrev, Y. Miloslavina, M. Müller, A. R. Holzwarth and P. Jahns. 2010. Identification of a slowly inducible zeaxanthin-dependent component of non-photochemical quenching of chlorophyll fluorescence generated under steady-state conditions in *Arabidopsis*. *Biochimica et Biophysica Acta (BBA) - Bioenergetics* 1797(4): 466-475.
- Ogbonna, J. and H. Tanaka. 2000. Light requirement and photosynthetic cell cultivation - Development of processes for efficient light utilization in photobioreactors. *Journal of Applied Phycology* 12(3-5): 207-218.
- Oukarroum, A., G. Schansker and R. J. Strasser. 2009. Drought stress effects on photosystem I content and photosystem II thermotolerance analyzed using Chl a fluorescence kinetics in barley varieties differing in their drought tolerance. *Physiologia Plantarum* 137(2): 188-199.
- Oxborough, K. and N. R. Baker. 1997. Resolving chlorophyll a fluorescence images of photosynthetic efficiency into photochemical and non-photochemical components -

- Calculation of  $qP$  and  $F_v'/F_m'$  without measuring  $F_o'$ . *Photosynthesis Research* 54(2): 135-142.
- Papageorgiou, G. C. and Govindjee. 2014 (in press). The Non-photochemical Quenching of the Electronically Excited State of Chlorophyll a in Plants: Definitions, Timelines, Viewpoints, Open Questions. In *Non-Photochemical Quenching and Energy Dissipation In Plants, Algae and Cyanobacteria*. Dordrecht: Springer.
- Papageorgiou, G. C. and Govindjee. 2011. Photosystem II fluorescence: Slow changes—Scaling from the past. *Journal of Photochemistry and Photobiology B: Biology* 104(1): 258-270.
- Papageorgiou, G. and Govindjee. 1968a. Light-induced changes in the fluorescence yield of chlorophyll a in vivo. II. *Chlorella pyrenoidosa*. *Biophysical journal* 8(11): 1316-1328.
- Papageorgiou, G. and Govindjee. 1968b. Light-induced changes in the fluorescence yield of chlorophyll a in vivo. I. *Anacystis nidulans*. *Biophysical journal* 8(11): 1299-1315.
- Papageorgiou, G. C. and Govindjee, eds. 2004. *Chlorophyll a fluorescence: a signature of photosynthesis*. Dordrecht Maxwell, MA: Springer.
- Pazour, G., O. Sineshchekov and G. Witman. 1995. Mutational analysis of the phototransduction pathway of *Chlamydomonas reinhardtii*. *The Journal of Cell Biology* 131(2): 427-440.
- Peers, G., T. B. Truong, E. Ostendorf, A. Busch, D. Elrad, A. R. Grossman, M. Hippler and K. K. Niyogi. 2009. An ancient light-harvesting protein is critical for the regulation of algal photosynthesis. *Nature* 462(7272): 518-521.
- Perrine, Z., S. Negi and R. T. Sayre. 2012. Optimization of photosynthetic light energy utilization by microalgae. *Algal Research* 1(2): 134-142.
- Polle, J., S. Kanakagiri and A. Melis. 2003. *tla1*, a DNA insertional transformant of the green alga *Chlamydomonas reinhardtii* with a truncated light-harvesting chlorophyll antenna size. *Planta* 217(1): 49-59.
- Polle, J., S. Kanakagiri, E. Jin, T. Masuda and A. Melis. 2002. Truncated chlorophyll antenna size of the photosystems - a practical method to improve microalgal productivity and hydrogen production in mass culture. *International Journal of Hydrogen Energy* 27(11-12): 1257-1264.
- Rasala, B. A. and S. P. Mayfield. 2014. Photosynthetic biomanufacturing in green algae; production of recombinant proteins for industrial, nutritional, and medical uses. *Photosynthesis Research* 123(3):227-39.
- Rochaix, J. 2014. Regulation and Dynamics of the Light-Harvesting System. *Annual Review of Plant Biology* 65(0): 287-309.
- Rochaix, J. 2002. *Chlamydomonas*, a model system for studying the assembly and dynamics of photosynthetic complexes. *FEBS Letters* 529(1): 34-38.



- Rochaix, J., M. Goldschmidt-Clermont and S. Merchant. 1998. *The Molecular Biology of Chloroplasts and Mitochondria in Chlamydomonas*. Dordrecht: Springer.
- Ruban, A. V., M. P. Johnson and C. D. Duffy. 2012. The photoprotective molecular switch in the photosystem II antenna. *Biochimica et Biophysica Acta (BBA)-Bioenergetics* 1817(1): 167-181.
- Rupassara, S. I. 2008. Metabolite profiling of leaves and vascular exudates of soybean grown under free-air concentration enrichment. PhD diss. Urbana, IL: University of Illinois at Urbana-Champaign.
- Sayre, R. 2010. Microalgae: the potential for carbon capture. *Bioscience* 60(9): 722-727.
- Schaller, H. 2003. The role of sterols in plant growth and development. *Progress in Lipid Research* 42(3): 163-175.
- Sheehan, J., T. Dunahay, J. Benemann and P. Roessler. 1998. A Look Back at the U.S. Department of Energy's Aquatic Species Program: Biodiesel from Algae. NREL/TP-580-24190. Washington, D.C.: U.S. Department of Energy.
- Sirikhachornkit, A., J. W. Shin, I. Baroli and K. K. Niyogi. 2009. Replacement of  $\alpha$ -tocopherol by  $\beta$ -tocopherol enhances resistance to photooxidative stress in a xanthophyll-deficient strain of *chlamydomonas reinhardtii*. *Eukaryotic Cell* 8(11): 1648-1657.
- Stirbet, A., G. Riznichenko, A. Rubin and Govindjee. 2014. Modeling Chlorophyll a Fluorescence Transient: Relation to Photosynthesis. *Biochemistry (Moscow)* 79(4): 291-323.
- Stirbet, A. and Govindjee. 2012. Chlorophyll a fluorescence induction: A personal perspective of the thermal phase, the J-I-P rise. *Photosynthesis Research* 113(1-3): 15-61.
- Stirbet, A. and Govindjee. 2011. On the relation between the Kautsky effect (chlorophyll a fluorescence induction) and Photosystem II: Basics and applications of the OJIP fluorescence transient. *Journal of Photochemistry and Photobiology B: Biology* 104(1-2): 236-257.
- Stoop, J. M. H., J. D. Williamson and D. M. Pharr. 1996. Mannitol metabolism in plants: A method for coping with stress. *Trends in Plant Science* 1(5): 139-144.
- Strasser, R. J., M. Tsimilli-Michael and A. Srivastava. 2004. Analysis of the Chlorophyll a fluorescence transient. In *Chlorophyll a Fluorescence: a Signature of Photosynthesis*. Dordrecht: Springer.
- Strasser, R. J., A. Srivastava and M. Tsimilli-Michael. 2000. The fluorescence transient as a tool to characterize and screen photosynthetic samples. In *Probing Photosynthesis: Mechanisms, Regulation, and Adaptation*. New York: Taylor & Francis.

- Strasser, R. J. and Govindjee. 1991. The Fo and the OJIP fluorescence rise in higher plants and algae. In *Regulation of Chloroplast Biogenesis*. New York: Plenum Press.
- Strasser, R. J., M. Tsimilli-Michael, D. Dangre and M. Rai. 2007. Biophysical phenomics reveals functional building blocks of plants systems biology: a case study for the evaluation of the impact of mycorrhization with *Piriformospora indica*. In *Advanced Techniques in Soil Microbiology*. Berlin, Heidelberg: Springer.
- Takahashi, H., S. Clowez, F. Wollman, O. Vallon and F. Rappaport. 2013. Cyclic electron flow is redox-controlled but independent of state transition. *Nature Communications* 4:1-8.
- Tokutsu, R. and J. Minagawa. 2013. Energy-dissipative supercomplex of photosystem II associated with LHCSR3 in *Chlamydomonas reinhardtii*. *Proceedings of the National Academy of Sciences of the United States of America* 110(24): 10016-10021.
- Trentacoste, E. M., A. M. Martinez and T. Zenk. 2014. The place of algae in agriculture: policies for algal biomass production. *Photosynthesis Research*. 123(3): 305-315.
- Tsimilli-Michael, M. and R. J. Strasser. 2008. In vivo Assessment of Stress Impact on Plant's Vitality: Applications in Detecting and Evaluating the Beneficial Role of Mycorrhization on Host Plants. In *Mycorrhiza: State of the Art. Genetics and Molecular Biology, Eco-function, Biotechnology, Eco-physiology, Structure and Systematics*. Berlin, Heidelberg: Springer.
- Tyystjärvi, E. 2013. Photoinhibition of Photosystem II. *International Review of Cell and Molecular Biology* 300: 243-303.
- U.S. DOE. 2010. National algal biofuels technology roadmap. U.S. Department of Energy, Office of Energy Efficiency and Renewable Energy, Biomass Program.
- Ünlü, C., B. Drop, R. Croce and H. van Amerongen. 2014. State transitions in *Chlamydomonas reinhardtii* strongly modulate the functional size of photosystem II but not of photosystem I. *Proceedings of the National Academy of Sciences of the United States of America* 111(9): 3460-3465.
- Valluru, R. and W. Van den Ende. 2011. Myo-inositol and beyond-Emerging networks under stress. *Plant Science* 181(4): 387-400.
- Vicente, M. and J. Plasencia. 2011. Salicylic acid beyond defense: its role in plant growth and development. *Journal of Experimental Botany* 62(10): 3321-3338.
- Voegelé, R., M. Hahn, G. Lohaus, T. Link and I. Heiser. 2005. Possible roles for mannitol and mannitol dehydrogenase in the biotrophic plant pathogen *Uromyces fabae*. *Plant Physiology* 137(1): 190-198.
- Williams, P. J. L. B. and L. M. L. Laurens. 2010. Microalgae as biodiesel biomass feedstocks: Review analysis of the biochemistry, energetics economics. *Energy Environmental Science* 3(5): 554-559.

- Yusuf, M. A., D. Kumar, R. Rajwanshi, R. J. Strasser, M. Tsimilli-Michael, Govindjee and N. B. Sarin. 2010. Overexpression of  $\gamma$ -tocopherol methyl transferase gene in transgenic *Brassica juncea* plants alleviates abiotic stress: Physiological and chlorophyll a fluorescence measurements. *Biochimica et Biophysica Acta - Bioenergetics* 1797(8): 1428-1438.
- Zhou, Y., C. L. Schideman, Govindjee, S. I. Rupassara and M. J. Seufferheld. 2012. Improving the Photosynthetic Productivity and Light Utilization in Algal Biofuel Systems: Metabolic and Physiological Characterization of a Potentially Advantageous Mutant of *Chlamydomonas reinhardtii*. In *Photosynthesis: Research for Food, Fuel and Future - 15th International Conference on Photosynthesis, Symposium*. Beijing, China: Zhejiang University Press.

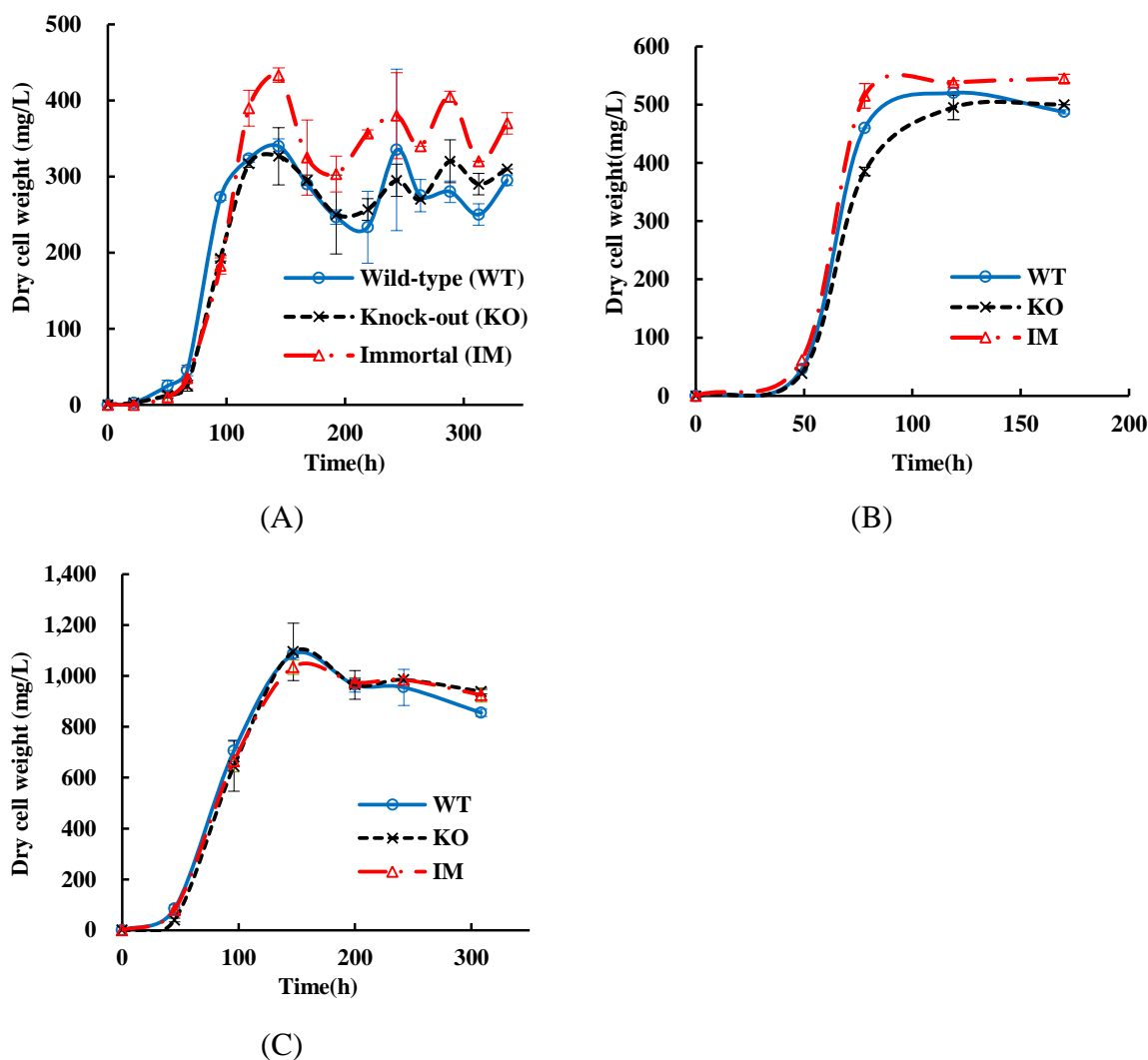
## 7.7 Figures and Tables

**Table 7-1. Parameters calculated from the Pn-E curves of all three *Chlamydomonas* strains (average values  $\pm$  standard deviations for six replicate measurements).**

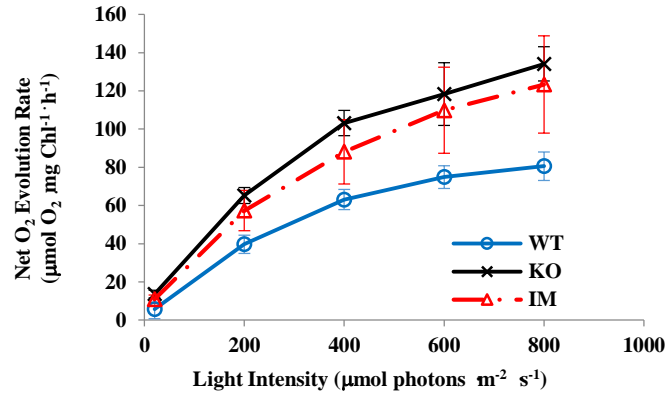
	<b>WT</b>	<b>KO</b>	<b>IM</b>
$P_{\max}$ , Maximum net O <sub>2</sub> evolution rate ( $\mu\text{mol O}_2 \text{ mg}^{-1} \text{ Chl } a \text{ h}^{-1}$ )	80.6 $\pm$ 7.5	134.1 $\pm$ 8.9	123.3 $\pm$ 25.4
$R_d$ , Dark respiration rate ( $\mu\text{mol O}_2 \text{ mg}^{-1} \text{ Chl } a \text{ h}^{-1}$ )	25.0 $\pm$ 3.4	40.3 $\pm$ 8.7	35.2 $\pm$ 5.3

**Table 7-2. Comparison of selected fluorescence parameters of the WT, KO and IM strains of *Chlamydomonas reinhardtii* for cultures grown under fluorescent lamps of two different light intensities (20 and 640  $\mu\text{mol photons m}^{-2} \text{s}^{-1}$ ) and sampled during the exponential phase. Presented values are averages  $\pm$  standard deviations for at least nine replicate measurements.**

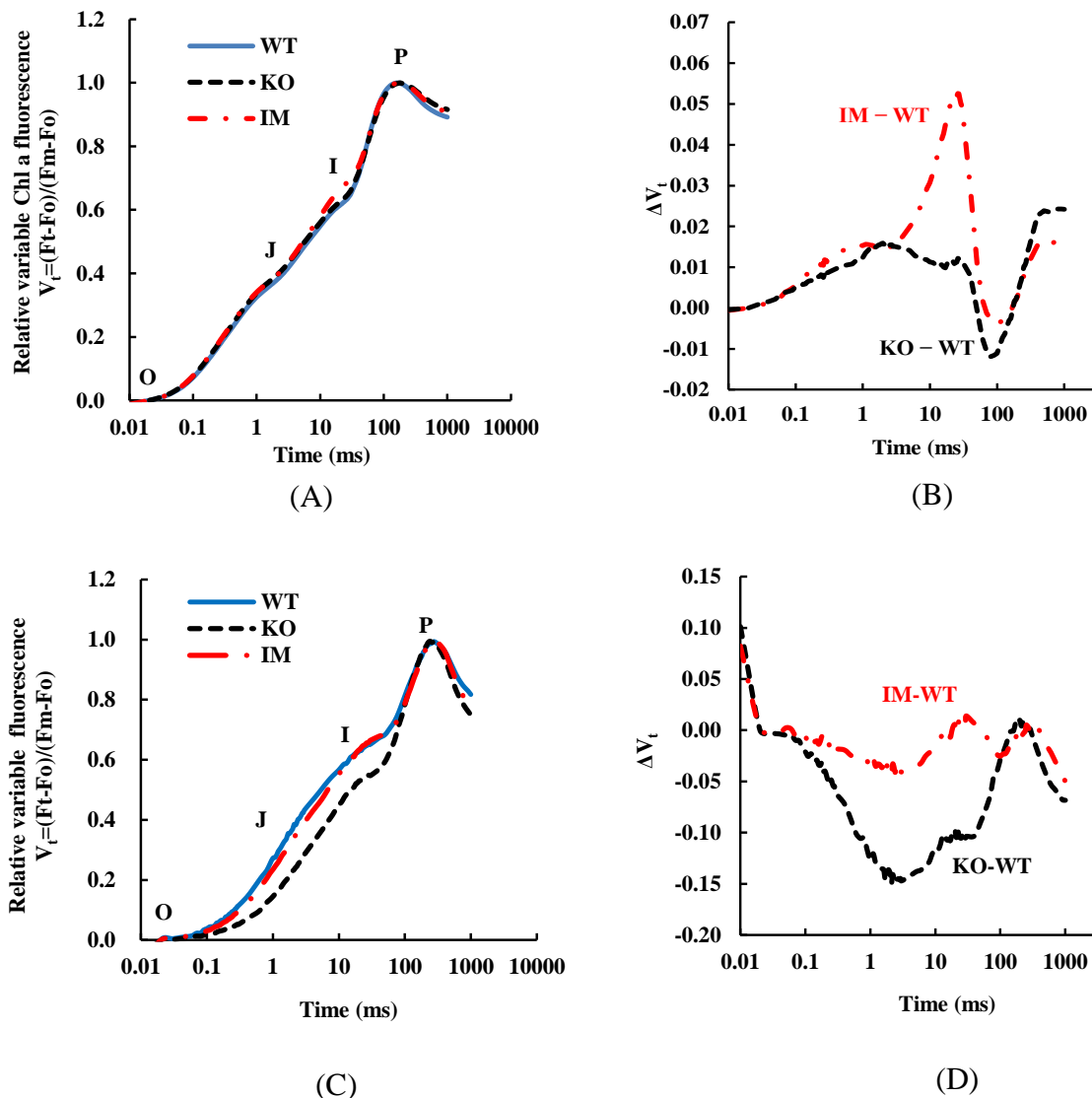
Fluorescence parameter symbols	Fluorescence parameter description	Wild-type (WT)	Knock-out Mutant (KO)	Immortal Mutant (IM)	(KO-WT) /WT	(IM-WT) /WT
<b>Low light condition: 20 <math>\mu\text{mol photons m}^{-2} \text{s}^{-1}</math></b>						
$F_o$	Initial (minimum) Chl fluorescence intensity	217 $\pm$ 34	244 $\pm$ 19	235 $\pm$ 9	12.5%	8.3%
$F_m$	Maximum Chl fluorescence intensity	954 $\pm$ 185	1115 $\pm$ 75	1097 $\pm$ 69	16.0%	15.0%
$F_v/F_m$	Maximum quantum yield of PSII photochemistry	0.77 $\pm$ 0.01	0.78 $\pm$ 0.02	0.79 $\pm$ 0.01	1.2%	1.9%
$F_v/F_o$	The ratio between maximum variable Chl fluorescence and initial fluorescence	3.37 $\pm$ 0.2	3.60 $\pm$ 0.49	3.67 $\pm$ 0.24	6.7%	8.8%
$F_o/F_m$	Quantum yield of excitation energy dissipation	0.23 $\pm$ 0.01	0.22 $\pm$ 0.02	0.21 $\pm$ 0.01	-4.0%	-6.3%
dV/dto	The initial slope of the double normalized (to $F_o$ and $F_m$ ) Chl fluorescence transient	0.684 $\pm$ 0.01	0.71 $\pm$ 0.08	0.73 $\pm$ 0.02	4.5%	6.2%
<b>High light condition: 640 <math>\mu\text{mol photons m}^{-2} \text{s}^{-1}</math></b>						
$F_o$	Minimum fluorescence intensity	377 $\pm$ 58	185 $\pm$ 6	322 $\pm$ 10	-50.9%	14.5%
$F_m$	Maximum fluorescence intensity	626 $\pm$ 35	490 $\pm$ 37	754 $\pm$ 85	-21.7%	20.4%
$F_v/F_m$	Maximum quantum yield of PSII photochemistry	0.40 $\pm$ 0.08	0.62 $\pm$ 0.04	0.57 $\pm$ 0.05	55.1%	41.8%
$F_v/F_o$	The ratio between maximum variable fluorescence and initial fluorescence	0.69 $\pm$ 0.23	1.66 $\pm$ 0.26	1.34 $\pm$ 0.25	139.3%	93.4%
$F_o/F_m$	Quantum yield of excitation energy dissipation	0.60 $\pm$ 0.08	0.38 $\pm$ 0.04	0.43 $\pm$ 0.05	-36.8%	27.9%
dV/dto	The initial slope of the double normalized (to $F_o$ and $F_m$ ) Chl fluorescence transient	0.41 $\pm$ 0.09	0.19 $\pm$ 0.02	0.34 $\pm$ 0.03	-54.7%	16.3%



**Figure 7-1. Dry cell weight growth curves of *Chlamydomonas reinhardtii* algae grown under fluorescent light of three different light intensities for three different strains: wild-type (WT), knock-out mutant (KO) and spontaneous mutant (IM). (A) 10  $\mu\text{mol photons m}^{-2} \text{s}^{-1}$ ; (B) 20  $\mu\text{mol photons m}^{-2} \text{s}^{-1}$ ; (C) 640  $\mu\text{mol photons m}^{-2} \text{s}^{-1}$ . Two culture replicates were used, and average values are plotted with error bars showing the standard deviation. These cultures were grown at 24 °C under mixotrophic conditions with TAP medium.**

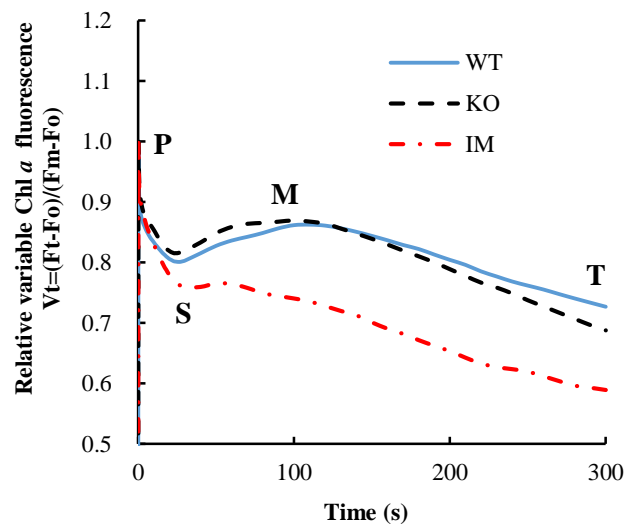


**Figure 7-2. Net photosynthetic O<sub>2</sub> evolution rate (P<sub>n</sub>) as a function of light intensity (P<sub>n</sub>-E curves) for WT, KO and IM cells of *Chlamydomonas reinhardtii* cultured under fluorescent light of 60  $\mu\text{mol photons m}^{-2} \text{ s}^{-1}$ , and collected during the exponential growth phase. The light source was a red LED with a peak wavelength at 650 nm. Three separate culture replicates were used and duplicate measurements were made for each culture replicate (n=6); results are presented as averages  $\pm$  standard deviations.**

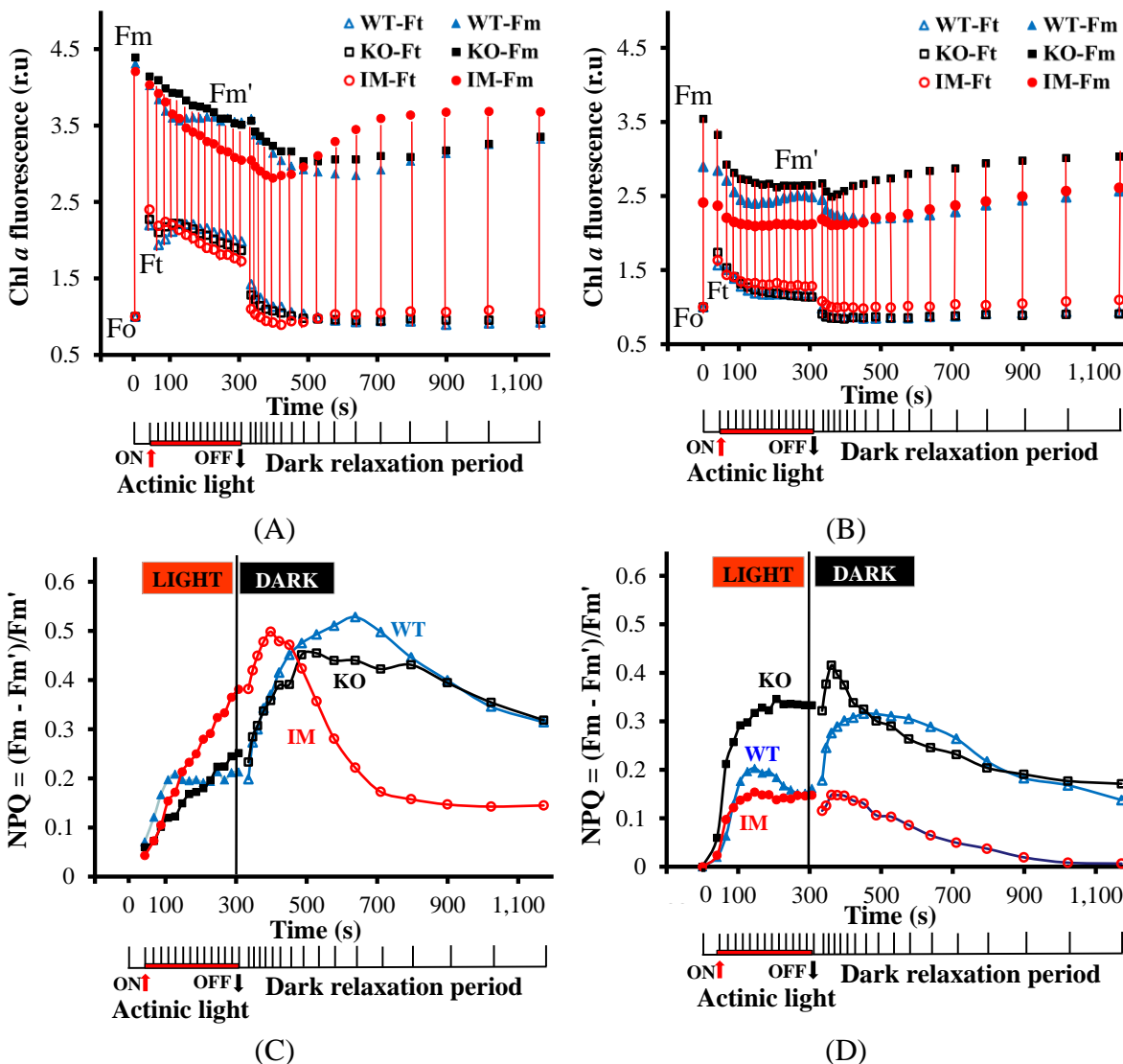


**Figure 7-3. OJIP Chl *a* fast fluorescence transients in WT, KO, and IM *Chlamydomonas reinhardtii* strains grown under fluorescent light of (A) 20  $\mu\text{mol photons m}^{-2} \text{s}^{-1}$  (low light) or (B) 640  $\mu\text{mol photons m}^{-2} \text{s}^{-1}$  (high light). Data were double normalized at  $F_0$  and  $F_m$ , and are presented on a logarithmic time scale in the 0-1 s range; data points are averages of nine independent measurements. (C) and (D) Difference curves (IM - WT) and (KO - WT) of the respective fluorescence transients shown in panel (A) and (B).**

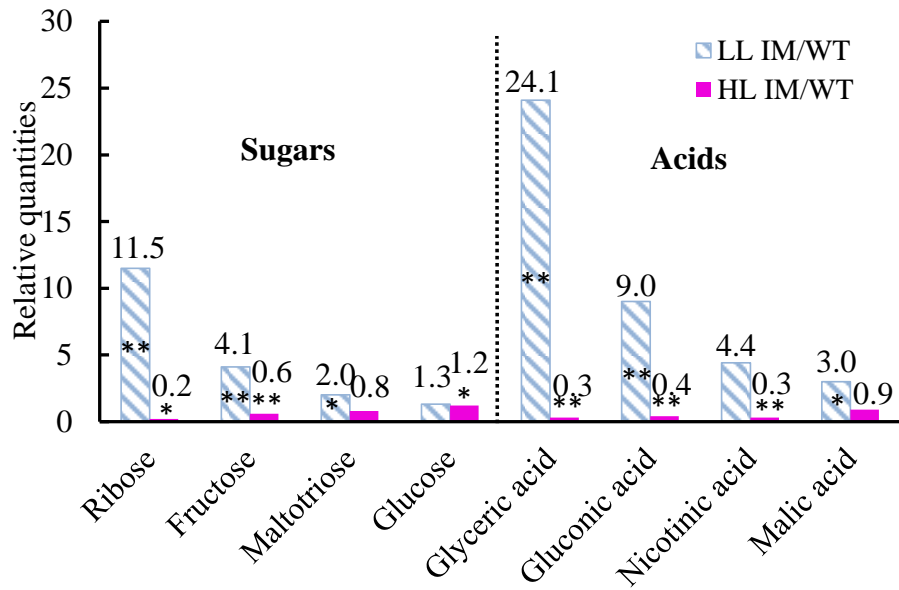




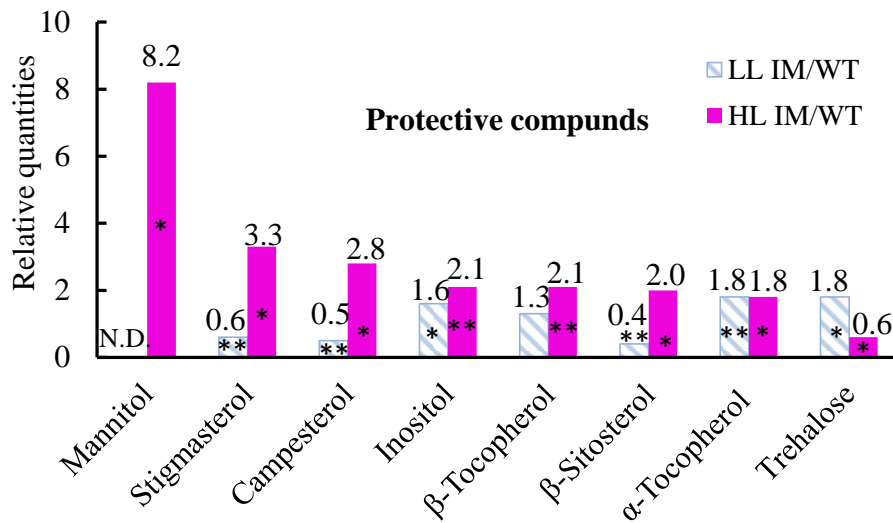
**Figure 7-4.** The PSMT part of Chl *a* fluorescence transients of three *Chlamydomonas reinhardtii* strains (WT, KO, and IM) grown under 20  $\mu\text{mol photons m}^{-2} \text{s}^{-1}$  fluorescent light. Data were double normalized at  $F_0$  and at  $F_m$ ; and are presented as the average values of at least nine independent measurements.



**Figure 7-5. Chl *a* fluorescence data obtained with Pulse Amplitude Modulation (PAM) instrument (Walz) in saturated pulse mode for three *Chlamydomonas* strains (WT, KO and IM) grown under fluorescent lamps of (A) low light (20  $\mu\text{mol photons m}^{-2} \text{s}^{-1}$ ) and (B) high light (640  $\mu\text{mol photons m}^{-2} \text{s}^{-1}$ ); (C) NPQ kinetic curves obtained using the data shown in (A); and (D), NPQ kinetic curves obtained using the data shown in (B). Data points are averages of nine independent measurements and normalized at  $F_0$ . During the 5 min "Light" period, samples were illuminated with actinic light ( $\sim 600 \mu\text{mol photons m}^{-2} \text{s}^{-1}$ ;  $\lambda = 665 \text{ nm}$ ) and they also received a saturating pulse (8,000  $\mu\text{mol photons m}^{-2} \text{s}^{-1}$ ;  $\lambda = 665 \text{ nm}$ ) every 20 s, or longer (time sequence of these light pulses is shown in the lower part of each panel). The actinic light was turned off during the 20 min "Dark" relaxation period, but the samples still received the series of saturating light pulses.**



(A)



(B)

**Figure 7-6. Comparison of key metabolites for (A) carbon metabolism and (B) oxidative stress protection for IM and WT cultures sampled during the exponential phase under fluorescent light of two different intensities: low light (LL, 20  $\mu\text{mol photons m}^{-2} \text{s}^{-1}$ ) and high light (HL, 640  $\mu\text{mol photons m}^{-2} \text{s}^{-1}$ ) conditions. Relative quantities were calculated as the ratio of metabolite levels in IM cells to the levels in WT cells. Three biological replicates and three analytical replicates were averaged in this analysis ( $n = 9$ ). Statistically significant metabolite differences are denoted with a “\*” ( $p < 0.05$ ) or “\*\*” ( $p < 0.01$ ) in t-test. N.D. indicates not detected.**